Université de Paris

École doctorale MTCI

Laboratoire UTCBS

CONCEPTION OF NANOSIZED HYBRID LIPOSOME/POLYMER PARTICLES FOR HYDROPHILIC DRUG DELIVERY

Par Shayan AHMED

Thèse de doctorat de Pharmacochimie

Dirigée par Dr. Nathalie MIGNET

Présentée et soutenue publiquement

Devant un jury composé de :

Françoise Chuburu, PU	Université de Reims	Rapporteur
Vincent Faivre, MCU-HDR	Université Paris Saclay	Rapporteur
Fabienne Testard, HDR	CEA	Examinateur
Khair Alhareth, MCU	Université de Paris	Membre invité
Nathalie Mignet, DR-HDR	Université de Paris	Directrice de thèse

à ma famille,

Acknowledgment

I would like to express my gratitude to my supervisor Dr. Nathalie Mignet for all the knowledge, guidance, support and time she provided to make this thesis possible. A real appreciation to Dr. Nathalie Mignet for acting as a sounding board during the discussions, for continually being available to meet, and for having confidence in me to pursue new ideas. Without her mentorship and tireless encouragement this work would not have been possible. Moreover, I would like to thank her for giving me the great opportunities and support to present my work at several conferences and specially for the visit to Biomat'X laboratory at MGILL University, Canada.

Likewise, I would like to thank Dr. Khair Alhareth, who taught me everything I had to know about Liposomes preparation and characterization. He generously provided me the time and guided me throughout the project. His guidance and spirit have been invaluable in my personal and academic development. His utter believe and trust in me were the key factors what kept me motivated in every situation.

Special thanks to Dr. Yohann Corvis and Dr. Johanne Seguin, for their support regarding physico-chemical characterization and in vitro part of the project, respectively. I am also thankful to René Lai-Kuen for his help in optical imaging.

In addition, my appreciations go to the Vector and Molecular Imaging and Targeted Therapy team for welcoming me and helping me including Daniel Scherman, Cyrille Richard, Karine Andrieux, Vincent Boudy, Philippe Espeau, Caroline Roques, Pascal Houze, Rabah Gahoual, Hélène Dhotel, Geoffroy Goujon, Thomas Lecuyer, Lucie Valero, Morgane Renault-Mahieux, Brice Couillaud, Hai-Doan Do, Jianhua Liu, Louise Fliedel, Xiaojing Liu, Panpan Ma, Asad ur Rehman and Master students Pinar Caklikaya, Arlen Euan, Silvia Collina and Salma Rabie for their assistance.

I would like to thank Dr. Maryam Tabrizian for giving me the opportunity through Fonds France-Canada por la Recherche (FFCR) project to integrate her laboratory for *in vitro* tests in 3D microfluidic chip at Biomat'X Laboratory, McGILL university, Canada. It would have been hopeless for me to achieve this project without the help of Dr. Hugo Salmon and Nicholas Distasio. I thank all the members of Biomat'X lab for their friendship and support.

I would like to thank HEC Pakistan, University Paris Descartes and the Doctoral School MTCI for giving me the opportunity to pursuit PhD degree.
I would like to thank all my friends including Rameez Mumtaz, Zaheer Mumtaz, Saad Misbah, Amit Kumar Pundir, Diana Kudina Osseyran, Rameez Ishaq, Bilal Mustafa Memon and Imtiaz Maitlo, Waseem Chishti, Hira Niazi and Matti Ullah.

In particular, I would like to thank to Dr. Shariq Rajput who guided me in every situation, since I arrived in France until now. His advice, availability and guidance in terms of all local and administrative issues kept my thesis journey out of troubles that helped me to develop myself personally and professionally.

I owe thanks to a very special person, my fiancée, Faiza Khan for her continuous and unfailing love, support and understanding during my pursuit of PhD degree, that made the completion of my thesis possible. I greatly value her care and deeply appreciate her believe in me. Without her love, affection and care this journey could not be so beautiful.

Finally, I cannot begin to thank my family enough for their unwavering love and support over the years. Words alone cannot express my gratitude to my parents, Muhammad Farooq and Alia Batool, without whom, I never could have completed my PhD journey. I would never be able to pay back the love and affection showered upon by my parents. Thank to my brothers, Salman Ahmed and Zeeshan Ahmed for always helping and supporting me in every situation. I greet you all for the selfless love, care, pain and sacrifice you did to shape my life.

Abstract

Nanomedicine is the application of nanotechnology for health. These particles in the nanosize range are used as drug delivery tools, diagnostic agents or enhancers of therapies. This thesis is part of the drug delivery strategies using organic compounds with low toxicity to serve as nanocarriers. Liposome is the first nanocarrier approved by the FDA to deliver doxorubicin. This phospholipid-based nano-carrier has the potential to carry hydrophilic and lipophilic drugs, but it also possesses some disadvantages like drug leakage in particular of small hydrophilic drugs. To cope with these limitations, we have designed a Hybrid liposome/polymer (HLP), made with a lipidic shell and a poloxamer core. The idea behind this replacement of the aqueous core with a polymeric core was to improve its features, in particular to increase the core viscosity in order to make it suitable to a wide range of drugs. During the thesis, various methods were applied to possibly prepare homogeneous hybrid nanoparticles, comparing the thin film hydration, manual and automatized ethanolic injection method using the syringe pump technique. The physio-chemical characterization of these nanoparticles was achieved by transmission electron microscopy, dynamic light scattering, nanoparticle tracking analysis, tunable resistive pulse sensing, densitometry and thermal analysis. The results revealed that the size of nanoparticles was within the range of 100 to 200 nm and PDI within the range of 0.1 to 0.3. Differential scanning calorimetry and colorimetric assay confirmed the presence of poloxamer inside the liposome shell. Various molecules were encapsulated in order to evaluate the range of molecular size drugs which could benefit from this technology. Encapsulation of Rhodamine, Doxorubicin and siRNA was evaluated. Non-ionic HLP was designed for the encapsulation of rhodamine and doxorubicin, which presented slow release, whereas positively charged HLP were conceived to encapsulate siRNA. siRNA activity against GFP expression was tested on endothelial cells seeded in 96 well plate and 3D micro-chip, in the presence and absence of TNF-α. The HLP encapsulating siRNA downregulated the GFP expression in the absence of TNF-α when compared to controls. Convincingly, the delay was observed in release of rhodamine and doxorubicin encapsulated in non-ionic HLP and on the other hand the cationic HLP formulation proved to be good candidate for siRNA delivery. To conclude, we conceived and obtained during this PhD, liposomes with thickened core and showed that they were able to allow a slower release of small hydrophilic drugs as regard to liposomes. During this PhD, we also found a novel method to characterize poloxamer by thermal analysis, and we showed that our homemade tubing system coupled with a syringe pump apparatus achieved reproducible, precisely controlled production of the HLP formulation which can be scaled up.

Résumé

La nanomédicine est l'application des nanotechnologies pour la santé. Ces particules de taille dans le domaine des nanos sont utilisées comme systèmes de délivrance de substances actives, d'agents d'imagerie ou comme potentialisateur de thérapies existantes, comme la radiothérapie. Cette thèse s'inscrit dans le cadre de nanoparticules pour la délivrance de principe actif. Les liposomes sont les premiers nanomédicaments qui ont été acceptés par la Food and Drug Administration pour une utilization humaine. Ces transporteurs constitués de phospholipids naturels ont la possibilité de transporter des molecules hydrophiles et lipophiles, néanmoins ils possèdent quelques désavantages comme la libération rapide de molécules hydrophiles. Afin d'améliorer la retention de molécules hydrophiles dans ces transporteurs, l'objectif de cette thèse a été de concevoir des liposomes avec un coeur liquide plus visqueux que celui de liposomes conventionnels. Nous avons choisi d'utiliser des excipients acceptables pour la clinique, et avons utilisé le poloxamère P407 afin de densifier le coeur aqueux de ces nano-objets. Le travail de cette thèse a consisté à étudier la préparation de ces liposomes hybrides afin d'obtenir des objets peu polydisperses, de démontrer que le coeur des liposomes obtenus était en effet plus dense que ceux de liposomes non polymériques et d'évaluer l'encapsulation et la liberation de trois sortes de molecules modèles de taille différente.

Dans un premier temps, une revue de la littérature sur les nanogels a été réalisée. Après selection des constituants, une méthode de caractérisation de poloxamères a été mise au point par calorimétrie. Puis, trois méthodes de preparation de ces liposomes hybrides ont été comparées, l'hydratation d'un film lipidique, la precipitation anti-solvent manuelle et automatisée. Cette étude a démontré que la méthode de preparation par pousse seringue mise en place au cours de cette thèse était plus efficace pour former des particules homogènes. Enfin, l'encapsulation et la libération de rhodamine, doxorucine et siRNA ont ainsi été étudiées. Nous avons montré que la libération de rhodamine et doxorubicine était ralentie lorsque ces molecules était encapsulée dans des liposomes hybrides non chargés. Pour l'encapsulation de siRNA, nous avons eu recours à des liposomes hybrides positivement chargés par association de lipids ou polymers cationiques dans la formulation. Ces dernières formulations ont montré qu'elles pouvaient induire l'extinction de la green fluorescent protein exprimées par des cellules endothéliales en culture 2D ou sur microchip.

Table of Contents

Abbreviation Abbreviations and symbols 1

Thesis Outline 2

Chapter 1: Introduction 4

1.1. Cancer 4

1.2. Nanomedicines 5

Chapter 2: Advancement in Nanogel Formulations Provides Controlled Drug Release. Review of the Literature 9

2.1. Introduction 9

2.2. Drug Release Mechanism for Nanogels 11

2.3. Nanogels with Trigger Responsive Behavior 14

2.3.1. Thermo-Sensitive Triggered Release. 14

2.3.2. pH Sensitive Release. 16

2.3.3. Redox-Responsive Release 19

2.3.4. Photo-Sensitive Release 22

2.3.5. Enzymatic Responsive Release 24

2.4. Conclusion 26

Chapter 3. Rationale of the Project 27

3.1. Why Liposomes? 27

3.2. Why Thickened Core Liposomes 27

3.3. Why Non-Ionic Lipid? 28

3.4. Why Non-Ionic Polymer? 28

3.5. Why Rhodamine B? 29

3.6. Why Doxorubicin Hydrochloride? 30

3.7. Why siRNA? 32

Chapter 4. Sub-ambient DSC Analytical Method Development for Quantitative Determination of Poloxamers solutions: application to the Characterization of Nano-formulations for Drug Delivery.....35
4.1. Introduction.....35
4.2. Materials.....36
4.3. Material and Methods.....37
4.3.1. Preparation of Polymeric Aqueous Solutions.....37
4.3.2. Thermal Analysis.....37
4.3.3. Density Analysis.....37
4.3.4. Thermal Microscopy.....38
4.3.5. Calibration Curves.....38
4.4. Results and Discussion.....38
4.4.1. Thermal Transitions at High Temperatures.....38
4.4.2. Densitometry Evaluation.....39
4.4.3. Thermal transitions at low temperatures.....40
4.4.4. The Evaluation of the Effect on Seaks at sub-ambient Temperature due to P407 Concentration.....42
4.5. Conclusion.....44
Chapter 5: Optimization of Syringe Pump Device for Production of Nanosized Hybrid Liposome/Poloxamer Particles and their Characterization.....46
5.1. Introduction.....46
5.2. Materials.....48
5.3. Methods.....48
5.3.1. Methods of Preparation of the Formulations.....48
5.3.2. Evaporation of Ethanol.....51
5.3.3. Densitometry.....51
5.3.4. Ultrafiltration by Centrifugation.....52
5.3.5. Physicochemical Characterization.....52

5.3.6. Calorimetric Assay (Baleux Assay) 53
5.3.7. Stability Study 53
5.4. Results and Discussion 54
5.4.1. Conception of the Formulations 54
5.4.2. Optimization of the Experimental Conditions for Push Syringe 54
5.4.3. Physicochemical Characterization 62
5.4.4. Differential Scanning Calorimetry (DSC) 64
5.4.5. Calorimetric Assay (Baleux Assay) 67
5.4.6. Influence of Temperature on HLP Formulations Size 67
5.4.7. Lipid Poloxamer Interaction Evidence 70
5.4.8. Stability 71
5.5. Conclusion 72
Chapter 6. Drug Modelling, Encapsulation and Cytotoxicity Assay of Hybrid Liposome/Poloxamer Particles Encapsulating Hydrophilic Anti-Cancer Drug Delivery 73
6.1. Introduction 73
6.2. Materials 74
6.3. Methods 74
6.3.1. Preparation of the Formulations by Syringe Pump Apparatus 74
6.3.2. Ultrafiltration by Centrifugation 75
6.3.3. Dynamic Light Scattering (DLS) 75
6.3.4. Loading Content and Encapsulation Efficiency 75
6.3.5. *In Vitro* Release 76
6.3.6. Cytotoxicity Tests 76
6.3.7. Statistical Analysis 77
6.4. Results and Discussion 77
6.4.1. Effect of Variables on Drug Modelling 77
6.4.2. Encapsulation Efficiency and Loading Content 80

6.4.3. *In Vitro* Release Kinetics 81
6.4.4. Cytotoxicity 83
6.5. Conclusion 85
Chapter 7. Conception of Positively Charged Hybrid Liposome/Poloxamer Nano Carriers for siRNA Delivery 86
7.1. Introduction 86
7.2. Materials 88
7.3. Methods 88
7.3.1. Preparations of the Formulations 88
7.3.2. Dynamic Light Scattering (DLS) 89
7.3.3. Nanoparticle Tracking Analysis 89
7.3.4. Ultrafiltration by Centrifugation 90
7.3.5. Gel Electrophoresis 90
7.3.6. Ribo Green Assay 90
7.3.7. Microchip Fabrication 91
7.3.8. Three-Dimensional Cell Culture in Micro-Chip 92
7.3.9. Fixation and Staining of Cells for Confocal Imaging 92
7.3.10. GFP Fluorescence Quantification 92
7.4. Results and Discussion 93
7.4.1. Formulation Preparation 93
7.4.2. Encapsulation Efficiency and Loading Content 96
7.4.3. Treatment of Cell with siRNA Formulation 97
7.5. Conclusion 108
Chapter 8. Global Discussion, Original Contributions, Conclusions and Future Perspectives 109
Formulation Rational Design 110
Comprehensive Nanoparticle's Characterization 112
Lipid/poloxamer Nanoparticle: Morphology and Configuration 113

Drug Retention and Release 113
In vitro Assessment of HLP 114
Perspectives for HLPs 114
Conclusion 115
Reference 117
Annex 143

List of Figures

1	Figure 1.1. Multifunctional nanoparticles structures which makes nanomedicines versatile.	07
2	Figure 2.1. Schematic representation of the network construction of hydrogels, microgels and nanogels.	11
3	Figure 2.2. Drug release from nanogels.	13
4	Figure 3.1. Diagram of liposomes.	27
5	Figure 3.2. Structure of DOPC (1,2 Dioleooyl-sn-glycero-3-phosphocholine).	28
6	Figure 3.3. Structure of Poloxamer P407 (PEO-PPO-PEO).	29
7	Figure 3.4. Structure of rhodamine B.	29
8	Figure 3.5. Structure of Doxorubicin HCL.	30
9	Figure 3.6. Picture of, A) Doxil structure and B) Doxorubicin pathway in cancer cell.	31
10	Figure 3.7. Structure of siRNA.	32
11	Figure 3.8. Diagram of, A) Patisiran (Pegylated liposome encapsulating siRNA) and B) siRNA pathway for gene silencing.	34
12	Figure 4.1. Graphical illustration of Micellization and gelification behavior of poloxamer in aqueous environment.	36
13	Figure 4.2. DSC curve of the P407 solution for the high temperature screening at function of polymer concentration: (–) 1%, (–) 5%, (–) 10%, (–) 15%, and (…) 20%.	29
14	Figure 4.3. Calibration curves, A) Temperature micellization and B) Heat flow derivation integration for various P407 concentration.	29
15	Figure 4.4. Density calibration curve of the P407 solution, A) 25 and B) 37 °C.	40
16	Figure 4.5. DSC curve of the P407 solution at the sub-ambient temperature screening at function of polymer concentration: (–) 0.1%, (–) 5%, (–) 10%, and (–) 15%.	41
17	Figure 4.6. Weight normalized DSC curve of PPO solution (5%).	42
18	Figure 4.7. Thermal microscopic images at sub-ambient temperature of P407 5% with Rhodamine dye (0.1 mg.mL-1) at (A) -15 °C, (B) -4.4 °C and (C) -0.4 °C.	42
19	Figure 4.8. Thermal data of the tightly-bound (A, B), loosely-bound (C, D), and (E, F) free water in P407 environment as function of P407 concentration.	44

20	Figure 5.1. Graphical representation of the formulation, A) Conventional Liposomes, B) HLPout and C) HLP.	50
21	Figure 5.2: Pictorial presentation of whole setup of Syringe pump preparation technique.	51
22	Figure 5.3. Comparison between two Tube System T-1 (left) and T-2 (right), (a) Pictorial illustration, (b) Graphical representation of size and PDI of liposomes obtained with different flow rate of each tube system (n=3).	56
23	Figure 5.4. TEM images and DLS size measurement of HLP (P407 0.5%) prepared by A) Dry film hydration technique, B) ethanolic injection technique and C) Push syringe technique.	58
24	Figure 5.5. Tube system and formulation optimization Graphical presentation of hydrodynamic average size of HLP (A) and of polydispersity index (B) of formulation obtained. with different poloxamer (P407) percentages at different flow rates (0.5, 1, 5, 10, and 37 mL.min-1).	59
25	Figure 5.6. Calibration curve for Poloxamer volumetric mass.	61
26	Figure 5.7. (A) Conventional liposomes as spherical unilaminar vesicles of variable sizes (24-329 nm), (B) HLPout. as heterogenous mixture with non-definite shape particles with size range (30-445), and (C) HLP as unilaminar vesicles of variable sizes (50-188 nm).	64
27	Figure 5.8. Derived DSC curves obtained (A) P407 5%, (B) HLPout, before filtration, (C) HLP, before filtration, (D) HLPout, after filtration, and (E) HLP after filtration.	65
28	Figure 5.9. Calibration curve for Polaxamer P407 by calorimetric analysis.	67
29	Figure 5.10. Study of the effect of temperature on the size and PDI of formulations A) Liposomes, B) HLP (P407 0.5%), C) HLP, and D) HLP_{out}.	69
30	Figure 5.11. Stability test graph corresponds to the difference in size and PDI of conventional liposomes, HLP, and HLPout with in a period of 2 months at 4°C.	71
31	Figure 6.1. Calibration curve for different poloxamer and rhodamine concentration, A) P407 5% - Rho 0.5 mg.mL-1, B) P407 0.5% - Rho 0.5 mg.mL-1, C) P407 0.5% - Rho 0.05 mg.mL-1 and D)Calibration curve P407 0% - Rhodamine mg.mL-1.	79

32	Figure 6.2. A) Encapsulation efficiency and loading content of rhodamine B inside Cls and HLP. B) Encapsulation efficiency and loading content of doxorubicin inside Cls and HLP. Two-way ANOVA p=0.01, **.	81
33	Figure 6.3. Release of Rhodamine B from nonionic lipids vesicles with and without poloxamer.	82
34	Figure 6.4. Release of Doxorubicin from nonionic lipids vesicles with and without poloxamer.	83
35	Figure 6.5. In vitro cell viability curves.	84
36	Figure 7.1. Structure of DMAPAP lipid.	87
37	Figure 7.2. Structure of Polyethylenimine (Branched).	87
38	Figure 7.3. Calibration curves for siRNA quantification at different concentration, A) siRNA in the absence of siRNA and B) siRNA in the presence of P407.	96
39	Figure 7.4. Confocal imaging of endothelial cells treated with different conditions, A) Non treated, B) Lipofectamine + scrambled siRNA, C) Lipofectamine + siRNA, D) CL-DMAPAP-siRNA and E) HLP-DMAPAP-siRNA in the absence of TNF-a.	98
40	Figure 7.5. Confocal imaging of endothelial cells treated with different conditions, A) Non treated, B) Lipofectamine + scrambled siRNA, C) Lipofectamine + siRNA, D) CL-PEI-siRNA and E) HLP-PEI -siRNA in the absence of TNF-a.	99
41	Figure 7.6. Confocal imaging of endothelial cells treated with different conditions, A) Non treated, B) Lipofectamine + scrambled siRNA, C) Lipofectamine + siRNA, D) CL-DMAPAP-siRNA and E) HLP-DMAPAP-siRNA in the presence of TNF-a.	100
42	Figure 7.7. Confocal imaging of endothelial cells treated with different conditions, A) Non treated, B) Lipofectamine + scrambled siRNA, C) Lipofectamine + siRNA, D) CL-PEI-siRNA and E) HLP-PEI -siRNA in the presence of TNF-a.	101
43	Figure 7.8. Quantitative analysis of GFP down regulation of siRNA encapsulated in cationic formulations in comparison to positive and negative controls in the absence of TNF-a.	102
44	Figure 7.9. Quantitative analysis of GFP down regulation of siRNA encapsulated in cationic formulations in comparison of positive and negative controls in the presence of TNF-a.	103

45	Figure 7.10. Confocal imaging of 3D endothelial cells culture in micro-chip treated with different conditions, A) Non treated, B) Lipofectamine + scrambled siRNA, C) Lipofectamine + siRNA, D) L-DMAPAP-siRNA and E) HLP-DMAPAP-siRNA in the absence of TNF-a.	105
46	Figure 7.11. Confocal imaging of 3D endothelial cells culture in micro-chip treated with different conditions, A) Non treated, B) Lipofectamine + scrambled siRNA, C) Lipofectamine + siRNA, D) CL-PEI-siRNA and E) HLP-PEI-siRNA in the absence of TNF-a.	106
47	Figure 8.1. The diagram projects the slope of nanomedicine journey.	109

List of Tables

1	Table 2.1: Examples of thermo-sensitive nanogels with their drug component, release percent, temperature and time of experiment.	15
2	Table 2.2: Examples of pH-sensitive nanogels with their drug component, release percent, pH and time of experiment.	17
3	Table 2.3: Examples of redox responsive nanogels with their drug component, release percent, reducing agent and time of experiment.	20
4	Table 2.4: Examples of photo-sensitive nanogels with their drug component, release percent, irradiation and time of experiment.	23
5	Table 2.5: Examples of enzyme sensitive nanogels with their drug component, release percent, enzyme and time of experiment.	25
6	Table 5.1. DLS measurements of Liposomes produced with thin film and ethanolic injection method n=3.	55
7	Table 5.2. Re numbers obtained by T-1 and T-2 tube system obtained with different flow rate.	57
	Table 5.3. Volumetric mass of different formulations as function of the ethanol/water ratio at 25 °C.	60
8	Table 5.4. Volumetric mass of different formulations after ethamol/water evaporation upto 25-35 + MilliQ water at 25 and 37°C.	61
9	Table 5.5. DLS results of size and PDI for CL, HLP_{out} and HLP.	62
10	Table 5.6. Experimental and variation in temperature of micellization.	66
11	Table 5.7. Table represents the onset temperature and the enthalpy data of free water, loosely- and tightly-bound freezable water peaks.	70
12	Table 6.1. Factors and levels for the experimental design	77
13	Table 6.2. Encapsulation efficiency percent (EE%), loading capacity (LC%) and particle size (PS) values for nine prepared formulations with different concentration of P407 and Rhodamine.	78
15	Table 6.3. IC50 ($mg.ml^{-1}$) values as function of Lipid and P407 on NIH/3T3 and BNL cells.	84

16	Table 7.1. List of the various formulation tested in our study with their components.	93
17	Table 7.1. DLS and NTA results for the different CL and HLP formulations described this table with or without charge containing siRNA. Size represents the mean hydrodynamic average diameter by intensity and the PDI the polydispersity index. The values and standard deviation are given for 9 values, triplicates measured 3 times each (n=3).	95
18	Table 7.3. RiboGreen assay for encapsulation efficiency and loading content siRNA encapsulated in CL and HLP (n=3).	96

Abbreviation

Ago2: Argonaute 2

C%: Concentration Percent

CL: Conventional Liposome

CRGO: Chitosan Modified Reduced

CQ4P: Combretastatin A 4 Phosphate

DLS: Dynamic Light Scattering

DMAPAP: (2-{3-[Bis-(3-amino-propyl)-amino]-propylamino}-*N*-ditetradecyl carbamoyl methyl-acetamide

DOPC: 1,2 Dioleooyl-sn-glycero-3-phosphocholine

DOX: Doxorubicin Hydrochloride

DS: Diclofenac Sodium

DSC: Differential Scanning Calorimetry

EGM 2: Endothelial Growth Medium 2

FDA: Food and Drug Authority

GFP: Green Fluorescent Protein

GL: Gelliposome

GSH: Glutathione

HLP: Hybrid Liposome/Poloxamer

HLP_{in}: Hybrid Liposome/Poloxamer Inside

HLP_{out}: Hybrid Liposome/Poloxamer Outside

IC50: Inhibition concentration 50

LSCT: Low Critical Solution Temperature

MASC: methacrylateed succinyl chitosan

MCG: Metothrexate Carbopol Gel

MCNG: Metothrexate Loaded Chitin Nanogel Grapheneoxide.

MWCO: Molecular Weight Cut- off

NIPAM: poly(N-isopropylacrylamide)

NIPAAm: poly(N-isopropylacrylamide)

NMR: Nuclear Magnetic Resonance

NP: Nanopore

NT: Non-Treated

NTA: Nanoparticle tracking analysis

P407: Poloxamer 407

PDI: Polydispersity

PEEK: Polyether Ether Ketone

PEG: Polyethylene Glycol

PEI: Polyethyleneimine

PEO: Polyethylene oxide

P-Gp: P-Glycoprotein

PPO: Polyethylene oxide

Rhod: Rhodamin B

TEM: Transmission Electron Microscopy

T_{fus}: Fusion Temperature

T_{mic}: Micellization Temperature

TNF-α: Tumor Necrosis Factor Alpha

TRPS: Tunable Resistive Pulse Sensing

siRNA: Short Interfering Ribonucleic Acid

SUV: Small Uni-lamellar Vesicles

VPTT: Volume Phase Transition Temperature

Thesis Outline

This thesis focused on the formulation of thicken core liposomes called hybrid liposomes containing a polymer interior core to encapsulate hydrophilic drugs with the help of automated microfluidic system. The thesis comprised of 8 chapters.

In chapter 1, a global introduction of the thesis project is presented, with the general description and pathways regarding nanomedicine and cancer.

Chapter 2 is a review that we have recently submitted to a special issue of International Journal of Pharmaceutics. It covers the various release mechanisms study on nanogels. We described the various release profiles described in the literature as a function of triggered/stimuli release.

The Chapter 3 is a short chapter describing the rationale of the project which highlights and explains the reason why we selected each component composition of our Hybrid Liposome/Poloxamer (HLP) formulation such as Lipid, poloxamer, Rhodamine, Doxorubicin and also the mechanism of the drugs which were encapsulated in our hybrid liposomes, Doxorubicin and siRNA.

Chapter 4 to 7 highlights the data obtained during the practical work performed.

First, I developed a novel method of quantification for poloxamers which is explained in chapter 4. This is the first effective method performed at sub-ambient temperature by DSC to quantify poloxamer.

Chapters 5, 6 and 7 cover the data about the hybrid liposome polymer (HLP) formulation preparation, characterization, stability and kinetics and *in vitro* studies. Chapter 5 introduces the optimization of our homemade design tubing system for preparing HLP formulation and optimization of formulation to determine which method and composition is optimal for our formulation. The Chapter 6 provides the loading/encapsulation efficiency, cytotoxicity test and stability test of the optimal formulation prepared in the previous chapter while encapsulating doxorubicin or rhodamine as model drugs. Chapter 7 explains the thesis work performed in Canada for one and a half month mobility at the University of McGill, Biomat'X la. The encapsulation of anti-GFP siRNA was done in our HLP formulation with or without cationic charges and tested to verify their efficiency against GFP expressing endothelial cells grown in cells or in a 3D chip.

Finally, the Chapter 8 discusses the relevance of our work within the nanomedicine context and highlights the major contributions of this work. It also gives future perspectives to move the

HLP formulation towards *in vivo* studies and to understand technical advancement of homemade microfluidic tubing system to prepare wide range of liposomes.

The annex: some of the data of chapters 5 and 6 were described in an article accepted by International Journal of Pharmaceutics in May 2019.

Chapter 1: Introduction

1.1. Cancer

Cancer is a problematic healthcare condition where cells grow and proliferate uncontrollably (Nussbaumer et al., 2011). Cancer cells alteration is space-time dependent which lead to malignant neoplasm. Cancer is the second biggest cause of death in the world (Hassanpour and Dehghani, 2017). Since 2018, according to WHO, cancer caused more than 10 million deaths worldwide which is expected to rise up to or more than 20 million death rate by 2035 (Li et al., 2017). Cancer usually present four stages divided according to the severity which depends on the cell proliferation and spreading. Cancer can be gender specific, age specific or general in both sexes and for all ages. As in case of gender specific cancer are the prostate for men, breast cancer and uterine cancer for women. The age specific cancer includes blood cancer and brain cancer are mostly in children, whereas lung bronchus and colon are general in all cases. Each type of cancer has its own pathway and nature which makes it hard to understand and render the conception of therapy complicated.

The treatment of cancer includes surgery, radiations, chemicals (drugs) and more recently immunotherapy. Cancer surgery is simply the removal of the affected area, whereas radiotherapy focused on the radiation of x-rays and γ-rays. Radiotherapy often causes skin problems, adverse effects and non-specific targeting to the normal tissues. Chemotherapy is still the backbone for cancer treatment. There is a long list of drugs for cancer treatment and their selectivity depends on the suitability against specific cancer, but the core issue is their toxicity and multi drug resistance. The cancer treatments are meant to harms mutant cells but unfortunately the normal cells are also getting affected. To avoid this unwanted effect of drugs on normal cells, scientists are working for several decades to design a safe and secure drug delivery system that can reach to the targeted site easily. Several drugs used as an anti-cancer therapy according to their mechanism of action, these includes antibodies, siRNA, antimetabolites, DNA interacting agents and others (Sikes, 2007). Most of the anticancer studies are based on DNA interacting agents and RNA interference (Gurova, 2009; Oh and Park, 2009). There are thousands of new cases and deaths due to cancer each year, which is big thing to worry, on the other hand the treatment of cancer is also painful and difficult as in many cases patients die during the treatment. The cancer taken at initial stages respond to chemotherapeutic drugs better but in metastatic phase of cancer, 90% of the chemotherapeutic treatments fails, which is due to overpopulation of malignant cells and increase of the internal fluid pressure which impeach the drugs to reach the tumor and induce new or adaptive drug resistance

(Dreaden et al., 2014). Multi-drug resistance is mostly facilitated by MDR1 P-glycoprotein (P-Gp). Many different approaches were applied to reverse the MDR but is challenging to minimize the chemotherapy hindrance. The recent discovery of immune checkpoints inhibitors represents a turning point in the field to overcome MDR leading to the Nobel Prize of Asuku Honjo and James Allison in 2018. Antibodies directed against these targets made impressive effects in what is called immunotherapy with the first cases of treated patients having melanoma (ref antiPD1). The blockade of these immune checkpoints is being applied now on all possible cancer to evaluate the efficacy of this treatment which is far better tolerated than chemotherapy. In the US, it was reported that about 45% of the US citizen were eligible for cancer checkpoint inhibitor treatment in 2018 (Haslam and Prasad, 2019). However, there are still limitations as the percentage of the patients estimated to respond the treatment was 12.5% in 2018 and 85-90% of the patients declare autoimmune side effects (Heinzerling et al., 2019).

As regard to the population, which is not eligible to these new treatments, another possible means to overcome cancer resistance is the use of drug delivery systems. For scientists, the emergence of nanotechnology is becoming one of the major field of interest in term of overcoming multi drug resistance (Niazi et al., 2016). Several carriers were designed for cancer drug delivery such as, dendritic nanocarriers, liposomes, micelles and polymers.

1.2. Nanomedicines

The concept of nanotechnology was described by Richard Feynman in late 1950's. His work inspired many scientists including Norio Taniguchi who coined the term 'Nanotechnology' in 1974. Literal meaning of the word Nano is dwarf-sized which is derived from the Greek word nanus, meaning which cannot be seen by human eye. Nanotechnology opened a whole new era of science which provided a latest platform for nanoscience and nanoengineering. The nanotechnology field grew rapidly as people from different fields found it of interest and pursued to exploit this new concept in their respective fields such as engineering, chemistry, biology, medicine and others.

Nanomedicine is the term for designing the application of the nanotechnologies for health, for the prevention, treatment and diagnosis (Boulaiz et al., 2011). It is an emerging field of nanotechnnology which leads to the transition of conventional medicines to smart medicine. Nanomedicine exploits the properties of nanosystems by modifying and engineering them up to the cellular level for patient care and diagnostic purposes. The space of development, modification and improvement in the nanomedicine field is still high in order to help in cancer

treatment, targeted drug delivery, diagnosis and imaging (Shi et al., 2017). Nanomedicine deals with the materials at the nanometer scale, such as nanoparticles, nanorobots, and others (Fang and Zhang, 2010; Yang et al., 2019).

Since last 3 decades' drug delivery systems are the most reported nanomedicines with thousands of articles published and more than 100 clinical trials reported, but still there are some limitations which need to be solved (Alhareth et al., 2017). Variety of nanocarriers such as liposomes, lipoplexes, polyplexes, lipid nanoparticles, nanoemulsions, nanogels, hybrid nanoparticles and others are described in the literature (Ahmed et al., 2019; Bencherif et al., 2009; Bozzuto and Molinari, 2015; Mignet et al., 2008; Zhang et al., 2013). These nanocarriers gained a real interest among scientists as they have the advantage to protect the drug from degradation, to improve the delivery at the targeted site, and may help the passage of certain barriers.

Moreover, nanomedicine offers the advantage over conventional medicines to be able to enter the cells or cancer site, thanks to their small nanometer size (Shubhika, 2013). Nanomedicine in cancer can overcomes the P-Gp mediated drug resistance by preventing multi drug resistance pathway. Nanomedicine can extend drug circulation and reduce their toxicity. These advantages make nanomedicine valuable in comparison to conventional medicine as shown for micelles, polymers and many other carriers encapsulating drugs (Niazi et al., 2016; Tran et al., 2017). Particularly in the case of oncology treatments some nanomedicines underwent clinical trials. These nanomedicines include nanoparticles which can be lipid based, virus based, polymer based, inorganic, or drug conjugates according to their application. The versatile nature of nanomedicine in terms of their physico-chemical characteristics such as size, morphology and surface properties allow customizing them according to the nature of the disease (Bregoli et al., 2016), Figure 1.1. Nanomedicine can be designed as carriers for poorly soluble drugs, degradable drugs, and drugs with a fast clearance. Indeed, nanocarriers can enhance the stability of hydrophilic or hydrophobic drugs by encapsulation or entrapment, and work as a multi-drug compartment to provide advances in cancer treatment (Wicki et al., 2015). However, despite more than 10000 scientific reports on nanomedicines for cancer, there are only about 50 nanomedicine approved by the FDA, out of which 6 are for cancer indication. The number of

approved nanomedicines is low because of their size range from 1 to 100 nm, which is defined as the criteria for medicines to be considered as nanomedicine (Seleci et al., 2016).

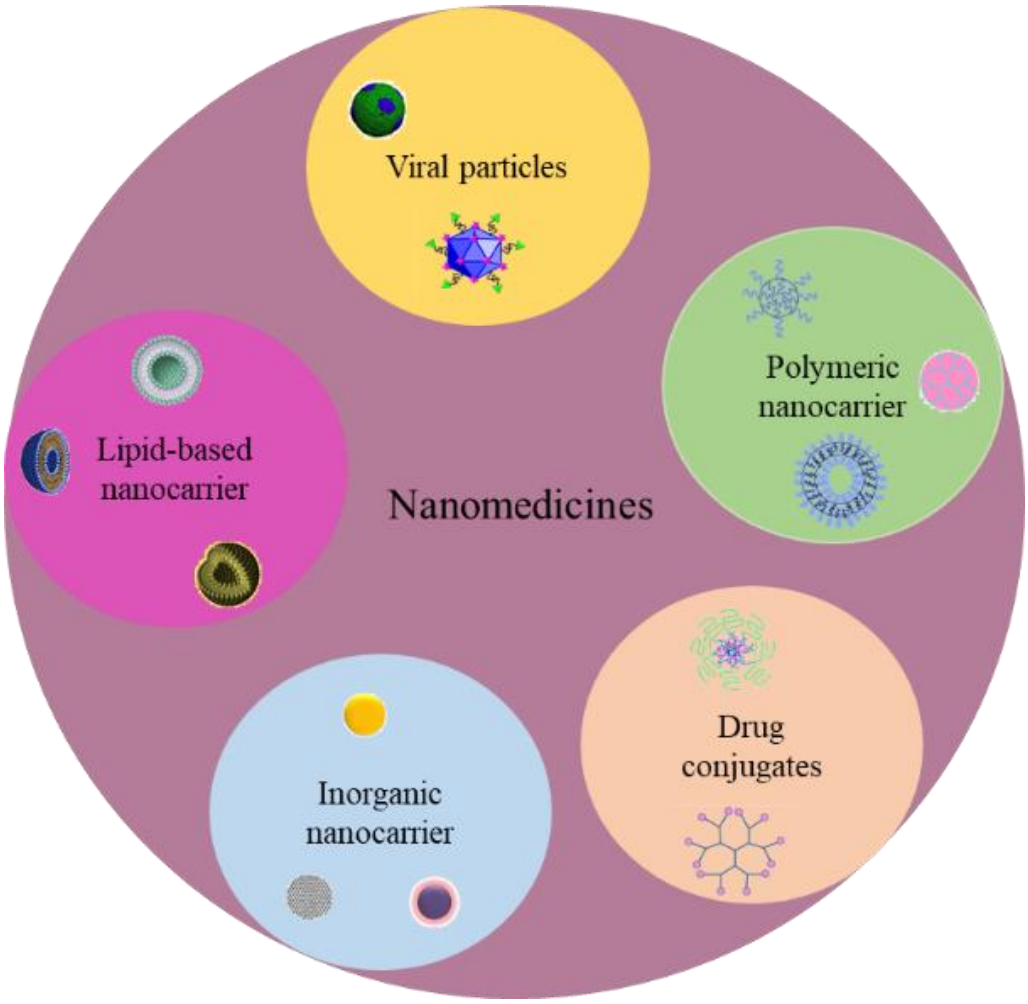

Figure 1.1. Multifunctional nanoparticles structures which makes nanomedicines versatile.

Among all the nanomedicine carriers described for cancer treatment, liposome is the most successful and studied nanocarrier for drugs. The first nanocarrier approved by the FDA for the anticancer drug doxorubicin was a liposome, and the same is true for the first nanocarrier accepted for siRNA delivery. This is why, we focused on the interests and limits of these auto assembled carriers. Liposomes were first described in 1961 (Bangham et al., 1965). These lipid vesicles are composed of natural or synthetic phospholipids. They form vesicles with an aqueous core, which can be used as a drug delivery system for hydrophilic and hydrophobic drugs. Hydrophilic drugs are encapsulated in the aqueous core of liposome, whereas hydrophobic drug entraps in lipid bilayer. The advantage of liposomes, is that due to their phospholipidic composition, they are less prone to induce an immune response (Hughes et al., 2010). The PEG coating increases the stability and reduces the interactions with circulating

proteins leading to an increased circulation time of the encapsulated drug (Milla et al., 2012). Addition of cholesterol within the membrane can also contribute to an increased stability. For nucleic acid delivery, liposomes have been modified and are usually composed of positively charged lipids. Electrostatic attraction between nitrogen of liposomes and phosphates of the nucleic acid leads to the formation of complexes called lipoplexes. The overall positive charge of the lipoplexes promotes the internalization of the nucleic acids within the cells (Tranchant et al., 2004).

Despite these reports and achievement to the clinic, liposomes still exhibit some limits in terms of small hydrophilic drug delivery for instance, which are released too fast to benefit from this carrier. Moreover, the incorporation of cationic lipids for nucleic acid delivery also represents a limit as these charges introduce toxicity and fast elimination of the lipoplexes. This is why we were interested in non-cationic carriers made of natural phospholipid for their safety, but with a thickened core to provide a higher stability in terms of drug release. Nanogels with an external lipidic bilayer might be of high interest to answer these limitations, which is why, we first made a literature survey on nanogels, which is the topic of chapter 2.

Chapter 2: Advancement in Nanogel Formulations Provides Controlled Drug Release. Review of the Literature

2.1. Introduction

Hydrogels are tri-dimensional network of cross-linked hydrophilic polymers; they swell and expand by absorbing important amount of water or biological fluids without losing their structure. Hydrogel are largely used for biomedical applications, especially for tissue engineering scaffolds (Peppas et al., 2000). Moreover, their ability to retain and release a therapeutic molecule is exploited for several applications in pharmaceutical sciences. Controlling their swelling ratio is a crucial step in order to develop hydrogel based pharmaceutical dosage forms with controlled release properties (Bettini et al., 1994; Lin et al., 2014; Rizwan et al., 2017).

Hydrogels are usually classified according to the nature of the polymer crosslinking; i) reversible physical hydrogels which are formed via physical processes of entanglements. Physical crosslinks are feeble interactions within gel networks like van der Waals, electrostatic interactions or hydrogen bonding (Eckmann et al., 2014), ii) permanent chemical hydrogels in which crosslinking is formed by covalent bonds between different functional groups present on the polymer chains, iii) dual-network hydrogel which formed by the combination of physical and chemical processes (Ullah et al., 2015). In addition, crosslinking may take place during the preparation of hydrogel or after the application at a precise location of the human body (in situ), thanks to specific physiological conditions such as temperature (Yu and Ding, 2008a). Advances in polymer chemistry leads to the development of smart hydrogels which have swelling properties dependent on external stimuli. Smart hydrogels may change their dimension or/and structure according to different environmental conditions. Innovative design of smart hydrogels have been realized for specific purposes, including wound dressings, tissue repair and pharmaceutical formulations with controlled drug release delivery (Ferreira et al., 2018; Li and Su, 2018; Sood et al., 2016). Hydrogels containing nanoparticles, liposomes, nanocrystals or nanoparticles, are also described in the literature, these promising formulations offers more stability and sustained release of encapsulated drug (Gao et al., 2014; Grijalvo et al., 2016; Lin et al., 2014; Shimoda et al., 2012).

Hydrogels are macroscopic networks which can be designed as micro or nano sized colloidal particles, called microgel or nanogel depending on their size as shown in Figure 2.1. These colloidal particles present a promising approach for the development of drug delivery systems

offering controlled drug release. Micro and nanogel combine the properties of hydrogel and micro/nanoparticles. They are characterized in terms of cross-link density and swelling ratio, like macroscopic hydrogel, and also in terms of mean average size, size distribution and colloidal stability, like micro/nanoparticles (Pelton, 2000).

The transition of hydrogel to nanogel was the major breakthrough in the drug delivery field. This opens the possibility of gel interaction at cellular level and can be injected intravenously. Nanogels formation improved the stability and stimuli responsive characteristics, while restricting the swelling ability (Vashist et al., 2017).

The term 'Nanogel' was first proposed by Vingradov and co in 1999 to describe a new drug carrier designed for the delivery of anti-sense oligonucleotides, it was made of cross-linked networks of water–soluble nonionic polymer (PEG) and cationic polymer, polyethyleneimine (PEI) (Vinogradov et al., 1999). The term nanogel was then used to describe particles sized between 10 and 200 nm, composed of crosslinked polymers and possessed the property of swelling in an aqueous environment.

Nanogels can be formed with various structures such as core shell nanoparticles, hollow nanogels, double walled and yolk shell structure (Liu et al., 2015; Sahu et al., 2017a; Shoueir et al., 2017; Xing et al., 2011). Nanogels can be prepared by using different cross-linking methods such as ionic cross-linking, crystallization, cross-linking polymerization, radiation cross-linking and functional group cross-linking (Yallapu et al., 2011). A wide variety of natural and synthetic polymer can be used to formulate nanogels. Their composition can be tuned to ensure the biocompatibility and the biodegradability of nanogels (Kabanov and Vinogradov, 2009; Sharma et al., 2016).

The size is the main advantage of nanogels comparing to bulk hydrogel. The nano size of allows nanogels to penetrate where larger hydrogels are restricted. Nanogels present a high potential as advanced drug delivery systems, thanks to their multifunctionality and stability in biological fluids (Soni et al., 2016). In addition, nanogels have present a high drug loading capacity due to their swelling capacity. Small therapeutic molecules, biological molecules and even nanoparticles can be loaded into nanogels. Like for any other nanoparticles, loading can be achieved by i) physical entrapment, through electrostatic, van der Waals and/or hydrophobic interactions or, ii) covalent attachment or iii) controlled self-assembly (Kabanov and Vinogradov, 2009; Soni et al., 2016). Moreover, the capacity of nanogels to incorporate a high amount of drug is accompanied with sustained release of entrapped molecules. A customized

design could offer triggered drug release ability which could be controlled by several stimuli like temperature, pH, ion-exchange, light and others (Zha et al., 2011).

This review is focusing on the potential of nanosized hydrogel in controlling the release of entrapped therapeutic molecules. We discuss first the mechanisms of drug release from nanogels, then summarize and comment the release profiles provided by different examples of nanogels reported in the literatures.

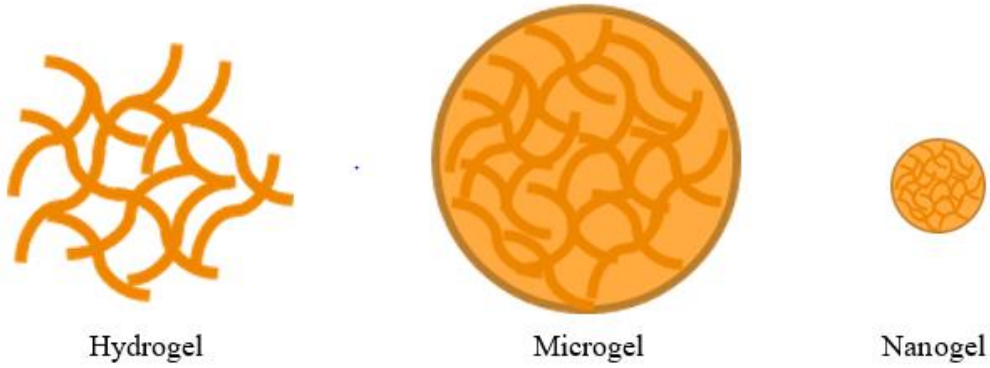

Figure 2.1. Schematic representation of the network construction of hydrogels, microgels and nanogels

2.2. Drug Release Mechanism for Nanogels

Drug delivery systems, aiming to enhance the drug concentration at the pathological site, are usually designed to carry drug and to provide a controlled release. To achieve an optimal therapeutic effect, factors affecting the drug release should be considered during the design stages. These factors are related to i) drug-material interactions which are determined by several features including hydrophilicity/hydrophobicity of drug and carrier, ii) biodegradability mechanisms and clearance time of the carrier (Felice et al., 2014). Regulate the rate of both drug release profile and biodegradation along with stability in circulation is rather challenging. In addition, a burst release phenomenon, which is an initial large bolus release of drug after the administration of the drug delivery system, or its placement in release medium, is observed for many drug delivery systems (Felice et al., 2014; Huang and Brazel, 2001). The nanogel have the tendency to release the drug quickly in the form of burst release. This led to the loss of hydrophilic and hydrophobic drugs in the circulation just after the administration and small amount of drug remain intact with nanogel and reach to the target site (Soni and Yadav, 2016). To control the release of the drug, the combination of polymer or modified polymers should be

used that can help the drug to release slower in controlled manner from the nanogel. Three main release mechanisms are involved in the release of drug from hydrogels and their nanostructure form: i) Diffusion, in which the drug release is governed by Fick's law. The polymer chain retard the solute release by reducing the average free volume available to the solute, by increasing the hydrodynamic drug experienced by the solute, and by acting as physical obstructions (Amsden, 1998). ii) Physical triggers such as temperature, irradiation and others can also cause swelling or degradation of polymeric network to control the release, in which slow or faster drug diffusion takes place. The kinetics of release is controlled by the increase in releasing area produced by the triggering phenomenon (Bettini et al., 1994). iii) Chemically release mechanism, in which drug release is based on the degradation of polymeric chain inducing hydrolysis of gel network leaks to surface erosion (Lin and Metters, 2006).

Nanogels with responsive behavior and triggered drug release are reported in the literature and termed as Smart nanogels as shown in Figure 2.2. Chemical or physical triggers lead to a change in their swelling behavior or cause the degradation of polymeric network and structure which influence the drug release profile. The main physical triggers reported are temperature, pressure, electrical and magnetically fields, whereas chemical triggers are pH, ionic change, enzymes and chemical agents, that changes the polymer-solvent interactions (Luckanagul et al., 2018; Ullah et al., 2015; Zhu et al., 2019).

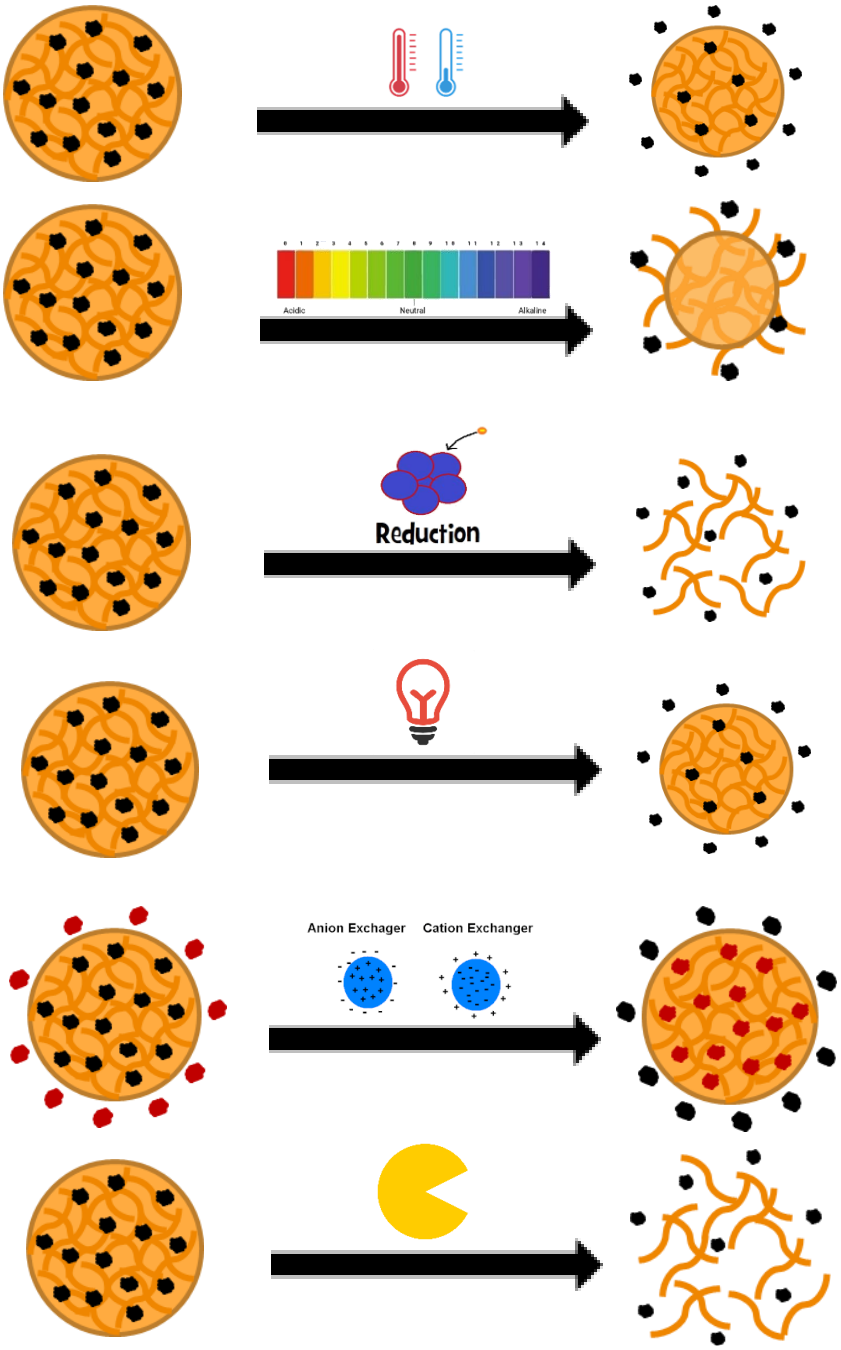

Figure 2.2. Drug release from nanogels, (a) Drug release can be induced by external energy (temperature) applied to nanogels that induces degradation, deswelling or structural transition of the nanogel polymer chains, (b) Change in pH results in deionization of polymer network and release of electrostatically bound drug, (c) Drug release due to degradation of reduction-sensitive polymer chains or cross-links, (d) Diffusion of the drug from nanogels due to the light irradiation, (e) Multivalent low-molecular cations or poly-ions of either charge can displace drugs having the same charge sign from electrostatic complexes with ionic nanogel, (f) Drug release due to degradation of enzyme-degradable polymer chains or cross-links.

2.3. Nanogels with Trigger Responsive Behavior

2.3.1. Thermo-Sensitive Triggered Release.

Temperature triggered hydrogels have the capability to swell and de-swell with temperature variation thanks to their composition based on thermosensitive polymers (Klouda and Mikos, 2008a). The temperature triggered hydrogels can be classified into two systems, positive responsive system and negative responsive system according to their low critical solution temperature (LCST), (i) Positive temperature hydrogels shrinks at temperature lower than LCST and swells at temperature higher than LCST, (ii) Negative temperature hydrogels shows swelling property at temperature lower than LCST and shrinks at temperature higher than LCST (Sood et al., 2016).

Several nanogels are reported as temperature responsive and most of them are composed of temperature sensitive polymer with additional material like lipids and silica etc. these nanogels swell or shrink with temperature variation and changes its volume, which is called volume phase transition temperature (VPTT), this variation on volume is usually exploited to enhance encapsulation and to control the release of drug (Bergueiro and Calderõn, 2015; Lu et al., 2011). Examples of temperature sensitive nanogels are summarized in Table 2.1. Poly(N-isopropylacrylamide) PNIPAM is used as thermosensitive polymer in several nanogel formulations. PNIPAM shrinks at temperature higher than LCST due to the exclusion of water from the vicinity of the PNIPAM chains, this property makes it a polymer of choice for designing controlled release gel-based formulation. Lu et al, in 2013, designed a microgel composed of PNIPAM and lipids (termed it as lipogel) and evaluated its temperature-triggered drug release behavior using calcein as drug model. The results showed the release of calcein up to 20% at 22°C in 8 hours, on the other hand at 37°C the release reached to 80% in 8 hours (Lu et al., 2013a). PNIPAM was also used in combination with acrylic acid (PNIPAM-co-AA) by Bardajee et al, in order to prepare nanogels based on salep (polysaccharide) modified graphene oxide. Nanogels were loaded with Doxorubicin (DOX) or Diclofenac sodium (DS) and results showed a faster release of both drugs at 42°C than 37°C. DS release was faster than DOX as DOX showed strong interaction with the polymeric chain of nanogel (Bardajee and Hooshyar, 2017). Later on, Bardajee and Hooshyar proposed another PNIPAM nanogel carrier for anti-cancer therapy based on PNIPAM grafted on sodium alginate modified graphene oxide nanogel. Doxorubicin loaded nanogel subjected to 37 °C and 42 °C buffer solution at pH 5.0 and showed 75% release at 42°C and 45% at 37 °C (Bardajee and Hooshyar, 2018). Lou et al prepared a dual sensitive nanogel, thermo- sensitive and redox-sensitive, composed of poly (2-

lactobionamidoethyl methacrylamide), poly (sulfobetaine methacrylate) and PNIPAM. In this study, the release rate of DOX was significantly enhanced in the presence of Glutathione (GSH). After 24h, release was 20% at 30°C without GSH, whereas around 50% at 40°C without GSH and 90% drug release at 40°C in the presence of GSH. The release was affected by temperature in the presence of redox condition as the PNIPAAM nanogel dissociation occurs in the presence of GSH (Lou et al., 2017).

Table 2.1: Examples of thermo-sensitive nanogels with their drug component, release percent, temperature and time of experiment.

Composition/ Carrier	Drug/Loaded component	Release %	Temp	Time	Reference
Poly(N-isopropylacrylamide) microgel	Calcein	20% 80%	22°C 37°C	8 h	(Lu et al., 2013a)
N-isopropylacrylamide graft-copolymerization onto salep modified graphene oxide	Doxorubicin + Graphene oxide	30, 50%	37,42 °C	8 h	(Bardaje e and Hooshy ar, 2017)
	Doxorubicin - Graphene oxide	45, 70%	37,42 °C	3 h	
	Diclofenac Na + Graphene oxide	60, 75%	37,42 °C	8 h	
	Diclofenac Na – Graphene oxide	90, 100%	37,42 °C	3 h	
Poly(N-isopropylacrylamide) grafted onto sodium alginate-modified graphene oxide	Doxorubicin	45% 75 %	37°C 42 °C	16 h	(Bardaje e and Hooshy ar, 2018)
Thermo-sensitive fibrinogen-graft-poly (N-isopropyl acrylamide) nanogels	5-FU/Megestrol acetate	45 % 70%	25°C 37 °C	72 h	(Rejinol d et al., 2014)

Poly (2-lactobionamidoethyl methacrylamide) poly (sulfobetaine methacrylate) poly(N-isopropylacrylamide)	Doxorubicin	90% + GSH 20% - GSH	40°C 30°C	24 h	(Lou et al., 2017)
Arginine–glycine–aspartic acid containing peptide and transferrin conjugated to poly (*N*-isopropylacrylamide-*co*-propyl acrylic acid) nanogel	Peptides	35% 80%	27 °C 37 °C	71 h	(Quan et al., 2009)
N-isopropylacrylamide and acrylicacid in the presence of β-cyclodextrin	Doxorubicin	82% 85% 90%	25°C 37°C 42 °C	10 h	(Yi et al., 2017)
PEG-Based ether- anhydride triblock copolymer	Doxorubicin	60% 80% 90%	25°C 37°C 45°C	48 h	(Zhao et al., 2010)

2.3.2. pH Sensitive Release.

The pH value varies in different tissues of human body including dysregulated cellular microenvironments, such as inflammation or cancer. Therefore, pH triggered release systems have a great potential to achieve a specific release of drugs at the pathological site. pH-sensitive nanogels are composed of crosslinked polyelectrolytes with weak acidic or basic groups or the combination of both (Zha et al., 2011). The ionization degree of the polyelectrolyte chain changes according to the variation of the environmental pH value, The deprotonation leads to a rise in osmotic pressure, swelling and porosity of the polymer which causes the release of electrostatically bound molecules (Tan et al., 2010).

The pH sensitive nanogels and theirs release profile are listed in Table 2. Zhang et al designed self-assembled crosslinked hyaluronic acid (HA) nanogels loaded with cisplatin and doxorubicin as a controlled drug delivery system for osteosarcoma. This nanogel was found to be stable at physiological pH, while it sizes and swelling properties were modified at pH 6.8 and 5.5. It swelled from 56 to 386 nm within 24h at pH 6.8 and dissociate. This destruction was even faster at pH 5.5, where the gel swelled from 57 nm to 473 nm in 12 h. Its drug release profile showed an increase in doxorubicin release with decrease of pH (Zhang et al., 2018).

Likewise, Yang et al in 2017 proposed pH-triggered chitosan nanogels via an ortho ester-based cross-linker for efficient drug- loading and chemotherapy. Methacrylated succinyl-chitosan was polymerized with ortho-ester diacrylamide to form chitosan nanogel with pH sensitive properties. The release of doxorubicin from nanogel was measured at various pH. At pH 7.4, 6.0 and 5.0 the doxorubicin release was 8.2%, 64.9% and 86.0%, respectively (Yang et al., 2017). Xue and his team proposed the sodium alginate nanogel for sustained drug release which is due to electrostatic interaction between drug and the sodium alginate. The *in vitro* release was carried out at pH 5.0 and 7.4 to comprehend the dissociation of Drug and nanogel due to disintegration of Ca^{2+}. The results showed the complete release of DOX at low pH in 60 hours and on the other hand at pH 7.4, the release was just 38% (Xue et al., 2015). Other examples of pH-sensitive nanogels are given in Table 2.2.

Table 2.2: Examples of pH-sensitive nanogels with their drug component, release percent, pH and time of experiment.

Composition/ Carrier	Drug/Loaded component	Release %	pH	Time	Reference
Cisplatin crosslinked hyaluronic acid (HA) nanogel	Doxorubicin + cisplatin	38.5% 60.1% 86.0%	7.4 , 6.8 5.5	72 h	(Zhang et al., 2018)
Methacrylated succinyl chitosan (MASCS) polymerized with ortho ester-based linkage	Doxorubicin	8.2% 64.9% 86.0%	7.4 6.0 5.0	168 h	(Yang et al., 2017)
Chitosan-based hydrogel conjugated with tetrakis(4-aminophenyl) porphyrin (NH_2-TPP) and 2,4,6-tris(p-formylphenoxy)-1,3,5-triazine	Porphyrin	22% 7% 1%	5 6.8 7.4	12 days	(Belali et al., 2018)

Egg yolk /polysaccharide nanogels	Curcumin	Uncross linked nanogel 75% Crosslinked nanogel 80%	2.4 7.5	2 h 6 h	(Zhou et al., 2018)
Sodium alginate pH responsive nanogel	Doxorubicin	100% 40%	5 7.4	6 h	(Xue et al., 2015)
Dextrin N,N'-methylene bisacrylamide	Doxorubicin	60% 35%	5.5 7.4	76 h	(Das et al., 2017)
Metotraxate Carbopol gel (MCG) Methotrexate Loaded Chitin Nanogel (MCNG)	Methotrexate	MCG 100% MCNG 92%	5.5 5.5	3 days 5 days	(Panonnummal and Sabitha, 2018)
Poly (PEGMEMA-*co*-FuMaMA-*co*-HEMA nanogels	Doxorubicin	17.6 5.8	5.4 7.4	30 days	(Chambre et al., 2018)
Aldehyde dextran nanogel	Doxorubicin	66% 28% 9%	2.0 5.0 7.4	72 h	(Su et al., 2018)
Hyaluronic acid nanogels	Doxorubicin	9.3% 88.4%	7.4 5.0	168 h	(Yang et al., 2017a)
Bleomycin-Chitosan	Bleomycin	50-55% 85% 85% 35%	4.0 5.0 6.0 7.0	96 h	(Sahu et al., 2017b)
Poly (vinyl alcohol) based nanogel	Paclitaxel	21.2% 90%	7.4 5.0	30 h	(W. Chen et al., 2017a)

Dendritic polyglycerols Nanogels	Doxorubicin	15% 60%	7.4 5.0	96 h	(Zhang et al., 2014)
Fish gelatin methacryloyl	Doxorubicin	11% 4%	4.5 7.4	72 h	(Kang et al., 2019)
Chitosan/Sodium triphosphate nanogel Magnetic nanoparticle / Chitosan / Sodium triphosphate nanogel	Doxorubicin	55 65 60 75	7.4 5.3 7.4 5.3	96 h	(Sadighian et al., 2017)

2.3.3. Redox-Responsive Release

Reports of redox responsive release systems are increasing due to the presence of redox-active stimuli in human tissues and cells. Glutathione (GSH) is the most reported stimulus for drug release and several GSH-responsive nano vehicles were developed for targeted intracellular drug delivery. GSH is present in abundance inside the intracellular fluid (about 2–10 mM) and extracellular fluid (about 2–20 μM) (Cheng et al., 2011).

In 2017 a bio-reducible cross-linked dextrin nanogels coated with Plerixafor designed by Zhang et al, a CXCR4 antagonist, for targeting metastatic breast cancer. The proposed nanogel was loaded with Doxorubicin and a redox responsive Dox release was expected, thanks to disulfide bonds of dextrin derivatives. The release profile indicated that in non-reducing conditions at pH 7.4 and 5.0, the release of Dox from the nanogel was similar and around 30%, however in reducing conditions in the presence of 10mm GSH at pH 5.0, Dox release from the nanogel reached 70% (Zhang et al., 2017). Another nanogel model for anti-tumor therapy was proposed by Huang and his team. The nanogel was composed of copolymer Methoxy poly(ethylene glycol)−poly(L-phenylalanine-co-L-cystine) and encapsulated Doxorubicin. The Dox release profile showed a responsive release under reducing environment at 10 mM GSH (Huang et al., 2015).

A new formulation of injectable hydrogel containing nanogel for combination therapy by local delivery of an anti-angiogenesis, combretastatin-A4 Phosphate (CA4P) and an anticancer, doxorubicin proposed by Jing Yang and his coworkers. Nanogel of poly (acrylic acid-co-4-vinylphenylboronic acid) was loaded with Dox and incorporated into hydrogel containing CA4P in order to release CA4P and DOX sequentially. DOX release profiles from the nanogel

showed a release of 24.7% without GSH and 64.1% with GSH at pH 7.4 in 84 h. The release of Dox was due to redox stimuli-responsive properties related to the presence of disulfide linkages on the polymer (Jing Yang et al., 2018). Another example of redox-responsive nanogel was described by Lee and his team. They designed thiol conjugated hyaluronic acid loaded with siRNA. The release profile confirms that in the presence of reducing agent, GSH, the –s-s- linkages cleaved and siRNA release was faster than without reducing agent (Lee et al., 2007). A list of nanogel formulation with redox responsive release are listed in Table 2.3.

Table 2.3: Examples of redox responsive nanogels with their drug component, release percent, reducing agent and time of experiment.

Composition/ Carrier	Drug/Loaded component	Release %	Reducing condition	Time	Reference
Di-thio-di-propionic acid in tri-polyphosphoric acid cross-linked poly(ethylenimine) nanogel. Nanogel ratio i) (2:1:0), ii) (2:1:0.05) and iii) (2:1:0.1)	Carboxylic fluorescein	i) 8.2, 8.1, 8.5, and 8.3% ii) 7.17, 49.6, 50.0, and 51.9% iii) 9.39, 41.1, 49.9, and 54.9%	Dithiothreitol 0 mM, 2 mM, 5 mM, 10 mM	24 h	(Guo and Kim, 2017)
Dox+ Dextrin nanogel coated with AMD3100	Doxorubicin	70% 29.2%	5.0 pH 10 mM GSH 5.0 and 7.4 pH 10µM GSH	24 h	(Zhang et al., 2017)
Methoxy poly (ethylene glycol) poly(*L*-phenylalanine-co-*L*-cystine) (mpeg−P(LP-co-LC)) nanogel	Doxorubicin	28.1% 74.7%	37 °C 0 mM GSH 10 mM GSH	72 h	(Huang et al., 2015)

Poly (acrylic acid-co-4-vinylphenylboronic acid) nanohydrogels	Combretastatin-A4 Phosphate and Doxorubicin	15.8% 22.9% 66% 83.9%	pH 6.5 - GSH pH 6.5 + GSH pH 7.4 - GSH pH 7.4 + GSH	14 days	(Jing Yang et al., 2018)
i) Poly (ethylene glycol)-b-poly(2-(hydroxyethyl) methacrylate-co-acryloyl carbonate) (PEG-P(HEMA-co-AC)) \nanogel ii) 1,4 butadiamine (non-reducing nanogel)	Protein	i) 96 % i) 30 % ii) 30 %	10 mM DTT 0 mM DTT 10 mM DTT	22 h	(W. Chen et al., 2013)
Thiol-conjugated \hyaluronic acid HA nanogel	siRNA	5.8% ≈17% ≈55% ≈70% 100%	GSH 0 mM 0.1 mM 1 mM 5 mM 10 mM	2 h 2 h 2 h 2 h 1 h	(Lee et al., 2007)
Cyclo(Arg-Gly-Asp) peptide (crgd) decorated disulfi de (SS) containing poly(vinyl alcohol) nanogels (crgd-SS-ngs)	Doxorubicin	≈20% 61% 65% ≈78%	GSH 0 mM, 7.4 pH 10 mM, 7.4 pH 0 mM, 5.5 pH 10 mM, 5.5pH+ 7.4pHafter 4 h	48 h	(W. Chen et al., 2017b)
Disulfide-cross-linked polypeptide nanogel with near-infrared fluorescence property	Doxorubicin	68% 88%	PBS GSH 10 mM	10 h	(Xing et al., 2012)

Poly(oligo(ethylene glycol) methacrylates-ss-acrylic acid) (P(oegmas-ss-AA)) nanogels	Doxorubicin	≈35% ≈25% ≈23% ≈32% ≈22% ≈20% ≈65% ≈62% ≈60% 	0 mM GSH pH 4.5 pH 6.5 pH 7.4 2 μM GSH pH 4.5 pH 6.5 pH 7.4 10 mM GSH pH 4.5 pH 6.5 pH 7.4	100 h	(H. Yang et al., 2015)
Disulfide cross-linked dextrin	siRNA	0% 70%	PBS +pH7.4 DTT + pH 7.4	12 h	(Li et al., 2018)
Fluorescent carbon nanogel	Paclitaxel	≈3% ≈37% ≈65% ≈100%	0 mM GSH 3 mM GSH 6 mM GSH 10 mM GSH	24 h	(Choi et al., 2019)

2.3.4. Photo-Sensitive Release

Light sensitive nanogels are composed of polymers bearing photoactive groups like azobenzene, spirobenzopyran or cinnamonyl. When these polymers are subjected to light exposure, their double bonds undergo a transition from trans to cis inducing a change in the shape and size of the nanogel (Alvarez-Lorenzo et al., 2009; Jiang et al., 2006). Another category of light sensitive nanogels is the hybrid nanogels which combines polymer and noble metals. In this case, metals converts light energy to heat which causes the transition in the polymer structure (Timko et al., 2010). Photo-sensitive nanogels have the ability of cis-trans isomerization, and upon exposure to specific radiations, nanogels can swell or shrink due to alteration in temperature, which trigger the release of drugs (Molina et al., 2015). For instance, azo-dextran nanogels encapsulating aspirin showed an improvement of aspirin release by light exposure, which can be explained by the fact that light exposure induced a photo-isomerization

of azobenzene, which led to faster release in case of Z-isomers than E-isomers. (Patnaik et al., 2007). A core-shell hybrid nanogel, made by coating the Ag-Au bimetallic NP core with a thermo-responsive nonlinear poly(ethylene glycol) based hydrogel have been reported in the literature by Wu et al. The nanogel showed faster release of Temozolomide when subjected to near infra-red light than without NIR light. This was explained by the fact that Ag-Au nanoparticles absorbs light and convert it to heat, causing the disruption of the polymer chain (Wu et al., 2010). Later on, a research team of Qin et al designed amphiphilic chitosan derivatives coated single-wall carbon nanotubes encapsulated in thermo/pH sensitive nanogel. This nanogel showed photosensitive properties as the release of Doxorubicin was 27% without NIR irradiation and up to 45% with irradiation at pH 7.4, at 25 °C (Qin et al., 2015). Examples of photo responsive release nanogels are listed in Table 2.4.

Table 2.4: Examples of photo-sensitive nanogels with their drug component, release percent, irradiation and time of experiment.

Composition/ Carrier	Drug/Loaded component	Release %	Irradiation	Time	Reference
Chitosan-modified graphene oxide (CRGO) Incorporated in NIPAM nanogel (DOX- CGN)	Doxorubicin	5 % - NIR 18.81% + NIR	3 min irradiation of in Near infra-red	3 h	(Wang et al., 2013)
Adamantine (AD)-conjugated copolymer, poly [poly (ethylene glycol) monomethyl ether metharcylate]-co-poly(N-(2-hydroxypropyl)-methacrylamide)-co-poly(N-adamantan-1-yl-2-methacrylamide) (PPEGMA-co-PHPMA-co-PADMA), and β-cyclodextrin (β-CD)-functionalized poly(amidoamine) Nanogel	Doxorubicin or Indocyanine green (ICG	20% - NIR 90% + NIR	3 min irradiation of in Near infra-red	16 h	(Zan et al., 2015)

Ag–Au@PEG–Hyaluronic hybrid nanogels	Temozolomide	PSG 1 50% PSG 2 58% PSG 3 75%	5 min irradiation of in Near infra-red	24 h	(Wu et al., 2010)
Azo-Dextran nanogel	Rhodamine, aspirin	---	UV irradiation	400	(Patnaik et al., 2007)
Chitosan coated carbon nanotubes encapsulated PNIPAAm	Doxorubicin	27% - NIR 45% + NIR	Near infra-red	48 h	(Qin et al., 2015)
Poly(NIPAM-Aam) nanogel	Curcumin	47% - NIR 70% + NIR	Near infra-red	92 h	(Wang et al., 2014)

2.3.5. Enzymatic Responsive Release

Enzyme sensitive nanogel systems are inspiring approach taking profit of the enzyme dependent process in the human body. Made with polymers sensitive to enzymatic hydrolysis, these nanogels changes physically and chemically upon exposure to enzymes. This approach is more sensitive and specific than the other approaches of triggered sensitive nanogel. The more common polymers are sensitive to proteases, lipases, phosphatases and endonucleases hydrolysis (Hu et al., 2012). Three years after Yang proposed a design for enzyme responsive nanogel loaded with Doxorubicin. Methacrylated Hyaluronic Acid was copolymerized with di (ethylene glycol) diacrylate to formulate an enzyme responsive nanogel. The release profile could be adjusted at various pH ,at 37 °C, in presence of various enzymes (Table 5) (C. Yang et al., 2015). A lipase responsive nanogel was developed by Xiong in 2012. The nanostructure composed of a triple layered nanogel (Polyethylene shell, poly(ε-caprolactone) fence and polyphosphoester core) showed a release of vancomycin dependent on the presence of pseudomonas lipase in the release medium (Xiong et al., 2012). Dual responsive alginate-keratin nanogel was proposed by Sun and co. The nanogel was designed to be redox and enzyme sensitive. The encapsulated doxorubicin showed the highest release (around 80%) in presence of GSH and trypsin (Sun et al., 2017). The detailed release profile of enzyme sensitive nanogels are listed in Table 2.5.

Table 2.5: Examples of enzyme sensitive nanogels with their drug component, release percent, enzyme and time of experiment.

Composition/ Carrier	Drug/Loaded component	Release %	Enzyme	Time	Reference
Methacrylated Hyaluronic acid nanogels	Doxorubicin	28% 60% 57% 63% 53% 64% 62% 74%	No enzyme pH 7.4 No enzyme pH 5.0 HAase pH 7.4 HAase pH 5.0 Lipase pH 7.4 Lipase pH 5.0 Multi-enzyme pH 7.4 Multi-enzyme pH 5.0	120 h	Yang et al 2015
Alginate-Keratin composite nanogel	Doxorubicin	11% 14% 27% 70% 80%	PBS 10 μM GSH 10 mM GSH 0.04mM Trypsin 10mM GSH+0.04mM Trypsin	48 h	Sun et al 2017
Lipase-sensitive polymeric triple-layered nanogel	Vancomycin	10 ± 1% ≈40% ≈70% 86 ± 3%	Without P. Lipase 0.5 mg/mL P.Lipase 1 mg/mL P.Lipase 1 mg/mL P. Lipase + ALP	48 h	Xiong et al 2012

2.4. Conclusion

Nanogels are one of the most promising drug delivery systems that could provide a controlled release of the entrapped drug. Several designs of nanogels with stimuli response property and triggered release were discussed in this review, results showed better control of the drug release when nanogel is designed as smart nanogel, drug release has occurred when the release medium containing the chemical trigger or when the physical trigger is applied. The reported design of smart nanogels showed great potential to deliver the drug specifically to the biological microenvironment where the release trigger is available, this scientific advance in the drug formulation should be the first step for developing and marketing new pharmaceutical dosage forms based on smart nanogels.

However, the drug release is often evaluated using experimental conditions that simplify the biological condition; phosphate buffer solution as release media which can slightly be modified according to the study objective by adding the chemical trigger or applying the physical trigger. Besides, the percentage of released drugs is dependent on the volume of release media, which is usually determined, based on the solubility of encapsulated drugs. A better understanding of drug release from nanogel, using mathematical modeling and more relevant *in vitro* models, may accelerate the exploitation of smart nanogels for clinical use.

Chapter 3. Rationale of the Project

3.1. Why Liposomes?

Liposomes are microscopic sphere-shaped sack of phospholipid molecules enclosing a water droplet, especially designed artificially to carry drug as shown in Figure 3.1. Many therapies have been upgraded with liposome formulations in terms of their stability, cellular uptake, release and biodistribution (Ding et al., 2006; Hua and Wu, 2013; Koning and Storm, 2003; Metselaar and Storm, 2005; Stenekes et al., 2000). The biocompatible and biodegradable nature with their exceptional capability to encapsulate the wide range of drugs as they encapsulate both, hydrophilic as well as hydrophobic drugs make them unique and versatile (L.-J. Chen et al., 2017, p.; Kube et al., 2017). Despite of increasingly potential application of liposomes as therapeutic tools, it is still being challenged by their physical and chemical instability, which may result in increased bilayer permeability , drug leakage, and fusion ability with each other (Guan et al., 2015). To reduce these problems a system with viscous core and lipid shell have been introduced in which both lipid and polymer unified to yield a notionally controlled and slow release drug delivery system (Mandal et al., 2013). The preparation of liposomes can be achieved by several different methods such as ethanolic injection, reverse-phase evaporation, freeze-drying and thin film hydration (Torchilin and Weissig, 2003). In this study, liposomes were prepared with the help of a push syringe device based on the principle of microfluidic and ethanolic injection methods.

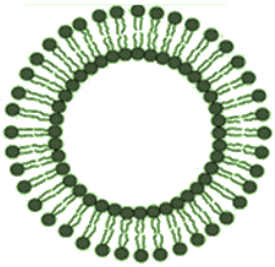

Figure 3.1. Diagram of liposomes

3.2. Why Thickened Core Liposomes

Liposomes and polymers for drug delivery have already been discussed in the literature, their potential as drug delivery systems is exploited in many applications. The liposomes safety, offered by their bio-inspired composition and design, which is an essential reason to give them more and more attention in order to develop new liposomes-based formulations by combining two strategies (Barenholz, 2012; Guan et al., 2015; Lu et al., 2013b; Mandal et al., 2013; Zhang

et al., 2013). However, an improvement in their design is required to increase their stability and the release profile of encapsulated drugs. In addition, a technical advancement of preparation methods is needed to improve reproducibility. Different hybrid liposome and polymer systems were presented in recent years, but this study is to transform them into reproducible and reliable with better encapsulation properties and characteristics.

3.3. Why Non-Ionic Lipid?

The DOPC (1,2 Dioleooyl-sn-glycero-3-phosphocholine) is a neutral lipid without any charges Figure 3.2. DOPC was used to prepare small unilamellar vesicles (SUV) which are non-ionic liposome formulation (Maheux et al., 2016). In literature the liposomal formulations are mostly cationic, but the highly cationic charge liposomes also cause cytotoxicity (Knudsen et al., 2015). DOPC and other non-ionic lipids are an ultimate solution for drug delivery without inducing any toxicity. The idea of keeping the formulation simple is to minimize the problem which arrive in the lot of complicated formulation in terms of their reproducibility, toxicity and structural changes due to physical or chemical interactions.

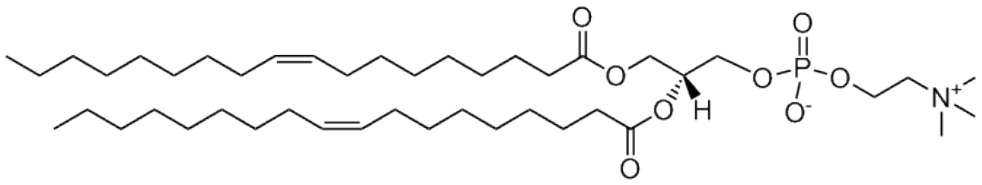

Figure 3.2. Structure of DOPC (1,2 Dioleooyl-sn-glycero-3-phosphocholine)

3.4. Why Non-Ionic Polymer?

Polymers are the widely used component in the field of nanomedicines. Their need is increasing day by day as it acquire variable nature, reversible properties and controllable characteristics (Banik and Brown, 2014). The negatively charged polymers activates the hypersensitive reactions (Szebeni et al., 2002; van den Hoven et al., 2013). Poloxamers have been introduced in the late 1950s and since then they have been suggested for various applications especially in pharmaceutical field. They are formed from copolymers arranged in triblocks of consisting of ethylene oxide (EO) and propylene oxide (PO) parts. X and y values can have modulated producing a collection of Poloxamer derivatives. In the case of Poloxamer 407 x and y are equal to 95-105 and 54-60, respectively as shown in Figure 3.3. Poloxamer P407, was selected as it is already approved by FDA and used in many formulations because of its absence of toxicity (Fakhari et al., 2017). Poloxamer 407 formulations led to improved solubilization of poorly

water-soluble drugs and extended release profile for many pharmaceutical applications for example, oral, rectal, topical, ophthalmic, nasal and injectable preparations (Dumortier et al., 2006). The poloxamer P407 is a thermosensitive polymer, characterized by a sol-gel transition temperature, since below this temperature, the systems remain as fluids and favor the development of injectable formulations, but remain as semisolids close to the physiological temperature (Klouda and Mikos, 2008b; Yu and Ding, 2008b). These properties will be more detailed in chapter 4.

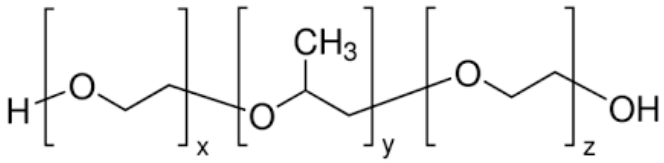

Figure 3.3. Structure of Poloxamer P407 (PEO-PPO-PEO)

3.5. Why Rhodamine B?

Rhodamine is a pink color fluorescent compound that has been used quite frequently in as adrug model for release studies in the pharmaceutical field and also in several other fields (Iyer and Eddington, 2019; Losic et al., 2012; Pepe et al., 2017; Reina et al., 2015; Zhang et al., 2011). Rhodamine is structurally [9-(2-carboxyphenyl)-6-diethylamino-3-xanthenylidene]-diethylammonium chloride as shown in Figure 3.4. It has excitation at 490 nm and emission at 580 nm which is easily detectable and quantified easily for the concentration. In our study we developed a drug modelling to understand the detailed nature of our formulation depending on the effect of polymer and model drug itself (Chapter 6).

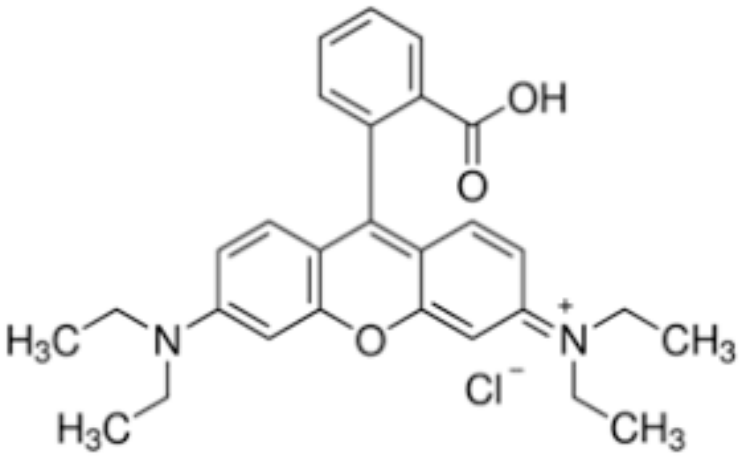

Figure 3.4. Structure of rhodamine B

3.6. Why Doxorubicin Hydrochloride?

The Doxorubicin is the most used anti-cancer drug in clinical and pre-clinical studies because of its efficacy against cancer especially solid tumors such as ovarian, breast and bladder cancer (Green and Rose, 2006; Rivankar, 2014). Doxorubicin was initially isolated form bacteria, Streptomyces peucetius which produce in the form of red pigments called daunorubicin (Arcamone et al., 1968). It was considered toxic since the study in 1967 raise the questions about its toxicity. The scientist changed this molecule by genetic alteration of this bacteria and produce a compound called Adriamycin which now called Doxorubicin (Arcamone et al., 1969). The structural IUPAC name of doxorubicin is (8S,10S)-10-(4-amino-5-hydroxy-6-methyl-tetrahydro-2H-pyran-2-yloxy)-6,8,11-trihydroxy-8-(2-hydroxyacetyl) -1-methoxy-7,8,9,10-tetrahydrotetracene-5,12-dione as shown in Figure 3.5. It is also used a lot in the research studies as it is red in color and can be detected with fluorescent spectrophotometer, it has excitation at 490 nm and emission at 595 nm.

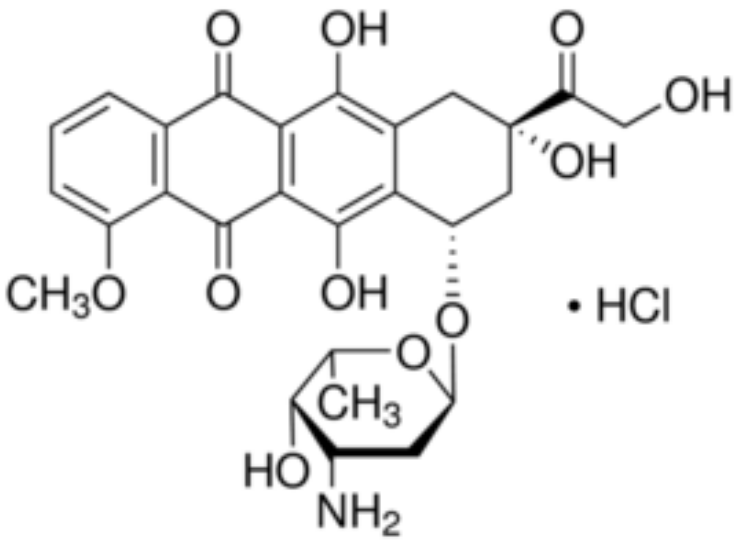

Figure 3.5. Structure of Doxorubicin HCL

In the huge list of anticancer drugs, doxorubicin is one of the most discussed nanomedicine. Doxorubicin is widely used as antineoplastic drug. It belongs to anthracycline family, which is mostly known as DNA interacting agent, that bind with DNA and cause potent destruction in cancer cells in solid tumour. Doxorubicin follows two mechanisms, first, DNA interaction and second, oxidative stress to cells, proteins and DNA as shown in Figure 3.6 (Tokarska-Schlattner et al., 2006). Despite of its potency and efficacy, doxorubicin alone was restricted in clinical trial as it produced serious complication and their dose dependent cardiotoxicity. The first approved nanomedicine approved by FDA in 1995 is 'Doxil' (Barenholz, 2012; Poljaková et al., 2008). Doxil is a pegylated liposomes encapsulating Doxorubicin, which help to decrease the toxicity of Doxorubicin and improved its pharmacokinetics (Xing et al., 2015). There are several other lipid based or polymer based nanoparticles with doxorubicin which shown success under clinical trials as they are easy to prepare and have better encapsulation efficiency with controlled release (Danson et al., 2004; Ferrari, 2005).

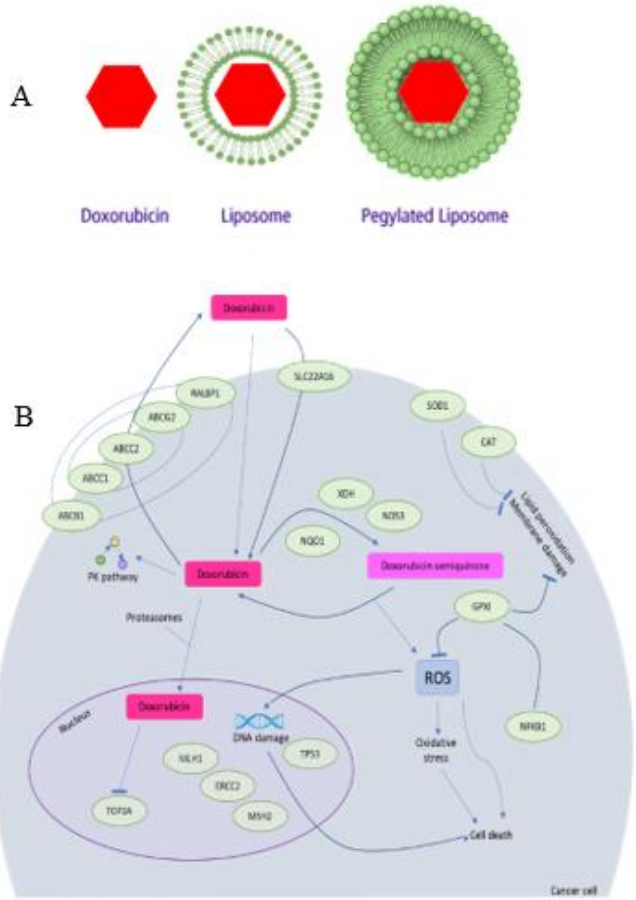

Figure 3.6. Picture of, A) Doxil structure and B) Doxorubicin pathway in cancer cell

3.7. Why siRNA?

Similarly, siRNA approach for gene silencing is considered as one of the most remarkable approach for cancer treatment (Fire et al., 1998, 1991; Mahmoodi Chalbatani et al., 2019). siRNA is short interfering or silencing RNA class of double stranded RNA with a size of 20 to 25 bp as shown in Figure 3.7. It has ability to silence a gene by interfering with gene expression by cleaving the mRNA after transcription which is responsible for the production of any specific protein which called post transcriptional silencing. It is a natural process which function as anti-viral activity.



Figure 3.7. Structure of siRNA

A carrier is required for siRNA based RNA interference therapy to cope with their negatively charged nature and non-specific targeting (Reischl and Zimmer, 2009). For both type of treatment, liposome is considered as the optimal carrier for their delivery, but the improvement is still required for lipid-based siRNA delivery system. RNA interference is a natural process and an effective strategy for gene silencing as shown in Figure 3.8.

As the RNAi machinery is being discovered in parts, the RNAi mechanism is getting clearer with the passage of time. In the last few years, significant understandings have been expanded in clarifying the RNAi mechanism. The first step consists in the initiating step, which involves binding of the RNA nucleases to dsRNA and its cleavage into discrete ≈21- to ≈25-nucleotide RNA fragments. In a second step, siRNAs join a multi-nuclease complex, called RISC, which degrades the homologous single-stranded mRNAs. The subsequent siRNA as a feature of a multiprotein RNA-inducing silencing complex is focused to the complementary RNA species which is then cleaved. Currently, little is known about the RNAi intermediates, RNA-protein complexes, and mechanisms of formation of different complexes during RNAi. In addition to various missing links in the process of RNAi, the molecular basis of its systemic spread is also largely unknown (Agrawal et al., 2003). Argonaute 2 (Ago2) is acknowledged by biochemical investigation as protein in RISC responsible for mRNA cleavage, and the crystal structure of RNA bound Ago2 has been reported, revealing key connection. Ago2 cleave the sense strand of siRNA duplex in the same manner as it cleaves mRNA substrates as shown in figure 3. By

means of chemical modifications we can alter the siRNA potency *in vitro*. siRNAs with highly stabilized uncleavable sense strands can be highly active (Bumcrot et al., 2006).

The viral vectors are very efficient in gene delivery, they are highly toxic but still most used for gene therapy (Hacein-Bey-Abina et al., 2010; Metzner and Dangerfield, 2011). On the other hand, synthetic non-viral vectors are much safer, but their ability of transfection is not efficient enough (Breton et al., 2011). The diligent efforts of researchers are trying to make non-viral vectors more efficient and to understand their limitations (Kostarelos and Miller, 2005). Several non-viral vectors are described in literature such as liposomes, polymer, nanocrystals, inorganic, micelles and proteins (Ventola, 2017). Most of them have cationic charges for better entrapment efficiency. The first liposome based siRNA therapy used for treating polyneuropathy of hereditary transthyretin-mediated (hATTR) was approved by FDA in 2018, named Patisiran (Alnylam pharmaceuticals) (Wahlich et al., 2019). This formulation is containing cationic charged pegylated liposomes of 100 nm in size encapsulating siRNA.

The idea to design thickened core liposomes was also to evaluate if these nanocarriers would possibly encapsulate siRNA with a limited amount of cationic charges. The addition of low amount of positive charges associated to the viscosity of the core could potentially improve the transport and release of siRNA from non-toxic nanocarriers. This will be the topic of chapter 7.

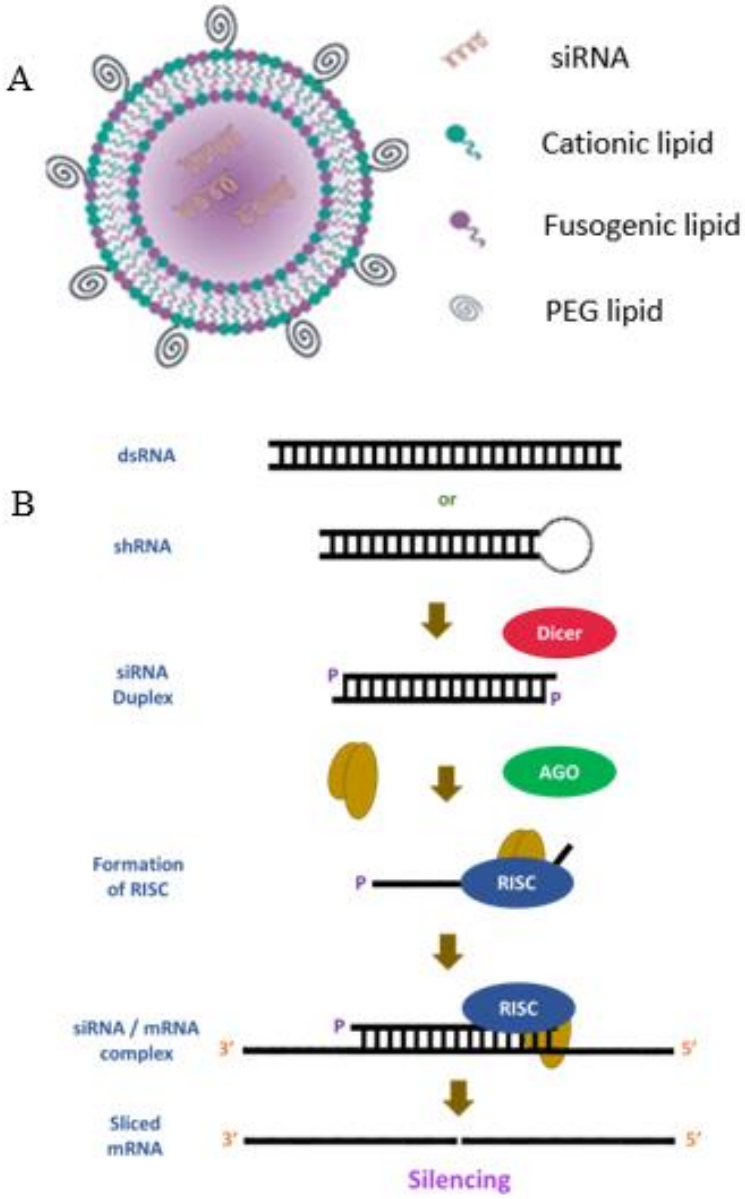

Figure 3.8. Diagram of, A) Patisiran (Pegylated liposome encapsulating siRNA) and B) siRNA pathway for gene silencing.

Chapter 4. Sub-ambient DSC Analytical Method Development for Quantitative Determination of Poloxamers solutions: application to the Characterization of Nano-formulations for Drug Delivery.

4.1. Introduction

Poloxamer is a thermosensitive polymer (Devi et al., 2013; Yapar and Ýnal, 2013). The poloxamer molecular weight as well as its polyoxypropylene/polyoxyethylene ratio have an impact on its physico-chemical properties, as well as in the *in vitro* and *in vivo* behavior of the polymeric carrier (J. Chen et al., 2013; Hemelryck et al., 2019). Commonly, due the sol/gel reversible behavior and micelles formation, poloxamer solution are useful for the drug encapsulation in the aqueous phase at room temperature, and then for targeting delivery and sustained release of the encapsulated drug in its gel phase. Indeed, thermo-sensibility of Poloxamer attracts notably pharmaceutical researchers to investigate more thermal responsive behavior regarding its applications as drug stabilization enhancer and drug carrier for optimized delivery. Poloxamer used as drug carriers can reduce the hepatic uptake of the active ingredient and, therefore can increase the time of half-life of the drug in the body (Mitchell et al., 2012). Moreover, poloxamer can be used to solubilize and stabilize drugs, nanocrystals for long period of time in terms of their size and to provide steric stabilization to lipid carriers (Bodratti and Alexandridis, 2018; Moghimi et al., 1991; Tuomela et al., 2016; Wu and Lee, 2009).

Thermal characteristics of poloxamer entities are often investigated close to their micellization and gelification points, thus at relatively high temperatures. Such transformations correspond to morphological organization change of the polymeric chains at the molecular level. The dehydration of PPO present in poloxamer, due to the increase in temperature, leads to a reversible process called micellization (Figure 4.1). The water bound with polymers have already been discussed in the literature. Three transitions have been described and classified as free, freezing and non-freezable water which highlights the difference in polymer composition and water holding ability (Bag and Valenzuela, 2017; Hatakeyama et al., 2010).

Therefore, lipid/polymer interactions might be also studied at lower temperatures. In the present study it has been demonstrated for the first time that P407/H_2O systems present two unreported signals (around -14 and -4 °C). This surprising result lays out a third parameter after micellization and gelification in terms of quantification, qualification and analyzing poloxamer

behavior in the case of single component systems on the one hand, and poloxamer/carriers or poloxamer/drug system on the other hand.

Recently, hydrations of polymers or lipids have been extensively studied using differential scanning calorimetry (DSC), nuclear magnetic resonance (NMR), and some other methods. (Yamauchi and Hasegawa, 1993) The results from all of these tools suggested that different types of water interacting with the amphiphilic molecule dispersed in the aqueous environment can be encountered. Taking into consideration the facts that polymer can be found in various pharmaceutical preparation thermal analysis may represent a non-destructive and sensitive analytical method development for quantitative determination of polymers such as poloxamers. In the present study, thermal analysis was used to establish a new method for determining poloxamer concentration in aqueous solutions.

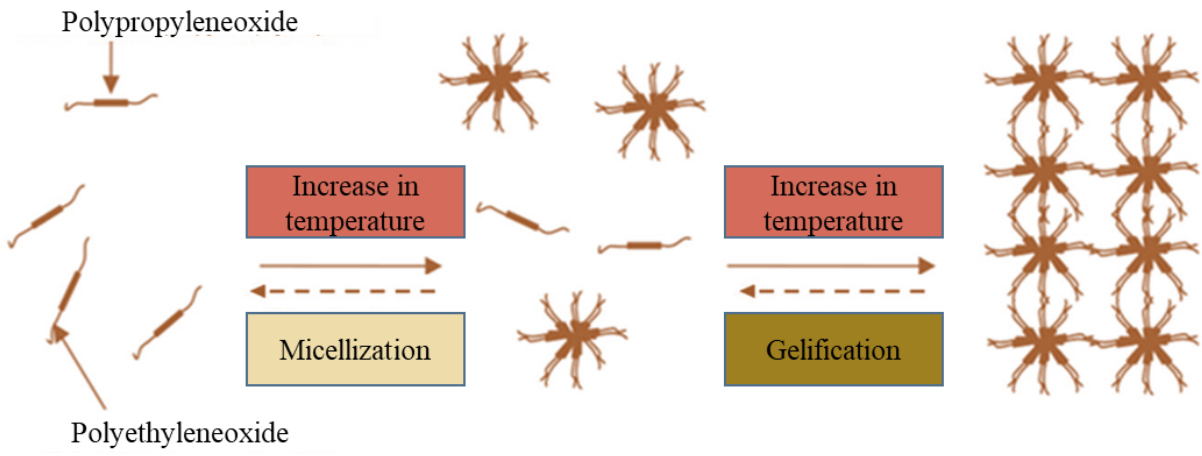

Figure 4.1. Graphical illustration of Micellization and gelification behavior of poloxamer in aqueous environment.

4.2. Materials

The poloxamers (P407) were supplied by BASF (BASF, Germany) under the trade name of Kolliphor®. Polypropylene oxide (PPO) was purchased from Sigma Aldrich with an average molecular weight of (1,000 g/mole). Commercial batches of P407 was provided by BASF, Germany. Milli-Q purified water was used to prepare the aqueous solutions and when water is required.

4.3. Material and Methods

4.3.1. Preparation of Polymeric Aqueous Solutions

Various concentrations of P407 aqueous solutions: "0.1, 0.5, 1, 5, 10, 15, 20" % w/v were prepared. The 20% w/v solution was prepared and used as the stock solution for preparation of the remaining concentrations by accurately weighing the corresponding amount of poloxamer and adding it to the right volume of Milli-Q purified water and magnetically stirring this mixture at 4°C for approximately 2 hours or until a homogenous solution is obtained. The same method was used to prepare aqueous solutions of 10% w/v of each of polypropylene glycol "PPO".
For thermal microscopy the poloxamer solution of 5% is prepared in the same way as discussed in above and 0.1 $mg.mL^{-1}$ of rhodamine dye.

4.3.2. Thermal Analysis

The Differential Scanning Calorimetry (DSC) experiments were performed on differential scanning calorimeter 822e (Mettler-Toledo, Switzerland) previously calibrated with high purity indium (T_{fus} = 156.6°C, $\Delta_{fus}H$ = 28.45 $J.g^{-1}$) and zinc (T_{fus} = 419.6°C, $\Delta_{fus}H$ = 107.5 $J.g^{-1}$). DSC experiments for high temperature were performed at temperature starting from 5 to 60 °C at 1 K.min-1 scan rate under dry air (60 mL.min-1). Thermal analysis for sub-ambient temperature was performed at temperature starting from -5 to -25°C and from -25 to 30 °C at the rate of 1 $K.min^{-1}$ under dry nitrogen gas. Empty aluminum pan of 100 µL was hermetically sealed and holed from the top by means of a small pin of controlled size (0.7 mm) and used as a reference. In order to understand the behavior of our formulation system upon heating and cooling, all experiments ran by taking 80 µL of samples in 100 µL of pan and hermetically sealed.

4.3.3. Density Analysis

The density was measured by using a Densimeter (Anton Paar DMA™ 4500 M). Experiments were performed at 25 and 37 °C. The U-tube was washed with Milli-Q water then with Ethanol 96% and dried with Air. The oscillating U-tube is filled with about 1.5 mL of sample with a plastic syringe. The U-View™ camera function shows and records live images of the oscillating U-tube to ensure that there are no bubbles and that the U-tube is entirely filled with the sample.

4.3.4. Thermal Microscopy

P407 5% with rhodamine transition were observed as function of the temperature by means of LTS 420 Linkam heating cell (Microvision Instruments, Evry, France) placed under a SMZ 168 microscope (Motic, Kowloon, Hong Kong). Temperature range from -50 to 30 °C at 2 °C.min^{-1}. Cooling of the system was achieved using a T95-HS Linkam device with liquid nitrogen automatically flowed through the cell. The pictures were taken each 0.2 °C with a Moticam 2500, 5.0M pixels, from Motic.

4.3.5. Calibration Curves

Normalized enthalpy ΔH (J.g^{-1}) and (J.C^{-1}.g^{-1}) for the low and high temp DSC, respectively, and the density values (g.cm^{-3}) at each investigated temperature were plotted versus the poloxamer concentrations.

4.4. Results and Discussion

4.4.1. Thermal Transitions at High Temperatures

The DSC translate this micellization behavior into transition peaks which depends on the concentration and temperature (Wanka et al., 1994). The diluted polymer P407 presents in the state of unimers at low temperatures but with the increase in concentration or temperature it turns to form aggregates of unimers and leads to micelles formation (Artzner et al., 2007; Aswal and Goyal, 2004; Mortensen and Pedersen, 1993). The transition peaks of micellization for different concentration of Poloxamer are presented in Figure 4.2. The results confirms that the size of the peaks is directly proportional to the concentration, whereas the shift of the peaks towards higher or lower temperature also depends on the concentration of the poloxamer (Alexandridis et al., 1994). DSC peaks shift in terms of temperature for micellization is inversely proportional to the concentration of the poloxamer. So peak shift to high temperature when concentration is low and peak shift towards low temperature when concentration is high, as micellization is concentration dependent and its thermos-responsive behavior for high concentration require low temperature form micelles and vice versa as shown in Figure 4.2. The peak area of micellization corresponds to the Polypropylene oxide chain size and can be translated into the concentration of poloxamer in any solution. By measuring temperature of micellization for several P407 aqueous solutions in the 1% to 20% range of concentrations, the relation between T_{mic} and P407 concentration ($C_{\%}$) allowed us to obtain a linear correlation that is fitting by the following equation, $T_{mic} = -0.53 \times C_{\%} + 26.0$ ($r^2 = 0.99999$) and relation between

heat flow and P407 concentration ($C_{\%}$) allowed us to obtain correlation that is fitting by the following equation, $H_{flow} = 0.02798 \times C_{\%}$ ($r^2 = 0.99786$) as shown in figure 4.3 A and B. But the restriction was its precision with low concentration of poloxamer detection as peaks are not enough sensitive to indicate the concentration of poloxamer less than 1% in the solution.

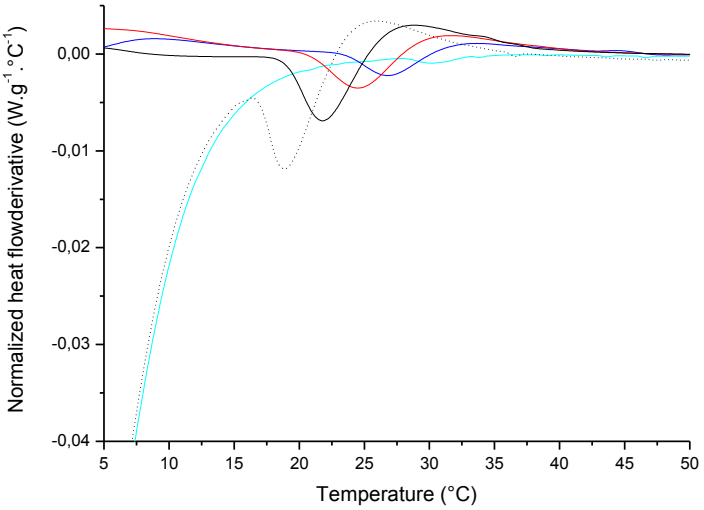

Figure 4.2. DSC curve of the P407 solution for the high temperature screening at function of polymer concentration: (–) 1%, (–) 5%, (–) 10%, (–) 15%, and (···) 20%.

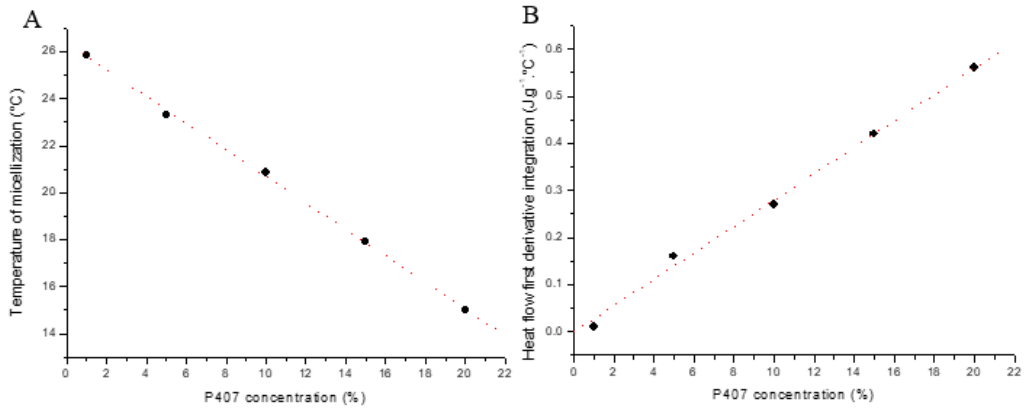

Figure 4.3. Calibration curves, A) Temperature micellization and B) Heat flow derivation integration for various P407 concentrations.

4.4.2. Densitometry Evaluation

Density of an organic molecule solution is proportional to the solute concentration. However, to our knowledge, it has not been clearly demonstrated for macromolecules. This is due to the poloxamer solution links to the concentration as they are directly proportional to each other.

This work has highlighted the dependence between density and concentration of poloxamer solutions. Indeed, different concentrations of poloxamer P407 solutions were verified by density analysis as shown in Figure 4.4 A and B. This gives us another way of quantifying the poloxamer which can be used as a complementary method for DSC at high temperature. By measuring density for several P407 aqueous solutions in the 1% to 20% range of concentrations, the relation between density (D) and P407 concentration ($C_{\%}$) at 25 and 37 °C allowed us to obtain a linear correlation that is fitting by the following equations, $D_{25} = 0.00104 \times C_{\%} + 26.0$ ($r^2 = 0.99797$) and $D_{37} = 0.00102 \times C_{\%}$ ($r^2 = 0.99218$) as shown in figure 4.4 A and B. These linear curve with different concentrations of poloxamer helped to determine the density of poloxamer in the different formulations which is presented and discussed in Chapter 5.

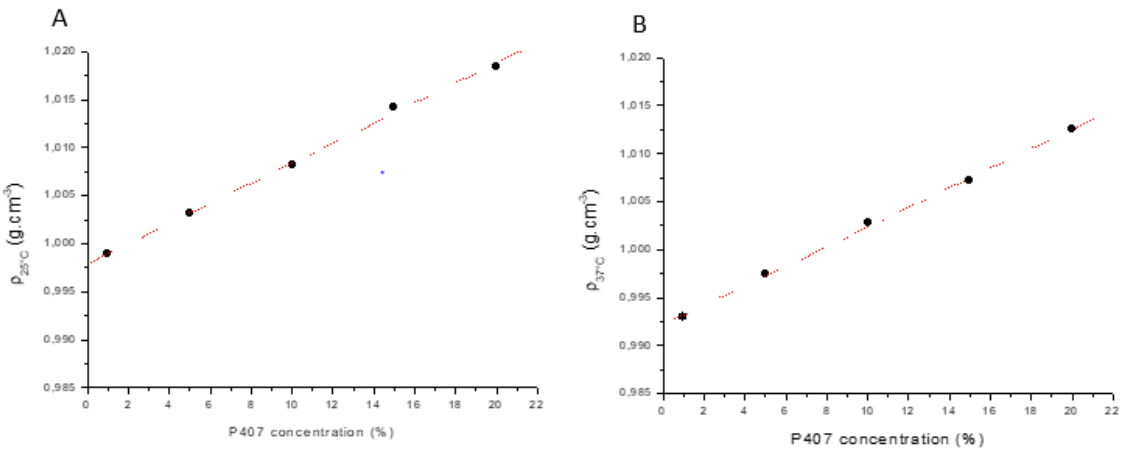

Figure 4.4. Density calibration curve of the P407 solution, A) 25 and B) 37 °C.

4.4.3. Thermal transitions at low temperatures

Numerous concentrations of P407 were analyzed at sub-ambient temperature range. Three water peaks were observed for concentrations starting from 0.1% w/v till the 20% w/v concentrations namely peak I, II and III from higher to lower temperature value on the thermogram as shown in Figure 4.5. By comparison with previous results obtained with PEG (*i.e.* PEO moieties) thermal analysis at the sub-ambient temperature range, one can assign peaks I to free water signal and peaks II/III to freezable water (Yamauchi and Hasegawa, 1993).

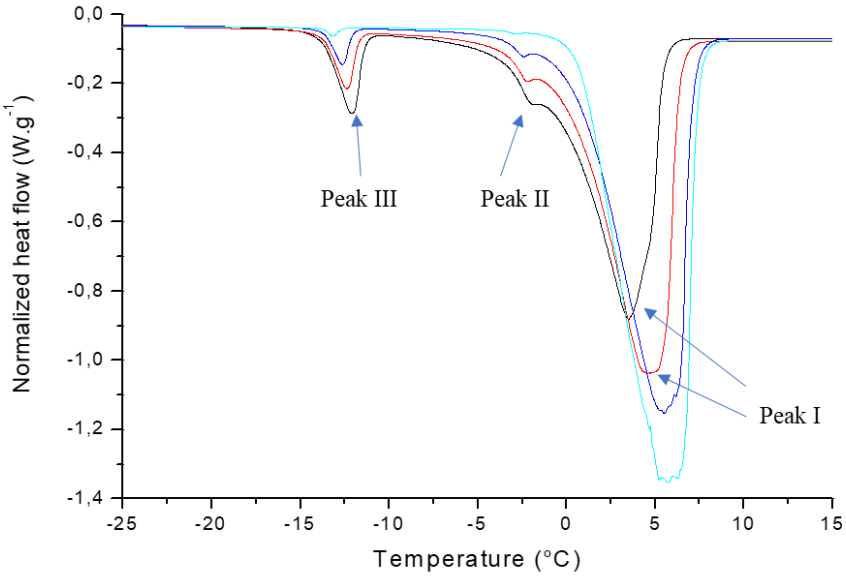

Figure 4.5. DSC curve of the P407 solution at the sub-ambient temperature screening at function of polymer concentration: (–) 0.1%, (–) 5%, (–) 10%, and (–) 15%.

In order to distinguish between peak II and III assignment, PPO solution was also analyzed by thermal analysis. Interestingly, a signal was obtained at -4 and 0 °C (Figure 4.6), proving that Peak II obtained for P407 solution is due the loosely-bound freezable water signal. As far as peak III is concerned, it corresponds to the tightly-bound freezable water signal due to PEO presence in the poloxamer, for signal of PEG (PEO) we attributed it as peak III which is described in literature (Huang and Nishinari, 2001; Yamauchi and Hasegawa, 1993). These results have been confirmed by thermal microscopy experiments by using rhodamine as dye as shown in Figure 4.7. Slight change of opacity of the system (two freezable water transitions at -15 and -4.4 **°C**) with the increase in temperature and melting of the system for the free water thermal transition at – 0.4 **°C** corresponds to the three peaks of DSC at sub-ambient temperature.

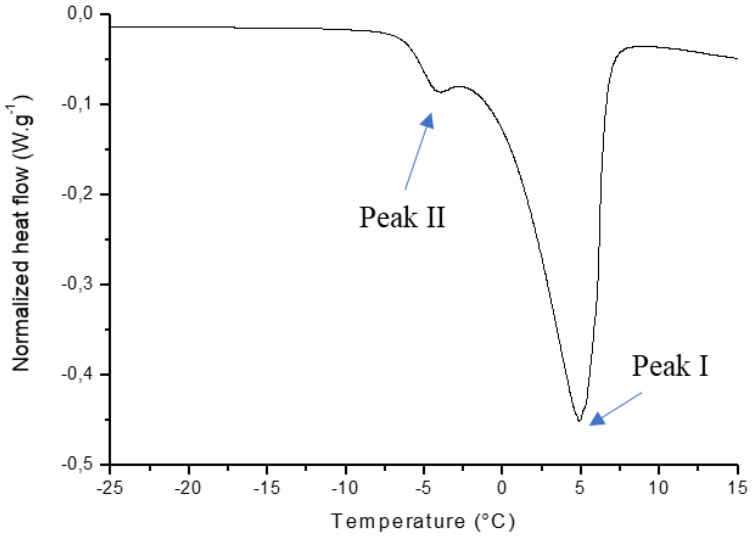

Figure 4.6. Weight normalized DSC curve of PPO solution (5%).

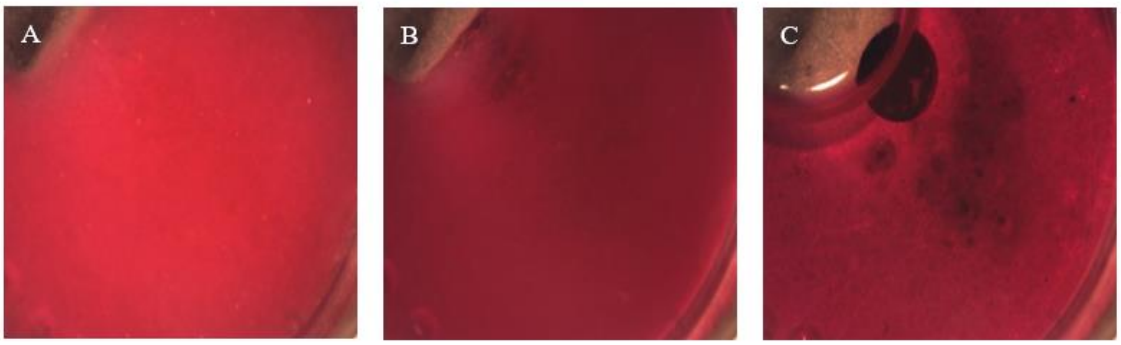

Figure 4.7. Thermal microscopic images at sub-ambient temperature of P407 5% with Rhodamine dye (0.1 mg.mL^{-1}) at (A) -15 °C, (B) -4.4 °C and (C) -0.4 °C.

4.4.4. The Evaluation of the Effect on Seeks at Sub-ambient Temperature due to P407 Concentration

The sub-ambient temperature screening brings new approach in poloxamer characterization. Indeed, the freezable water temperature transitions are independent regarding the poloxamer concentration (Figure 4.8 A, C, E), contrary to the higher temperature screening. Therefore, poloxamer quantification might be simplify in the sub-ambient range evaluation, especially if other parameters like entrapment or interactions with exogenous species are involved with the polymer. In order to emphasize this fact, normalized enthalpy calibration curves were plotted as function of P407 concentration of each freezable water signal, as it has been done for the high temperature thermal screening. The latter curves are presented on Figure 4.8 B, D, F. It is

noteworthy that DSC limit of detection for the P407/water systems measured at the lower temperatures is improved compared to that of the P407/water systems measured at the higher temperatures (0.1% vs. 1%). By measuring the enthalpy for several P407 aqueous solutions in the 0.1% to 20% range of concentrations at sub ambient temperature, the relation between enthalpy and P407 concentration ($C_{\%}$) allowed us to obtain a linear correlation that is fitting by the following equations, tightly-bound freezable water $\Delta H = 1.266 \times C_{\%}$ ($r^2 = 0.99696$), loosely-bound freezable water $\Delta H = 1.4487 \times C_{\%}$ ($r^2 = 0.99934$) and free water $\Delta H = -9.071 \times C_{\%} + 328.18$ ($r^2 = 0.99703$) as shown in figure 4.8 B, C and E. Interestingly, extrapolation of PeakIII ΔH at [P407] = 0% is 328.28 $J.g^{-1}$, which is close to melting enthalpy of pure water (333.6 $J.g^{-1}$). This result validates the thermal analysis tool at the sub-ambient temperature range to quantify polymer solutions with high sensitivity.

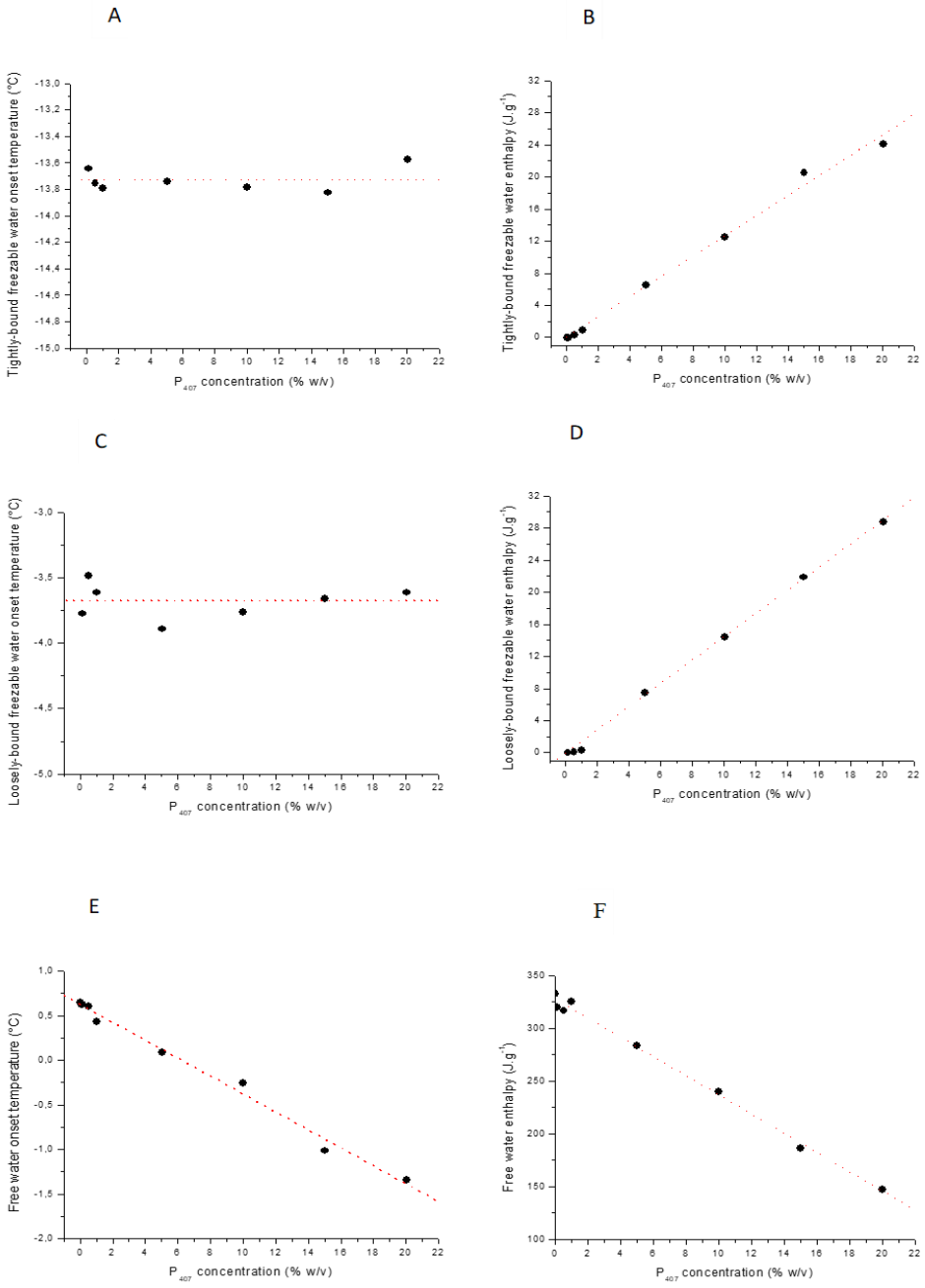

Figure 4.8. Thermal data of the tightly-bound (A, B), loosely-bound (C, D), and (E, F) free water in P407 environment as function of P407 concentration.

4.5. Conclusion

This study for characterizing poloxamer P407 by DSC and densitometry provided additional information and understanding of poloxamer behavior in different formulations which are discussed in chapter 5. The conventional DSC experiments at high temperature provide us the structural confirmation of the formulation and also provided the insight to our formulation

system in terms of the organization of our formulation. The densitometry results support the data obtained by DSC at high temperature. The third study was carried out for the optimization and development of the new method to discover peaks at sub-ambient temperature for the characterization of poloxamer. The results produced by DSC at sub-ambient temperature have proved that this method is more precise and accurate than conventional methods for the quantification of poloxamer. The three different peaks at sub-ambient temperature are well defined in terms of the water interaction with the poloxamer molecules. Unlike high temperature screening, poloxamer P407 concentration doesn't influence the peak II and III transitions at sub-ambient temperature screening. Thermal microscopy indicated the change in opacity of the poloxamer formulation with the change in temperature which supports the results from DSC at low temperature. The results of DSC at sub-ambient temperature conducted confirms the presence of peaks which demonstrated that peak I, II and III belongs to free water, water attached to PPO and water attached to PEO moieties, respectively. These methods allow us to further investigate the characteristics of HLP formulations which are discussed in Chapter 5.

Chapter 5: Optimization of Syringe Pump Device for Production of Nanosized Hybrid Liposome/Poloxamer Particles and their Characterization

5.1. Introduction

The liposomes as a carrier brought the revolution in the drug delivery field and became the first FDA approved nano-drug carrier in 1995 (Barenholz, 2012). Liposomes are bi-layer lipid vesicles composed of phospholipid chains with an aqueous core. Initially designed to mimic cell membranes *in vitro*, they were consequently proposed as drug delivery system (Gregoriadis and Florence, 1993). Due to high loading capacity as well as similarity with cell membrane, liposomes have been implemented to serve in several applications in the field of pharmaceuticals, such as cancer diagnosis and therapy (Torchilin, 2005). Potential application of liposomes as therapeutic tools is still being challenged by their physical and chemical instability, which may result in increased bilayer permeability and drug leakage (Guan et al., 2015). In order to improve the stability of liposomes, many approaches have been suggested such as liposome surface coating with PEG polymer. However, the use of an external coating also reduce liposomes cellular uptake (Wollina et al., 2003; Zhang et al., 2013). More recently, a new approach has been investigated in order to alleviate the limitations of liposomes; a system composed of a polymeric-core and a lipid shell have been introduced, in this nanosystem both lipid and polymer are unified to yield theoretically stable particles, enhanced encapsulation, controlled and modified release drug delivery system (Mandal et al., 2013).

Liposomes can be prepared by different techniques which are already well described in the literature such as ethanolic injection method, film hydration and several others (Patil and Jadhav, 2014; Shaker et al., 2017). The conventional ethanol injection technique provides the advantage of being simple to form vesicles without the application of a lot of energy and the possibility of scale up (Akbarzadeh et al., 2013; Batzri and Korn, 1973; Wagner et al., 2002). Automatization of the process by the merger of ethanolic injection technique with a syringe pump apparatus enhanced the reproducibility while reducing the variability related to the experimenter. Additionally, it allows to achieve a large scale production of liposomes (Pham et al., 2012; Pradhan et al., 2008).

Some polymers form 3D structures in contact with water. Hydrophilic polymers swells when hydrated and expand by the absorption of water (Peppas, 2000). Poloxamers are non-ionic copolymers arranged in triblock of EOx-POy-EOx consisting of ethylene oxide (EO) and

propylene oxide (PO) parts, x and y values can have modulated producing a collection of poloxamer derivatives. Poloxamers exhibit low critical solution temperature (LCST). The poloxamer based nanogels have the particularity to be temperature responsive. Small nanogel (Pluronic/PEI) particles around 120 nm swelled drastically to over 400 nm when temperature rapidly decreased below LCST (Lee et al., 2008).

In the literature hybrid structures of liposomes with polymer or gel are termed differently such as gelliposome or lipogels. These structures design different compositions which possess various characteristics. To control the release of drug, Kim et al formulated hybrid liposomal lipid bilayers with a Poly(Poly(*N*-Isopropylacrylamide-co-acrylic Acid) core (Kim et al., 1997). In 2015, Guan et al prepared gelliposomes composed of liposomes with a gelatin core to enhance the stability and the structure of liposomes (Guan et al., 2015).

In our case, we were interested in developing interiorly viscous core liposomes with no additional charges or chemical component to avoid the risk of toxicity. The most similar works in the literature were carried by Chandaroy and his team who proposed the hybrid Liposomes and very low concentration of Pluronic with particle size under 200 nm, another similar work in the literature was done by Zhang et al. His team proposed interiorly thickened liposomes with high poloxamer concentration of poloxamer (Chandaroy et al., 2001; Zhang et al., 2013). This approach led to an increase of liposomes stability and provided controlled release of encapsulated drugs. The obtained micro particles having an average size of 1.2 µm and exhibiting an important polydispersity (Zhang et al., 2013). In order to enhance the encapsulation of drug and slow their release while keeping a good pharmacokinetics profile, it would be preferable to obtain monodisperse nanoparticles with controlled preparation process. In this work, we aimed to obtain nanosized hybrid liposome/polymer particles with enhanced inner core viscosity using an optimum concentration of poloxamer, that should enhance the encapsulation and delay the release of drug. For this purpose, an appropriate preparation method with controlled experimental conditions had to be set-up.

To control the release, a system with lipid shell and polymeric viscous core, namely Hybrid liposome/polymer (HLP), has been designed. For this purpose, we setup a syringe pump apparatus equipped with homemade tubing system. The validation of push syringe techniques for formulation preparation was started by comparing the DLS and TEM results for size and PDI with formulation produced by dry film hydration and ethanolic injection techniques. HLP formulation consisting of poloxamer (5% w/v) was found to be optimal when produced at injection rates of 5 $mL.min^{-1}$. Then, we tend to characterize the HLP with DLS, TEM, TRPS,

thermal analysis and densitometry in comparison with a polymer added after formation of the liposomes (HLP_{out}). The selected conditions and composition resulted in nanocarriers which are highly reproducible with mono-disperse size distribution with an average size of 206 ± 4.8 nm and a polydispersity index of 0.15 ± 0.015. Densitometry and thermal analysis results confirmed the formation of HLP. Interestingly, HLP were stable over 2 months. Our homemade tubing system coupled with syringe pump apparatus achieved reproducible, precisely controlled production for the HLP formulation which can be scale up.

In this chapter, we developed a hybrid liposome/poloxamer (HLP) which is also termed hybrid liposome/poloxamer inside (HLP_{in}) formulation using a syringe pump apparatus coupled with a homemade tubing system. We first optimized the composition and the experimental parameters in order to obtain small size and monodispersed particles. The optimal formulation was extensively characterized in term of physico-chemical properties.

5.2. Materials

DOPC (1,2 Dioleooyl-sn-glycero-3-phosphocholine) was purchased from Avanti polar Lipids (Alabaster, Alabama, USA), Poloxamer 407 (P407), also known by its trade name as Kolliphor P407 was provided by BASF (Ludwigshafen, Germany), Doxorubicin Hydrochloride (Sigma Aldrich, France), Rhodamine B (Sigma Aldrich, France), Iodine and Potassium Iodine were provided by Prolab (Briare, France). Water was purified on Milli-Q system from Millipore (Fontenay-sous-bois, France), Ethanol 96% was purchased from Carlo-Erba reagents (Val-de-Reuil, France). Ultra-filtration units Vivaspin®20 were purchased from Sartorius (Geottingen, Germany), ultra-filtration units NANOSEP 300k was purchased from PALL filtron (Massachusetts, USA), Dialysis device Microfloat-A-lyzer 100 KD was purchased from spectrum laboratories (CA, USA). Polyether ether ketone (PEEK) tubes, T-shaped connectors and ferrules were purchased from IDEX Health & Science (Oak Harbor, WA, USA).

5.3. Methods

5.3.1. Methods of Preparation of the Formulations

5.3.1.1. Dry Film Hydration Method

Thin film of DOPC was made in the round bottom flask by evaporating ethanol from the solution of DOPC (2 $mg.mL^{-1}$) solubilized in ethanol with the help of rotary evaporator at 35°C

for 30 minutes. Later, the thin layer was hydrated with poloxamer solution (0.5%) and immidiately transfered to sonication bath for 15 minutes. formulation. Finally the formulation was recovered and characterised by DLS and TEM.

5.3.1.2. Ethanolic Injection Method

The ethanolic injection method is a simple method. Poloxamer solution (P407 0.5%) was poured in a small vial and stirred at 750 rpm with the help of magnetic stirrer. Meanwhile ethanolic solution of DOPC (2 $mg.mL^{-1}$) was added drop by drop into the poloxamer solution (ratio 10:1 for poloxamer solution and DOPC solution) and kept it on stirring for 2 hour. Evaporation of the ethanol achieved by using Rotary Evaporator (rotating rate 60 rpm, 35 °C, pressure 10 mbar). Evaporation was performed untill 1/3 of the total sample evaporated and quantity was made sufficient with Milli-Q® water in the end.

5.3.1.3. Preparation of the Formulations by Syringe Pump Apparatus

In this work, three formulations were designed: Conventional non-ionic liposomes, Hybrid liposome/poloxamer (HLP) and Hybrid liposome/poloxamer outside (HLP_{out}) as shown in Figure 5.1.

Conventional liposomes (CLs) were prepared by the ethanolic injection method using a syringe pump apparatus (Harvard apparatus PHD 2000) as shown in Figure 5.2. One syringe (1 mL) was filled with ethanolic solution of DOPC (20 $mg.mL^{-1}$, 25.4 $\mu mol.mL^{-1}$) and another syringe (10 mL) was filled with Milli-Q® water. Both syringes were fixed on the syringe pump apparatus, injection speed was set to 0.5 $mL.min^{-1}$ for the lipid solution and 5 $mL.min^{-1}$ for the aqueous solution. Apparatus ran for 1 min giving final volume of 5.5 mL, yielding a final concentration of DOPC (2 mg/mL, 2.54 $mmol.mL^{-1}$).

Hybrid liposome/poloxamer (HLP) was prepared using the same procedure as liposomes preparation. The aqueous phase was replaced by poloxamer 407 (P407) solution at different concentration (0.5, 5 and 10 % w/v). Different flow rates of P407 solution injection (0.1, 1, 5, 10 and 37 $mL.min^{-1}$) were tested in order to choose the optimal value. Ratio of the injection flow rates between the lipid solution and the P407 solution was kept at 1:10 for all experiments.

Liposomes with gel outside termed as Hybrid liposome/poloxamer outside (HLP_{out}). HLP_{out} was prepared by first preparing conventional liposomes with concentration of DOPC (4 $mg.mL^{-1}$, 5.08 $mmol.\ mL^{-1}$). A poloxamer solution (10 % w/v) was prepared. Liposome suspension and

poloxamer solution were then mixed with 1:1 volume ratio to obtain final concentration of lipid and poloxamer similar to HLP.

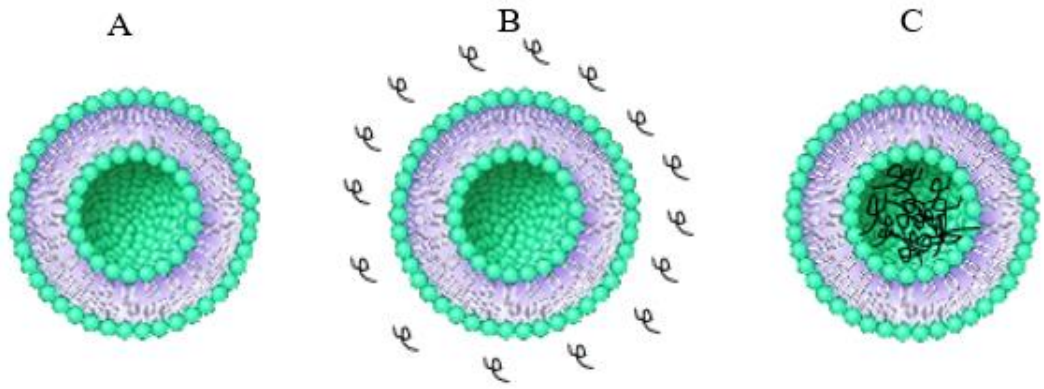

Figure 5.1. Graphical representation of the formulation, A) Conventional Liposomes, B) HLP_{out} and C) HLP_{in} or HLP.

In case of rhodamine or Doxorubicin HCL (DOX) encapsulation, the formulations were prepared by following the same procedure discussed above for each formulation. The only difference was the addition of rhodamine or DOX (0.5 $mg.mL^{-1}$ and 5 $mg.mL^{-1}$, respectively) in aqueous phase or in poloxamer solution during preparation.

The theoretical calculation of Reynolds Number to determine the laminar flow in the tubes was computed using the equation,

$$Re = \frac{\rho V D}{\mu}$$

Where ρ represents the fluid density, V is the linear velocity of the solution, D the tube diameter and μ the dynamic viscosity of the fluid. The density of a 5% P407 solution was experimentally determined by densitometry (DMA™ 4500 M, Anton Paar) performed at 20 °C.

Where ρ = 1.00612 kg/L, V is the linear velocity which depends on the injection rate, D = 0.25 mm, the viscosity of poloxamer (P407 0.5%) μ = 2.29 cP.

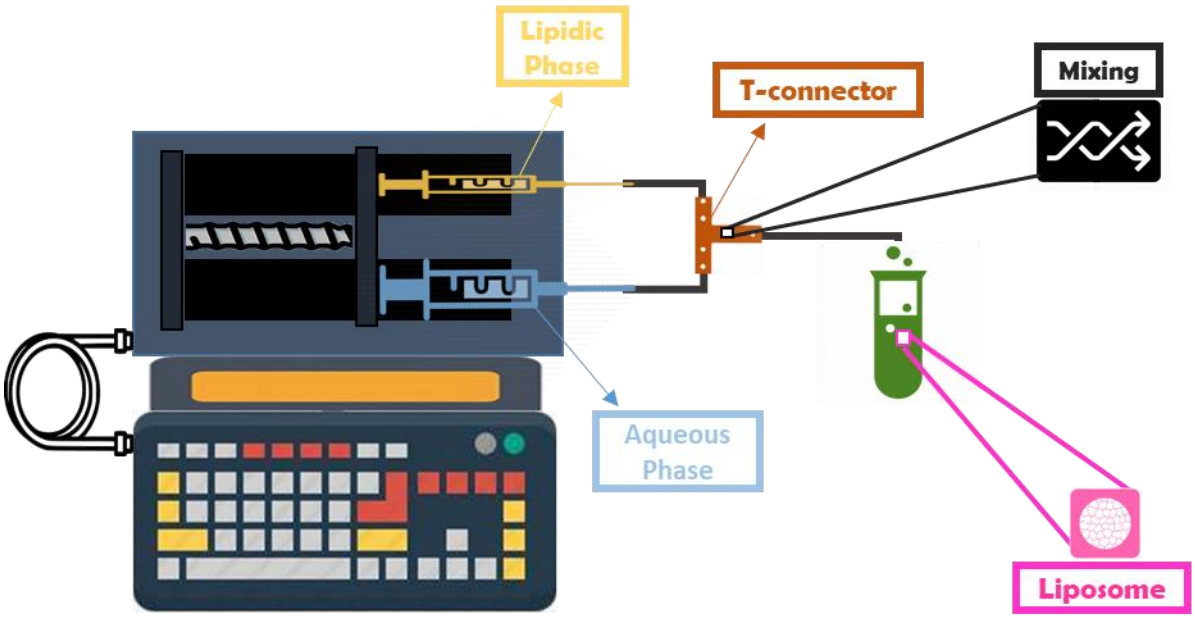

Figure 5.2: Pictorial presentation of whole setup of Syringe pump preparation technique.

5.3.2. Evaporation of Ethanol

The removal of ethanol was performed using a rotary evaporator. The formulation was collected in an evaporation flask and treated by using a rotavapor (Rotavapor R-144, Büchi, Switzerland) at the following conditions (rotating rate 60 rpm, 35 °C, pressure 10 mbar). These conditions applied for 15-20 min to achieve 25-35% evaporation and 30-40 minutes to achieve 60-65% evaporation of formulation measured by weight which were later adjusted with by adding Milli-Q® water.

5.3.3. Densitometry

The density was measured by using a Densitometer (Anton Paar DMA™ 4500 M). Densitometry analysis is based on the principle of oscillating U-tube to determine the density of samples based on an electronic measurement of the frequency of oscillation, from which the density value is calculated. Experiments were performed at temperature 25 and 37 °C. The U-tube was washed with Milli-Q® water then with ethanol 96% following by drying with air, before and after each utilization. The oscillating U-tube was filled with about 1.5 mL of sample with a syringe. The U-View ™ camera function shows and records live images of the oscillating U-tube to ensure that there should be no bubbles and that the U-tube is entirely filled with the sample.

5.3.4. Ultrafiltration by Centrifugation

Ultrafiltration column (Pall Filtron, USA) with 300 kDa molecular weight cut-off (MWCO) were used to separate free poloxamer and non-encapsulated rhodamine B from liposomal suspension. The filtration was carried out by centrifugation at 13000 rpm for 30 min in a refrigerated bench-top centrifuge (Hettich Rotanta 460 RF, Germany) at 4 °C.

5.3.5. Physicochemical Characterization

5.3.5.1. Dynamic Light Scattering (DLS)

The liposome, HLP and HLP_{out} diameters were determined at 25 °C by quasi-elastic light scattering using a Zetasizer Nanoseries Nano-ZS (Malvern Instruments, France). The scattering was measured at a 173° fixed angle and the position at 4.65. Each sample was run for 3 measurements. Results were expressed as the average hydrodynamic diameter and the standard deviation of the triplicate.

For temperature study, the option for trendline vs temperature was selected with the same conditions used for size and PDI measuring experiment. The only difference was to record the size and PDI after each 10 °C increase, which was set from 15 to 55 °C. The result data was expressed by the help of graphs.

5.3.5.2. Transmission Electron Microscopy (TEM)

The liposome, HLP and HLP_{out} formulations were observed by Transmission Electron Microscopy (TEM). Briefly, 10 µL of the sample was deposited on a carbon-coated copper grids, excess solution was removed after 2 min by a filter paper. This was followed by the application of 5 µL of uranyl acetate 1% to the same grid for 2min, excess stain was then removed with filter paper. Sample is subsequently air-dried at room temperature. The grid placed on a slide was inserted in the microscope. The sample analysis was performed with a JEOL JEM 100 S (JEOL Ltd Tokyo, Japan) TEM operating at 80 kV. TEM images were captured using an Orius Sc 200 digital Camera (Gatan-Roper Scientific, Evry, France).

5.3.5.3. Tunable Resistive Pulse Sensing (TRPS)

Measurements were made using a qNano system from IZON Science equipped with an upper and a lower fluid cell, each one containing an Ag/AgCl electrode. The measurements were done using electrolyte (standard provided with Izon kit) solution and a pressure of 0 mbar to allow the passage of the particles through the pore. The membrane stretch was comprised between 45 and 47 mm and the voltage were adjusted in order to have a baseline current between 120 and 145 nA. Data were acquired using Izon Control Suite V3.1. Each acquisition presented is the result of the passage of at least 500 liposomes. The liposome size and concentration were calculated after the measurement of the calibrated particles solutions with Nano-pore (NP250) allowing a measurement of a total size range between 100 and 400 nm according to manufacturer. The results were determined using the IZON Control Suite software.

5.3.5.4. Thermal Analysis

The Differential Scanning Calorimetry (DSC) experiments were performed on the differential scanning calorimeter 822e (Mettler-Toledo, Switzerland) previously calibrated with high purity indium (T_{fus} = 156.6 °C, $\Delta_{fus}H$ = 28.45 $J.g^{-1}$) and zinc (T_{fus} = 419.6 °C, $\Delta_{fus}H$ = 107.5 Jg^{-1}). DSC experiments were performed at temperature starting from 5 to 60 °C at 1 $K.min^{-1}$ scan rate under dry air (60 $mL.min^{-1}$). Empty aluminum pan of 100 µL was hermetically sealed and holed from the top by means of a small pin of controlled size (0.7 mm) and used as a reference.

5.3.6. Calorimetric Assay (Baleux Assay)

Poloxamer quantification was carried out by a colorimetric assay as previously described by Baleux et al (Baleux and Champetier, 1972). Briefly, 12.5 µL Iodine solution (iodine solution at 10 mg/mL and potassium iodide solution at 20 mg/mL) was added to 1 mL of diluted sample. The absorbance of the complex was measured after 5 min at 540 nm using UV-Vis spectrophotometer (Varian CARY® 100). linearity was checked for standard solutions with concentration ranging from 0.05 to 100 $\mu g.ml^{-1}$. Poloxamer concentration of samples were calculated using calibration curve with r^2 of 0.99.

5.3.7. Stability Study

Stability tests were carried out for CLs, HLP and HLP_{out} formulations for 2 months. The three formulations were prepared, filtered and kept at 4 °C. The liposome and HLP diameters were

determined at 25 °C by quasi-elastic light scattering using a Zetasizer Nanoseries Nano-ZS (Malvern Instruments, France).

5.4. Results and Discussion

5.4.1. Conception of the Formulations

In this study, a hybrid composition of lipid and polymer was selected to achieve a formulation that offers an improved encapsulation and controlled release of the encapsulated drug. The lipid used for this formulation was DOPC and the polymer used was poloxamer 407 (P407). The designed formulation is referred as Hybrid liposome/poloxamer or Hybrid liposome/poloxamer inside (HLP_{in} or HLP). Regarding physicochemical properties, the HLP system is expected to increase the viscosity and the density of the liposome core by incorporating poloxamer into the aqueous core of the liposomes. This approach should enhance the entrapment of drug and avoid its fast release.

5.4.2. Optimization of the Experimental Conditions for Push Syringe

All formulations were prepared according to the principle of ethanolic injection with the help of a syringe pump device and tubing system that we developed (methods section 2.1). The preparation of formulations with the syringe pump apparatus combines two main principles, the ethanolic injection and microfluidics. The instrumental setting was designed to provide fully controlled and reproducible experimental conditions due to minimum experimenter influence, in addition to offer the possibility to scale up the production (Charcosset et al., 2015). From a formulation standing point, the main advantage is to produce a narrow size distribution of liposomes in a single step, without extrusion or sonication. However, to generate a reproducible formulation having relevant characteristics, several parameters needed to be setup, i) optimization of experimental setup, ii) optimization of formulation regarding the lipid and poloxamer ratio, and iii) optimization of formulation regarding the solvent content.

5.4.2.1. Preparation of HLP Formulations by Thin Film Hydration Method and Ethanolic Mnjection Method

Thin film hydration and Ethanolic injection method are two most studied method for liposomes preparation (Shaker et al., 2017). Both methods were carried out for producing liposomes. The idea behind this study was to characterize the HLP formulation produced by ethanolic injection

method and thin film hydration method and to compare these results with the results with push syringe method with our newly homemade designed tubing system. The DLS results shown that the HLP (0.5%) produced with thin film hydration technique possess size (51 ± 4.2) and PDI (0.36 ± 0.1), whereas, Liposomes prepared from Ethanolic injection method are bigger on size around 100 nm and polydispersity was 0.19 ± 0.5. We prepared each formulation at least 3 times and measure with DLS as shown in Table 5.1.

Ethanolic injection is a very simple process and became the ultimate choice as it produce the formulation with better PDI (Pons et al., 1993). Later, we tried to automatize ethanolic injection method by merging it with microfluidics to minimize the external influence under controlled conditions.

Table 5.1. DLS measurements for liposomes produced with Thin film hydration and ethanolic injection method n=3.

Method	Size	PDI
Thin film Hydration	51 ± 4.2	0.36 ± 0.1
Ethanolic injection	98 ± 12	0.19 ± 0.5

5.4.2.2. Optimization of the Experimental Setup

In order to optimize the conditions for formulations preparation, the influence of two instrumental parameters on the final preparation properties was studied a) the tubing internal diameter and b) the injection flow rate. The HLP formulation with poloxamer concentration (0.5% w/v) was used for the optimization of the experimental conditions. For this experiment, two types of tubbing systems with different compositions and internal diameters were considered in order to select the most suitable to prepare the formulations as emphasized in Figure 5.3. Both preparation systems are comprised of 3 distinctive tubes connected to each other by the intermediate of T-shaped connector (Figure 5.3 A). T-1 tube system was composed of two polyethylene inlet tubes having a 1 mm internal diameter followed after the junction by one outlet tube of 250 µm internal diameter composed of polyether ether ketone (PEEK) which is high performance engineering thermoplastic inert to water and the most common chemical solvents (Haleem and Javaid, 2019). Whereas, T-2 preparation system composed of three PEEK tubes with the same internal diameter (250 µm). HLP formulation was prepared using both

preparation systems according to the procedure described in preparation of the formulations (section: 2.2.1).

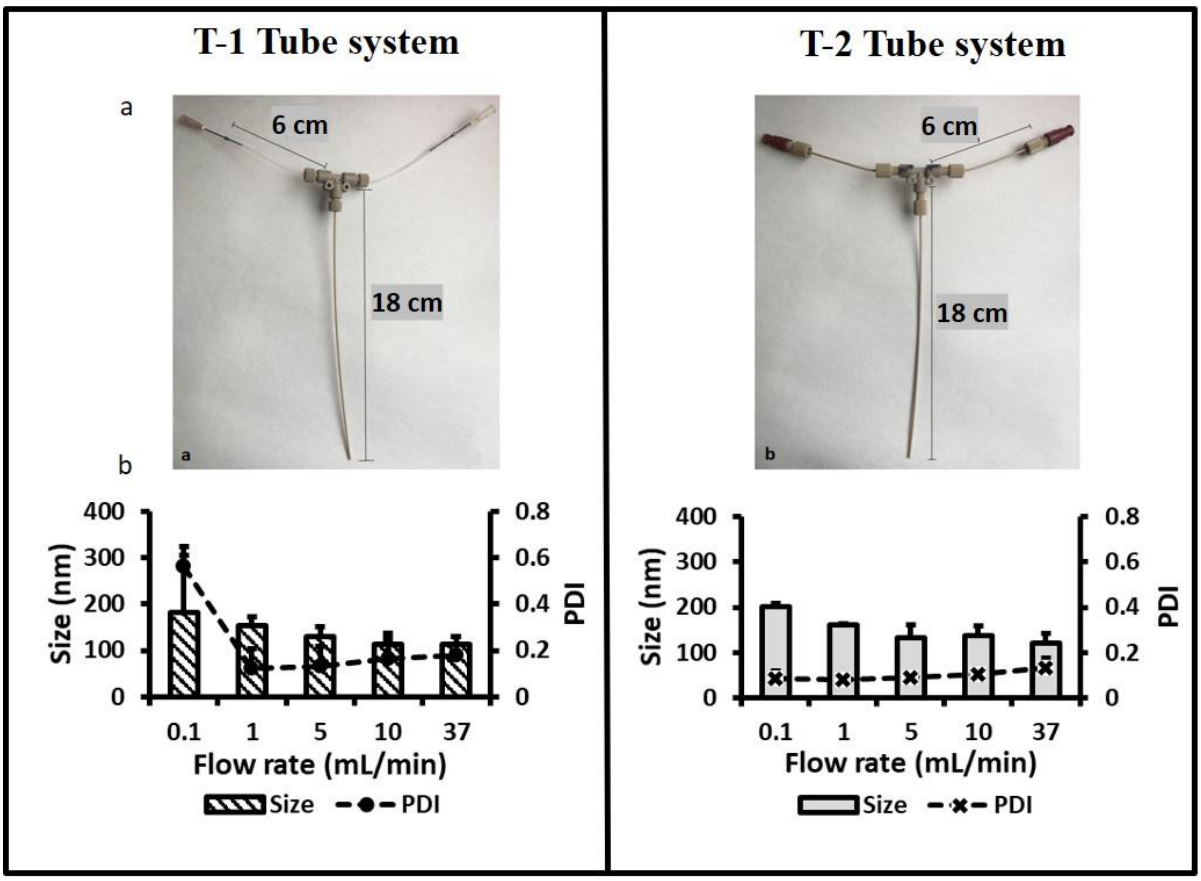

Figure 5.3. Comparison between two Tube System T-1 (left) and T-2 (right), (a) Pictorial illustration, (b) Graphical representation of size and PDI of liposomes obtained with different flow rate of each tube system (n=3).

The second parameter requiring optimization was the injection flow rate. For that purpose, HLP formulation was prepared using different injection flow rates (0.1 mL.min^{-1}, 1 mL.min^{-1}, 5 mL.min^{-1}, 10 mL.min^{-1}, 37 mL.min^{-1}). The optimal injection flow rate was selected according to the DLS characterization of the final preparation (Figure 5.3 B: left and right, respectively). First, we verified that both preparation systems would generate to laminar flow which is necessary to obtain liposomes (Yu et al., 2009). For this purpose, we calculated the Reynolds (Re) number for both preparation systems depending on the injection flow rate. As described in the literature, a Reynold number lower than 2000 is representative of laminar flow conditions, favorable for liquid mixing and to the formation of smaller and uniform size liposomes with low PDI (Bessoth et al., 1999; Jahn et al., 2004; Yu et al., 2009). The Reynold number was calculated for each tube (Table 5.2). Regardless of the flow rates employed, Re number was

systematically well within the range of 2000 and lower for the T-2 tube than the T-1 tube demonstrating the formation of a laminar flow and (Table 5.2). Therefore, the different configurations T-1 and T-2 were suitable for the formation of liposomes.

Table 5.2. Re numbers obtained by T-1 and T-2 tube system obtained with different flow rate

Flow Rate ($mL.min^{-1}$)	Reynolds number T-1 tube	Reynolds number T-2 tube
0.1	0.06	0.01
1	0.56	0.07
5	2.80	0.35
10	5.60	0.70
37	20.7	2.59

All preparations produced had acceptable range of average hydrodynamic size and PDI except in the case of the lowest infusion flow rate (0.1 $mL.min^{-1}$) with Tube-1 system. The comparison showed that the polydispersity (PDI) of the liposomes obtained from T-1 tube was significantly higher than the PDI obtained from T-2 preparation system, as the average PDI for all flow rates was 0.232 and 0.098 respectively. As the T-2 preparation system exhibited lower Re number than T-1 system at each flow rate (see Table 2), this could explain the formation of formulations with slightly better PDI obtained with the T-2 tube system (Figure 5.2 B: left and right).

The two preparation systems designed to be used in conjunction with the syringe pump demonstrated to be suitable for the production of CLs and HLP formulations in a robust manner. This instrumental approach has the advantage to provide an optimal usage of the volume of the different solutions by minimizing the dead volume of the preparation system. In addition, because it relies on the use of PEEK tubbing readily available, it appears as particularly cost-effective approach which can be easily implemented. On the basis of Re numbers and PDI of HLP, Tube-2 system was considered further for optimizing lipid/poloxamer ratio according to the injection flow rate.

5.4.2.3. HLP Prepared by all Three Techniques and their Comparison

In this experiment we prepared HLP formulation (P407 0.5 %) with dry film hydration, ethanolic injection method and the push syringe technique. Earlier, both film hydration and ethanolic injection techniques produced liposomes with the size less than of 200 nm, which is a desired size for any nanoparticle to cross the cell membrane (Bozzuto and Molinari, 2015). HLP formulation (P407 0.5 %) prepared by ethanolic injection method looks more mono dispersed than dry film hydration as shown in Figure 5.4. The amount of poloxamer to be incorporated was evaluated. When poloxamer concentration was increased up to 5% and more, it was difficult to form HLP by both methods (ethanolic injection method and dry film hydration method). The Poloxamer is a surfactant and some poloxamer have been shown to deconstruct the liposomal membrane at high concentration, therefore there is probably a threshold not to be reached to preserve membrane integrity (Pembouong et al., 2011). Nevertheless, the syringe pump device allowed us to prepare HLP with higher concentration of poloxamer by simple mixing without any huge external influence to produce energy such as sonication, heating, stirring and others, which are discussed in later experiments.

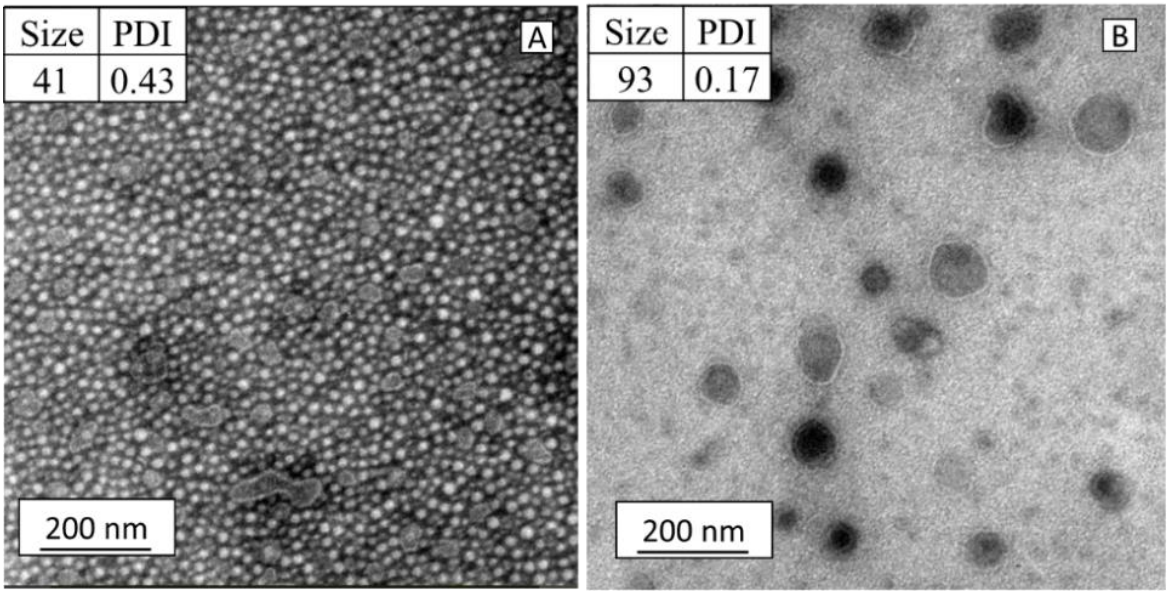

Figure 5.4. TEM images and DLS size measurement of HLP (P407 0.5%) prepared by A) Dry film hydration technique, B) ethanolic injection technique and C) Push syringe technique.

5.4.2.4. Optimization of the Formulation Regarding Lipid and Polymer Ratio

The lipid and polymer ratio adjustment were the next phase to attain the intended formulation. The lipid to poloxamer ratio was optimized at fixed lipid concentration and varying poloxamer concentration using various flow rates. The average hydrodynamic size and PDI of liposomes

are decreases with small concentration of poloxamer (Chandaroy et al., 2001; Zhang et al., 2013) HLP with poloxamer 0.5% had the smallest size and PDI but at this concentration, it was thought difficult to increase the liposome inner core viscosity. HLP with poloxamer 5% was found optimal as it exhibits an average size within acceptable range and a slightly better PDI than HLP with poloxamer 10%, as shown in Figure 5.5.

Finally, the formulation with the optimal average size and PDI was obtained with the T-2 tube system at a flow rate of 5 ml.min^{-1} with 5% of P407 in HLP. These parameters were also set for the other two formulations taken as controls, Conventional liposomes (CL) and Hybrid liposome/poloxamer outside (HLP_{out}) in which the poloxamer was added after the formation of liposomes.

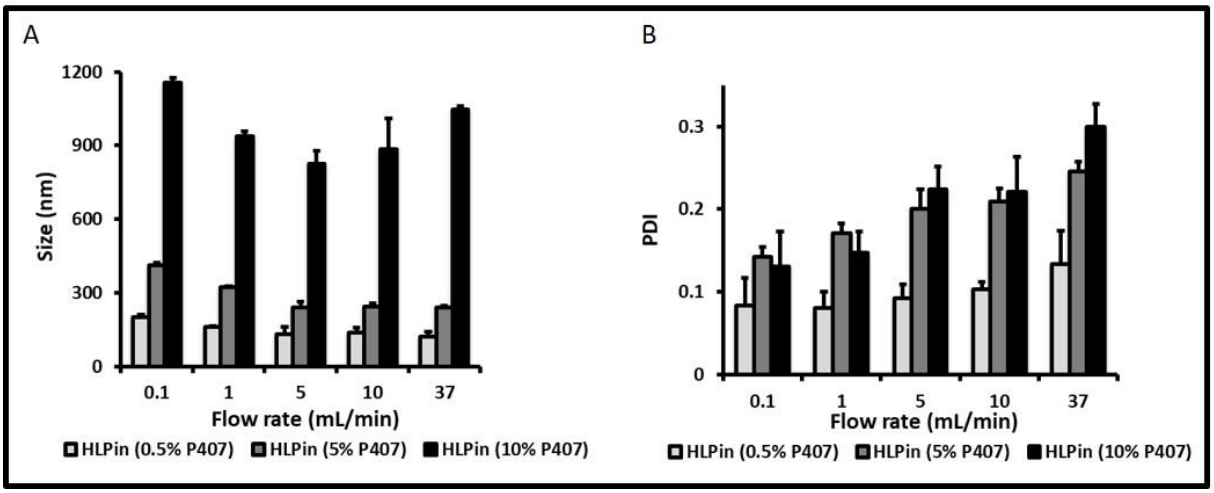

Figure 5.5. Tube system and formulation optimization Graphical presentation of hydrodynamic average size of HLP (A) and of polydispersity index (B) of formulation obtained. with different poloxamer (P407) percentages at different flow rates (0.5, 1, 5, 10, and 37 mL.min^{-1}).

5.4.2.5. Optimization of the Formulation Regarding the Solvent Content

Density analysis was performed in order i) to optimize the evaporation procedure with respect to HLP integrity, and ii) to evidence the internalization of the polymer within the liposomes.

As far as the validation of the evaporation procedure is concerned, it has been demonstrated that the control of ethanol/water quantity in the formulation is necessary to prevent liposomes from dissolving (in case of too high quantity of ethanol, *e.g.* 10% in the present study) or aggregating (in case of water over-evaporation).

To optimize the evaporation procedure, the obtained formulations were evaporated up to 25-35% and 60-75% at controlled temperature and pressure. The percentages were determined and adjusted by weighing the samples after evaporation. As it can be seen in Table 5.3, the

difference in volumetric found only in the case of volumetric mass of HLP and HLP_{out} formulation evaporated up to 25-35%. In the case of non-evaporated formulations, a slight differentiation was noticed by comparing conventional liposome formulations and water/ethanol 90/10 v/v solutions volumetric masses.

Table 5.3. Volumetric mass of different formulations as function of the ethanol/water ratio at 25 °C

Formulation	Volumetric mass ($g.cm^{-3}$) 25 °C		
	Without evap.	25-35% evap. + q.s.	60-75% evap. + q.s.
Milli-Q water	0.99705	0.99705	0.99705
Water/ethanol (90/10, v/v)	0.98462	0.99637	0.99702
Conventional liposomes	0.98644	0.99634	0.99685
HLP_{out}	0.99743	1.00214	1.00236
HLP	0.99171	0.99881	1.00325

Interestingly, densitometry analysis has also demonstrated that with 25-35% of evaporation of the ethanol/water medium, less than 0.3% of ethanol was remaining in the final formulations.

Similarly, volumetric mass was quite comparable for the HLP and HLP_{out} formulations with 60-75% evaporation + q.s. Milli-Q® water. These results could be explained by relative disruption of the liposomes membrane leading to the same P407/lipid system.

The presence of poloxamer inside the liposomes makes them stable and suitable for *in vivo* administration (Çağdaş et al., 2014; Zhang et al., 2013). Furthermore, once the overall formulation procedure has been optimized (*i.e.* 5% P407, 25-35% evaporation + q.s. Milli-Q® water), densitometry experiments help to have a first insight into HLP and HLP_{out} properties differentiation. For that purpose, a poloxamer density calibration curve has been firstly established as shown in in Figure 5.6 and highlights the fact that volumetric mass of aqueous solution of P407 is directly proportional to the polymer concentration. This could be helpful to estimate the poloxamer amount in the HLP formulations.

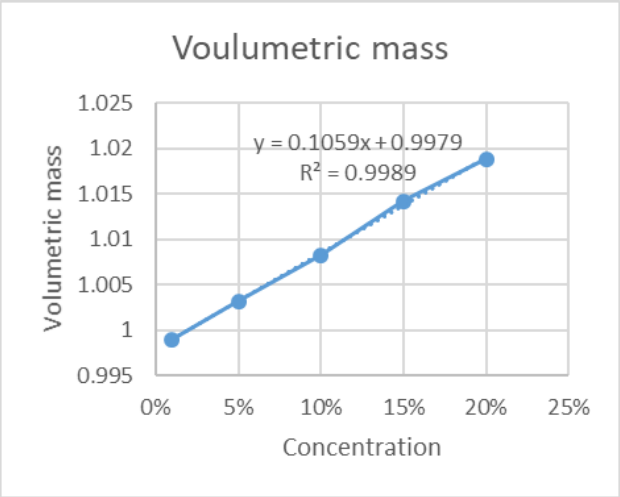

Figure 5.6. Calibration curve for Poloxamer volumetric mass

As far as the present results are concerned, a 5% P407 solution have a volumetric mass of 1.00253 g.cm^{-3} at 25 °C. This density value is similar to that of the optimized HLP$_{out}$ formulation, possibly due to the fact that P407 in the HLP$_{out}$ formulation is present in the continuous medium. For the HLP formulation, the density is lower compared to the 5% P407 solution but higher compared to the conventional liposome prepared the same way. This suggests that the polymer is encapsulated within the liposomes. To apprehend the HLP and HLP$_{out}$ behavior at body temperature, densitometry experiments were also performed at 37 °C (Table 5.4). A similar behavior was observed, indicating that the liposome as well as the poloxamer entities undergo no change at that temperature. We assume that, at the body temperature, the encapsulation efficiency should be the same as at room temperature. These results will comfort the further *in vitro* and *in vivo* experiments. As far as the current results are concerned, a 5% P407 solution have a volumetric mass of 0.99816 g.cm^{-3} at 37 °C.

Table 5.4. Volumetric mass of different formulations after ethanol/water evaporation up to 25-35% + q.s. Milli-Q® water at 25 and 37 °C

Formulation	Volumetric mass (g.cm^{-3}) 25°C	Volumetric mass (g.cm^{-3}) 37°C
Milli-Q water	0.99705	0.99328
Conventional liposomes	0.99634	0.99263
HLP$_{out}$	1.00214	0.99766
HLP	0.99881	0.99431

To resume, the densitometry experiment demonstrated that 25-35% of evaporation of the continuous medium was the best range to optimize the HLP formulations by maintaining its required characteristics. Concurrently, this procedure allows removing the maximum of ethanol to make the HLP formulations biocompatible. Moreover, densitometry showed that the continuous phase was denser for HLPout as regard to HLP giving a first indication that liposome inner core was denser in HLP as regard to HLP_{out}. The formulations retained with the help of the densitometry experiments were then filtrated and considered for further characterization studies such as physicochemical experiments, within the objective of accessing the poloxamer encapsulated inside liposome for the HLP formulations.

5.4.3. Physicochemical Characterization

5.4.3.1. Dynamic Light Scattering (DLS)

The results of the particle sizing of our formulations are summarized in Table 5.5. The table shows the z-average diameters, the polydispersity index obtained for the various liposome, HLP and HLP_{out} formulations. The z-average diameter values are the mean of measurements repeated on 5 samples of each formulation of CL, HLP and HLP_{out}. The data shows that the measurements are reproducible for each formulation. In addition, the results show that the size is dependent of the formulation composition. We obtained nanoscale particle size within a range suitable for systemic delivery. This was definitely an advances as regard to the microscale particles gelliposomes reported in the literature (Guan et al., 2015; Zhang et al., 2013)

Table 5.5. DLS results of size and PDI for CL, HLP_{out} and HLP

Formulation	Size (nm)	PdI
CL	91 ± 12.8	0.22 ± 0.019
HLP_{out}	183 ± 5.5	0.17 ± 0.016
HLP	206 ± 4.8	0.15 ± 0.015

The physical characterization of liposomes, HLP and HLP_{out} is of great importance in understanding their stability and suitability for the variety of applications. After size

determination, the TEM imaging was carried out to examine the morphological difference between the formulations.

5.4.3.2. Transmission Electron Microscopy (TEM) and Tunable Resistive Pulse Sensing (TRPS)

TEM images of liposome, HLP and HLP_{out} revealed the structure and morphology of each system. The morphology of these formulations was different from each other (as shown in Figure: 5.7 left panel). The liposome exhibits various morphologies lose their defined shape related to the effect of grid drying. HLP_{out} exhibited more defined structures with few clusters. The deformation of the HLP_{out} vesicles can be explained by a significant amount of free poloxamer in the continuous medium. Interestingly, HLP showed regular structures under TEM observations (Figure 5.7 A, B, and C, left panel).

To complete the DLS and TEM data, the number of nanoparticles obtained were determined using tunable resistive pulse-sensing. The liposomes and HLP_{out} tend to exhibit a main size distribution between 150 to 200 nm with concentration 1.4×10^9 particles/mL and from 170 to 250 nm with concentration 1.5×10^9 particles/mL respectively (Figure 5.7 A and B graph, right panel). HLP tends to exhibit a broader range from 150 to 200 nm with concentration 7.0×10^8 particles/mL (Figure 5.7 C graph at right). These interpretations indicate that the HLP formulation may contain encapsulated poloxamer as it contains a smaller number of particles, which can be due to more homogeneous shape and size as observed in TEM images and a better PDI obtained with DLS. The poloxamer inside the liposome might provide stability, strength and viscosity to the core of liposomes (Zhang et al., 2013). In order to verify this hypothesis, thermal analysis experiments were performed. from 5 to 60 °C, as the poloxamer suspension presents a micellization transition in this range of temperature, and since the poloxamer environment may impact such a transition.

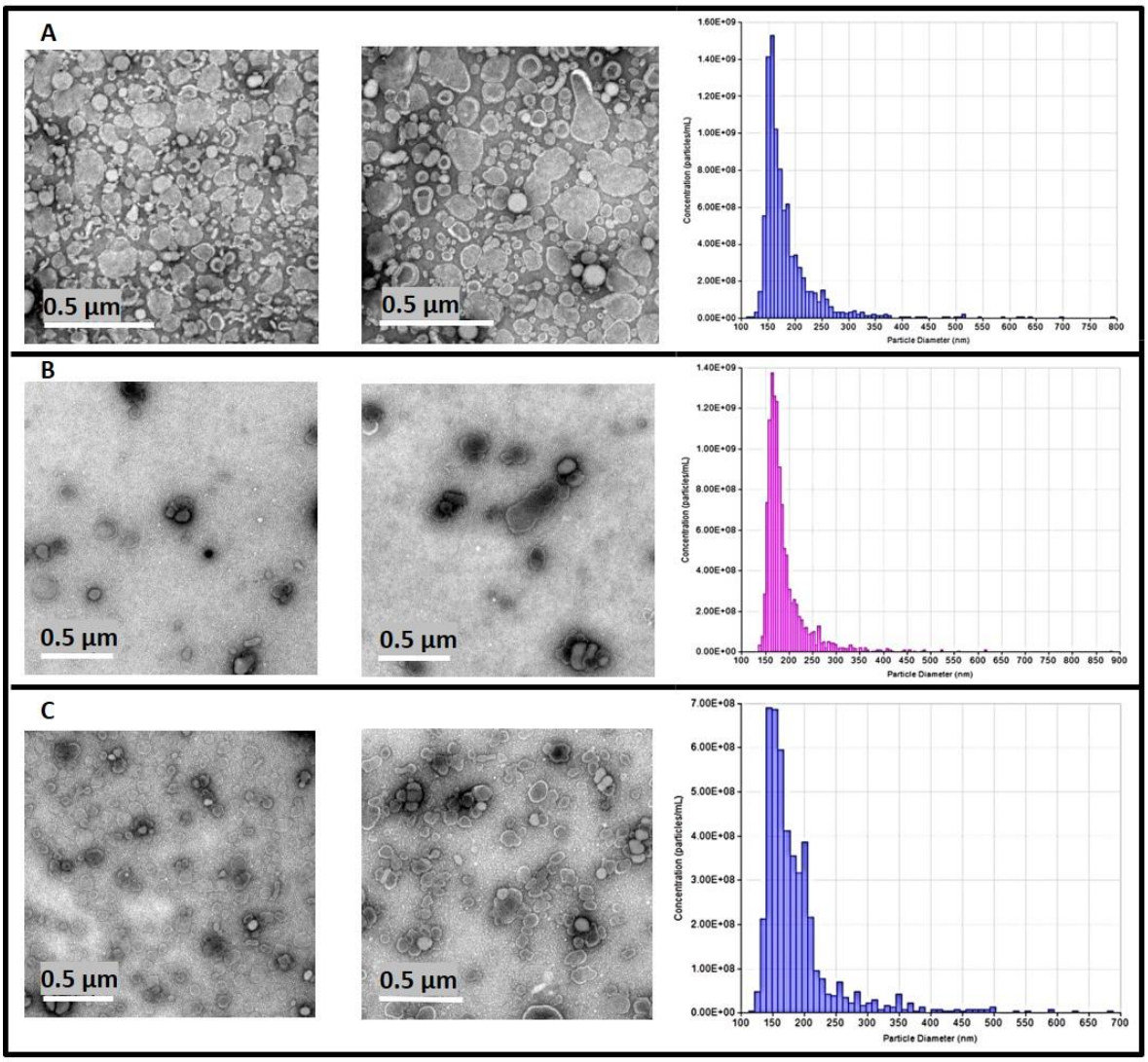

Figure 5.7. (A) Conventional liposomes as spherical unilaminar vesicles of variable sizes (24-329 nm), (B) $HLP_{out.}$ as heterogenous mixture with non-definite shape particles with size range (30-445), and (C) HLP as unilaminar vesicles of variable sizes (50-188 nm) .

5.4.4. Differential Scanning Calorimetry (DSC)

Poloxamer behavior as a function of temperature in aqueous medium is well known and discussed in numerous publications (J. Chen et al., 2013; Dumortier et al., 2006; Pembouong et al., 2011). Indeed, one can have access to the poloxamer micellization transition by deriving the heat flow vs. temperature signal obtained from the DSC analysis of the poloxamer solution. An endothermic signal is then obtained with a peak position corresponding to the micellization temperature. This transition corresponds to the removal of water (likely dehydration process) from PPO of the PEO-PPO-PEO chains of the poloxamer during the micelles formation (Alexandridis et al., 1994; Ur-Rehman et al., 2010). Since the micellization temperature

decreases with concentration, and since the signal area in proportional to the concentration, the micellization temperature is inversely proportional to peak height. As can be seen in Figure 5.8, no difference in micellization was noticed between P407 5% aqueous solution, unfiltered HLP and HLP_{out} formulations (Fig. 5.8 A, B, and C). This is due to the fact that free poloxamer influences the thermal transition of the overall lipid/polymer systems. But once HLP and HLP_{out} were filtrated, one can easily distinguish both formulations since their temperatures of micellization are shifted to higher temperatures (Figure 5.8 D and E).

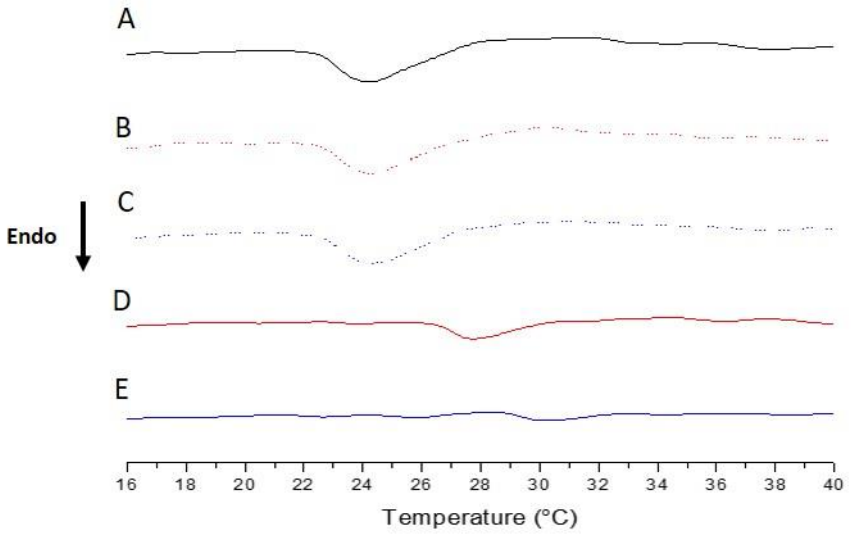

Figure 5.8. Derived DSC curves obtained (A) P407 5%, (B) HLP_{out}, before filtration, (C) HLP, before filtration, (D) HLP_{out}, after filtration, and (E) HLP after filtration.

Interestingly, P407 temperature of micellization (T_{mic}) for filtered HLP is 5.5 °C higher than that of both unfiltered HLP and free P407 5% formulations. As far as filtered HLP_{out} is concerned, P407, the micellization temperature is 3.6 °C higher than that of both unfiltered HLP_{out} and free P407 5% formulations (see experimental ΔT_{mic} data in Table 5.6). These differences are indicative of the stabilization of liposome by the poloxamer at this concentration. The more stable formulation being the HLP.

Table 5.6. Experimental and variation in temperature of micellization

Formulation	Experimental T_{mic} (°C)	Experimental ΔT_{mic} (°C)	P407 %	Extrapolated T_{mic} (°C)	EffectiveΔT_{mic} (°C)
Free P407	23.6	–	5.0%	–	–
HLP	23.6	–	5.0%	–	–
HLP_{out}	23.6	–	5.0%	–	–
Filtrated HLP	29.1	5.5	3.4%	24.2	4.9
Filtrated HLP_{out}	27.2	3.6	2.3%	24.8	2.4

This result should support our former hypothesis of encapsulated poloxamer in the HLP vesicles only if we can certify that decrease in P407 quantity after the filtration process is not the only factor responsible of such a shift in the temperature of micellization. To evaluate the concentration contribution to T_{mic} data for filtrated HLP and HLP_{out} formulations, a T_{mic} *vs.* concentration curve calibration has been established shown in chapter 4, and then correlated to calorimetric assay of poloxamer in filtrated in and out formulations. The results of the latter experiment are presented hereafter in part 4.4 and are also considered for some data in Table 5.6. By measuring temperature of micellization for several P407 aqueous solutions in the 5% to 20% range of concentrations, the relation between T_{mic} and P407 concentration ($C_{\%}$) allowed us to obtain a linear correlation that is fitting by the following equation, $T_{mic} = -0.53 \times C_{\%} + 26.0$ ($r^2 = 0.99999$). P407 concentration will be later determined by calorimetric assay, allowing to recalculate the temperature of micellization (extrapolated T_{mic}) that would correspond to phase transition temperature taking into consideration the polymer concentration decrease due to the filtration. Finally, the extrapolated T_{mic} allows determining the effective variation of temperature of micellization (effective ΔT_{mic}) between the filtered and unfiltered formulations, independently of P407 variation in concentration. The latter result clearly indicates that the effective increase of 4.9 °C for filtrated HLP T_{mic} is due to the poloxamer encapsulation within the liposomes. By similarity, the effective increase of 2.4 °C for filtrated HLP_{out} T_{mic} can be explain by i) a percentage of poloxamer entrapped in the liposomes, and/or ii) a specific interaction between poloxamer and the DOPC. It is noteworthy to mention here that mixtures of unorganized DOPC and poloxamer do not modify the temperature of micellization of poloxamer compared to that of free poloxamer as shown in Chapter 4.

5.4.5. Calorimetric Assay (Baleux Assay)

To determine the quantity of poloxamer entrapped inside the liposomal shell, calorimetric assay was carried out by means of poloxamer/KI_3 interactions. This has been made possible since we demonstrated that DOPC presence does not influence the quantification of poloxamer by such a technique. To evaluate the concentration contribution to calorimetric assay data for filtrated HLP and HLP_{out} formulations, an absorbance *vs.* concentration curve calibration has been established as shown in Figure 5.9. The estimated percentages of entrapped poloxamer for the filtrated HLP and HLP_{out} formulations were 67% and 45%, respectively. The distinguishable data between these two formulations confirm the TEM images previously described. Indeed, HLP have higher amount of entrapped poloxamer than HLP_{out}. Additionally, the results obtained allow us to interpret the DSC data.

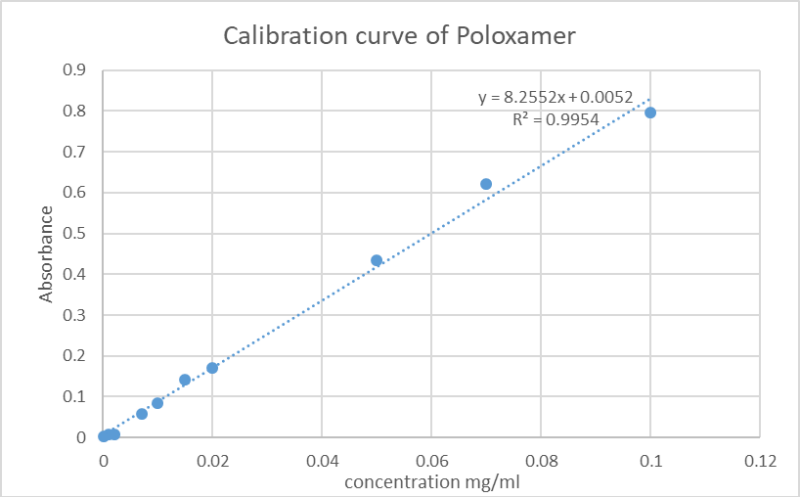

Figure 5.9. Calibration curve for Polaxamer P407 by calorimetric analysis.

5.4.6. Influence of Temperature on HLP Formulations Size

The polymer solutions have the tendency to form micelles by the influence of temperature (Khoshnood et al., 2016). Our main formulation HLP contains poloxamer (P407) which is a thermosensitive polymer that have tendency to form micelles and gel, depending on the concentration and the temperature (Bodratti and Alexandridis, 2018). To evidence the presence of poloxamer inside the HLP and to support the data collected from colorimetric and calorimetric assays, a DLS trendline vs temperature experiment was performed. It gave us the fair reason in support of poloxamer presence by indicating the micellization due to temperature rise. Indeed, we noticed an alteration in size and PDI of the HLPs at a temperature around 25 °C, but not for the liposomes. This temperature was similar to the endothermic peak observed in DSC colorimetric experiment which correspond to micellization. For this experiment, similar

formulations were prepared CL, HLP (P407 0.5%), HLP (P407 5%), HLP_{out}. HLP (P407 0.5%) is an intermediate formulation with a lower poloxamer concentration All the formulations were passed through filtration process to remove the free poloxamer.

This study shows that temperature had no effect on CL formulation in term of size and PDI as there was no poloxamer in the formulation. The HLP (P407 0.5%) has shown slight alteration as the concentration of poloxamer was very low but in case of our main formulation HLP (P407 5%), the size decreases up to 52 nm from 134 to 82 nm and PDI increases from 0.2 to 0.5. Whereas in the case of $HLP_{out,}$ the size decreases only up to 30 nm from 120 to 90 nm and PDI increases from 0.16 to 0.30. These data are consistent with a micellization of the poloxamer which enlarge the distribution of the particles measured by DLS reflected by the PDI increase outside and inside the liposome. We observed that the HLP has biggest size among all the formulation and it also has the maximum decrease in size and maximum increase in PDI, which is the evidence that this formulation contains more Poloxamer than the rest of the formulations and its bigger size indicate the presence of poloxamer inside as shown in Figure 5.10.

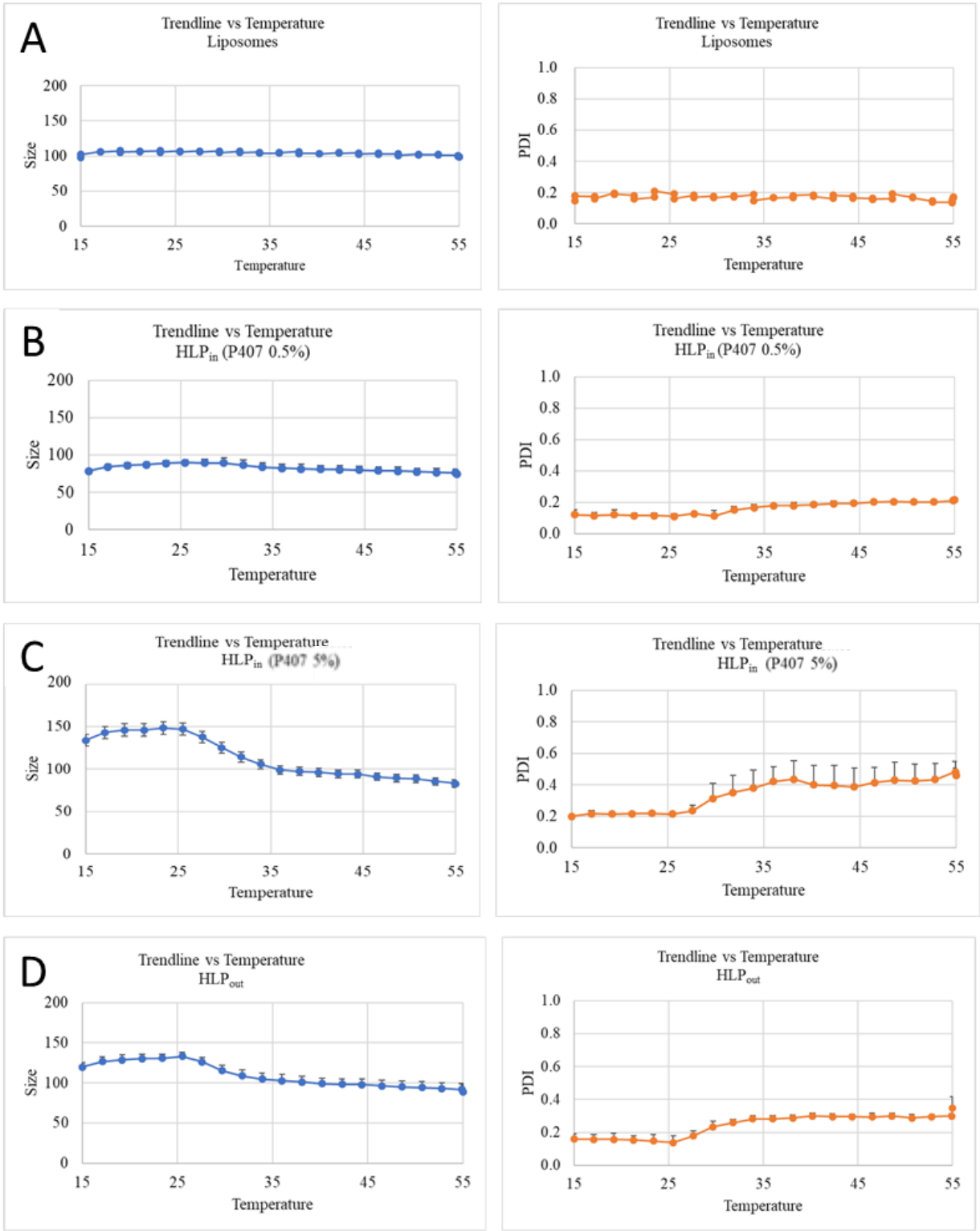

Figure 5.10. Study of the effect of temperature on the size and PDI of formulations A) Liposomes, B) HLP (P407 0.5%), C) HLP, and D) HLP_{out}.

5.4.7. Lipid Poloxamer Interaction Evidence

Thermal analysis at high temperature being concentration dependent on the one hand, and non-quantitative via enthalpy measurements, the sub-ambient temperature range has been considered in order to get more insight into the lipid poloxamer interactions for the HLP formulations. The corresponding DSC curves obtained were analyzed. The onset temperature as well as the enthalpy data of free water, loosely- and tightly-bound freezable water peaks were determined and gathered in Table 5.7. The filtered and non-filtered have presented all the three peaks. Whereas after HLP filtration, the filtrate does not present any Peak II or Peak III, indicating that classic HLP preparation allows a better encapsulation efficiency compared to the HLP_{out} (presence of P407 in the filtrate, *i.e.* outside of the liposome). The fact that Peak III signal is not observed for filtrates of HLPout indicates that P407 outside of the DOPC liposomes induce disruption of the latter, forming micelles with P407 PPO moieties self-assembled within the outer part of the micelle.

Table 5.7. Table represents the onset temperature and the enthalpy data of free water, loosely- and tightly-bound freezable water peaks.

Sample		Tightly-bound water		Loosely-bound water		Free water	
Lipogel		$T_{PeakIII}$ (°C)	$\Delta H_{PeakIII}$ ($mJ.g^{-1}$)	T_{PeakII} (°C)	ΔH_{PeakII} ($mJ.g^{-1}$)	T_{PeakI} (°C)	ΔH_{PeakI} ($J.g^{-1}$)
HLP	nonfiltered	-17.3	28.5	-11.2	382.2	-0.7	290.2
	filtered 1	-16.5	10.5	-7.2	223.0	0.0	295.6
	filtered 2	-16.4	32.7	-6.4	244.4	1.8	329.8
	filtrate 1	----	----	----	----	1.3	326.2
	filtrate 2	----	----	----	----	0.0	325.9
HLP_{out}	nonfiltered	-16.5	41.9	-7.3	867.1	0.8	297.0
	filtered 1	-15.3	127.3	-6.1	533.2	2.3	313.2
	filtered 2	-16.3	120.2	-6.2	428.1	1.7	326.5
	filtrate 1	----	----	-8.6	18.8	-2.0	347.0
	filtrate 2	----	----	-9.1	191.7	-1.1	343.6

5.4.8. Stability

The liposome stability is the limit to which a drug substance or product retains the same properties and characteristics, throughout its period of storage and use (Winterhalter and Lasic, 1993). Stability study of liposome, HLP_{out} and HLP formulations carried in terms of measurement of average size and PDI. The samples (n=3) were kept at 4 °C during the whole experiment of 2 months as shown in Figure 5.11. The results were compared between day 0 and day 58 in terms of average size and PDI. In case of conventional liposomes and HLP no significant difference was observed in terms of their average size and PDI. Whereas in $HLP_{out,}$ formulation, the change in average size and PDI was observed that may be due to presence of substantial amount of P407 which leads to liposomal membrane disruption. The stability study was also discussed previously by Guan et al showing that the stability of liposomes was definitely improved in gel core liposomes (Guan et al., 2015).

The stability of our formulation was notable in comparison of HLP_{out} formulation used as control. This experiment confirms that our main formulation HLP was stable enough and should be considered for next experiments. Therefore, we first assessed its cytotoxicity in two different cell lines.

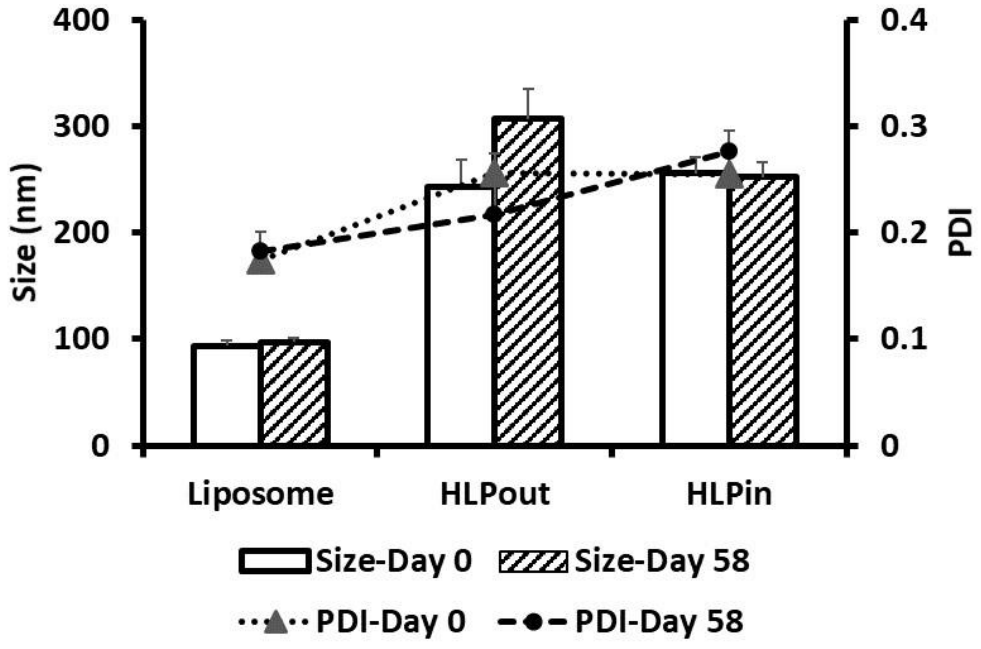

Figure 5.11. Stability test graph corresponds to the difference in size and PDI of conventional liposomes, HLP, and HLP_{out} with in a period of 2 months at 4°C.

5.5. Conclusion

HLP nanoparticles formulation was effectively produced by using syringe pump system. It has been validated as better technique to produce our HLP formulation when compared with dry film hydration and ethanolic injection method. The physicochemical characterization of our HLP systems opens a path for better understanding of formulating vesicles encapsulating polymers. The formation of HLP was confirmed by DSC and density analysis. HLP formulation found to be stable for 2 months of storage. In conclusion, HLP present different physiognomies to be used as controlled drug delivery systems. Our homemade designed syringe pump tubing achieved reproducible, economical, precisely controlled fabrication for the liposomes, HLP formulations which can be scale up with a minimal influence of experimenter.

Chapter 6. Drug Modelling, Encapsulation and Cytotoxicity Assay of Hybrid Liposome/Poloxamer Particles Encapsulating Hydrophilic Anti-Cancer Drug Delivery

6.1. Introduction

The cancer is simply defined as cell growth and uncontrollable cell division. The most common treatments for cancer are surgery, chemotherapy and radiotherapy (Falzone et al., 2018). The main reason behind the failure of chemotherapeutic agents for cancer treatment is the large amount of free drug unable to reach the targeted site, inducing a high toxicity for sane tissues (Olusanya et al., 2018). To reduce their toxicity and enhance their accumulation at the tumor site, the encapsulation of these chemotherapeutic agents has been proposed. This strategy led to a number of different nano-carrier designs, that are mostly composed of lipids or polymers for API delivery at the cancer site (Balzus et al., 2017; Kieler-Ferguson et al., 2017). These advancements in nanomedicine allows innovation in the pharmaceutical field and fascinates scientists more and more. The nano sized formulations are becoming more versatile with continuous improvement in designs (Kumar et al., 2013).

Our project is inspired by the approach of interiorly thickened liposomes instead of coating liposomes from outside, which makes the liposomes more efficient without losing its original characteristics due to outer coating by PEG or other compound, which neglect the direct contact of liposomal membrane and cell membrane.

The poloxamer P407 used in this strategy is a non-ionic triblock copolymer PEO-PPO-PEO (Kamboj and Verma, 2015). The theory behind this study was to exploit the viscosity of the poloxamer solution (Reeve and Hinsberg, 2005) to maintain slightly longer the drug within the liposomes Indeed, liposomes are well known nanocarriers composed of phospholipids designed to potentially carry drugs. However, liposomes suffer in terms of leakage of small hydrophilic drugs. To control the release, a system with lipid shell and polymeric viscous core, namely Hybrid liposome/polymer (HLP), has been designed, which is discussed in detail in chapter 5. This chapter enlightens the efficiency of our nanosystem (HLP) to verify its capacity, safety and release profile.

The main idea behind this study was to evaluate the encapsulation, retention and release kinetics of one model drug and a cytotoxic drug within an HLP system. The factorial design in 3^2 (2 factors at 3 levels) was used for this experimental design. The concentration factor of drug and polymer content was divided in three levels. The nanoparticles were characterized on the basis

of particle size, encapsulation efficiency, and loading content. Then, we studied the cytotoxicity of the designed formulation on two different cell lines, murine fibroblast NIH/3T3 and liver normal epithelial BNL (TIB75) cell lines.

6.2. Materials

DOPC (1,2 Dioleooyl-sn-glycero-3-phosphocholine) was purchased from Avanti polar Lipids (Alabaster, Alabama, USA), Poloxamer 407 (P407), also known by its trade name as Kolliphor P407 was provided by BASF (Ludwigshafen, Germany), Doxorubicin Hydrochloride (Sigma Aldrich, France), Rhodamine B (Sigma Aldrich, France), Iodine and Potassium Iodine were provided by Prolab (Briare, France). Water was purified on Milli-Q system from Millipore (Fontenay-sous-bois, France), Ethanol 96% was purchased from Carlo-Erba reagents (Val-de-Reuil, France). Ultra-filtration units Vivaspin®20 were purchased from Sartorius (Geottingen, Germany), ultra-filtration units NANOSEP 300k was purchased from PALL filtron (Massachusetts, USA), Dialysis device Microfloat-A-lyzer 100 KD was purchased from spectrum laboratories (CA, USA). Polyether ether ketone (PEEK) tubes, T-shaped connectors and ferrules were purchased from I`DEX Health & Science (Oak Harbor, WA, USA).

6.3. Methods

6.3.1. Preparation of the Formulations by Syringe Pump Apparatus

In this work, three formulations were designed: Conventional non-ionic liposomes, Hybrid liposome/poloxamer (HLP) and Hybrid liposome/poloxamer outside (HLP_{out}).

Conventional liposomes (CLs) were prepared by the ethanolic injection method using a syringe pump apparatus (Harvard apparatus PHD 2000). One syringe (1 mL) was filled with ethanolic solution of DOPC (20 $mg.mL^{-1}$, 25.4 $\mu mol.mL^{-1}$) and another syringe (10 mL) was filled with Milli-Q® water containing rhodamine or DOX solution (0.5 $mg.mL^{-1}$ and 5 $mg.mL^{-1}$, respectively). Both syringes were fixed on the syringe pump apparatus, injection speed was set to 0.5 $mL.min^{-1}$ for the lipid solution and 5 $mL.min^{-1}$ for the rhodamine or Doxorubicin aqueous solution. Apparatus ran for 1 min giving final volume of 5.5 mL, yielding a final concentration of DOPC (2 mg/mL, 2.54 $mmol.mL^{-1}$).

Hybrid liposome/poloxamer (HLP) was prepared using the same procedure as liposomes preparation. The rhodamine or Doxorubicin aqueous solution was replaced by poloxamer 407

(P407) solution containing rhodamine or Doxorubicin (0.5 $mg.mL^{-1}$ and 5 $mg.mL^{-1}$, respectively). Ratio of the injection flow rates between the lipid solution and the P407 solution was kept at 1:10 for all experiments. The removal of ethanol was performed using a rotary evaporator. The formulation was collected in an evaporation flask and treated by using a rotavapor (Rotavapor R-144, Büchi, Switzerland) at the following conditions (rotating rate 60 rpm, 35 °C, pressure 10 mbar). These conditions applied for 15-20 min to achieve 25-35% evaporation and 30-40 minutes to achieve 60-65% evaporation of formulation measured by weight which were later adjusted with by adding Milli-Q® water.

6.3.2. Ultrafiltration by Centrifugation

Ultrafiltration column (Pall Filtron, USA) with 300 kDa molecular weight cut-off (MWCO) were used to separate free poloxamer and non-encapsulated rhodamine B from liposomal suspension. The filtration was carried out by centrifugation at 13000 rpm for 30 min in a refrigerated bench-top centrifuge (Hettich Rotanta 460 RF, Germany) at 4 °C.

6.3.3. Dynamic Light Scattering (DLS)

The liposome, HLP and HLP_{out} diameters were determined at 25 °C by quasi-elastic light scattering using a Zetasizer Nanoseries Nano-ZS (Malvern Instruments, France). The scattering was measured at a 173° fixed angle and the position at 4.65. Each sample was run for 3 measurements. Results were expressed as the average hydrodynamic diameter and the standard deviation of the triplicate.

6.3.4. Loading Content and Encapsulation Efficiency

The liposome and HLP formulations encapsulating rhodamine B (0.5 $mg.mL^{-1}$) or doxorubicin (5 $mg.mL^{-1}$)were filtered as described in section 3.3. The sample remained on the filter was re-suspended with Milli-Q® water in order to make up to the initial volume and quantified by spectrofluorometer using a Varian CARY® spectrofluorometer at excitation 490 nm and emission 580 nm for rhodamine and at excitation 490 nm and emission 595 nm for doxorubicin. linearity was checked for standard solutions with concentration ranging from 0.075 to 1 $\mu g.ml^{-1}$ for rhodamine and 1 to 25 $\mu g.ml^{-1}$ for doxorubicin. Rhodamine and doxorubicin concentration of samples were calculated using calibration curve with r^2 of 0.98 and 0.97, respectively. The solutions of rhodamine B and rhodamine B with P407 5% were taken as controls. Loading content and encapsulation efficiency were calculated by using the following equations:

$$Loading\ Content\ (\%) = \left(\frac{weight\ of\ loaded\ drug}{weight\ of\ drug\ loaded\ particles}\right) \times 100$$

$$Encapsulation\ Efficiency\ (\%) = \left(\frac{weight\ of\ loaded\ drug}{weight\ of\ drug\ in\ feed}\right) \times 100$$

6.3.5. *In Vitro* Release

A stock solution of rhodamine B (0.5 $mg.mL^{-1}$) was used to prepare two different samples: solution of rhodamine B encapsulated within liposomes and rhodamine B encapsulated within HLP formulation. Dialysis device (Micro Float-A-Lyzer, France) was filled with the required volume of each sample and kept floating in a beaker with PBS at 37 °C using an agitation rate of 60 rpm, volume of medium to volume of sample ratio was fixed at 1:1000. At defined points, 1 mL of samples were removed from the release medium and replaced with fresh PBS to maintain the volume constant. The amount of rhodamine B released was monitored by spectrofluorometer (Varian CARY®) at 580 nm. *In vitro* release test was performed in triplicates. A similar procedure was followed for Doxorubicin Phosphate (5 $mg.mL^{-1}$) release study.

6.3.6. Cytotoxicity Tests

The murine fibroblast NIH/3T3 (ATCC® CRL1658™) and liver normal epithelial BNL 1ME A.7R.1 (ATCC® TIB75™) cell lines were purchased from the American Type Culture Collection (ATCC, Manassas, USA). The cell line NIH/3T3 was grown at 37 °C and 5% CO_2 in DMEM containing 2 mM L-glutamine, 100 U/mL penicillin and 100 µg/mL streptomycin, 10% bovine serum, whereas cell line BNL was grown in the same medium just replacing the bovine serum by a fetal one. Cells were plated onto 96-well plates at 20000 cells per well in 100 µL of culture medium. Twenty-four hours after plating, 100 µL of medium containing the compound of interest (final concentrations ranging from 0.06-2 mg/mL in terms of lipid or 1.5-50 mg/mL in terms of P407, in 2-fold dilutions) was added to the wells. After 24h of exposure, the cell viability was evaluated using the MTT test. Then, the absorbance was read at 560 nm in a microplate reader (Infinite F200 Pro - TECAN). Results are expressed in percent of viability compared to the same concentration of solvent.

6.3.7. Statistical Analysis

The graph Pad Prism software was used to analyses the data and determine statistical significance between groups for cytotoxicity and release test. Cytotoxicity experiment data was treated with Gaussian nonlinear regression fit and two-way ANOVA was applied $p<0.001$, ***. The release test graphs presented one phase decay nonlinear regression fit and student t test was applied $p=0.0001$, ***. All the experiments were performed in triplicates.

6.4. Results and Discussion

6.4.1. Effect of Variables on Drug Modelling

The literature lack of full information about the different factors that affects encapsulation and particle sizes (Ghanbarzadeh et al., 2014a). This study highlights the modelling of drug for better insight of the effects of variables in our formulations which are generally not described in lots of other formulations in the literature. In our work, instead of encapsulating the drug directly into our formulation, we designed a drug modelling as an intermediate way to confirm and analyze the effects of some independent variables on our formulations. For this we developed the factorial design as 3^k, where 3 denotes the levels of the variation of the chosen factors and k denotes the factors affecting the development (Kumar et al., 2014). This experimental design simplify the technique to achieve the cause-effect relationship between each individual variables in our formulations with the least experimental work, and reproducible results (Ghanbarzadeh et al., 2014b). The two variables were focused, the concentration of poloxamer and rhodamine as shown in Table 6.1. The three levels were defined and total nine formulations were prepared for encapsulation efficiency and characterization of CL and HLP. The formulations were prepared according to the poloxamer concentration which are CL (0% P407), HLP (0.5% P407) and HLP (5% P407). Each formulation was then divided into three categories according to the encapsulated rhodamine concentration.

Table 6.1. Factors and levels for the experimental design

Variables	Units	Levels		
		0	1	2
Rhodamine concentration	[mg/mL]	0.01	0.05	0.5
P407 concentration	%w/v	0	0.5	5

These variables are the concentration of the polymer in the nanoparticles and the drug itself. Rhodamine B was used as drug model for this experimental design. This evaluation helped us to understand the detailed technical modifications in our formulation and to confirm the exact effect due to individual variables, such as concentration of P407 and Rhodamin, on liposomes and HLP performance and characteristics.

The mean of the encapsulation efficiency, particle size, PDI and loading capacity for the 9 formulations of the batches prepared is presented on table 2 with the respective standard deviation. Each formulation was prepared in 3 different batches to confirm the results and to ensure the reproducibility.

Three levels of concentrations were chosen for each factor, which were defined on the basis of the single factor experiment result and possibility of preparing liposome samples at the maximum and minimum levels. The results show the hydrodynamic diameter, PDI, encapsulation efficiency, and loading content as shown in the Table 6.2.

Table 6.2. Encapsulation efficiency percent (EE%), loading capacity (LC%) and particle size (PS) values for nine prepared formulations with different concentration of P407 and Rhodamine

Formulation	P407 w/v%	Rhod mg/mL	EE% ± SD	LC% ± SD	Size ± SD	PDI ± SD
F1	0	0.05	57 ± 4.3	1 ± 0	129 ± 38	0.13 ± 0.01
F2	0	0.25	74 ± 8	9 ± 1	100 ± 27	0.15 ± 0.02
F3	0	0.5	81 ± 6.2	20 ± 2	95 ± 0.9	0.20 ± 0.01
F4	0.5	0.05	71 ± 9	2 ± 0	126 ± 32	0.23 ± 0.02
F5	0.5	0.25	76 ± 3.6	9 ± 0	116 ± 3.2	0.23 ± 0.01
F6	0.5	0.5	77 ± 2	19 ± 0.5	108 ± 1.8	0.20 ± 0.09
F7	5	0.05	63 ± 1.5	2 ± 0	178 ± 77	0.26 ± 0.02
F8	5	0.25	73 ± 8	9 ± 1	130 ± 14	0.19 ± 0.01
F9	5	0.5	75 ± 4	19 ± 1.1	125 ± 6.5	0.20 ± 0.02

Examining the values obtained for encapsulation efficiency of CL and HLP for rhodamine, the values obtained show dependence on the drug content. The calibration curves for different concentration of P407 and Rhodamine are shown in Figure 6.1. The difference in the EE% between the CL and HLPs is more pronounced in the case of the least levels of drug for both cases.

The loading content show the same behavior in both cases (CL and HLP), there is a difference when examining the formulations with lowest amount of drug, but when the initial drug concentration was increased, the values got close to each other. The EE% and LC% values can mean that the system is saturated when using high quantity of drug (Crommelin and van Bloois, 1983), which is not allowing a difference between the encapsulation values. (Moghimi and Hunter, 2000).

The average size of each formulations is within the range of 95-180 nm and PDI was in the range of 0.13-0.26. The average size of each formulation was suitable and fall in the range of the appropriate size of delivery systems aimed at crossing biological barriers when compared with the literature (Gaumet et al., 2008).

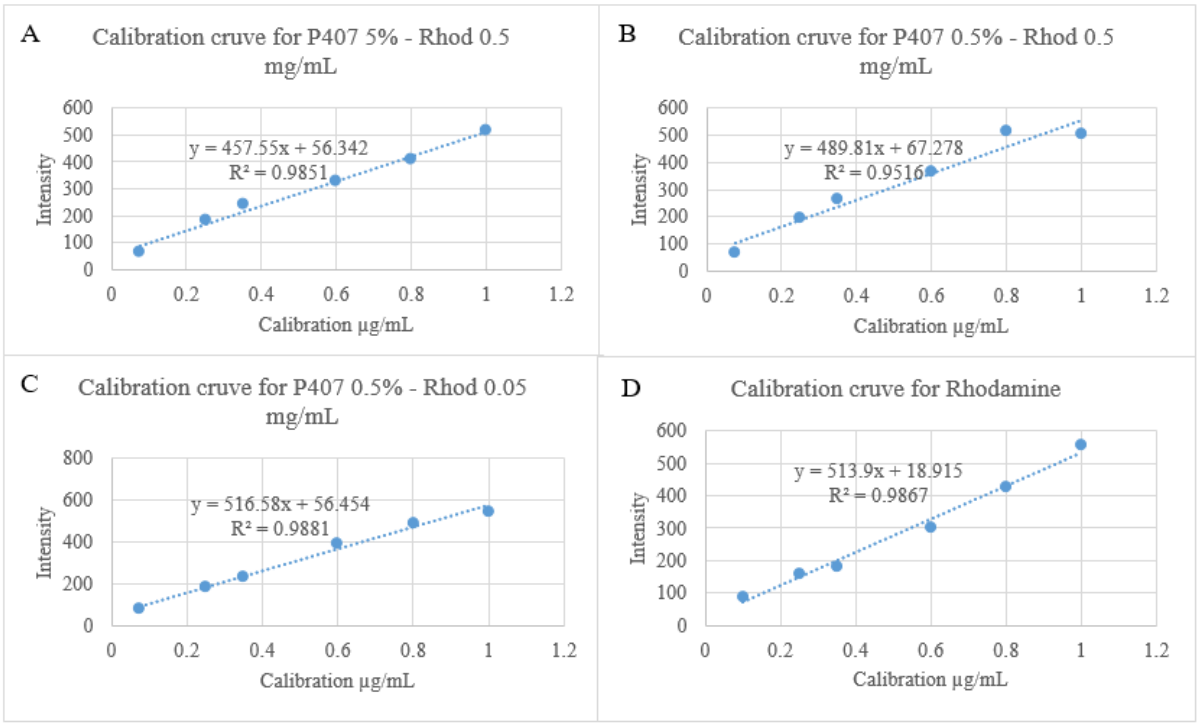

Figure 6.1. Calibration curve for different poloxamer and rhodamine concentration, A) P407 5% - Rho 0.5 mg.mL^{-1}, B) P407 0.5% - Rho 0.5 mg.mL^{-1}, C) P407 0.5% - Rho 0.05 mg.mL^{-1} and D)Calibration curve P407 0% - Rhodamine mg.mL^{-1}.

6.4.2. Encapsulation Efficiency and Loading Content.

The main idea to design this lipid/polymer hybrid a carrier was to improve the encapsulation and/or the release kinetic of hydro-soluble drugs. For the evaluation of encapsulation ability, Rhodamine B was used as a model drug and doxorubicin as a drug. As described above, nine different formulations were prepared with different concentrations of P407 (0%, 0.5%, and 5%) and drug solution (0.01 $mg.mL^{-1}$, 0.05 $mg.mL^{-1}$, and 0.5 $mg.mL^{-1}$) were used to evaluate the effect of the initial drug solution concentration on the encapsulation efficiency and loading content. Rhodamine or doxorubicin were added in H_2O or P407 solution and encapsulated during the preparation of conventional liposomes (CL) and hybrid liposome/polymer HLP (Poloxamer 5%), respectively. The encapsulation efficiency and loading content of HLP were compared to those of liposomes (Figure 6.2 A for rhodamine and B for doxorubicin). For both nanosystems, EE % and LC % were increased for both drugs when increasing the initial concentration. Differences in encapsulation values between CLs and HLP were significant for the low initial concentrations of drugs. It was previously reported that the interior content of liposomes is a key factor for increasing encapsulation (Guan et al., 2015). This implies that the incorporation of rhodamine in thickened liposomes should have been greater than encapsulating rhodamine in empty liposome. However, no difference was observed at the highest concentrations, 0.5 $mg.mL^{-1}$ and 5 $mg.mL^{-1}$ for rhodamine and doxorubicin, respectively.

To examine if these two formulations could exhibit a different release kinetics, a release study was carried out on these two formulations. The highest concentrations for both drugs were used for the release study, this choice was made considering the volume of the release medium and the limit of detection of the spectrofluorometer.

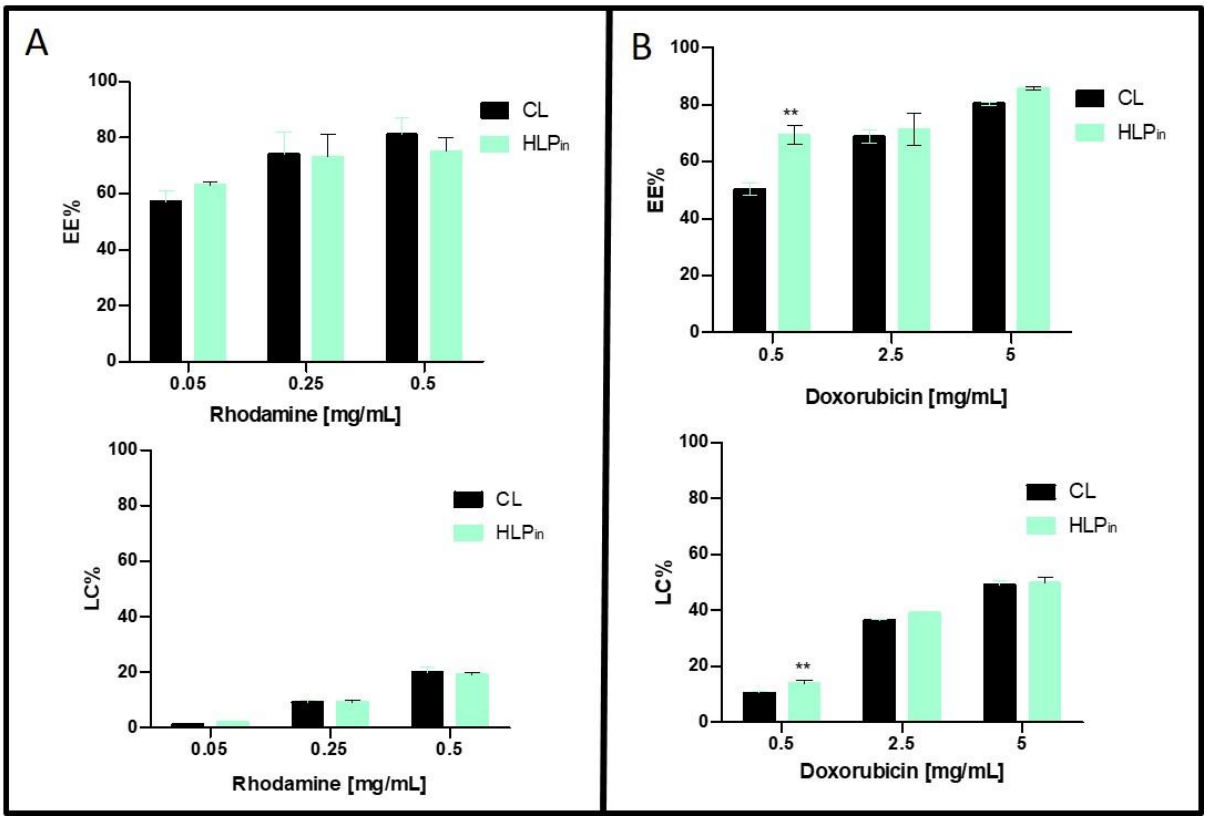

Figure 6.2. A) Encapsulation efficiency and loading content of rhodamine B inside Cls and HLP. B) Encapsulation efficiency and loading content of doxorubicin inside Cls and HLP. Two-way ANOVA p=0.01, **.

6.4.3. *In Vitro* Release Kinetics

In vitro release studies were conducted to determine the difference between drug solutions (rhodamine or doxorubicin), encapsulated drug in liposomes and HLP for 24 hours (Figure 6.3 and 6.4, respectively). All the experiments were performed in triplicates at 37 °C. The half-life of rhodamine solution, rhodamine release from CL and HLP were close around 1.83, 1.34 and 2.18 hours, respectively. However, the final release from these formulations after 24 h was significantly different. It reached 94% for the rhodamine solution, 91% for CL and only 73% for HLP. This significant variance is probably due to the viscous core of HLP which lead to a slower release of rhodamine.

In vitro kinetics were also carried out with doxorubicin. The final release of doxorubicin from these formulations after 30 h was significantly different which was 96% for the doxorubicin solution, 56% for CL and 89% for HLP. Interestingly, the release of doxorubicin from HLP displayed delayed release of drug comparing to CLs. The amount of doxorubicin released

during the first hour was relatively lower as compared to the one of CLs. Noteworthy, HLP exhibited a release half-life of doxorubicin 3 times higher than the one with CL. This substantial variation between the CLs and HLP might probably be attributed to the inner core viscosity of HLP which led to delayed and slower release of doxorubicin.

The release of doxorubicin from CLs reached to a plateau around 4 hours whereas a large part of drug payload remained associated to the nano system. In contrast, a continuous release throughout the experiment was observed in the case of HLP, this may be explained by the presence of poloxamer in the nano system which released into the release medium that improving the Dox solubility. The characteristic of poloxamer to keep the drugs solubilized and stable in term of their size has been described in previous literature. (Bodratti and Alexandridis, 2018; Couillaud et al., 2019; Devi et al., 2013).

If we compare HLP to Gelliposomes (GLs) formulation described in the literature by Zhang et al, the kinetic profile of our formulation was in first order and not biphasic. This could be explained by the fact that the HLP core was viscous but not gelified like GLs. Moreover, the sustained release of the rhodamine and Dox in HLP was faster than GLs which have a relatively bigger particle size (1.2µm) and higher amount of poloxamer.

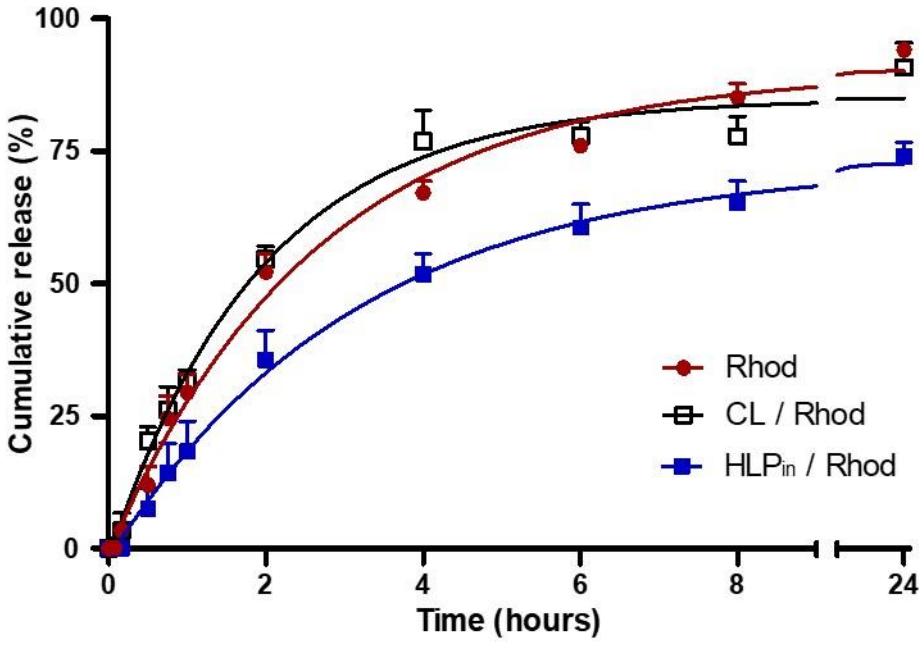

Figure 6.3. Release of Rhodamine B from nonionic lipids vesicles with and without poloxamer. Formulation composition: (•) Rhodamine solution, (▫) Liposome encapsulating Rhodamine, (▪) HLP encapsulating Rhodamine. One phase decay nonlinear regression fit and student t test p=0.0001, ***.

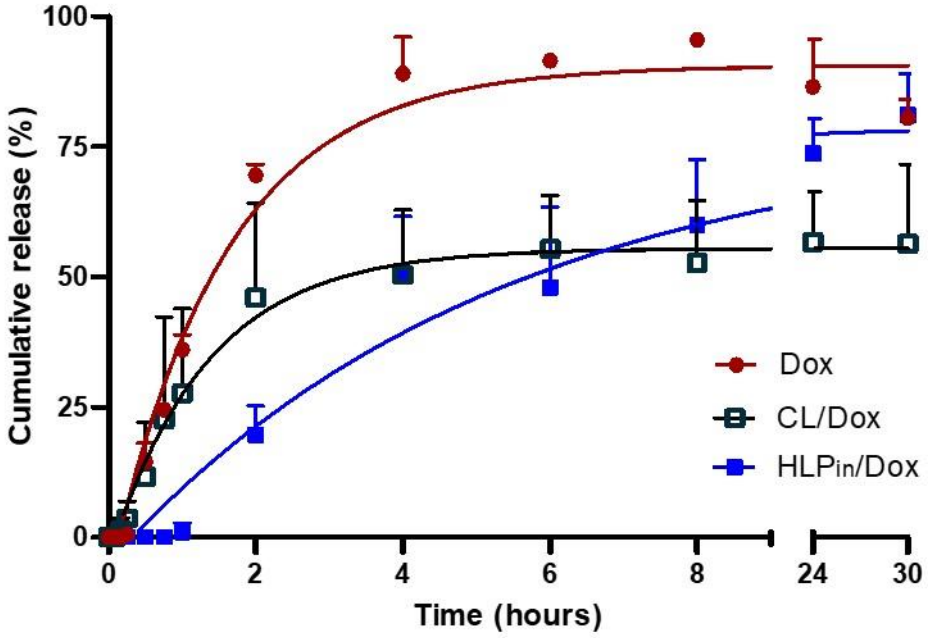

Figure 6.4. Release of Doxorubicin from nonionic lipids vesicles with and without poloxamer. Formulation composition: (•) Doxorubicin solution, (▫) Liposome encapsulating Doxorubicin, (▪) HLP encapsulating Doxorubicin. One phase decay nonlinear regression fit and student t test p=0.0001, ***.

6.4.4. Cytotoxicity

To investigate the cytotoxicity of our formulations *in vitro*, the study was carried out on two different mouse cell lines, NIH 3T3 fibroblast and BNL epithelial liver cells because they both are suitable for transfection studies. Both the cell lines were treated with each formulation (CL, HLP_{out}, HLP, and P407 10%). The viability results for each cell lines are presented in Figure 6.5 A and B, as a function of lipid (left) and P407 concentration (right).

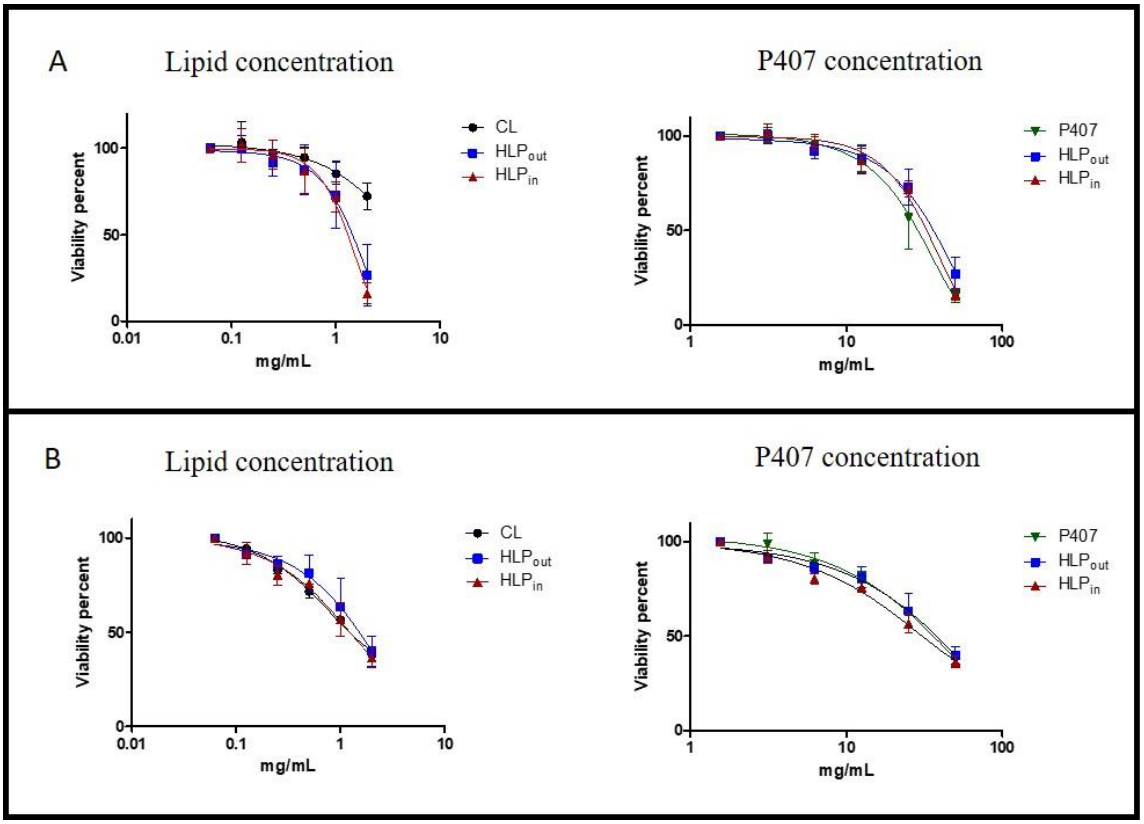

Figure 6.5. *In vitro* cell viability curves A) Graphs for cell line NIH/3T3 cell viability in relation of Lipid and P407 concentration, left and right respectively B) Graphs for cell line TIB75 cell viability in relation of Lipid and P407 concentration, left and right respectively. Gaussian nonlinear regression fit, and two-way ANOVA was applied $p<0.05$.

The mean inhibition concentration 50 (IC50) values determined for each curve is shown in Table 6.3. Cytotoxicity results obtained for HLP and HLP_{out} formulations in both cell lines were similar to the cytotoxicity of conventional liposomes and poloxamer P407.

Table 6.3. IC50 ($mg.ml^{-1}$) values as function of Lipid and P407 on NIH/3T3 and BNL cells

Cell lines		CL	HLP_{out}	HLP	P407
NIH 3T3 (IC50)	Lipid	>2	1.4 ± 0.1	1.5 ± 0.2	--
	P407	--	37.9 ± 5.5	35.2 ± 5 .8	28.1 ± 7.6
BNL (IC50)	Lipid	1.3 ± 0.2	1.5 ± 0.4	1.3 ± 0.2	--
	P407	--	36.6 ± 12.8	32.7 ± 7.0	38.5 ± 4.7

In BNL cell line the IC50 value was approximately 1.5 mg/mL in terms of lipid and 35 mg/mL in terms of P407. However, on NIH/3T3 cells, liposome showed low toxicity with 80% of

viability at 2 mg.mL^{-1} of lipids ($p<0.001$, ***). Hybrid lipid/poloxamer formulations induced a little toxicity in NIH3T3 cell line, probably due to P407 because IC50 was around 35 mg.mL^{-1} The MTT assay revealed no cytotoxicity over the concentration of poloxamer in our preparations (approximately 30 mg.mL^{-1} for HLP and 25 mg.mL^{-1} for HLP_{out}, measured after filtration by calorimetric assay). This can be ascribed to the biocompatible nature of lipid and poloxamer in our formulations.

6.5. Conclusion

All the formulation encapsulating drugs were effectively produced by using syringe pump system. We have shown previously that the poloxamer inside the liposome could provide a higher density to the internal core of liposomes as regard to conventional liposomes. This increased density did not increase the encapsulation of small molecules such as rhodamine or doxorubicin. However, we observed that the release kinetic was improved when adding poloxamer in. The encapsulation and loading content percent can be influenced by the alteration of polymer and drug concentration up to certain concentration. In our study, the initial drug concentration was the most significant factor affecting the encapsulation efficiency and loading capacity. The range of poloxamer did not influence the concentration, and probably a larger amount of poloxamer would be needed to impact the encapsulation efficiency, however it is possible that other polymers could also be chosen in order to increase the viscosity of the core, such as gelatin, PEI, different type of poloxamer and others for different application or nature of the drug.

In vitro release of HLP showed slow release in comparison of CL in 24 hours for rhodamine and 30 hours for doxorubicin. The release study showed that the drug release from HLP is delayed from the one of conventional liposomes. Moreover, the HLP formulation had shown no cytotoxicity.

We have established in this first study that HLP system is a potential delivery system for therapeutic application due to the characteristics of delayed drug release, and possess the same loading capacity as CL. The system could still benefit from improvement by modifying the polymer or its concentration, however, we thought that the current HLP system could be further studied for the encapsulation of different drugs with different characteristics. To establish the size range of hydrophilic molecules which could benefit from the system, we evaluated in the next chapter the possibility to encapsulate small nucleic acids, such as siRNA.

Chapter 7. Conception of Positively Charged Hybrid Liposome/Poloxamer Nano Carriers for siRNA Delivery

7.1. Introduction

Liposomes formulations are the most studied and the first FDA approved nanoparticles for drug delivery. Liposomes are utmost nano-carriers to encapsulate a high number of different drug molecules for clinical application. Liposomes still suffers in terms of the small hydrophilic drugs leakage, fast release and tendency to fuse with each other. In order to cope with these limitations, we intended to formulate lipidic auto-assembled nanoparticles with polymers in order to form liposomes with a viscous internal core, we called Hybrid liposome/polymer (HLP). HLP formulation and characterization have been discussed in chapter 5 and in our publication (Ahmed et al., 2019). Interiorly thickened core liposomes have been described before (Zhang et al., 2013), however, the HLP we reported, was the only described system with a quantification of the amount of poloxamer encored in the liposomes. The quantification of poloxamer was monitored by the help of differential scanning calorimetry (DSC) and colorimetric analysis by UV spectrophotometer.

In our previous study, we have shown that small molecules such as rhodamine and doxorubicin could be encapsulated into HLPs with E.E% around 75%. To enlarge the application of our HLPs, we were interested to know if they would be able to carry a small nucleic acid, such as siRNA, solely by physical encapsulation related to viscosity, or if the addition of a small amount of positive charges would be necessary for siRNA encapsulation and retention. For this purpose, we introduced the cationic lipid DMAPAP (RPR209120) or the polymer PEI known for their high transfection ability (Ewe et al., 2017; Höbel and Aigner, 2010; Tranchant et al., 2004).

The cationic lipid, DMAPAP 2-{3-[bis-(3-amino-propyl)-amino]-propylamino}-N-ditetradecyl carbamoyl methyl-acetamide (RPR209120), synthesized in our lab, UTCBS as shown in Figure 7.1 (Breton et al., 2011; Tranchant et al., 2004). DMAPAP lipids have been used as gene delivery vector in many studies (Ficai and Grumezescu, 2017; Manta et al., n.d.; Valero et al., 2018). Non-ionic HLP formulation was prepared to encapsulate the small hydrophilic drugs. In order to see whether cationic lipid was needed to encapsulate more efficiently siRNA, DMAPAP was added to the HLP formulation within the lipid part.

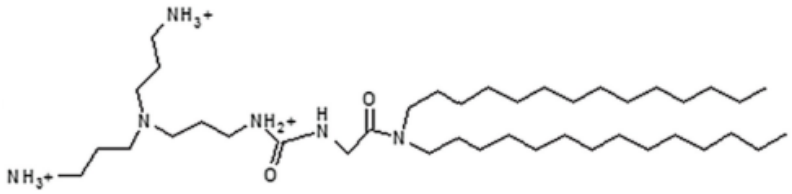

Figure 7.1. Structure of DMAPAP lipid

Polyethylenimines are synthetic water-soluble polymer, with linear or branched chains as shown in Figure 7.2 (Tang and Szoka, 1997). PEI is high in cationic charge density potential polymer that can be highly protonated due to abundance of nitrogen group in its structure, which forms 'proton sponge', a polymeric network (Boussif et al., 1995). It forms non-covalent complex with siRNA. The complex protects the siRNA from degradation and increase their intracellular release and uptake (Höbel and Aigner, 2010). PEI has advantages over other transfecting agents as it has high transfection efficiency with almost no toxicity in cells. PEI transfecting technique is also cost effective in comparison to other commercially available transfecting agents (Wirth et al., 2011). In our project, we decided to use PEI in parallel study with DMAPAP lipid to see the difference in the performance of the two formulations in terms of their encapsulation and release of siRNA. PEI was used in minimum quantity to see the encapsulation with minimum cationic charges and added as the polymeric component.

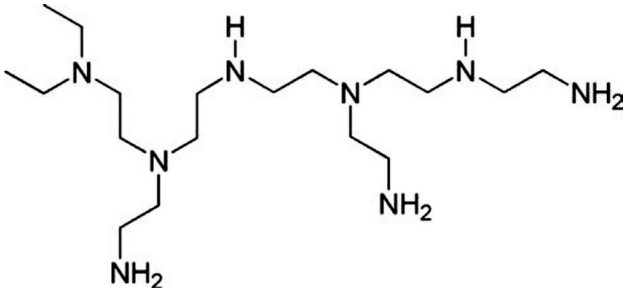

Figure 7.2. Structure of Polyethylenimine (Branched)

In order to produce positively charged HLPs, we merged two methods, ethanolic injection and microfluidics, as described in chapter 5. A syringe pump device connected with a home-made designed tubing system was applied to produce nano-sized Hybrid liposome/poloxamer particles. The aim of this study was to formulate and select the best formulation for siRNA delivery among conventional liposomes (CL) and HLP formulation with or without cationic charges. The formulations were characterized by dynamic light scattering and nanoparticle

tracking analysis. *In-vitro* experiments have been carried out on GFP expressing endothelial cells in 96 wells plate and 3D micro-chip cell culture, in the presence and absence of TNF-α. Confocal imaging was carried out for qualitative and quantitative analysis. Noteworthy, the *in vitro* experiments have been performed during my stay in Canada, in Mc Gill University where I stayed for one and a half months, from October to November 2019.

7.2. Materials

DOPC (1,2 Dioleooyl-*sn*-glycero-3-phosphocholine) was purchased from Avanti polar Lipids (Alabaster, Alabama, USA), poloxamer 407 (P407), also known by its trade name as Kolliphor P407 was provided by BASF (Ludwigshafen, Germany), Polyethylenimine, branched (Sigma Aldrich, USA), DMAPAP (UTCBS laboratory, France). Water was purified on Milli-Q system from Millipore (Fontenay-sous-bois, France), Cationic lipids DMAPAP (2-{3-[Bis-(3-amino-propyl)-amino]-propylamino}-*N*-ditetradecyl carbamoyl methyl-acetamide, or dimyristoylaminopropylaminopropyl) were synthesized as described in previous publication (Mignet et al., 2008), Chloroform (was purchased from Carlo-Erba reagents (Val-de-Reuil, France), and Ethanol 96% was purchased from Carlo-Erba reagents (Val-de-Reuil, France). Ultra-filtration units Vivaspin®20 were purchased from Sartorius (Geottingen, Germany), ultra-filtration units NANOSEP 300k was purchased from PALL filtron (Massachusetts, USA), Dialysis device Microfloat-A-lyzer 100 KD was purchased from spectrum laboratories (CA, USA), Polyether ether ketone (PEEK) tubes and T-shaped connectors and ferrules were purchased from IDEX Health & Science (Oak Harbor, WA, USA), Micro-chip 150 x 150 mm (Eden Microfluidics, France).

7.3. Methods

7.3.1. Preparations of the Formulations

7.3.1.1. Preparation of Cationic Conventional Liposomes and Cationic Hybrid Liposomes/Poloxamer Nanoparticle with DMAPAP and siRNA

Cationic conventional liposomes (CLs) were prepared by the ethanolic injection method using a syringe pump apparatus (Harvard apparatus PHD 2000). One syringe (1 mL) was filled with ethanolic solution of DMAPAP and DOPC with a ratio 1:10 (20 $mg.mL^{-1}$) and another syringe (10 mL) was filled with Milli-Q® water containing siRNA (30 nM). Both syringes were fixed on the syringe pump apparatus, injection speed was set at 0.5 $mL.min^{-1}$ for the lipid solution and 5 $mL.min^{-1}$ for the aqueous solution. Apparatus ran for 1 min giving a final volume of 5.5

mL, yielding a final concentration of DMAPAP and DOPC at 2 mg/mL with a ratio 1:10. Cationic hybrid liposome/poloxamer (HLP) was prepared using the same procedure as liposomes preparation, apart from that the aqueous phase was replaced by a solution of poloxamer 407 (P407) containing siRNA (30 nM) at concentration (5% w/v) with flow rates fixed at 5 $mL.min^{-1}$.

7.3.1.2. Preparation of Cationic Conventional Liposomes and Cationic Hybrid Liposomes/Poloxamer Nanoparticle with PEI and siRNA

Cationic conventional liposomes and cationic hybrid liposome/poloxamer (HLP) with PEI prepared with the same procedure which is described in Chapter 6. Cationic conventional liposomes (CLs) were prepared by the ethanolic injection method using a syringe pump apparatus (Harvard apparatus PHD 2000). One syringe (1 mL) was filled with an ethanolic solution of DOPC (20 $mg.mL^{-1}$, 25.4 $\mu mol.mL^{-1}$) and another syringe (10 mL) was filled with Milli-Q® water containing siRNA (30 nM) and PEI (30 $\mu g.mL^{-1}$). Both syringes were fixed on the syringe pump apparatus, injection speed was set at 0.5 $mL.min^{-1}$ for the lipid solution and 5 $mL.min^{-1}$ for the aqueous solution. Apparatus ran for 1 min giving final volume of 5.5 mL, yielding a final concentration of DOPC (2 mg/mL, 2.54 $mol.L^{-1}$). Hybrid liposome/poloxamer (HLP) was prepared using the same procedure as liposomes preparation. The aqueous phase was replaced by poloxamer 407 (P407) solution containing siRNA (30 nM) and PEI (30 $\mu g.mL^{-1}$) (ratio PEI/Poloxamer:) at concentration (5% w/v) with the flow rates 5 $mL.min^{-1}$.

7.3.2. Dynamic Light Scattering (DLS)

The cationic liposome, cationic HLP diameters were determined at 25 °C by quasi-elastic light scattering using a Zetasizer Nanoseries Nano-ZS (Malvern Instruments, France). The scattering was measured at a 173° fixed angle and the position at 4.65. Each sample was run for 3 measurements. Each formulation prepared at least three times, measured and the results were expressed as the average hydrodynamic diameter and the standard deviation.

7.3.3. Nanoparticle Tracking Analysis

Nanoparticle Tracking Analysis (NTA) was conducted to measure the size of cationic CL and HLP nanoparticles by NanoSight 300 (NanoSight, Amesbury, United Kingdom) with a 640 nm laser at t = 25°C. Each formulation was diluted 1/500 in Milli-Q and measurements were performed in dynamic flow mode controlled with built in syringe pump at level 60. The particle

size is reported as hydrodynamic diameter, determined by following the 2-D trajectory of each particle over a tracking time with the Software NanoSight NTA 3.4.

7.3.4. Ultrafiltration by Centrifugation

Ultrafiltration columns (Pall Filtron, USA) with 300 kDa molecular weight cut-off (MWCO) were used to separate free poloxamer and non-encapsulated siRNA from CL and HLP formulations. The filtration was carried out by centrifugation at 13,000 rpm for 30 min in a refrigerated bench-top centrifuge (Hettich Rotanta 460 RF, Germany) at 4 °C.

7.3.5. Gel Electrophoresis

Gel electrophoresis was performed to verify the encapsulation of siRNA in the formulations as described in section 3.1. The formulations were filtered before performing gel electrophoresis. The mixtures were loaded into 1% (w/v) agarose gel at 80 V/cm in TAE buffer (40 mM Triacetate and 1mM EDTA at pH 8.3) siRNA was revealed with EtBr and visualized under UV light.

7.3.6. Ribo Green Assay

The siRNA formulation was diluted with 100 µL TE buffer to make 2 µg/mL. This concentration was further diluted to prepare the different concentration for calibration curve. One hundred microliters of each concentration were transferred to a 96-well plate. A total of 100 µL of diluted RiboGreen dye (1:200 dilutions in Tris-EDTA (TE) buffer) was added to each siRNA concentration. Fluorescence measurements were made after 5 minutes of incubation at ambient temperature using a TECAN instrument (at emission wavelength 525 nm). The quantification of siRNA encapsulated was carried out by the same procedure which is discussed earlier for calibration curve. After filtration the siRNA in the filtrate of each sample was quantified on the basis of which quantity of encapsulated siRNA was determined. All measurements were corrected for background fluorescence from a solution containing only buffer and RiboGreen dye.

7.3.7. Microchip Fabrication

7.3.7.1. Tube Channels Embossing

The microchip fabrication was carried out by cutting wire 1 mm in diameter with desired length using a razor edge or a wire cutter. The hot embossing press (Eden microfluidics) was heated up till 170 °C until the temperature was stabilized. Following sandwich was made, from top to bottom: teflon sheet-counter mold-Flexdym foil- wire mold - silicon substrate - teflon sheet. The sandwich was pressed for $90s$. Pressure was removed and sandwich was gently taken out and cooled slowly. Teflon sheet was removed, and sandwich was gently demolded by using isopropyl alcohol. The holes were punched at the end of each tube for inputs and outputs. Molded foil was dried with nitrogen or pressurized air and placed in a covered dish to avoid dust contamination. Embossed foils placed into the UV-ozone cleaner and exposed to the device for $30min$ with 70% ethanol for sterilization.

7.3.7.2. Studs Fabrication

The aluminum mold was heated at $215°C$, until temperature was reached and stable. Each slot was filled with Flexdym beads and waited for 30 min. More beads were added till each slot was completely filled. Mold was removed, cooled down and demolded with isopropyl alcohol. Each stud was pierced with a syringe needle of the proper gauge (18 or 21, i.e. $574\mu m$). The needle was heated by using a flame before removing gently through the stud. The studs at $180°C$ were baked on a Si wafer to transfer the Si smoothness. Each stud was pressed gently, after one minute the wafer was removed and cooled down before collecting the final studs.

7.3.7.3. Assembly of the Microchip

The microchannel layer of smooth embossed Flexdym sheet overlaid on smooth Flexdym sheet which was already overlaid on a coverslip. Studs were positioned on the punched inputs and outputs and baked for at least $30min$ in an oven at $80°C$. Chips were exposed to powerful UV for less than a 1 minute (Dymax, light curving systems) for sterilization. Chips were rinsed successively with 70% ethanol, sterilized mQ/PBS and finally 0.1% sterile gelatin solution. Then microdevices placed in a humidified $37°C$ incubator overnight.

7.3.8. Three-Dimensional Cell Culture in Micro-Chip

Endothelial cells at a concentration of 1.5 million cells/mL in Endothelial growth medium (EGM-2) containing 4% dextran sulfate was injected through the inputs of each micro-channel. Chips were placed in upside down position to favor seeding on the top side and incubated at $37°C$ for 30 mins . Then, chips were seeded again and placed upright position to favor the bottom side seeding. Medium was changed after every 2 hours (EGM-2 medium) two times. TNF-a (20ng/mL in DMEM/F12) was added on the same day after seeding. Incubate the chip overnight. Cells were treated with the formulations incubated for 4 hours and then replaced with EGM-2 medium and incubated overnight.

7.3.9. Fixation and Staining of Cells for Confocal Imaging

After cell treatments the microchannels were rinsed twice with PBS. Paraformaldehyde 4% in PBS was injected and incubated for 15min at room temperature protected from light. Again, the cells were rinsed twice with PBS. Cells were rinsed with PBS-T (0.1% Tween-20) for staining of intracellular structures (Actin and DAPI), and injected with PBS containing 0.1% Triton X-100 for permeabilization, incubated at room temperature for 10min and then again rinsed with PBS-T. For Blocking non-specific binding sites cells rinsed with PBS-T containing 1% BSA and incubated for 30min followed by PBS-T rinsing. Finally, cells were incubated with mixture of phalloidin-i594 (Abcam, 1/1000 in PBS-T) and DAPI (1/2000 from 10 mg/mL stock in PBS-T) for 30min and rinsed with PBS-T twice.

7.3.10. GFP Fluorescence Quantification

Fiji ImagJ-win64 software was used to quantification analysis of GFP fluorescence. The same images were selected as qualitative analysis. The image was split into multi-color into single channels and then to grayscale before proceeding. The binary image was created, and threshold was adjusted to highlight the structures to measure. Later, background was subtracted to neglect the noise and background pixels. The binary version of the image was created with only two-pixel intensities: black = 0 and white = 255. The binary image was selected, and particles were analyzed. The numbers appeared corresponded to data for individual image in “Display Results” option which later transferred on excel and graphs were made.

7.4. Results and Discussion

7.4.1. Formulation Preparation

The CL and HLP formulations were prepared in a similar manner as described in Chapter 5. In order to entrap siRNA, little amount of cationic charges was added to conventional liposomes and hybrid liposome/poloxamer nanoparticle formulations. DMAPAP is a branched polyamine lipid initially developed in the UTCBS as shown in Figure 7.1. PEI is a branched of linear polyamine polymer Figure 7.2. Both lipid and polymer have been shown in the 90s to allow the encapsulation and internalization of nucleic acid into cells leading to transfection (Byk et al., 1998; Tang and Szoka, 1997).

Polyethyleneimine (PEI) cationic polymer and cationic lipid (DMAPAP, RPR209120) were added to these formulations which provides positively charged property to CL and HLP. Basically, 6 formulations have been prepared, conventional liposomes, conventional liposomes containing the cationic lipid DMAPAP, conventional liposomes containing positively charged polymer PEI, Hybrid lipid/polymer, Hybrid lipid/polymer containing the cationic lipid DMAPAP, Hybrid lipid/polymer containing the positively charged polymer PEI.

Table 7.1. List of the various formulations tested in our study with their components.

	Sample	DOPC	Poloxamer	DMAPAP	PEI	siRNA
1	CL + siRNA	✓	✗	✗	✗	✓
2	HLP + siRNA	✓	✓	✗	✗	✓
3	CL + DMAPAP + siRNA	✓	✗	✓	✗	✓
4	HLP + DMAPAP + siRNA	✓	✓	✓	✗	✓
5	CL + PEI + siRNA	✓	✗	✗	✓	✓
6	HLP + PEI + siRNA	✓	✓	✗	✓	✓

In this study, positive charges were added to the CL and HLP formulations by the addition of DMAPAP or PEI. The first approach was to modify the lipidic part by the addition of DMAPAP

lipid and the second approach was to add PEI polymer to the formulation. These modifications were made to see the difference between two approaches and to give us an idea about each individual formulation. The preparation of all the formulations was carried out by the microfluidic tubing system connected with the push syringe, as described in the method section. Only the formulations on which siRNA has been added, have been characterized.

7.4.1. Physico-Chemical Characterization

7.4.1.1.Dynamic Light Scattering and Nanoparticle Tracking Analysis

DLS was used to verify the size and PDI of our nanoparticles within the suitable range of 100 to 200 nm. All the preparations produced, had acceptable range of average hydrodynamic size and PDI as shown in Table 2. The comparison showed that the polydispersity (PDI) of all the conventional liposomes (CL) formulation obtained were significantly higher than the PDI obtained for HLP formulations. The HLP formulation slightly had better PDI due to the presence of poloxamer which stabilize and provide definite shape and size to the liposomes as already discussed in chapter 5. Concerning the positively charged formulations, all the formulations except CL + PEI + siRNA were within the range of 90-50 nm and PDI from 0.15-0.25, which indicates that the microfluidic method we developed was suitable for producing liposomes and HLP with DMAPAP (RPR209120) (Tranchant et al., 2004) and PEI. This increase in the PDI observed for CL + PEI + siRNA tend to show that maybe the PEI and siRNA were not incorporated but rather formed micelles of PEI/siRNA and CL, whereas for HLPs, the size increase with PEI could reflect a real internalization of PEI within the HLPs.

Nanoparticle tracking analysis was carried out for further confirmation of the size of our cationic CL and HLP formulations in complementary to DLS results. Only in case of NTA the samples were diluted 1/500 in Milli-Q and injected in the micro-channel of the device with the help of syringe. NTA revealed that the size of all the formulations were in the range of 140-180 nm as shown in Table 2. The difference between the DLS and NTA results may be due to the dilution, as the samples measured by NTA were diluted, which was not the case when the size of the samples was measured by DLS.

Table 7.2. DLS and NTA results for the different CL and HLP formulations described this table with or without charge containing siRNA. Size represents the mean hydrodynamic average diameter by intensity and the PDI the polydispersity index. The values and standard deviation are given for 9 values, triplicates measured 3 times each (n=3).

Sample	DLS		NTA
	Size	PDI	Size
CL + siRNA	104 ± 20	0.23 ± 0.03	--
CL + DMAPAP + siRNA	113 ±10	0.25 ± 0.06	172 ± 1.3
CL + PEI + siRNA	97 ± 0.1	0.34 ±0.02	180 ± 4.3
HLP + siRNA	124 ± 15	0.18 ± 0.04	--
HLP + DMAPAP + siRNA	122 ± 16	0.16 ± 0.02	174 ± 2.7
HLP + PEI + siRNA	143 ± 12	0.17 ± 0.05	143 ± 1.7

7.4.2. Encapsulation Efficiency and Loading Content

The main idea to design this cationic hybrid lipid/polymer carrier was to improve the encapsulation of siRNA. We wondered if the sole fact to thicken the core of liposomes would be enough to entrap siRNA, which cannot be encapsulated within neutral conventional liposomes. To determine the encapsulation of siRNA within the various formulations, the formulations were filtered after preparation by ultrafiltration column as described in method section 3.6. The non-encapsulated siRNA was removed and collected in form of filtrate. The filtrate was collected to perform a RiboGreen assay for siRNA encapsulation efficiency. The calibration curve was made with known concentrations of siRNA with or without P407 to determine the unknown concentration in the filtrate as shown in Figure 7.3 A and B, respectively. The encapsulation efficiency and loading content of non-cationic HLP was compared to those of non-cationic liposomes (Table 7.3) for siRNA. For both nano-systems, differences in encapsulation values between CLs and HLP were clearly seen as we used the same initial amount of siRNA for preparation as shown in Table 7.3.

Figure 7.3. Calibration curves for siRNA quantification at different concentration, A) siRNA in the absence of siRNA and B) siRNA in the presence of P407.

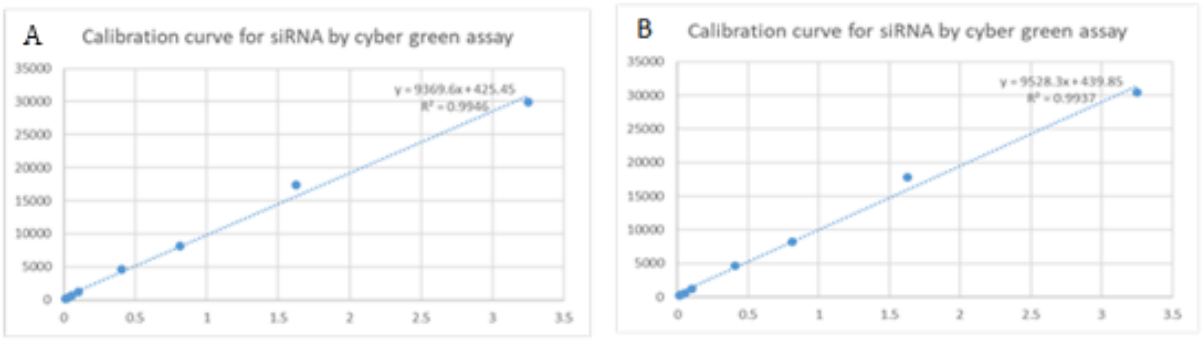

Table 7.3. RiboGreen assay for encapsulation efficiency and loading content siRNA encapsulated in CL and HLP (n=3).

Sample	E.E%	L.C%
siRNA + CL	8.45 ±0.21	0.016 ±0.009
siRNA + HLP	96.7 ±0.88	0.144 ±0.003

Incorporation of siRNA in thickened liposomes was repeatedly found to be greater than encapsulating siRNA in empty liposomes. We were quite surprised though to obtain such an encapsulation efficiency. Initially, it was considered that the value might have been artificially increased by the presence of poloxamer within the filtrate but no evidence of artifact was found when the calibration curve of siRNA was prepared in the presence of poloxamer with same concentrations of siRNA used for the calibration curve without poloxamer as shown in Figure 7.3 A and B.

7.4.3. Treatment of Cell with siRNA Formulation

7.4.3.1.Transfection of siRNA Encapsulated in CL-PEI, CL-DMAPAP, HLP-PEI and HLP-DMAPAP Formulations in the Absence and Presence of TNF-α in Wells

This study was carried out to validate the competence of our cationic formulations for siRNA delivery. The transfection of siRNA was performed in two different *in vitro* conditions. first condition was normal GFP expressing endothelial mice cells and the second was induced inflammatory GFP expressing mice cells by TNF-α, which is a well-known inflammatory mediator that enhance the endothelial cell permeability (Royall et al., 1989; Sainson et al.,

2008). For inducing inflammation, the cells were incubated overnight in the presence of TNF-α before treating them with siRNA formulations. Later, the cells with and without TNF-α were treated with siRNA formulations in opti-mem medium for 4 hours, then opti-mem medium replaced with EGM-2 medium and incubated overnight. Cells were washed after 24 hours, fixed and stained for confocal imaging. The confocal images were treated with the help of Fiji imageJ-win64 software. The conditions were non-treated cells (NT), cells treated with complex of lipofectamine + scrambled siRNA (negative control, lipo + scrambled), complex of lipofectamine + siRNA (positive control, lipo + siRNA), and formulation 3,4,5 and 6 which are described in Table 1.

In the first condition without TNF-α treatment, confocal imaging showed the difference in GFP expression. GFP down-regulation can be seen in the cells treated with the lipofectamine-siRNA, HLP-DMAPAP-siRNA and HLP-PEI-siRNA, when compared with non-treated cells and cells treated with complex of lipofectamine + scrambled siRNA. These results provide the qualitative analysis of gene knockdown and efficiency of siRNA encapsulated in cationic HLP formulation as shown in Figure 7.4 and 7.5. Whereas, CL-DMAPAP-siRNA and CL-PEI-siRNA cationic formulations under the same condition in the absence of TNF-α doesn't show down-regulation in comparison to the complex of lipofectamine + scrambled siRNA and non-treated cells as shown in Figure 7.4 and 7.5. This might be due to the fact that liposomes with low positive charges, in absence of poloxamer viscosity were not able to retain the siRNA.

In the second condition, after treating the cells with TNF-α in order to induce inflammation and to see whether the internalization of siRNA is improved, did not give expected results. It looks like there is almost no down regulation of GFP in all conditions as shown in Figure 7.6 and 7.7. This hindrance in siRNA efficiency effect may be due to some interruption of silencing pathways by TNF- α activation, that induces multiple morphological and physiological changes in EC gene expression (Fràter-Schröder et al., 1987; Sato et al., 1986)

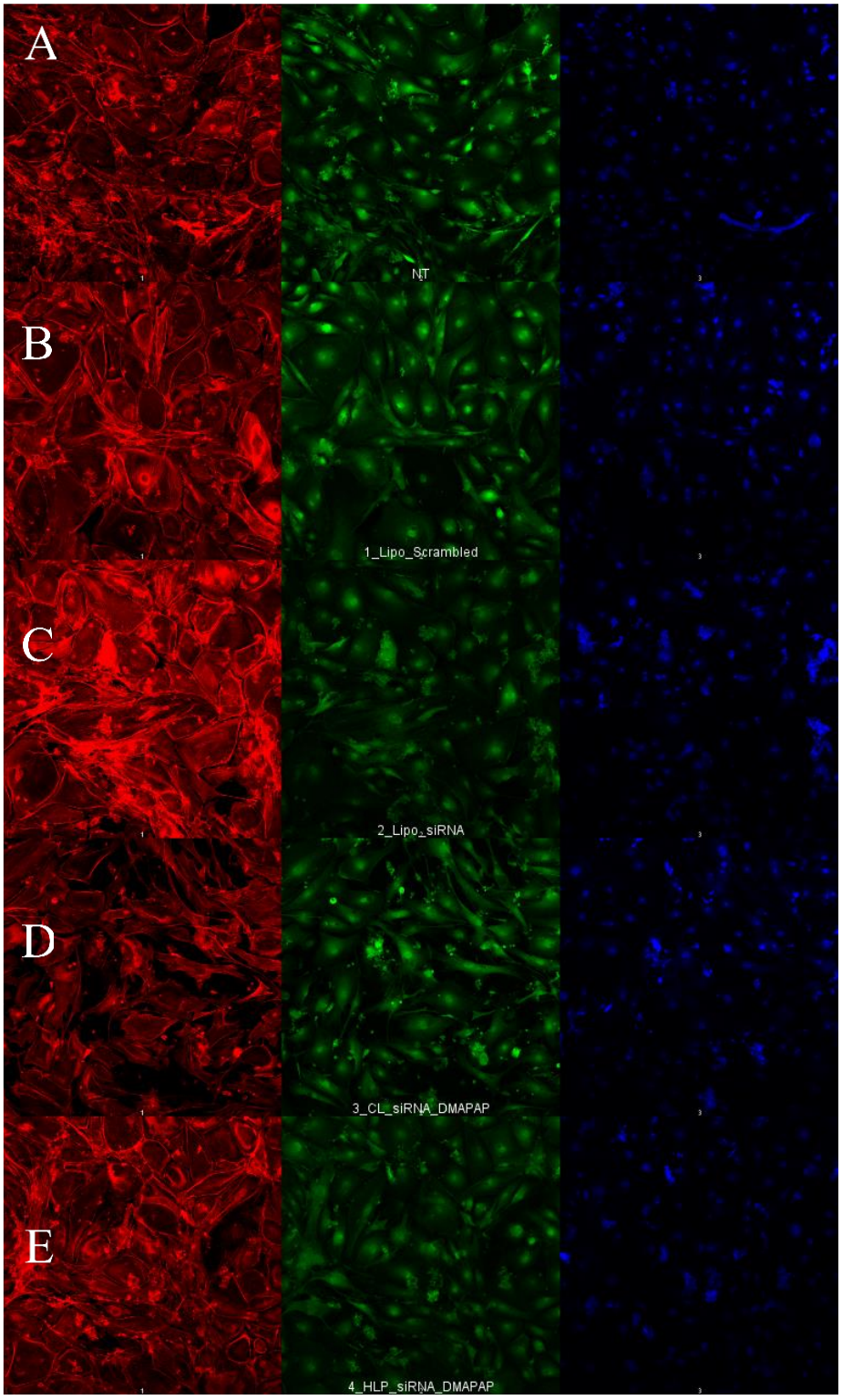

Figure 7.4. Confocal imaging of endothelial cells treated with different conditions, A) Non treated, B) Lipofectamine + scrambled siRNA, C) Lipofectamine + siRNA, D) CL-DMAPAP-siRNA and E) HLP-DMAPAP-siRNA in the absence of TNF-a.

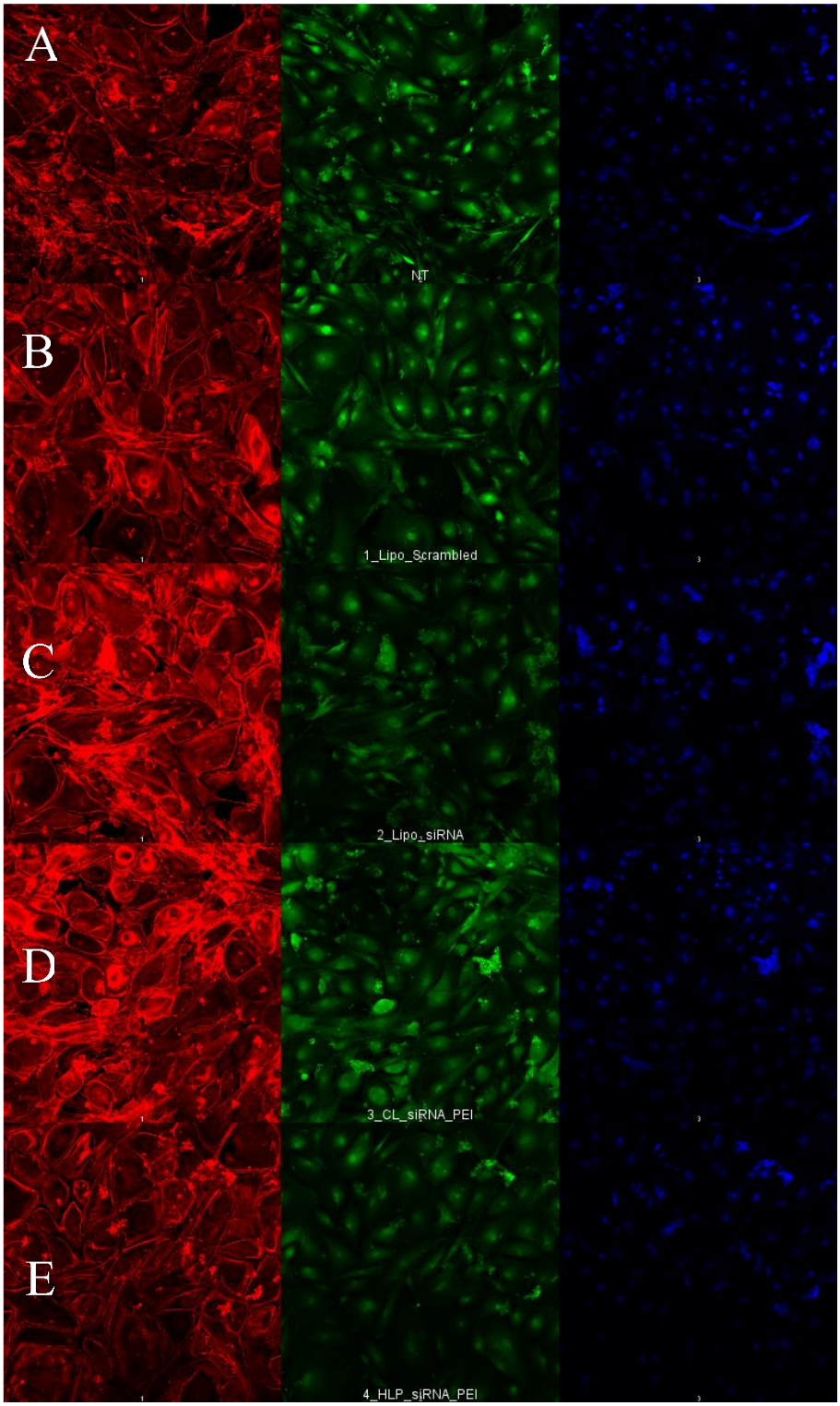

Figure 7.5. Confocal imaging of endothelial cells treated with different conditions, A) Non treated, B) Lipofectamine + scrambled siRNA, C) Lipofectamine + siRNA, D) CL-PEI-siRNA and E) HLP-PEI -siRNA in the absence of TNF-a.

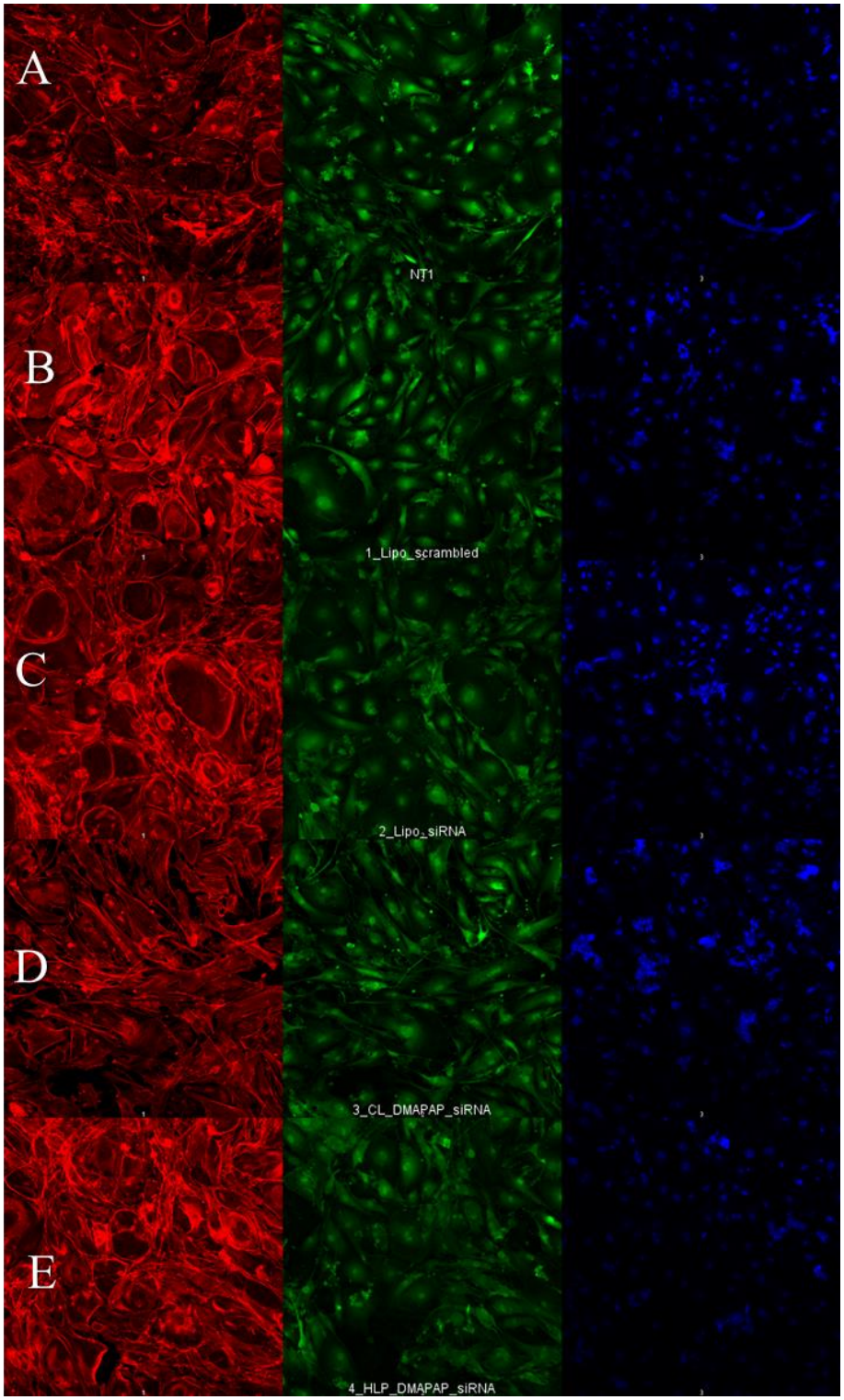

Figure 7.6. Confocal imaging of endothelial cells treated with different conditions, A) Non treated, B) Lipofectamine + scrambled siRNA, C) Lipofectamine + siRNA, D) CL-DMAPAP-siRNA and E) HLP-DMAPAP-siRNA in the presence of TNF-a.

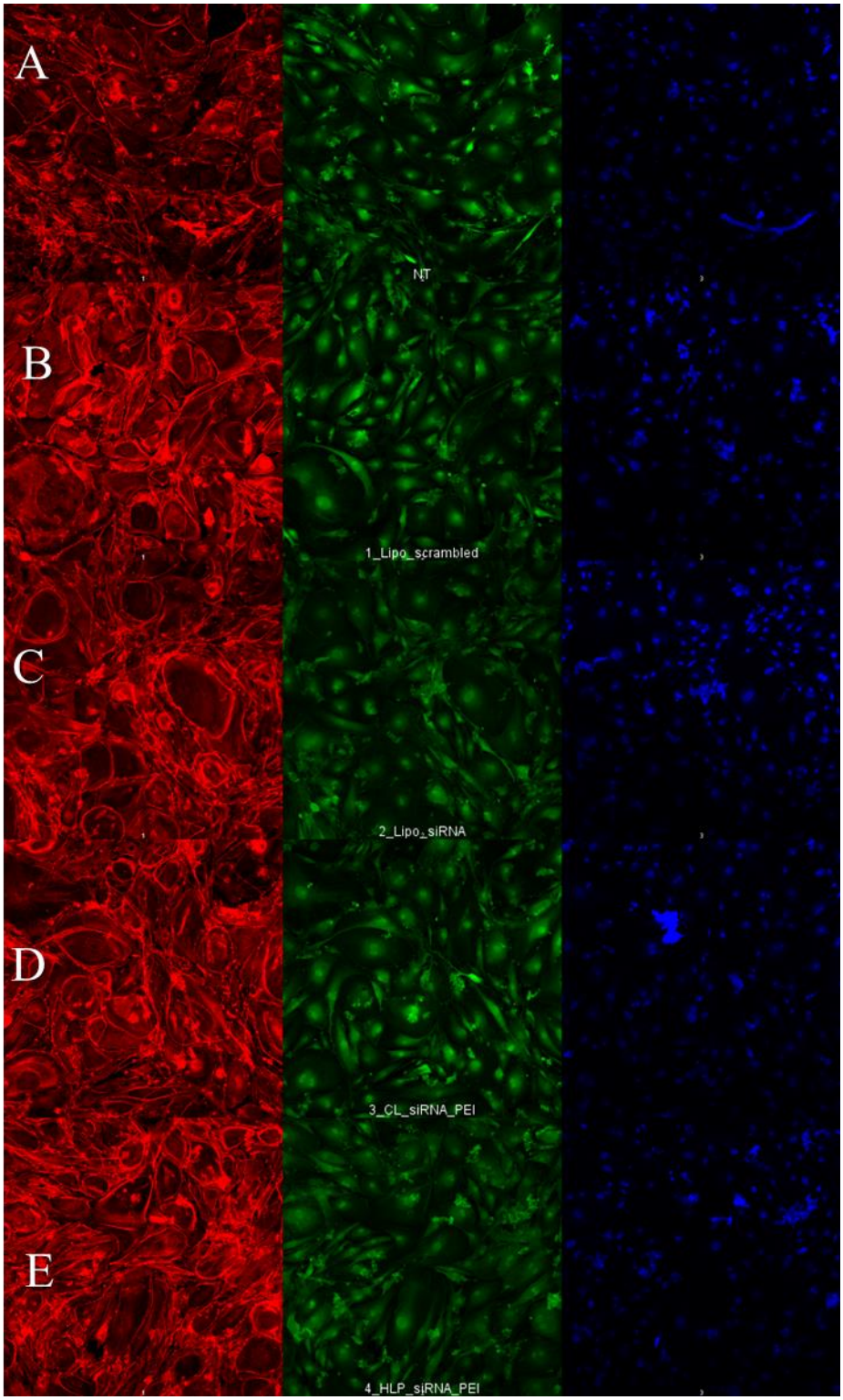

Figure 7.7. Confocal imaging of endothelial cells treated with different conditions, A) Non treated, B) Lipofectamine + scrambled siRNA, C) Lipofectamine + siRNA, D) CL-PEI-siRNA and E) HLP-PEI -siRNA in the presence of TNF-a.

7.4.3.2. Quantitative Analysis of the Efficiency of Cationic Formulation for siRNA Delivery and GFP Down Regulation in the Absence and Presence of TNF-α in Wells

Quantitative analysis was carried out for further confirmation of our qualitative analysis to verify the GFP expression down regulation. The GFP expression of the cells was quantified by taking the same images as analyzed for qualitative analysis. The GFP expression was calculated with the help of imageJ software for the confocal images by taking into account the number of cells while taking each nucleus (Dapi) into consideration. These results ensure that qualitative and quantitative analysis have shown similar kind of result. In the absence of TNF-α the DMAPAP containing formulations shows a down regulation when compared with positive and negative controls as shown in Figure 7.8, whereas in the presence of TNF-α the expression of GFP were not down regulated in all conditions as we have observed in the quantitative analysis of images as shown in Figure 7.9. This effect is due to TNF-α activation, that induces multiple morphological and physiological changes in EC gene expression (Fràter-Schröder et al., 1987; Sato et al., 1986). Surprisingly, there was the up-regulation of GFP in the presence of TNF-α, but the cause is unknown. All the conditions were in the triplicate, but the experiment was performed once that is why statistical analysis is not mentioned.

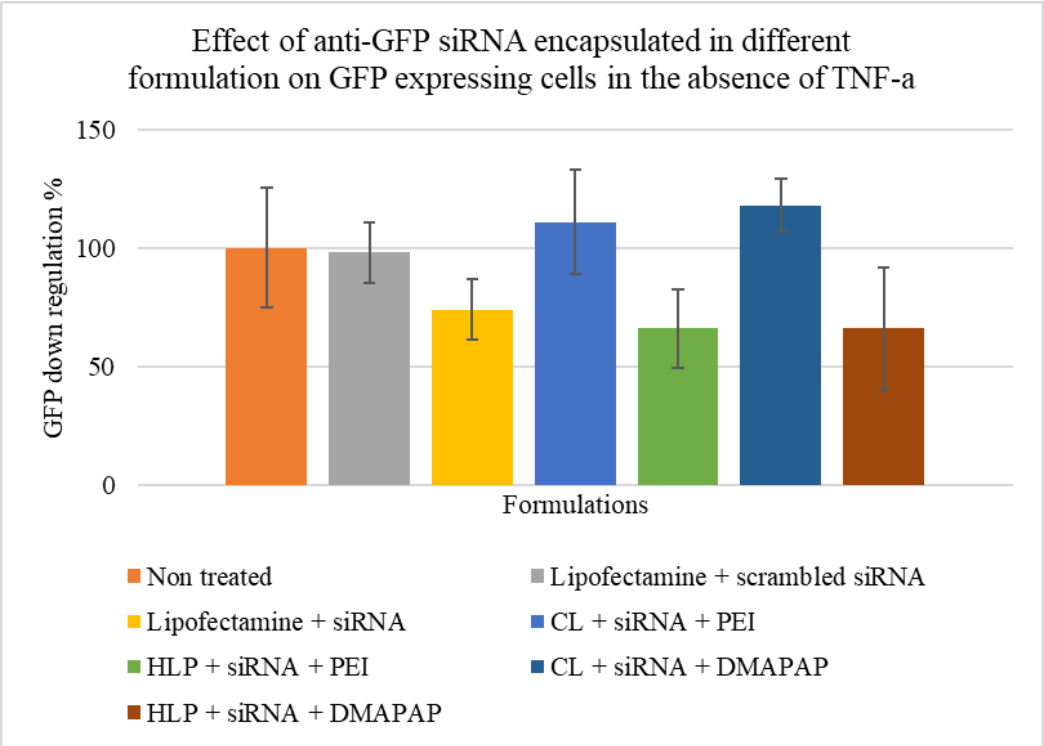

Figure 7.8. Quantitative analysis of GFP down regulation of siRNA encapsulated in cationic formulations in comparison to positive and negative controls in the absence of TNF-a.

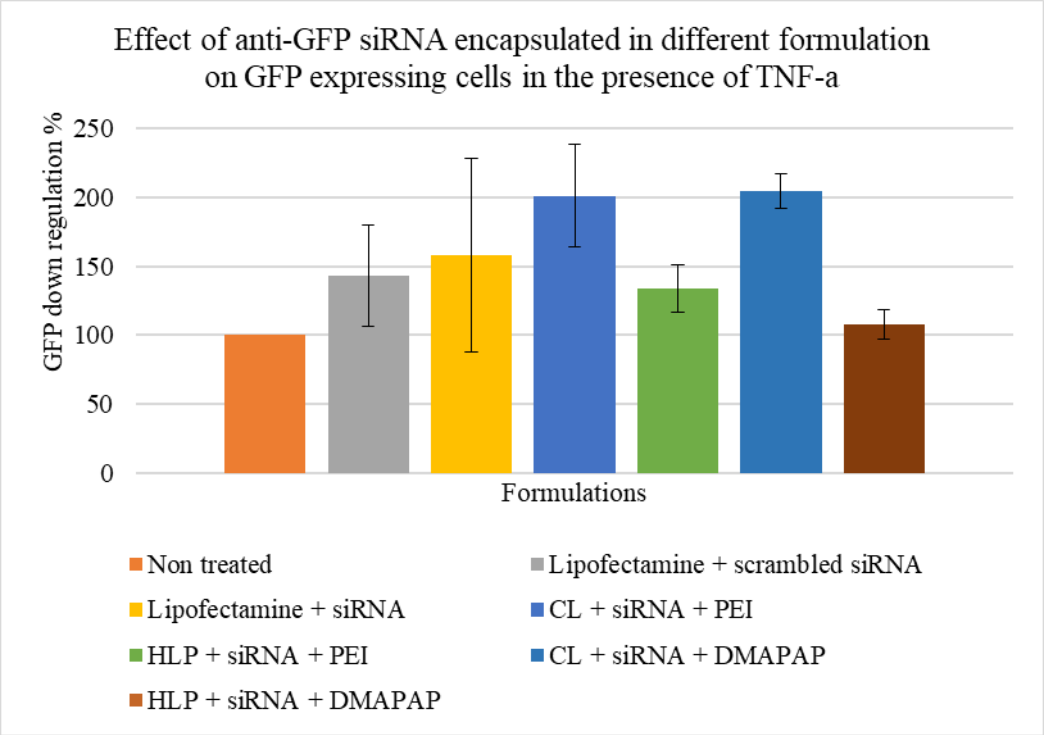

Figure 7.9. Quantitative analysis of GFP down regulation of siRNA encapsulated in cationic formulations in comparison of positive and negative controls in the presence of TNF-a.

7.4.3.3.Transfection of siRNA Encapsulated in CL-PEI and HLP-PEI and PEI Formulations in the Absence of TNF-α Inside Microchip in the Absence of TNF-α

A 3D cell culture modeling was initiated to have a better idea of cell proliferation and imaging in a 3-dimensional environment using a minimum amount of cell medium and formulations. Similar experiments as described before in wells, were carried out, on the same GFP expressing cells but inside the 3D culture microchip. The number of cells were almost the same in both microchip and each well or wells plate. The images were taken for the cells attached at the bottom side of the 3D microchip to have similar dimensions for all the conditions, throughout the experiment. The cells were seeded very well in the microchip treated with sterile gelatin 0.1% solution as could be seen by imaging GFP. Looking at transfection experiments, we found results consistent with the one obtained in 1D culture in wells. Positive control lipofectamine + siRNA, HLP-DMAPAP-siRNA and HLP-PEI-siRNA, were able to down-regulate GFP expression when compared to complex of lipofectamine + scrambled siRNA (negative control) and non-treated in the absence of TNF-α as shown in Figure 7.10 and 7.11. The CL formulations didn't show any down regulation in the absence of TNF- α. This may be due to the same fact as discussed earlier in Section 4.4, that liposomes with low in positive charges without the

poloxamer viscosity were not able to retain the siRNA and in case of CL + PEI + siRNA just form micelles of PEI/siRNA and CL not able to transfect. This 3D cell culture model gave us the possibility to produce similar results as performed in 96 wells plate while using a minimum amount of formulations and medium. The confocal images were treated with the help of imageJ software.

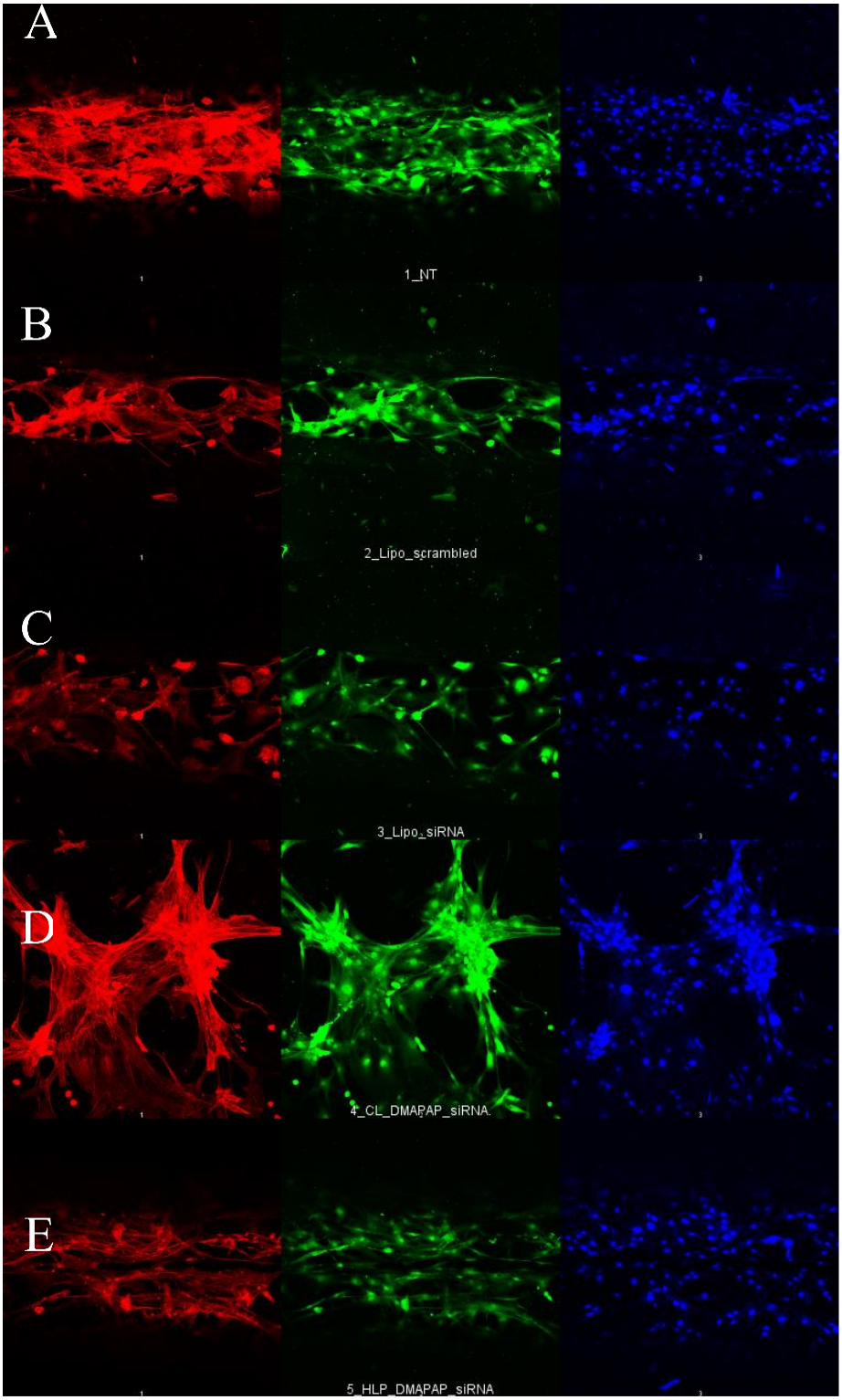

Figure 7.10. Confocal imaging of 3D endothelial cells culture in micro-chip treated with different conditions, A) Non treated, B) Lipofectamine + scrambled siRNA, C) Lipofectamine + siRNA, D) L-DMAPAP-siRNA and E) HLP-DMAPAP-siRNA in the absence of TNF-a.

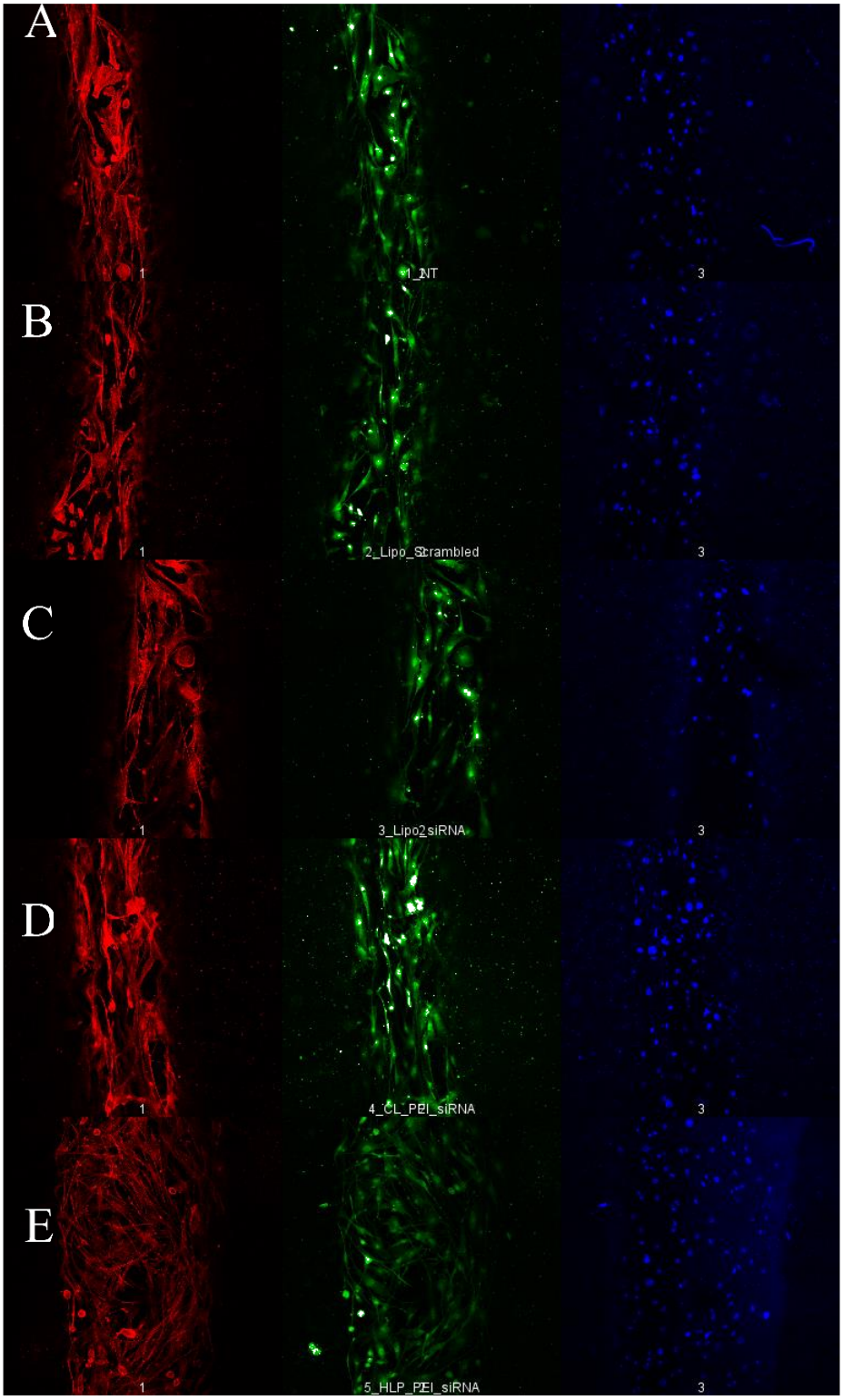

Figure 7.11. Confocal imaging of 3D endothelial cells culture in micro-chip treated with different conditions, A) Non treated, B) Lipofectamine + scrambled siRNA, C) Lipofectamine + siRNA, D) CL-PEI-siRNA and E) HLP-PEI-siRNA in the absence of TNF-a.

7.5. Conclusion

This study was conducted in terms of improving our formulation and extending its range of encapsulation of different drug molecules. This is the first example in the literature of a thickened core nanosized liposome described for siRNA delivery. The microfluidics device with our homemade tubing system have been successfully applied to produce cationic Cl and HLP formulations with good size and PDI. We showed that our formulation required positive charge for siRNA encapsulation. The cationic charges were provided to CL and HLP formulations with the addition of PEI polymer and DMAPAP lipid, at a certain level that can help encapsulation with inducing cytotoxicity. The idea was to provide low positive charge to our CL and HLP formulation to encapsulate siRNA without introducing toxicity. To evaluate the efficacy of the formulations, cells were successfully seeded in 24 wells plate and microchip model. The 3D cell culture model gave us the possibility to produce the same results while using minimum amount of the formulation and the medium. The 3D cell culture model also allows to image the cells in three dimensions and are more physiologically appropriate as cells in body work in 3D environment (Mazzoleni et al., 2009). Microfluidic cell culture model have been described before for endothelial cells (Sfriso et al., 2018).

These results showed that cationic HLP is able to down regulate GFP expression, indicating that the formulation is able to help siRNA cell internalization while releasing it inside the cells. It would obviously be interesting to investigate the internalization process of the HLPs and the intracellular siRNA release. It would also be interesting to evaluate if a better down regulation could be achieved when increasing the amount of DMAPAP into the HLPs, however, a compromise should be found between toxicity and efficacy. The interest of this approach could propose the delivery of a combination of drugs. As we have shown in chapter 6 that we were able to encapsulate and prolong the release of an anticancer drug into the HLPs, we could combine the approaches by blocking the expression of a gene for instance in a cancer context, as the combination studies are discussed in the literature (Oh et al., 2016; Peng et al., 2014; Qu et al., 2014; Yang et al., 2014, 2014; Yao et al., 2015). A similar approach could be proposed in a context of inflammation by releasing locally a drug, while inhibiting TNF alpha or another inflammation mediator.

Chapter 8. Global Discussion, Original Contributions, Conclusions and Future Perspectives

Nanotechnology is the vastly growing revolutionary field of science which contributes in different fields of application, among which nanomedicine. Nanomedicine is generally a broad term which changed the perspectives of researcher's idea for diagnosis, prevention and cure of the diseases by conventional drug delivery systems and it has potentially some possible applications in cancer, cardiovascular diseases, inflammation or rare diseases, but the clinical needs should be well identified to make sure that the nanomedicine is well designed and tailored for the specific application. (Moghimi et al., 2005). Their size ranges from 1 to 100 nm range and the tunable surface property make them unique and advantageous over conventional medicines. The initial goal of nanomedicine was to improve the conventional drug delivery systems to offer sustained release, increase the specificity towards target sites, improved pharmacokinetics profiles, enhance drug circulation time and reduce side effects of the drug (Bor et al., 2019). The engineered nanomaterial can avoid multi drug resistance, pass some biological barriers and can be used for diagnosis and even provide potentiation of therapies such as radiotherapy (Alexis et al., 2008; Lux et al., 2018). Despite their advantages and the recent advances, there are still many scientific and logistic challenges to transfer more efficiently nanocarriers to the clinic (Alhareth et al., 2017).

In the last decade, nanomedicine was considered to enter in a maturation step. The researchers in the field thinks that nanomedicine is between crest of over stated hope and rise of illumination and it still need efforts to reach the plateau of productivity as shown in Figure 8.1, inspired by Gartner hype cycle (Couvreur, 2019).

Several issues should be considered for the development of new medicines, including the clinical need or the manner by which drugs are administered or delivered. The route of administration and the design of the drug delivery system should be defined in an early stage of the development process. More information is required regarding the physico-chemical characteristics of nanomaterials and effect of the physiological environment on nano materials behavior (Couvreur, 2013). For the better future of nanomedicine, there is a need of more nanoscale platforms to design, prepare, and evaluate nanosized drug delivery systems. In the field of cancer, the nano-characterization laboratory (US-NCL) has performed a tremendous work to provide researchers and companies with the various protocols which should be followed to transfer nanoparticles to the clinic. In the last years, a similar idea was developed in Europe

with the European Characterization Laboratory (Eu-NCL) which aims at helping the transfer to clinic in all field of nanomedicine (Bremer- Hoffmann et al., 2018). Nevertheless, multidisciplinary research is required to advance in the field of nanomedicine with smart engineering, combination therapies, improving drug loading capacity, release, stability and safety (Moghimi et al., 2005).

In this thesis/work, the development of a new drug delivery system was investigated considering new challenges in the field of nanoparticles for drug delivery.

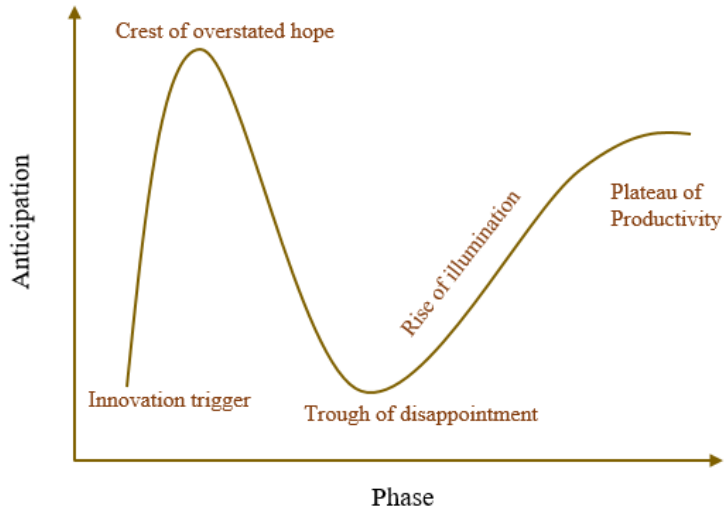

Figure 8.1. The diagram projects the slope of nanomedicine journey.

Formulation Rational Design

The rational design of the HLP formulation was to broaden the applications of liposomes. Thanks to the retention of a significant amount of drug for prolong period of time, which makes the formulation ideal. The aim of polymeric core was to provide viscosity to entrap the drug more efficiently and reduce drug leakage which is the common issue in case of liposome formulations. The additional excipient to the liposomes might bring cytotoxicity; necessitating a compromise between the added value of additives and their clinical safety.

The rational choice of the materials is primary criterion to acknowledge, before conception of a drug. The future possibility to transfer the drug to the patients depends on drug's adequate efficacy and safety, which are the two common issues in clinical trial (Singh and Loke, 2012). While keeping in mind the efficacy and safety, this study was begun with the selection of the

materials, based on the simple formulation where each component has a defined role. For the conception of HLP formulation, non-charged DOPC lipid were considered over charged lipids to avoid toxic effects from the lipids. DOPC liposomes are already been reported and discussed numerously in the literature. This phospholipid is the main constituent of cell membranes, and as such, the main component of Doxil® or Mepact® commercialized liposomes (Bulbake et al., 2017). In the literature, most reported liposomes have been prepared with other phospholipids such as DOPE, DOPS, DOPG or DSPC (Voss et al., 2018). We chose poloxamer P407 as it is also FDA approved as an inactive ingredient in a number of preparation such as parenteral, oral solutions, suspensions, ophthalmic and dermal formulations (Dumortier et al., 2006; Rowe et al., 1994). The thermoreversible sol/gel transition nature and viscous consistency of poloxamer P407 at certain concentration adds an extra factor. This polymeric core strengthens the liposomal bilayer and retain the hydrophilic drugs for prolong period of time, that makes it a good contender to be chosen as the interior core for the formulation. The approach of preparing hybrid liposome/poloxamer nanoparticle with thickened core was inspired by two studies described in the literature about liposomes with poloxamer inside the core. However, in those two studies, Chandaroy et al described liposomes with a very low concentration (less than 0.2% w/v) of poloxamer, whereas Zhang and his team prepared micro-sized particles with high concentration of poloxamer (~ 20% w/v) (Chandaroy et al., 2001; Zhang et al., 2013).

Adding poloxamer to lipid add even higher complexity to this challenge. The poloxamer quantification was therefore a key issue to address, first because, there is no precise poloxamer characterization in the literature, second, because the confirmation of our HLP formulation is reliant upon the concentration of encapsulated P407. DSC and densitometry analysis were carried out for this purpose. The endothermic peaks by DSC at high temperature have been well described to reflect the micellization and gelification processes. The onset of the micellization peak is concentration dependent which can complicate the interpretation of the quantification. Moreover, the other signature, relative to the sol/gel transition, is of low energy, therefore poorly sensitive. Fortuitously, while doing the study of DOPC lipid transition and poloxamer quantification and interaction with DOPC lipid, we discovered peaks at sub-ambient temperature related to the water bounded to poloxamer molecules in three states, free water, loosely and tightly bound water. These peaks later evaluated and we found that loosely bound water peak is not studied before at sub-ambient temperature and it corresponds to water attached to PPO molecules, where as tightly bound water corresponds to water attached to PEO (PEG) which already discussed in literature (Huang and Nishinari, 2001). Looking at water bound

polymer, rather than at the signatures of the polymer transitions was found to be more precise and accurate than quantification at high temperature at sub-ambient temperature, the temperature of water bound with poloxamer was independent of the poloxamer concentration which eased the quantification as regard to micellization and gelification peaks. The poloxamer quantification at sub-ambient temperature by DSC opens the new window for quantifying poloxamer in many formulations up to or less than 1% W/V, more accurately. The sub-ambient temperature transition peaks of water presence are also determined by thermal microscopy when the images were taken at -15, -4.4 and -0.4 °C related to water bound PPO, PEO and free water, respectively, where change in the opacity of poloxamer solution can be seen. The imaging was carried out just to visualize the changes at the sub-ambient temperature but this is not conclusive.

Comprehensive Nanoparticle's Characterization

After the rational selection of materials and their characterization, the most important step was to find an optimized method for the preparation of our HLP formulations. Several techniques of liposome preparation and their detailed characterization are already been discussed in the literature (Nkanga et al., 2019; Patil and Jadhav, 2014). Microfluidic is the emerging techniques for liposome preparation and can encapsulate both hydrophilic and lipophilic drugs (Carugo et al., 2016; Joshi et al., 2016). Scalable manufacturing methods for liposomes and their related systems were developed in the last decade to facilitate the transition of liposomal products from bench to clinic (Zizzari et al., 2017). The application of microfluidic tools for liposome manufacturing is based on the theory of a nanoprecipitation reaction resulting from rapid mixing at the nano-scale. A new manufacturing method based on microfluidic technologies allows enhancing the control of processing parameters, improving reproducibility and providing the possibility of using a reduced volume of solvents. Parameters like the concentration of each component, and the flow rate ratio influences the resultant nano-liposomal carriers. In our study, we optimized the parameters and conditions to achieve a tailored nanosystem. A robust assessment of nanoparticles using at least two characterization techniques are highly recommended, this can be explained by the fact that no single technique can fully characterize nanomaterials (Faria et al., 2018). The detailed study for characterization of our formulation led us to develop a method of solvent evaporation by evaluating the solvent concentration by comparing the densities of different formulations, and also the detailed size characterization with the help of different techniques such as TEM, DLS, TRPS and NTA. Several articles showed the discrepancies obtained using several size measurements methods (Coty and

Vauthier, 2018; Varenne et al., 2017, 2016). In our case, the size measured for our main formulation HLP was around 200 nm by all three techniques which was probably due to the homogeneity of the preparation. The stability is also the main concern about the nanomedicine as they can be altered with time. The HLP formulation was found stable up to two months of shelf-life in terms of the particle size.

Lipid/poloxamer Nanoparticle: Morphology and Configuration

The foremost challenge of the project was to confirm that poloxamer was inside the liposomes, and this was complicate to show as it is known that there is also some poloxamer which is interacting with the surface of the liposomes (Pembouong et al., 2011). The techniques such as DLS which give a size distribution do not allow to make a difference between poloxamer outside or inside the liposomes, which is why the controls such as conventional liposomes and HLP_{out} (poloxamer added after liposomes preparation) were compared with HLP (poloxamer added while liposomes preparation, as aqueous medium was replaced by P407 solution) to quantify the amount of poloxamer encapsulated inside as a polymeric core. The preparation based on microfluidic technique of similar configuration using another lipid and polymer was previously reported, liposome−hydrogel hybrid nanoparticles made up of DPPC:cholesterol:DCP as lipid and N-isopropylacrylamide as a polymer, core gelification was achieved after filtration using UV light exposure to initiate the polymerization (Hong et al., 2010).

Drug Retention and Release

The aim of designing nanocarriers is to use them as cargo for loading and delivering (bio)therapeutics. It is important to develop strategies to control their drug loading and release characteristics and to explore parameters that impact the drug loading efficiency and the release characteristics. to gather a better understanding of drug interaction with nanocarrier, in terms of retention and release, a widespread study of drug loading should be performed, the variation of the initial concentration of drug and initial concentration of nanocarrier should be planned, loading efficiency and loading content should be evaluated. This encapsulation and release study based on two hydrophilic molecules, rhodamine as drug model and doxorubicin as drug. Rhodamine drug modelling allowed us to understand the encapsulation and loading principles related to the drug concentration. Interestingly, poloxamer viscous core did not influence the encapsulation efficiency of HLP and showed the similar encapsulation efficiency like CL. The

release of rhodamine and doxorubicin from HLP was slow when compared to CL. These two results confirm the improvement release and encapsulation which are the major challenges in nanomedicine field.

In vitro Assessment of HLP

New relevant model to study bio-nano interactions is cells on chip, tissue on chip and organ on chip is a three-dimensional cell culture technique. The 3D cell culture is advanced technique of cell culturing after moving from cell monolayer 2D cultures to make more convincing framework (Pampaloni et al., 2007; Saji Joseph et al., 2019). It have some advantages and provide more logical information then simple monolayer cell culture, but the 3D cell culture techniques is still not fully developed as the reproducibility and extraction of cells can be limitation so 2D culture is still the most used method . In our case we need to do imaging of 3D cell culture after treating the GFP expressing endothelial cells with anti-GFP siRNA to see the down-regulation of green florescence. The cationic charges were added to HLP formulation for siRNA encapsulation and entrapment, two strategies were applied either to modify P407 polymeric core with cationic charges moiety such as PEI polymer or to modify DOPC lipidic shell with DMAPAP lipid. The experiment was performed on both, 2D and 3D cell cultures to compare them together in the presence and absence of TNF-α. The both strategies of modified HLP with cationic charge produced similar results for both type of cell cultures, HLP formulations down regulates the GFP expression in the absence of TNF-α. The treatment of endothelial cells with TNF-α was supposed to enhance the internalization but unexpectedly, no downregulation of GFP was observed.

Perspectives for HLPs

This study enlightens the improvement in terms of lipid polymer self-assembled nanoparticles. Our convincing results suggests that HLP formulation is a promising approach to carry and deliver the anticancer agents including hydrophilic drugs and gene therapy agents.

It was the first work in the laboratory, to design and evaluate thickened core liposomes, that we called HLP. To go further with this approach, some additional studies are needed to advance and optimize the HLP formulation, preparation method and evaluation protocols, improvements are required at several stages. These liposomes have already discussed in the literature with three different (low, medium and high) concentrations of poloxamer and we observed that an issue to be addressed was their size increase with increased polymer concentration (Ahmed et al., 2019; Chandaroy et al., 2001; Zhang et al., 2013). Nevertheless, it would be interesting to

increase the core viscosity by to entrap the nucleic acid without charges for instance. Increasing poloxamer concentration is an approach. Another convincible approach is using polymer other than poloxamer such as gelatin or cellulose if we select non-ionic polymers.

Credit to the controlled parameters of preparation by automatized syringe pump. The microfluidic mixing doesn't require any extra external driving force for liposome production without the immense influence of experimenter. The improvement in term of preparation and purification process could be possible by replacing the current method of ultra-filtration method by gel filtration. This modification will have automatized the filtration step by installing the gel-filtration device in-line with the syringe pump setup. Another improvement of our setup for preparation could be the in-line assessment of size distribution during the preparation, which can have achieved by coupling the Vasco-kin instrument (a portable DLS that provides the kinetic measurement of size) with our syringe pump setup.

The optimized HLP formulation will later need to be tested *in-vivo* for its cytotoxicity, bio-distribution and gene silencing to make this approach more convincing and to position HLP formulation as a good carrier for wide range of molecules. Doxorubicin loaded HLP should be evaluated *in vitro* and *in vivo* models to assess the benefit of what HLP formulation can offer in terms of doxorubicin efficacy, toxicity and therapeutic outcome. Finally, the possibility to encapsulate siRNA and transfect it to the cell was shown in 2D and 3D culture. This should be confirmed with more relevant siRNA sequences.

Conclusion

This work was the part of the nanomedicine context. We have tried to add some new features to the highly known liposomes nanocarriers, in terms of design, production, and evaluation. This study described a new design of a drug delivery system, a hybrid composition of polymer and lipid is suggested to combine the advantages of these materials. A new method of nanoparticle preparation based on the microfluidic basis was described and optimized in this work for reproducible production of the HLP formulation. The developed formulation was characterized using advanced technical tools to understand and to figure out the morphology of this new nanocarrier. The ability of HLP to carry a gene therapy agent, siRNA, was evaluated using an emerging model of cell culture on-chip.

In some ways, this study provided new knowledge and data regarding to the lipid/polymer nanoparticles and paved some new protocols for nanoparticle evaluation. The knowledge and

data assembled from this work open a new horizon of investigation and new research questions to be answered. In parallel, experimental protocols developed in this work will certainly use to advance different projects in our laboratory and will hopefully contribute to the answer to the ultimate question: how can we proceed in the cure for severe diseases using nanomedicine?

Reference

Agrawal, N., Dasaradhi, P.V.N., Mohmmed, A., Malhotra, P., Bhatnagar, R.K., Mukherjee, S.K., 2003. RNA Interference: Biology, Mechanism, and Applications. Microbiol Mol Biol Rev 67, 657–685. https://doi.org/10.1128/MMBR.67.4.657-685.2003

Ahmed, S., Corvis, Y., Gahoual, R., Euan, A., Lai-Kuen, R., Couillaud, B.M., Seguin, J., Alhareth, K., Mignet, N., 2019. Conception of nanosized hybrid liposome/poloxamer particles to thicken the interior core of liposomes and delay hydrophilic drug delivery. International Journal of Pharmaceutics 567, 118488. https://doi.org/10.1016/j.ijpharm.2019.118488

Akbarzadeh, A., Rezaei-Sadabady, R., Davaran, S., Joo, S.W., Zarghami, N., Hanifehpour, Y., Samiei, M., Kouhi, M., Nejati-Koshki, K., 2013. Liposome: classification, preparation, and applications. Nanoscale Res Lett 8, 102. https://doi.org/10.1186/1556-276X-8-102

Alexandridis, P., Holzwarth, J.F., Hatton, T.A., 1994. Micellization of Poly(ethylene oxide)-Poly(propylene oxide)-Poly(ethylene oxide) Triblock Copolymers in Aqueous Solutions: Thermodynamics of Copolymer Association. Macromolecules 27, 2414–2425. https://doi.org/10.1021/ma00087a009

Alexis, F., Rhee, J.-W., Richie, J.P., Radovic-Moreno, A.F., Langer, R., Farokhzad, O.C., 2008. New frontiers in nanotechnology for cancer treatment. Urol. Oncol. 26, 74–85. https://doi.org/10.1016/j.urolonc.2007.03.017

Alhareth, K., Sancey, L., Tsapis, N., Mignet, N., 2017. How should we plan the future of nanomedicine for cancer diagnosis and therapy? International Journal of Pharmaceutics, SFNano 2016 meeting 532, 657–659. https://doi.org/10.1016/j.ijpharm.2017.05.037

Alvarez-Lorenzo, C., Bromberg, L., Concheiro, A., 2009. Light-sensitive intelligent drug delivery systems. Photochemistry and Photobiology 85, 848–860. https://doi.org/10.1111/j.1751-1097.2008.00530.x

Amsden, B., 1998. Solute Diffusion within Hydrogels. Mechanisms and Models. Macromolecules 31, 8382–8395. https://doi.org/10.1021/ma980765f

Arcamone, F., Cassinelli, G., Fantini, G., Grein, A., Orezzi, P., Pol, C., Spalla, C., 1969. Adriamycin, 14-hydroxydaimomycin, a new antitumor antibiotic fromS. Peucetius var.caesius. Biotechnol. Bioeng. 11, 1101–1110. https://doi.org/10.1002/bit.260110607

Arcamone, F., Franceschi, G., Orezzi, P., Penco, S., Mondelli, R., 1968. The structure of daunomycin. Tetrahedron Letters 9, 3349–3352. https://doi.org/10.1016/S0040-4039(00)89489-7

Artzner, F., Geiger, S., Olivier, A., Allais, C., Finet, S., Agnely, F., 2007. Interactions between Poloxamers in Aqueous Solutions: Micellization and Gelation Studied by Differential Scanning Calorimetry, Small Angle X-ray Scattering, and Rheology. Langmuir 23, 5085–5092. https://doi.org/10.1021/la062622p

Aswal, V.K., Goyal, P.S., 2004. Small-angle neutron scattering from micellar solutions. J. Phys. 63, 8.

Bag, M.A., Valenzuela, L.M., 2017. Impact of the Hydration States of Polymers on Their Hemocompatibility for Medical Applications: A Review. Int J Mol Sci 18. https://doi.org/10.3390/ijms18081422

Baleux, B., Champetier, G., 1972. Dosage colorimétrique d'agents de surface non ioniques polyoxyéthylenes al'aide d'une solution iodo–iodurée. CR Acad. Sc. Paris (C) 274, 1617–1620.

Balzus, B., Sahle, F.F., Hönzke, S., Gerecke, C., Schumacher, F., Hedtrich, S., Kleuser, B., Bodmeier, R., 2017. Formulation and ex vivo evaluation of polymeric nanoparticles for controlled delivery of corticosteroids to the skin and the corneal epithelium. Eur J Pharm Biopharm 115, 122–130. https://doi.org/10.1016/j.ejpb.2017.02.001

Bangham, A.D., Standish, M.M., Watkins, J.C., 1965. Diffusion of univalent ions across the lamellae of swollen phospholipids. Journal of Molecular Biology 13, 238-IN27. https://doi.org/10.1016/S0022-2836(65)80093-6

Banik, B.L., Brown, J.L., 2014. Polymeric Biomaterials in Nanomedicine, in: Natural and Synthetic Biomedical Polymers. Elsevier, pp. 387–395. https://doi.org/10.1016/B978-0-12-396983-5.00024-7

Bardajee, G.R., Hooshyar, Z., 2018. A novel thermo-sensitive nanogel composing of poly(N-isopropylacrylamide) grafted onto alginate-modified graphene oxide for hydrophilic anticancer drug delivery. Journal of the Iranian Chemical Society 15, 121–129. https://doi.org/10.1007/s13738-017-1215-9

Bardajee, G.R., Hooshyar, Z., 2017. Drug release study by a novel thermo sensitive nanogel based on salep modified graphene oxide. Journal of Polymer Research 24, 49. https://doi.org/10.1007/s10965-016-1148-5

Barenholz, Y., 2012. Doxil®--the first FDA-approved nano-drug: lessons learned. J Control Release 160, 117–134. https://doi.org/10.1016/j.jconrel.2012.03.020

Batzri, S., Korn, E.D., 1973. Single bilayer liposomes prepared without sonication. Biochimica et Biophysica Acta (BBA) - Biomembranes 298, 1015–1019. https://doi.org/10.1016/0005-2736(73)90408-2

Belali, S., Karimi, A.R., Hadizadeh, M., 2018. Cell-specific and pH-sensitive nanostructure hydrogel based on chitosan as a photosensitizer carrier for selective photodynamic therapy. International Journal of Biological Macromolecules 110, 437–448. https://doi.org/10.1016/J.IJBIOMAC.2017.12.169

Bencherif, S.A., Siegwart, D.J., Srinivasan, A., Horkay, F., Hollinger, J.O., Washburn, N.R., Matyjaszewski, K., 2009. Nanostructured hybrid hydrogels prepared by a combination of atom transfer radical polymerization and free radical polymerization. Biomaterials 30, 5270–5278. https://doi.org/10.1016/j.biomaterials.2009.06.011

Bergueiro, J., Calderõn, M., 2015. Thermoresponsive nanodevices in biomedical applications. Macromolecular Bioscience 15, 183–199. https://doi.org/10.1002/mabi.201400362

Bessoth, F.G., deMello, A.J., Manz, A., 1999. Microstructure for efficient continuous flow mixing. Analytical Communications 36, 213–215. https://doi.org/10.1039/a902237f

Bettini, R., Colombo, P., Massimo, G., Catellani, P.L., Vitali, T., 1994. Swelling and drug release in hydrogel matrices: polymer viscosity and matrix porosity effects. European Journal of Pharmaceutical Sciences 2, 213–219. https://doi.org/10.1016/0928-0987(94)90025-6

Bodratti, A.M., Alexandridis, P., 2018. Formulation of Poloxamers for Drug Delivery. J Funct Biomater 9. https://doi.org/10.3390/jfb9010011

Bor, G., Mat Azmi, I.D., Yaghmur, A., 2019. Nanomedicines for cancer therapy: current status, challenges and future prospects. Therapeutic Delivery 10, 113–132. https://doi.org/10.4155/tde-2018-0062

Boulaiz, H., Alvarez, P.J., Ramirez, A., Marchal, J.A., Prados, J., Rodríguez-Serrano, F., Perán, M., Melguizo, C., Aranega, A., 2011. Nanomedicine: Application Areas and Development Prospects. Int J Mol Sci 12, 3303–3321. https://doi.org/10.3390/ijms12053303

Boussif, O., Lezoualc'h, F., Zanta, M.A., Mergny, M.D., Scherman, D., Demeneix, B., Behr, J.P., 1995. A versatile vector for gene and oligonucleotide transfer into cells in culture and in vivo: polyethylenimine. Proceedings of the National Academy of Sciences 92, 7297–7301. https://doi.org/10.1073/pnas.92.16.7297

Bozzuto, G., Molinari, A., 2015. Liposomes as nanomedical devices. Int J Nanomedicine 10, 975–999. https://doi.org/10.2147/IJN.S68861

Bregoli, L., Movia, D., Gavigan-Imedio, J.D., Lysaght, J., Reynolds, J., Prina-Mello, A., 2016. Nanomedicine applied to translational oncology: A future perspective on cancer

treatment. Nanomedicine: Nanotechnology, Biology and Medicine 12, 81–103. https://doi.org/10.1016/j.nano.2015.08.006

Bremer- Hoffmann, S., Halamoda- Kenzaoui, B., Borgos, S.E., 2018. Identification of regulatory needs for nanomedicines. Journal of Interdisciplinary Nanomedicine 3, 4–15. https://doi.org/10.1002/jin2.34

Breton, M., Leblond, J., Tranchant, I., Scherman, D., Bessodes, M., Herscovici, J., Mignet, N., 2011. Lipothioureas as Lipids for Gene Transfection: A Review. Pharmaceuticals (Basel) 4, 1381–1399. https://doi.org/10.3390/ph4101381

Bulbake, U., Doppalapudi, S., Kommineni, N., Khan, W., 2017. Liposomal Formulations in Clinical Use: An Updated Review. Pharmaceutics 9. https://doi.org/10.3390/pharmaceutics9020012

Bumcrot, D., Manoharan, M., Koteliansky, V., Sah, D.W.Y., 2006. RNAi therapeutics: a potential new class of pharmaceutical drugs. Nat Chem Biol 2, 711–719. https://doi.org/10.1038/nchembio839

Byk, G., Dubertret, C., Escriou, V., Frederic, M., Jaslin, G., Rangara, R., Pitard, B., Crouzet, J., Wils, P., Schwartz, B., Scherman, D., 1998. Synthesis, Activity, and Structure−Activity Relationship Studies of Novel Cationic Lipids for DNA Transfer. J. Med. Chem. 41, 224–235. https://doi.org/10.1021/jm9704964

Çağdaş, M., Sezer, A.D., Bucak, S., 2014. Liposomes as Potential Drug Carrier Systems for Drug Delivery, in: Sezer, A.D. (Ed.), Application of Nanotechnology in Drug Delivery. InTech. https://doi.org/10.5772/58459

Carugo, D., Bottaro, E., Owen, J., Stride, E., Nastruzzi, C., 2016. Liposome production by microfluidics: potential and limiting factors. Scientific Reports 6, 25876. https://doi.org/10.1038/srep25876

Chambre, L., Degirmenci, A., Sanyal, R., Sanyal, A., 2018. Multi-Functional Nanogels as Theranostic Platforms: Exploiting Reversible and Nonreversible Linkages for Targeting, Imaging, and Drug Delivery. Bioconjugate Chemistry 29, 1885–1896. https://doi.org/10.1021/acs.bioconjchem.8b00085

Chandaroy, P., Sen, A., Hui, S.W., 2001. Temperature-controlled content release from liposomes encapsulating Pluronic F127. Journal of Controlled Release 76, 27–37. https://doi.org/10.1016/S0168-3659(01)00429-1

Charcosset, C., Juban, A., Valour, J.-P., Urbaniak, S., Fessi, H., 2015. Preparation of liposomes at large scale using the ethanol injection method: Effect of scale-up and injection

devices. Chemical Engineering Research and Design 94, 508–515. https://doi.org/10.1016/j.cherd.2014.09.008

Chen, J., Zhou, R., Li, L., Li, B., Zhang, X., Su, J., 2013. Mechanical, Rheological and Release Behaviors of a Poloxamer 407/ Poloxamer 188/Carbopol 940 Thermosensitive Composite Hydrogel. Molecules 18, 12415–12425. https://doi.org/10.3390/molecules181012415

Chen, L.-J., Yang, C.-X., Yan, X.-P., 2017. Liposome-Coated Persistent Luminescence Nanoparticles as Luminescence Trackable Drug Carrier for Chemotherapy. Anal. Chem. 89, 6936–6939. https://doi.org/10.1021/acs.analchem.7b01397

Chen, W., Hou, Y., Tu, Z., Gao, L., Haag, R., 2017a. pH-degradable PVA-based nanogels via photo-crosslinking of thermo-preinduced nanoaggregates for controlled drug delivery. Journal of Controlled Release 259, 160–167. https://doi.org/10.1016/J.JCONREL.2016.10.032

Chen, W., Zheng, M., Meng, F., Cheng, R., Deng, C., Feijen, J., Zhong, Z., 2013. In Situ Forming Reduction-Sensitive Degradable Nanogels for Facile Loading and Triggered Intracellular Release of Proteins. Biomacromolecules 14, 1214–1222. https://doi.org/10.1021/bm400206m

Chen, W., Zou, Y., Zhong, Z., Haag, R., 2017b. Cyclo(RGD)-Decorated Reduction-Responsive Nanogels Mediate Targeted Chemotherapy of Integrin Overexpressing Human Glioblastoma In Vivo. Small 13, 1–9. https://doi.org/10.1002/smll.201601997

Cheng, R., Feng, F., Meng, F., Deng, C., Feijen, J., 2011. Glutathione-responsive nano-vehicles as a promising platform for targeted intracellular drug and gene delivery. Journal of Controlled Release 152, 2–12. https://doi.org/10.1016/J.JCONREL.2011.01.030

Choi, C.A., Ryplida, B., In, I., Park, S.Y., 2019. Selective redox-responsive theragnosis nanocarrier for breast tumor cells mediated by MnO2/fluorescent carbon nanogel. European Journal of Pharmaceutical Sciences 134, 256–265. https://doi.org/10.1016/J.EJPS.2019.04.027

Coty, J.-B., Vauthier, C., 2018. Characterization of nanomedicines: A reflection on a field under construction needed for clinical translation success. J Control Release 275, 254–268. https://doi.org/10.1016/j.jconrel.2018.02.013

Couillaud, B.M., Espeau, P., Mignet, N., Corvis, Y., 2019. State of the Art of Pharmaceutical Solid Forms: from Crystal Property Issues to Nanocrystals Formulation. ChemMedChem 14, 8–23. https://doi.org/10.1002/cmdc.201800612

Couvreur, P., 2019. Nanomedicine: From where are we coming and where are we going? J Control Release 311–312, 319–321. https://doi.org/10.1016/j.jconrel.2019.10.020

Couvreur, P., 2013. Nanoparticles in drug delivery: Past, present and future. Advanced Drug Delivery Reviews 65, 21–23. https://doi.org/10.1016/j.addr.2012.04.010

Crommelin, D.J.A., van Bloois, L., 1983. Preparation and characterization of doxorubicin-containing liposomes. II. Loading capacity, long-term stability and doxorubicin-bilayer interaction mechanism. International Journal of Pharmaceutics 17, 135–144. https://doi.org/10.1016/0378-5173(83)90027-3

Danson, S., Ferry, D., Alakhov, V., Margison, J., Kerr, D., Jowle, D., Brampton, M., Halbert, G., Ranson, M., 2004. Phase I dose escalation and pharmacokinetic study of pluronic polymer-bound doxorubicin (SP1049C) in patients with advanced cancer. British Journal of Cancer 90, 2085–2091. https://doi.org/10.1038/sj.bjc.6601856

Das, D., Rameshbabu, A.P., Ghosh, P., Patra, P., Dhara, S., Pal, S., 2017. Biocompatible nanogel derived from functionalized dextrin for targeted delivery of doxorubicin hydrochloride to MG 63 cancer cells. Carbohydrate Polymers 171, 27–38. https://doi.org/10.1016/J.CARBPOL.2017.04.068

Devi, D.R., Sandhya, P., Hari, B.N.V., 2013. Poloxamer: A Novel Functional Molecule For Drug Delivery And Gene Therapy. J. Pharm. Sci. 7.

Ding, B.-S., Dziubla, T., Shuvaev, V.V., Muro, S., Muzykantov, V.R., 2006. Advanced drug delivery systems that target the vascular endothelium. Mol. Interv. 6, 98–112. https://doi.org/10.1124/mi.6.2.7

Dreaden, E.C., Raji, I.O., Austin, L.A., Fathi, S., Mwakwari, S.C., Humphries, W.H., Kang, B., Oyelere, A.K., El-Sayed, M.A., 2014. P-Glycoprotein-Dependent Trafficking of Nanoparticle-Drug Conjugates. Small 10, 1719–1723. https://doi.org/10.1002/smll.201303190

Dumortier, G., Grossiord, J.L., Agnely, F., Chaumeil, J.C., 2006. A Review of Poloxamer 407 Pharmaceutical and Pharmacological Characteristics. Pharm Res 23, 2709–2728. https://doi.org/10.1007/s11095-006-9104-4

Eckmann, D.M., Composto, R.J., Tsourkas, A., Muzykantov, V.R., 2014. Nanogel Carrier Design for Targeted Drug Delivery. J Mater Chem B Mater Biol Med 2, 8085–8097. https://doi.org/10.1039/C4TB01141D

Ewe, A., Panchal, O., Pinnapireddy, S.R., Bakowsky, U., Przybylski, S., Temme, A., Aigner, A., 2017. Liposome-polyethylenimine complexes (DPPC-PEI lipopolyplexes) for

therapeutic siRNA delivery in vivo. Nanomedicine 13, 209–218. https://doi.org/10.1016/j.nano.2016.08.005

Fakhari, A., Corcoran, M., Schwarz, A., 2017. Thermogelling properties of purified poloxamer 407. Heliyon 3, e00390. https://doi.org/10.1016/j.heliyon.2017.e00390

Falzone, L., Salomone, S., Libra, M., 2018. Evolution of Cancer Pharmacological Treatments at the Turn of the Third Millennium. Front Pharmacol 9. https://doi.org/10.3389/fphar.2018.01300

Fang, C., Zhang, M., 2010. Nanoparticle-based theragnostics: integrating diagnostic and therapeutic potentials in nanomedicine. J Control Release 146, 2–5. https://doi.org/10.1016/j.jconrel.2010.05.013

Felice, B., Prabhakaran, M.P., Rodríguez, A.P., Ramakrishna, S., 2014. Drug delivery vehicles on a nano-engineering perspective. Materials Science and Engineering: C 41, 178–195. https://doi.org/10.1016/j.msec.2014.04.049

Ferrari, M., 2005. Cancer nanotechnology: opportunities and challenges. Nature Reviews Cancer 5, 161–171. https://doi.org/10.1038/nrc1566

Ferreira, N.N., Ferreira, L.M.B., Cardoso, V.M.O., Boni, F.I., Souza, A.L.R., Gremião, M.P.D., 2018. Recent advances in smart hydrogels for biomedical applications: From self-assembly to functional approaches. European Polymer Journal 99, 117–133. https://doi.org/10.1016/j.eurpolymj.2017.12.004

Ficai, D., Grumezescu, A.M., 2017. Nanostructures for Novel Therapy: Synthesis, Characterization and Applications. Elsevier.

Fire, A., Albertson, D., Harrison, S.W., Moerman, D.G., 1991. Production of antisense RNA leads to effective and specific inhibition of gene expression in C. elegans muscle. Development 113, 503–514.

Fire, A., Xu, S., Montgomery, M.K., Kostas, S.A., Driver, S.E., Mello, C.C., 1998. Potent and specific genetic interference by double-stranded RNA in Caenorhabditis elegans. Nature 391, 806–811. https://doi.org/10.1038/35888

Fràter-Schröder, M., Risau, W., Hallmann, R., Gautschi, P., Böhlen, P., 1987. Tumor necrosis factor type alpha, a potent inhibitor of endothelial cell growth in vitro, is angiogenic in vivo. Proc. Natl. Acad. Sci. U.S.A. 84, 5277–5281. https://doi.org/10.1073/pnas.84.15.5277

Gao, W., Vecchio, D., Li, Jieming, Zhu, J., Zhang, Q., Fu, V., Li, Jiayang, Thamphiwatana, S., Lu, D., Zhang, L., 2014. Hydrogel Containing Nanoparticle-Stabilized Liposomes for

Topical Antimicrobial Delivery. ACS Nano 8, 2900–2907. https://doi.org/10.1021/nn500110a

Gaumet, M., Vargas, A., Gurny, R., Delie, F., 2008. Nanoparticles for drug delivery: The need for precision in reporting particle size parameters. European Journal of Pharmaceutics and Biopharmaceutics 69, 1–9. https://doi.org/10.1016/J.EJPB.2007.08.001

Ghanbarzadeh, S., Khorrami, A., Arami, S., 2014a. Preparation of optimized Naproxen nano liposomes using response surface methodology. Journal of Pharmaceutical Investigation 44, 33–39. https://doi.org/10.1007/s40005-013-0098-8

Ghanbarzadeh, S., Khorrami, A., Arami, S., 2014b. Preparation of optimized Naproxen nano liposomes using response surface methodology. Journal of Pharmaceutical Investigation 44, 33–39. https://doi.org/10.1007/s40005-013-0098-8

Green, A.E., Rose, P.G., 2006. Pegylated liposomal doxorubicin in ovarian cancer. Int J Nanomedicine 1, 229–239.

Gregoriadis, G., Florence, A.T., 1993. Liposomes in Drug Delivery: Clinical, Diagnostic and Ophthalmic Potential. Drugs 45, 15–28. https://doi.org/10.2165/00003495-199345010-00003

Grijalvo, S., Mayr, J., Eritja, R., Díaz, D.D., 2016. Biodegradable liposome-encapsulated hydrogels for biomedical applications: a marriage of convenience. Biomaterials Science 4, 555–574. https://doi.org/10.1039/C5BM00481K

Guan, P., Lu, Y., Qi, J., Niu, M., Lian, R., Wu, W., 2015. Solidification of liposomes by freeze-drying: the importance of incorporating gelatin as interior support on enhanced physical stability. Int J Pharm 478, 655–664. https://doi.org/10.1016/j.ijpharm.2014.12.016

Guo, H., Kim, J.-C., 2017. Reduction-Sensitive Poly(ethylenimine) Nanogel Bearing Dithiodipropionic Acid. CHEMICAL & PHARMACEUTICAL BULLETIN 65, 718–725. https://doi.org/10.1248/cpb.c17-00029

Gurova, K., 2009. New hopes from old drugs: revisiting DNA-binding small molecules as anticancer agents. Future Oncol 5, 1685. https://doi.org/10.2217/fon.09.127

Hacein-Bey-Abina, S., Hauer, J., Lim, A., Picard, C., Wang, G.P., Berry, C.C., Martinache, C., Rieux-Laucat, F., Latour, S., Belohradsky, B.H., Leiva, L., Sorensen, R., Debré, M., Casanova, J.L., Blanche, S., Durandy, A., Bushman, F.D., Fischer, A., Cavazzana-Calvo, M., 2010. Efficacy of Gene Therapy for X-Linked Severe Combined Immunodeficiency. N Engl J Med 363, 355–364. https://doi.org/10.1056/NEJMoa1000164

Haleem, A., Javaid, M., 2019. Polyether ether ketone (PEEK) and its 3D printed implants applications in medical field: An overview. Clinical Epidemiology and Global Health. https://doi.org/10.1016/j.cegh.2019.01.003

Haslam, A., Prasad, V., 2019. Estimation of the Percentage of US Patients With Cancer Who Are Eligible for and Respond to Checkpoint Inhibitor Immunotherapy Drugs. JAMA Netw Open 2, e192535–e192535. https://doi.org/10.1001/jamanetworkopen.2019.2535

Hassanpour, S.H., Dehghani, M., 2017. Review of cancer from perspective of molecular. Journal of Cancer Research and Practice 4, 127–129. https://doi.org/10.1016/j.jcrpr.2017.07.001

Hatakeyama, T., Tanaka, M., Hatakeyama, H., 2010. Thermal Properties of Freezing Bound Water Restrained by Polysaccharides. Journal of Biomaterials Science, Polymer Edition 21, 1865–1875. https://doi.org/10.1163/092050610X486946

Heinzerling, L., de Toni, E.N., Schett, G., Hundorfean, G., Zimmer, L., 2019. Checkpoint Inhibitors. Dtsch Arztebl Int 116, 119–126. https://doi.org/10.3238/arztebl.2019.0119

Hemelryck, S.V., Dewulf, J., Niekus, H., van Heerden, M., Ingelse, B., Holm, R., Mannaert, E., Langguth, P., 2019. In vitro evaluation of poloxamer in situ forming gels for bedaquiline fumarate salt and pharmacokinetics following intramuscular injection in rats. International Journal of Pharmaceutics: X 1, 100016. https://doi.org/10.1016/j.ijpx.2019.100016

Höbel, S., Aigner, A., 2010. Polyethylenimine (PEI)/siRNA-mediated gene knockdown in vitro and in vivo. Methods Mol. Biol. 623, 283–297. https://doi.org/10.1007/978-1-60761-588-0_18

Hong, J.S., Stavis, S.M., DePaoli Lacerda, S.H., Locascio, L.E., Raghavan, S.R., Gaitan, M., 2010. Microfluidic Directed Self-Assembly of Liposome−Hydrogel Hybrid Nanoparticles. Langmuir 26, 11581–11588. https://doi.org/10.1021/la100879p

Hu, J., Zhang, G., Liu, S., 2012. Enzyme-responsive polymeric assemblies, nanoparticles and hydrogels. Chemical Society Reviews 41, 5933. https://doi.org/10.1039/c2cs35103j

Hua, S., Wu, S.Y., 2013. The use of lipid-based nanocarriers for targeted pain therapies. Front Pharmacol 4, 143. https://doi.org/10.3389/fphar.2013.00143

Huang, K., Shi, B., Xu, W., Ding, J., Yang, Y., Liu, H., Zhuang, X., Chen, X., 2015. Reduction-responsive polypeptide nanogel delivers antitumor drug for improved efficacy and safety. Acta Biomaterialia 27, 179–193. https://doi.org/10.1016/J.ACTBIO.2015.08.049

Huang, L., Nishinari, K., 2001. Interaction between poly(ethylene glycol) and water as studied by differential scanning calorimetry. Journal of Polymer Science Part B: Polymer Physics 39, 496–506. https://doi.org/10.1002/1099-0488(20010301)39:5<496::AID-POLB1023>3.0.CO;2-H

Huang, X., Brazel, C.S., 2001. On the importance and mechanisms of burst release in matrix-controlled drug delivery systems. Journal of Controlled Release 73, 121–136. https://doi.org/10.1016/S0168-3659(01)00248-6

Hughes, J., Yadava, P., Mesaros, R., 2010. Liposomal siRNA Delivery, in: Weissig, V. (Ed.), Liposomes: Methods and Protocols, Volume 1: Pharmaceutical Nanocarriers, Methods in Molecular Biology. Humana Press, Totowa, NJ, pp. 445–459. https://doi.org/10.1007/978-1-60327-360-2_31

Iyer, M.A., Eddington, D.T., 2019. Storing and releasing rhodamine as a model hydrophobic compound in polydimethylsiloxane microfluidic devices. Lab Chip 19, 574–579. https://doi.org/10.1039/C9LC00039A

Jahn, A., Vreeland, W.N., Gaitan, M., Locascio, L.E., 2004. Controlled Vesicle Self-Assembly in Microfluidic Channels with Hydrodynamic Focusing. J. Am. Chem. Soc. 126, 2674–2675. https://doi.org/10.1021/ja0318030

Jiang, H., Kelch, S., Lendlein, A., 2006. Polymers move in response to light. Advanced Materials 18, 1471–1475. https://doi.org/10.1002/adma.200502266

Jing Yang, W., Zhou, P., Liang, L., Cao, Y., Qiao, J., Li, X., Teng, Z., Wang, L., 2018. Nanogel-Incorporated Injectable Hydrogel for Synergistic Therapy Based on Sequential Local Delivery of Combretastatin-A4 Phosphate (CA4P) and Doxorubicin (DOX). ACS Applied Materials & Interfaces 10, 18560–18573. https://doi.org/10.1021/acsami.8b04394

Joshi, S., Hussain, M.T., Roces, C.B., Anderluzzi, G., Kastner, E., Salmaso, S., Kirby, D.J., Perrie, Y., 2016. Microfluidics based manufacture of liposomes simultaneously entrapping hydrophilic and lipophilic drugs. Int J Pharm 514, 160–168. https://doi.org/10.1016/j.ijpharm.2016.09.027

Kabanov, A. V., Vinogradov, S. V., 2009. Nanogels as Pharmaceutical Carriers: Finite Networks of Infinite Capabilities. Angewandte Chemie International Edition 48, 5418–5429. https://doi.org/10.1002/anie.200900441

Kamboj, V.K., Verma, P.K., 2015. Poloxamers based nanocarriers for drug delivery system.

Kang, M.G., Lee, M.Y., Cha, J.M., Lee, J.K., Lee, S.C., Kim, J., Hwang, Y.-S., Bae, H., 2019. Nanogels Derived from Fish Gelatin: Application to Drug Delivery System. Marine Drugs 17, 246. https://doi.org/10.3390/md17040246

Khoshnood, A., Lukanov, B., Firoozabadi, A., 2016. Temperature Effect on Micelle Formation: Molecular Thermodynamic Model Revisited. Langmuir 32, 2175–2183. https://doi.org/10.1021/acs.langmuir.6b00039

Kieler-Ferguson, H.M., Chan, D., Sockolosky, J., Finney, L., Maxey, E., Vogt, S., Szoka, F.C., 2017. Encapsulation, controlled release, and antitumor efficacy of cisplatin delivered in liposomes composed of sterol-modified phospholipids. Eur J Pharm Sci 103, 85–93. https://doi.org/10.1016/j.ejps.2017.03.003

Kim, J.-C., Bae, S.K., Kim, J.-D., 1997. Temperature-Sensitivity of Liposomal Lipid Bilayers Mixed with Poly(N-Isopropylacrylamide-co-acrylic Acid). J Biochem 121, 15–19. https://doi.org/10.1093/oxfordjournals.jbchem.a021558

Klouda, L., Mikos, A.G., 2008a. Thermoresponsive hydrogels in biomedical applications. European Journal of Pharmaceutics and Biopharmaceutics 68, 34–45. https://doi.org/10.1016/j.ejpb.2007.02.025

Klouda, L., Mikos, A.G., 2008b. Thermoresponsive hydrogels in biomedical applications. Eur J Pharm Biopharm 68, 34–45. https://doi.org/10.1016/j.ejpb.2007.02.025

Knudsen, K.B., Northeved, H., Kumar EK, P., Permin, A., Gjetting, T., Andresen, T.L., Larsen, S., Wegener, K.M., Lykkesfeldt, J., Jantzen, K., Loft, S., Møller, P., Roursgaard, M., 2015. In vivo toxicity of cationic micelles and liposomes. Nanomedicine: Nanotechnology, Biology and Medicine 11, 467–477. https://doi.org/10.1016/j.nano.2014.08.004

Koning, G.A., Storm, G., 2003. Targeted drug delivery systems for the intracellular delivery of macromolecular drugs. Drug Discov. Today 8, 482–483. https://doi.org/10.1016/s1359-6446(03)02699-0

Kostarelos, K., Miller, A.D., 2005. What role can chemistry play in cationic liposome-based gene therapy research today? Adv. Genet. 53, 71–118.

Kube, S., Hersch, N., Naumovska, E., Gensch, T., Hendriks, J., Franzen, A., Landvogt, L., Siebrasse, J.-P., Kubitscheck, U., Hoffmann, B., Merkel, R., Csiszár, A., 2017. Fusogenic Liposomes as Nanocarriers for the Delivery of Intracellular Proteins. Langmuir 33, 1051–1059. https://doi.org/10.1021/acs.langmuir.6b04304

Kumar, A., Chen, F., Mozhi, A., Zhang, Xu, Zhao, Y., Xue, X., Hao, Y., Zhang, Xiaoning, Wang, P.C., Liang, X.-J., 2013. Innovative pharmaceutical development based on

unique properties of nanoscale delivery formulation. Nanoscale 5, 8307–8325. https://doi.org/10.1039/c3nr01525d

Kumar, S., Xu, X., Gokhale, R., Burgess, D.J., 2014. Formulation parameters of crystalline nanosuspensions on spray drying processing: A DoE approach. International Journal of Pharmaceutics 464, 34–45. https://doi.org/10.1016/j.ijpharm.2014.01.013

Lee, H., Mok, H., Lee, S., Oh, Y.-K., Park, T.G., 2007. Target-specific intracellular delivery of siRNA using degradable hyaluronic acid nanogels. Journal of Controlled Release 119, 245–252. https://doi.org/10.1016/J.JCONREL.2007.02.011

Lee, S.H., Choi, S.H., Kim, S.H., Park, T.G., 2008. Thermally sensitive cationic polymer nanocapsules for specific cytosolic delivery and efficient gene silencing of siRNA: Swelling induced physical disruption of endosome by cold shock. Journal of Controlled Release 125, 25–32. https://doi.org/10.1016/j.jconrel.2007.09.011

Li, H., Zhou, Z., Zhang, F., Guo, Y., Yang, X., Jiang, H., Tan, F., Oupicky, D., Sun, M., 2018. A networked swellable dextrin nanogels loading Bcl2 siRNA for melanoma tumor therapy. Nano Research 11, 4627–4642. https://doi.org/10.1007/s12274-018-2044-6

Li, X., Su, X., 2018. Multifunctional smart hydrogels: potential in tissue engineering and cancer therapy. Journal of Materials Chemistry B 6, 4714–4730. https://doi.org/10.1039/C8TB01078A

Li, Z., Tan, S., Li, S., Shen, Q., Wang, K., 2017. Cancer drug delivery in the nano era: An overview and perspectives (Review). Oncology Reports 38, 611–624. https://doi.org/10.3892/or.2017.5718

Lin, C.-C., Metters, A.T., 2006. Hydrogels in controlled release formulations: Network design and mathematical modeling. Advanced Drug Delivery Reviews 58, 1379–1408. https://doi.org/10.1016/J.ADDR.2006.09.004

Lin, Z., Gao, W., Hu, H., Ma, K., He, B., Dai, W., Wang, X., Wang, J., Zhang, X., Zhang, Q., 2014. Novel thermo-sensitive hydrogel system with paclitaxel nanocrystals: High drug-loading, sustained drug release and extended local retention guaranteeing better efficacy and lower toxicity. Journal of Controlled Release 174, 161–170. https://doi.org/10.1016/J.JCONREL.2013.10.026

Liu, L., Du, P., Zhao, X., Zeng, J., Liu, P., 2015. Independent temperature and pH dual-stimuli responsive yolk/shell polymer microspheres for controlled release: Structural effect. European Polymer Journal 69, 540–551. https://doi.org/10.1016/J.EURPOLYMJ.2015.03.026

Losic, D., Atkins, G.J., Pivonka, P., Findlay, D., Aw, M.S., Khalid, K.A., Gulati, K., 2012. Characterization of drug-release kinetics in trabecular bone from titania nanotube implants. IJN 4883. https://doi.org/10.2147/IJN.S33655

Lou, S., Zhang, X., Zhang, M., Ji, S., Wang, W., Zhang, J., Li, C., Kong, D., 2017. Preparation of a dual cored hepatoma-specific star glycopolymer nanogel via arm-first ATRP approach. International journal of nanomedicine 12, 3653–3664. https://doi.org/10.2147/IJN.S134367

Lu, N., Yang, K., Li, J., Weng, Y., Yuan, B., Ma, Y., 2013a. Controlled Drug Loading and Release of a Stimuli-Responsive Lipogel Consisting of Poly(N -isopropylacrylamide) Particles and Lipids. The Journal of Physical Chemistry B 117, 9677–9682. https://doi.org/10.1021/jp402826n

Lu, N., Yang, K., Li, J., Weng, Y., Yuan, B., Ma, Y., 2013b. Controlled Drug Loading and Release of a Stimuli-Responsive Lipogel Consisting of Poly(N-isopropylacrylamide) Particles and Lipids. J. Phys. Chem. B 117, 9677–9682. https://doi.org/10.1021/jp402826n

Lu, X., Sun, M., Barron, A.E., 2011. Non-ionic, thermo-responsive DEA/DMA nanogels: Synthesis, characterization, and use for DNA separations by microchip electrophoresis. Journal of Colloid and Interface Science 357, 345–353. https://doi.org/10.1016/J.JCIS.2011.01.079

Luckanagul, J.A., Pitakchatwong, C., Ratnatilaka Na Bhuket, P., Muangnoi, C., Rojsitthisak, Pranee, Chirachanchai, S., Wang, Q., Rojsitthisak, Pornchai, 2018. Chitosan-based polymer hybrids for thermo-responsive nanogel delivery of curcumin. Carbohydrate Polymers 181, 1119–1127. https://doi.org/10.1016/J.CARBPOL.2017.11.027

Lux, F., Tran, V.L., Thomas, E., Dufort, S., Rossetti, F., Martini, M., Truillet, C., Doussineau, T., Bort, G., Denat, F., Boschetti, F., Angelovski, G., Detappe, A., Crémillieux, Y., Mignet, N., Doan, B.-T., Larrat, B., Meriaux, S., Barbier, E., Roux, S., Fries, P., Müller, A., Abadjian, M.-C., Anderson, C., Canet-Soulas, E., Bouziotis, P., Barberi-Heyob, M., Frochot, C., Verry, C., Balosso, J., Evans, M., Sidi-Boumedine, J., Janier, M., Butterworth, K., McMahon, S., Prise, K., Aloy, M.-T., Ardail, D., Rodriguez-Lafrasse, C., Porcel, E., Lacombe, S., Berbeco, R., Allouch, A., Perfettini, J.-L., Chargari, C., Deutsch, E., Le Duc, G., Tillement, O., 2018. AGuIX® from bench to bedside-Transfer of an ultrasmall theranostic gadolinium-based nanoparticle to clinical medicine. Br J Radiol 20180365. https://doi.org/10.1259/bjr.20180365

Maheux, S., Frache, G., Thomann, J.S., Clément, F., Penny, C., Belmonte, T., Duday, D., 2016. Small unilamellar liposomes as a membrane model for cell inactivation by cold atmospheric plasma treatment. Journal of Physics D: Applied Physics 49, 344001. https://doi.org/10.1088/0022-3727/49/34/344001

Mahmoodi Chalbatani, G., Dana, H., Gharagouzloo, E., Grijalvo, S., Eritja, R., Logsdon, C.D., Memari, F., Miri, S.R., Rad, M.R., Marmari, V., 2019. Small interfering RNAs (siRNAs) in cancer therapy: a nano-based approach. Int J Nanomedicine 14, 3111–3128. https://doi.org/10.2147/IJN.S200253

Mandal, B., Bhattacharjee, H., Mittal, N., Sah, H., Balabathula, P., Thoma, L.A., Wood, G.C., 2013. Core–shell-type lipid–polymer hybrid nanoparticles as a drug delivery platform. Nanomedicine: Nanotechnology, Biology and Medicine 9, 474–491. https://doi.org/10.1016/j.nano.2012.11.010

Manta, S., Delalande, A., Renault, G., Bureau, M.F., Lebertre, M., Marie, C., Scherman, D., Midoux, P., Mignet, N., Pichon, C., n.d. Positively charged microbubbles to target nucleic acid delivery with ultrasound 3.

Mazzoleni, G., Di Lorenzo, D., Steimberg, N., 2009. Modelling tissues in 3D: the next future of pharmaco-toxicology and food research? Genes Nutr 4, 13–22. https://doi.org/10.1007/s12263-008-0107-0

Metselaar, J.M., Storm, G., 2005. Liposomes in the treatment of inflammatory disorders. Expert Opin Drug Deliv 2, 465–476. https://doi.org/10.1517/17425247.2.3.465

Metzner, C., Dangerfield, J., 2011. Surface Modification of Retroviral Vectors for Gene Therapy. Viral Gene Therapy. https://doi.org/10.5772/20568

Mignet, N., Richard, C., Seguin, J., Largeau, C., Bessodes, M., Scherman, D., 2008. Anionic pH-sensitive pegylated lipoplexes to deliver DNA to tumors. International Journal of Pharmaceutics 361, 194–201. https://doi.org/10.1016/j.ijpharm.2008.05.017

Milla, P., Dosio, F., Cattel, L., 2012. PEGylation of Proteins and Liposomes: a Powerful and Flexible Strategy to Improve the Drug Delivery. CDM 13, 105–119. https://doi.org/10.2174/138920012798356934

Mitchell, S.J., Huizer-Pajkos, A., Cogger, V.C., McLachlan, A.J., Le Couteur, D.G., Jones, B., de Cabo, R., Hilmer, S.N., 2012. The Influence of Old Age and Poloxamer-407 on the Hepatic Disposition of Diazepam in the Isolated Perfused Rat Liver. Pharmacology 90, 233–241. https://doi.org/10.1159/000341724

Moghimi, S.M., Hunter, A.C., 2000. Poloxamers and poloxamines in nanoparticle engineering and experimental medicine. Trends in Biotechnology 18, 412–420. https://doi.org/10.1016/S0167-7799(00)01485-2

Moghimi, S.M., Hunter, A.C., Murray, J.C., 2005. Nanomedicine: current status and future prospects. The FASEB Journal 19, 311–330. https://doi.org/10.1096/fj.04-2747rev

Moghimi, S.M., Porter, C.J.H., Illum, L., Davis, S.S., 1991. The effect of poloxamer-407 on liposome stability and targeting to bone marrow: comparison with polystyrene microspheres. International Journal of Pharmaceutics 68, 121–126. https://doi.org/10.1016/0378-5173(91)90134-A

Molina, M., Asadian-Birjand, M., Balach, J., Bergueiro, J., Miceli, E., Calderón, M., 2015. Stimuli-responsive nanogel composites and their application in nanomedicine. Chemical Society Reviews 44, 6161–6186. https://doi.org/10.1039/C5CS00199D

Mortensen, K., Pedersen, J.S., 1993. Structural study on the micelle formation of poly(ethylene oxide)-poly(propylene oxide)-poly(ethylene oxide) triblock copolymer in aqueous solution. Macromolecules 26, 805–812. https://doi.org/10.1021/ma00056a035

Niazi, M., Zakeri-Milani, P., Najafi Hajivar, S., Soleymani Goloujeh, M., Ghobakhlou, N., Shahbazi Mojarrad, J., Valizadeh, H., 2016. Nano-based strategies to overcome p-glycoprotein-mediated drug resistance. Expert Opinion on Drug Metabolism & Toxicology 12, 1021–1033. https://doi.org/10.1080/17425255.2016.1196186

Nkanga, C.I., Bapolisi, A.M., Okafor, N.I., Krause, R.W.M., 2019. General Perception of Liposomes: Formation, Manufacturing and Applications. Liposomes - Advances and Perspectives. https://doi.org/10.5772/intechopen.84255

Nussbaumer, S., Bonnabry, P., Veuthey, J.-L., Fleury-Souverain, S., 2011. Analysis of anticancer drugs: A review. Talanta 85, 2265–2289. https://doi.org/10.1016/j.talanta.2011.08.034

Oh, H.R., Jo, H.-Y., Park, J.S., Kim, D.-E., Cho, J.-Y., Kim, P.-H., Kim, K.-S., 2016. Galactosylated Liposomes for Targeted Co-Delivery of Doxorubicin/Vimentin siRNA to Hepatocellular Carcinoma. Nanomaterials (Basel) 6. https://doi.org/10.3390/nano6080141

Oh, Y.-K., Park, T.G., 2009. siRNA delivery systems for cancer treatment. Adv. Drug Deliv. Rev. 61, 850–862. https://doi.org/10.1016/j.addr.2009.04.018

Olusanya, T.O.B., Haj Ahmad, R.R., Ibegbu, D.M., Smith, J.R., Elkordy, A.A., 2018. Liposomal Drug Delivery Systems and Anticancer Drugs. Molecules 23. https://doi.org/10.3390/molecules23040907

Pampaloni, F., Reynaud, E.G., Stelzer, E.H.K., 2007. The third dimension bridges the gap between cell culture and live tissue. Nat Rev Mol Cell Biol 8, 839–845. https://doi.org/10.1038/nrm2236

Panonnummal, R., Sabitha, M., 2018. Anti-psoriatic and toxicity evaluation of methotrexate loaded chitin nanogel in imiquimod induced mice model. International Journal of Biological Macromolecules 110, 245–258. https://doi.org/10.1016/J.IJBIOMAC.2017.10.112

Patil, Y.P., Jadhav, S., 2014. Novel methods for liposome preparation. Chem. Phys. Lipids 177, 8–18. https://doi.org/10.1016/j.chemphyslip.2013.10.011

Patnaik, S., Sharma, A.K., Garg, B.S., Gandhi, R.P., Gupta, K.C., 2007. Photoregulation of drug release in azo-dextran nanogels. International Journal of Pharmaceutics 342, 184–193. https://doi.org/10.1016/J.IJPHARM.2007.04.038

Pelton, R., 2000. Temperature-sensitive aqueous microgels. Advances in Colloid and Interface Science 85, 1–33. https://doi.org/10.1016/S0001-8686(99)00023-8

Pembouong, G., Morellet, N., Kral, T., Hof, M., Scherman, D., Bureau, M.-F., Mignet, N., 2011. A comprehensive study in triblock copolymer membrane interaction. Journal of Controlled Release 151, 57–64. https://doi.org/10.1016/j.jconrel.2011.01.007

Peng, Z., Wang, C., Fang, E., Lu, X., Wang, G., Tong, Q., 2014. Co-Delivery of Doxorubicin and SATB1 shRNA by Thermosensitive Magnetic Cationic Liposomes for Gastric Cancer Therapy. PLoS One 9. https://doi.org/10.1371/journal.pone.0092924

Pepe, A., Podesva, P., Simone, G., 2017. Tunable uptake/release mechanism of protein microgel particles in biomimicking environment. Sci Rep 7. https://doi.org/10.1038/s41598-017-06512-5

Peppas, N., 2000. Hydrogels in pharmaceutical formulations. European Journal of Pharmaceutics and Biopharmaceutics 50, 27–46. https://doi.org/10.1016/S0939-6411(00)00090-4

Peppas, N.A.A., Bures, P., Leobandung, W., Ichikawa, H., 2000. Hydrogels in pharmaceutical formulations. European Journal of Pharmaceutics and Biopharmaceutics 50, 27–46. https://doi.org/10.1016/S0939-6411(00)00090-4

Pham, T.T., Jaafar-Maalej, C., Charcosset, C., Fessi, H., 2012. Liposome and niosome preparation using a membrane contactor for scale-up. Colloids and Surfaces B: Biointerfaces 94, 15–21. https://doi.org/10.1016/j.colsurfb.2011.12.036

Poljaková, J., Eckschlager, T., Hřebačková, J., Hraběta, J., Stiborová, M., 2008. The comparison of cytotoxicity of the anticancer drugs doxorubicin and ellipticine to human

neuroblastoma cells. Interdisciplinary Toxicology 1, 186–189. https://doi.org/10.2478/v10102-010-0036-9

Pons, M., Foradada, M., Estelrich, J., 1993. Liposomes obtained by the ethanol injection method. International Journal of Pharmaceutics 95, 51–56. https://doi.org/10.1016/0378-5173(93)90389-W

Pradhan, P., Guan, J., Lu, D., Wang, P.G., Lee, L.J., Lee, R.J., 2008. A facile microfluidic method for production of liposomes. Anticancer Res. 28, 943–947.

Qin, Y., Chen, J., Bi, Y., Xu, X., Zhou, H., Gao, J., Hu, Y., Zhao, Y., Chai, Z., 2015. Near-infrared light remote-controlled intracellular anti-cancer drug delivery using thermo/pH sensitive nanovehicle. Acta Biomaterialia 17, 201–209. https://doi.org/10.1016/J.ACTBIO.2015.01.026

Qu, M.-H., Zeng, R.-F., Fang, S., Dai, Q.-S., Li, H.-P., Long, J.-T., 2014. Liposome-based co-delivery of siRNA and docetaxel for the synergistic treatment of lung cancer. Int J Pharm 474, 112–122. https://doi.org/10.1016/j.ijpharm.2014.08.019

Quan, C.Y., Chang, C., Wei, H., Chen, C.S., Xu, X.D., Cheng, S.X., Zhang, X.Z., Zhuo, R.X., 2009. Dual targeting of a thermosensitive nanogel conjugated with transferrin and RGD-containing peptide for effective cell uptake and drug release. Nanotechnology 20. https://doi.org/10.1088/0957-4484/20/33/335101

Reeve, L.E., Hinsberg, M.G., 2005. Process for the fractionation of polymers. US6977045B2.

Reina, G., Orlanducci, S., Cairone, C., Tamburri, E., Lenti, S., Cianchetta, I., Rossi, M., Terranova, M.L., 2015. Rhodamine/Nanodiamond as a System Model for Drug Carrier. J Nanosci Nanotechnol 15, 1022–1029. https://doi.org/10.1166/jnn.2015.9736

Reischl, D., Zimmer, A., 2009. Drug delivery of siRNA therapeutics: potentials and limits of nanosystems. Nanomedicine: Nanotechnology, Biology and Medicine 5, 8–20. https://doi.org/10.1016/j.nano.2008.06.001

Rejinold, N.S., Baby, T., Chennazhi, K.P., Jayakumar, R., 2014. Dual drug encapsulated thermo-sensitive fibrinogen-graft-poly (N-isopropyl acrylamide) nanogels for breast cancer therapy. Colloids and Surfaces B: Biointerfaces 114, 209–217. https://doi.org/10.1016/J.COLSURFB.2013.10.015

Rivankar, S., 2014. An overview of doxorubicin formulations in cancer therapy. J Cancer Res Ther 10, 853–858. https://doi.org/10.4103/0973-1482.139267

Rizwan, M., Yahya, R., Hassan, A., Yar, M., Azzahari, A., Selvanathan, V., Sonsudin, F., Abouloula, C., 2017. pH Sensitive Hydrogels in Drug Delivery: Brief History,

Properties, Swelling, and Release Mechanism, Material Selection and Applications. Polymers 9, 137. https://doi.org/10.3390/polym9040137

Rowe, R.C., Sheskey, P.J., Quinn, M.E., 1994. Handbook of Pharmaceutical Excipients.

Royall, J.A., Berkow, R.L., Beckman, J.S., Cunningham, M.K., Matalon, S., Freeman, B.A., 1989. Tumor necrosis factor and interleukin 1 alpha increase vascular endothelial permeability. American Journal of Physiology-Lung Cellular and Molecular Physiology 257, L399–L410. https://doi.org/10.1152/ajplung.1989.257.6.L399

Sadighian, S., Rostamizadeh, K., Hosseini, M.-J., Hamidi, M., Hosseini-Monfared, H., 2017. Magnetic nanogels as dual triggered anticancer drug delivery: Toxicity evaluation on isolated rat liver mitochondria. Toxicology Letters 278, 18–29. https://doi.org/10.1016/J.TOXLET.2017.06.004

Sahu, P., Kashaw, S.K., Kushwah, V., Sau, S., Jain, S., Iyer, A.K., 2017a. pH responsive biodegradable nanogels for sustained release of bleomycin. Bioorganic & Medicinal Chemistry 25, 4595–4613. https://doi.org/10.1016/j.bmc.2017.06.038

Sahu, P., Kashaw, S.K., Kushwah, V., Sau, S., Jain, S., Iyer, A.K., 2017b. pH responsive biodegradable nanogels for sustained release of bleomycin. Bioorganic & Medicinal Chemistry 25, 4595–4613. https://doi.org/10.1016/J.BMC.2017.06.038

Sainson, R.C.A., Johnston, D.A., Chu, H.C., Holderfield, M.T., Nakatsu, M.N., Crampton, S.P., Davis, J., Conn, E., Hughes, C.C.W., 2008. TNF primes endothelial cells for angiogenic sprouting by inducing a tip cell phenotype. Blood 111, 4997–5007. https://doi.org/10.1182/blood-2007-08-108597

Saji Joseph, J., Tebogo Malindisa, S., Ntwasa, M., 2019. Two-Dimensional (2D) and Three-Dimensional (3D) Cell Culturing in Drug Discovery, in: Ali Mehanna, R. (Ed.), Cell Culture. IntechOpen. https://doi.org/10.5772/intechopen.81552

Sato, N., Goto, T., Haranaka, K., Satomi, N., Nariuchi, H., Mano-Hirano, Y., Sawasaki, Y., 1986. Actions of tumor necrosis factor on cultured vascular endothelial cells: morphologic modulation, growth inhibition, and cytotoxicity. J. Natl. Cancer Inst. 76, 1113–1121.

Seleci, M., Ag Seleci, D., Joncyzk, R., Stahl, F., Blume, C., Scheper, T., 2016. Smart multifunctional nanoparticles in nanomedicine. BioNanoMaterials 17. https://doi.org/10.1515/bnm-2015-0030

Sfriso, R., Zhang, S., Bichsel, C.A., Steck, O., Despont, A., Guenat, O.T., Rieben, R., 2018. 3D artificial round section micro-vessels to investigate endothelial cells under physiological flow conditions. Sci Rep 8, 5898. https://doi.org/10.1038/s41598-018-24273-7

Shaker, S., Gardouh, A.R., Ghorab, M.M., 2017. Factors affecting liposomes particle size prepared by ethanol injection method. Res Pharm Sci 12, 346–352. https://doi.org/10.4103/1735-5362.213979

Sharma, A., Garg, T., Aman, A., Panchal, K., Sharma, R., Kumar, S., Markandeywar, T., 2016. Nanogel - An advanced drug delivery tool: Current and future. Artificial Cells, Nanomedicine and Biotechnology 44, 165–177. https://doi.org/10.3109/21691401.2014.930745

Shi, J., Kantoff, P.W., Wooster, R., Farokhzad, O.C., 2017. Cancer nanomedicine: progress, challenges and opportunities. Nat Rev Cancer 17, 20–37. https://doi.org/10.1038/nrc.2016.108

Shimoda, A., Yamamoto, Y., Sawada, S., Akiyoshi, K., 2012. Biodegradable nanogel-integrated hydrogels for sustained protein delivery. Macromolecular Research 20, 266–270. https://doi.org/10.1007/s13233-012-0054-x

Shoueir, K.R., Atta, A.M., Sarhan, A.A., Akl, M.A., 2017. Synthesis of monodisperse core shell PVA@P(AMPS-*co*-NIPAm) nanogels structured for pre-concentration of Fe(III) ions. Environmental Technology 38, 967–978. https://doi.org/10.1080/09593330.2016.1215351

Shubhika, K., 2013. Nanotechnology and medicine - The upside and the downside. International Journal of Drug Development and Research 5.

Sikes, R.A., 2007. Chemistry and pharmacology of anticancer drugs. Br J Cancer 97, 1713. https://doi.org/10.1038/sj.bjc.6604075

Singh, S., Loke, Y.K., 2012. Drug safety assessment in clinical trials: methodological challenges and opportunities. Trials 13, 138. https://doi.org/10.1186/1745-6215-13-138

Soni, G., Yadav, K.S., 2016. Nanogels as potential nanomedicine carrier for treatment of cancer: A mini review of the state of the art. Saudi Pharmaceutical Journal 24, 133–139. https://doi.org/10.1016/j.jsps.2014.04.001

Soni, K.S., Desale, S.S., Bronich, T.K., 2016. Nanogels: An overview of properties, biomedical applications and obstacles to clinical translation. Journal of Controlled Release 240, 109–126. https://doi.org/10.1016/j.jconrel.2015.11.009

Sood, N., Bhardwaj, A., Mehta, S., Mehta, A., 2016. Stimuli-responsive hydrogels in drug delivery and tissue engineering. Drug Delivery 23, 748–770. https://doi.org/10.3109/10717544.2014.940091

Stenekes, R.J., Loebis, A.E., Fernandes, C.M., Crommelin, D.J., Hennink, W.E., 2000. Controlled release of liposomes from biodegradable dextran microspheres: a novel delivery concept. Pharm. Res. 17, 690–695. https://doi.org/10.1023/a:1007526114744

Su, H., Zhang, W., Wu, Y., Han, X., Liu, G., Jia, Q., Shan, S., 2018. Schiff base-containing dextran nanogel as pH-sensitive drug delivery system of doxorubicin: Synthesis and characterization. Journal of Biomaterials Applications 33, 170–181. https://doi.org/10.1177/0885328218783969

Sun, Z., Yi, Z., Zhang, H., Ma, X., Su, W., Sun, X., Li, X., 2017. Bio-responsive alginate-keratin composite nanogels with enhanced drug loading efficiency for cancer therapy. Carbohydrate Polymers 175, 159–169. https://doi.org/10.1016/J.CARBPOL.2017.07.078

Szebeni, J., Baranyi, L., Savay, S., Milosevits, J., Bunger, R., Laverman, P., Metselaar, J.M., Storm, G., Chanan-Khan, A., Liebes, L., Muggia, F.M., Cohen, R., Barenholz, Y., Alving, C.R., 2002. Role of complement activation in hypersensitivity reactions to doxil and hynic PEG liposomes: experimental and clinical studies. J Liposome Res 12, 165–172. https://doi.org/10.1081/lpr-120004790

Tan, J.P., Tan, M.B., Tam, M.K., 2010. Application of nanogel systems in the administration of local anesthetics. Local and regional anesthesia 3, 93–100. https://doi.org/10.2147/LRA.S7977

Tang, M., Szoka, F., 1997. The influence of polymer structure on the interactions of cationic polymers with DNA and morphology of the resulting complexes. Gene Ther 4, 823–832. https://doi.org/10.1038/sj.gt.3300454

Timko, B.P., Dvir, T., Kohane, D.S., 2010. Remotely triggerable drug delivery systems. Advanced Materials 22, 4925–4943. https://doi.org/10.1002/adma.201002072

Tokarska-Schlattner, M., Zaugg, M., Zuppinger, C., Wallimann, T., Schlattner, U., 2006. New insights into doxorubicin-induced cardiotoxicity: The critical role of cellular energetics. Journal of Molecular and Cellular Cardiology 41, 389–405. https://doi.org/10.1016/j.yjmcc.2006.06.009

Torchilin, V., Weissig, V., 2003. Liposomes: A Practical Approach. OUP Oxford.

Torchilin, V.P., 2005. Recent advances with liposomes as pharmaceutical carriers. Nature Reviews Drug Discovery 4, 145–160. https://doi.org/10.1038/nrd1632

Tran, S., DeGiovanni, P.-J., Piel, B., Rai, P., 2017. Cancer nanomedicine: a review of recent success in drug delivery. Clin Trans Med 6, 44. https://doi.org/10.1186/s40169-017-0175-0

Tranchant, I., Thompson, B., Nicolazzi, C., Mignet, N., Scherman, D., 2004. Physicochemical optimisation of plasmid delivery by cationic lipids. J. Gene Med. 6, S24–S35. https://doi.org/10.1002/jgm.509

Tuomela, A., Hirvonen, J., Peltonen, L., 2016. Stabilizing Agents for Drug Nanocrystals: Effect on Bioavailability. Pharmaceutics 8. https://doi.org/10.3390/pharmaceutics8020016

Ullah, F., Othman, M.B.H., Javed, F., Ahmad, Z., Akil, H.Md., 2015. Classification, processing and application of hydrogels: A review. Materials Science and Engineering: C 57, 414–433. https://doi.org/10.1016/j.msec.2015.07.053

Ur-Rehman, T., Tavelin, S., Gröbner, G., 2010. Effect of DMSO on micellization, gelation and drug release profile of Poloxamer 407. International Journal of Pharmaceutics 394, 92–98. https://doi.org/10.1016/j.ijpharm.2010.05.012

Valero, L., Alhareth, K., Espinoza Romero, J., Viricel, W., Leblond, J., Chissey, A., Dhotel, H., Roques, C., Campiol Arruda, D., Escriou, V., Mignet, N., Fournier, T., Andrieux, K., 2018. Liposomes as Gene Delivery Vectors for Human Placental Cells. Molecules 23. https://doi.org/10.3390/molecules23051085

van den Hoven, J.M., Nemes, R., Metselaar, J.M., Nuijen, B., Beijnen, J.H., Storm, G., Szebeni, J., 2013. Complement activation by PEGylated liposomes containing prednisolone. Eur J Pharm Sci 49, 265–271. https://doi.org/10.1016/j.ejps.2013.03.007

Varenne, F., Botton, J., Merlet, C., Hillaireau, H., Legrand, F., Barratt, G., Vauthier, C., 2016. Size of monodispersed nanomaterials evaluated by dynamic light scattering: Protocol validated for measurements of 60 and 203nm diameter nanomaterials is now extended to 100 and 400nm. International Journal of Pharmaceutics. https://doi.org/10.1016/j.ijpharm.2016.10.016

Varenne, F., Rustique, E., Botton, J., Coty, J.-B., Lanusse, G., Ait Lahcen, M., Rio, L., Zandanel, C., Lemarchand, C., Germain, M., Negri, L., Couffin, A.-C., Barratt, G., Vauthier, C., 2017. Towards quality assessed characterization of nanomaterial: Transfer of validated protocols for size measurement by dynamic light scattering and evaluation of zeta potential by electrophoretic light scattering. Int J Pharm 528, 299–311. https://doi.org/10.1016/j.ijpharm.2017.06.006

Vashist, A., Kaushik, A.K., Ahmad, S., Nair, M., 2017. Nanogels for Biomedical Applications. Royal Society of Chemistry.

Ventola, C.L., 2017. Progress in Nanomedicine: Approved and Investigational Nanodrugs. P T 42, 742–755.

Vinogradov, S., Batrakova, E., Kabanov, A., 1999. Poly(ethylene glycol)–polyethyleneimine NanoGel™ particles: novel drug delivery systems for antisense oligonucleotides. Colloids and Surfaces B: Biointerfaces 16, 291–304. https://doi.org/10.1016/S0927-7765(99)00080-6

Voss, O.H., Lee, H.-N., Tian, L., Krzewski, K., Coligan, J.E., 2018. Liposome preparation for the analysis of lipid-receptor interaction and efferocytosis. Curr Protoc Immunol 120, 14.44.1-14.44.21. https://doi.org/10.1002/cpim.43

Wagner, A., Vorauer-Uhl, K., Kreismayr, G., Katinger, H., 2002. The Crossflow Injection Technique: An Improvement of the Ethanol Injection Method. Journal of Liposome Research 12, 259–270. https://doi.org/10.1081/LPR-120014761

Wahlich, J., Desai, A., Greco, F., Hill, K., Jones, A.T., Mrsny, R.J., Pasut, G., Perrie, Y., Seib, F.P., Seymour, L.W., Uchegbu, I.F., 2019. Nanomedicines for the Delivery of Biologics. Pharmaceutics 11. https://doi.org/10.3390/pharmaceutics11050210

Wang, C., Mallela, J., Garapati, U.S., Ravi, S., Chinnasamy, V., Girard, Y., Howell, M., Mohapatra, S., 2013. A chitosan-modified graphene nanogel for noninvasive controlled drug release. Nanomedicine: Nanotechnology, Biology and Medicine 9, 903–911. https://doi.org/10.1016/J.NANO.2013.01.003

Wang, H., Yi, J., Mukherjee, S., Banerjee, P., Zhou, S., 2014. Magnetic/NIR-thermally responsive hybrid nanogels for optical temperature sensing, tumor cell imaging and triggered drug release. Nanoscale 6, 13001–13011. https://doi.org/10.1039/C4NR03748K

Wanka, G., Hoffmann, H., Ulbricht, W., 1994. Phase Diagrams and Aggregation Behavior of Poly(oxyethylene)-Poly(oxypropylene)-Poly(oxyethylene) Triblock Copolymers in Aqueous Solutions. Macromolecules 27, 4145–4159. https://doi.org/10.1021/ma00093a016

Wicki, A., Witzigmann, D., Balasubramanian, V., Huwyler, J., 2015. Nanomedicine in cancer therapy: Challenges, opportunities, and clinical applications. Journal of Controlled Release 200, 138–157. https://doi.org/10.1016/j.jconrel.2014.12.030

Winterhalter, M., Lasic, D.D., 1993. Liposome stability and formation: Experimental parameters and theories on the size distribution. Chemistry and Physics of Lipids 64, 35–43. https://doi.org/10.1016/0009-3084(93)90056-9

Wirth, M., Fritsche, P., Stojanovic, N., Brandl, M., Jaeckel, S., Schmid, R.M., Saur, D., Schneider, G., 2011. A Simple and Cost-Effective Method to Transfect Small

Interfering RNAs Into Pancreatic Cancer Cell Lines Using Polyethylenimine: Pancreas 40, 144–150. https://doi.org/10.1097/MPA.0b013e3181f7e41c

Wollina, U., Dummer, R., Brockmeyer, N.H., Konrad, H., Busch, J.-O., Kaatz, M., Knopf, B., Koch, H.-J., Hauschild, A., 2003. Multicenter study of pegylated liposomal doxorubicin in patients with cutaneous T-cell lymphoma. Cancer 98, 993–1001. https://doi.org/10.1002/cncr.11593

Wu, G., Lee, K.Y.C., 2009. Interaction of Poloxamers with Liposomes: An Isothermal Titration Calorimetry Study. J. Phys. Chem. B 113, 15522–15531. https://doi.org/10.1021/jp906331m

Wu, W., Shen, J., Banerjee, P., Zhou, S., 2010. Core–shell hybrid nanogels for integration of optical temperature-sensing, targeted tumor cell imaging, and combined chemo-photothermal treatment. Biomaterials 31, 7555–7566. https://doi.org/10.1016/J.BIOMATERIALS.2010.06.030

Xing, M., Yan, F., Yu, S., Shen, P., 2015. Efficacy and Cardiotoxicity of Liposomal Doxorubicin-Based Chemotherapy in Advanced Breast Cancer: A Meta-Analysis of Ten Randomized Controlled Trials. PLOS ONE 10, e0133569. https://doi.org/10.1371/journal.pone.0133569

Xing, T., Mao, C., Lai, B., Yan, L., 2012. Synthesis of Disulfide-Cross-Linked Polypeptide Nanogel Conjugated with a Near-Infrared Fluorescence Probe for Direct Imaging of Reduction-Induced Drug Release. ACS Applied Materials & Interfaces 4, 5662–5672. https://doi.org/10.1021/am301600u

Xing, Z., Wang, C., Yan, J., Zhang, L., Li, L., Zha, L., 2011. Dual stimuli responsive hollow nanogels with IPN structure for temperature controlling drug loading and pH triggering drug release. Soft Matter 7, 7992. https://doi.org/10.1039/c1sm05925d

Xiong, M.-H., Bao, Y., Yang, X.-Z., Wang, Y.-C., Sun, B., Wang, J., 2012. Lipase-Sensitive Polymeric Triple-Layered Nanogel for “On-Demand” Drug Delivery. Journal of the American Chemical Society 134, 4355–4362. https://doi.org/10.1021/ja211279u

Xue, Y., Xia, X., Yu, B., Luo, X., Cai, N., Long, S., Yu, F., 2015. A green and facile method for the preparation of a pH-responsive alginate nanogel for subcellular delivery of doxorubicin. RSC Adv. 5, 73416–73423. https://doi.org/10.1039/C5RA13313K

Yallapu, M.M., Jaggi, M., Chauhan, S.C., 2011. Design and engineering of nanogels for cancer treatment. Drug Discovery Today 16, 457–463. https://doi.org/10.1016/J.DRUDIS.2011.03.004

Yamauchi, T., Hasegawa, A., 1993. Determination of PEG concentration in its aqueous solution using differential scanning calorimetry. Journal of Applied Polymer Science 49, 1653–1658. https://doi.org/10.1002/app.1993.070490918

Yang, C., Wang, X., Yao, X., Zhang, Y., Wu, W., Jiang, X., 2015. Hyaluronic acid nanogels with enzyme-sensitive cross-linking group for drug delivery. Journal of Controlled Release 205, 206–217. https://doi.org/10.1016/J.JCONREL.2015.02.008

Yang, G., Fu, S., Yao, W., Wang, X., Zha, Q., Tang, R., 2017a. Hyaluronic acid nanogels prepared via ortho ester linkages show pH-triggered behavior, enhanced penetration and antitumor efficacy in 3-D tumor spheroids. Journal of Colloid and Interface Science 504, 25–38. https://doi.org/10.1016/J.JCIS.2017.05.033

Yang, G., Wang, X., Fu, S., Tang, R., Wang, J., 2017b. pH-triggered chitosan nanogels via an ortho ester-based linkage for efficient chemotherapy. Acta Biomaterialia 60, 232–243. https://doi.org/10.1016/J.ACTBIO.2017.05.003

Yang, H., Wang, Q., Chen, W., Zhao, Y., Yong, T., Gan, L., Xu, H., Yang, X., 2015. Hydrophilicity/Hydrophobicity Reversable and Redox-Sensitive Nanogels for Anticancer Drug Delivery. Molecular Pharmaceutics 12, 1636–1647. https://doi.org/10.1021/acs.molpharmaceut.5b00068

Yang, J., Zhang, C., Wang, X., Wang, W., Xi, N., Liu, L., 2019. Development of micro- and nanorobotics: A review. Sci. China Technol. Sci. 62, 1–20. https://doi.org/10.1007/s11431-018-9339-8

Yang, T., Li, B., Qi, S., Liu, Y., Gai, Y., Ye, P., Yang, G., Zhang, W., Zhang, P., He, X., Li, W., Zhang, Z., Xiang, G., Xu, C., 2014. Co-delivery of Doxorubicin and Bmi1 siRNA by Folate Receptor Targeted Liposomes Exhibits Enhanced Anti-Tumor Effects in vitro and in vivo. Theranostics 4, 1096–1111. https://doi.org/10.7150/thno.9423

Yao, Y., Su, Z., Liang, Y., Zhang, N., 2015. pH-Sensitive carboxymethyl chitosan-modified cationic liposomes for sorafenib and siRNA co-delivery. Int J Nanomedicine 10, 6185–6197. https://doi.org/10.2147/IJN.S90524

Yapar, E., Ýnal, Ö., 2013. Poly(ethylene oxide)–Poly(propylene oxide)-Based Copolymers for Transdermal Drug Delivery: An Overview. Trop. J. Pharm Res 11, 855–866. https://doi.org/10.4314/tjpr.v11i5.20

Yi, P., Wang, Y., Zhang, S., Zhan, Y., Zhang, Y., Sun, Z., Li, Y., He, P., 2017. Stimulative nanogels with enhanced thermosensitivity for therapeutic delivery via β-cyclodextrin-induced formation of inclusion complexes. Carbohydrate Polymers 166, 219–227. https://doi.org/10.1016/J.CARBPOL.2017.02.107

Yu, B., Lee, R.J., Lee, L.J., 2009. Microfluidic Methods for Production of Liposomes. Methods Enzymol 465, 129–141. https://doi.org/10.1016/S0076-6879(09)65007-2

Yu, L., Ding, J., 2008a. Injectable hydrogels as unique biomedical materials. Chemical Society Reviews 37, 1473. https://doi.org/10.1039/b713009k

Yu, L., Ding, J., 2008b. Injectable hydrogels as unique biomedical materials. Chem Soc Rev 37, 1473–1481. https://doi.org/10.1039/b713009k

Zan, M., Li, J., Huang, M., Lin, S., Luo, D., Luo, S., Ge, Z., 2015. Near-infrared light-triggered drug release nanogels for combined photothermal-chemotherapy of cancer. Biomaterials Science 3, 1147–1156. https://doi.org/10.1039/C5BM00048C

Zha, L., Banik, B., Alexis, F., 2011. Stimulus responsive nanogels for drug delivery. Soft Matter 7, 5908. https://doi.org/10.1039/c0sm01307b

Zhang, B., Chen, J., Lu, Y., Qi, J., Wu, W., 2013. Liposomes interiorly thickened with thermosensitive nanogels as novel drug delivery systems. International Journal of Pharmaceutics 455, 276–284. https://doi.org/10.1016/j.ijpharm.2013.07.020

Zhang, F., Gong, S., Wu, J., Li, H., Oupicky, D., Sun, M., 2017. CXCR4-Targeted and Redox Responsive Dextrin Nanogel for Metastatic Breast Cancer Therapy. Biomacromolecules 18, 1793–1802. https://doi.org/10.1021/acs.biomac.7b00208

Zhang, R., Hummelgård, M., Lv, G., Olin, H., 2011. Real time monitoring of the drug release of rhodamine B on graphene oxide. Carbon 49, 1126–1132. https://doi.org/10.1016/j.carbon.2010.11.026

Zhang, X., Achazi, K., Steinhilber, D., Kratz, F., Dernedde, J., Haag, R., 2014. A facile approach for dual-responsive prodrug nanogels based on dendritic polyglycerols with minimal leaching. Journal of Controlled Release 174, 209–216. https://doi.org/10.1016/J.JCONREL.2013.11.005

Zhang, Y., Wang, F., Li, M., Yu, Z., Qi, R., Ding, J., Zhang, Z., Chen, X., 2018. Self-Stabilized Hyaluronate Nanogel for Intracellular Codelivery of Doxorubicin and Cisplatin to Osteosarcoma. Advanced Science 5. https://doi.org/10.1002/advs.201700821

Zhao, A., Zhou, S., Zhou, Q., Chen, T., 2010. Thermosensitive Micelles from PEG-Based Ether-anhydride Triblock Copolymers. Pharmaceutical Research 27, 1627–1643. https://doi.org/10.1007/s11095-010-0155-1

Zhou, M., Khen, K., Wang, T., Hu, Q., Xue, J., Luo, Y., 2018. Chemical crosslinking improves the gastrointestinal stability and enhances nutrient delivery potentials of egg yolk LDL/polysaccharide nanogels. Food Chemistry 239, 840–847. https://doi.org/10.1016/J.FOODCHEM.2017.07.019

Zhu, M., Lu, D., Wu, S., Lian, Q., Wang, Wenkai, Lyon, L.A., Wang, Weiguang, Bártolo, P., Saunders, B.R., 2019. Using green emitting pH-responsive nanogels to report environmental changes within hydrogels: a nanoprobe for versatile sensing. Nanoscale 11, 11484–11495. https://doi.org/10.1039/C9NR00989B

Zizzari, A., Bianco, M., Carbone, L., Perrone, E., Amato, F., Maruccio, G., Rendina, F., Arima, V., 2017. Continuous-Flow Production of Injectable Liposomes via a Microfluidic Approach. Materials (Basel) 10. https://doi.org/10.3390/ma10121411

Annex

Ahmed, S., Corvis, Y., Gahoual, R., Euan, A., Lai-Kuen, R., Couillaud, B.M., Seguin, J., Alhareth, K., Mignet, N., 2019. Conception of nanosized hybrid liposome/poloxamer particles to thicken the interior core of liposomes and delay hydrophilic drug delivery. International Journal of Pharmaceutics 567, 118488. https://doi.org/10.1016/j.ijpharm.2019.118488.

International Journal of Pharmaceutics 567 (2019) 118488

Contents lists available at ScienceDirect

International Journal of Pharmaceutics

journal homepage: www.elsevier.com/locate/ijpharm

Conception of nanosized hybrid liposome/poloxamer particles to thicken the interior core of liposomes and delay hydrophilic drug delivery

Shayan Ahmed[a,b,c], Yohann Corvis[a,b,c], Rabah Gahoual[a,b,c], Arlen Euan[a,b,c], Rene Lai-Kuen[d], Brice Martin Couillaud[a,b,c], Johanne Seguin[a,b,c], Khair Alhareth[a,b,c], Nathalie Mignet[a,b,c,*]

[a] Chemical and Biological Technologies for Health Unit (UTCBS), CNRS UMR8258, 75006 Paris, France
[b] UTCBS, INSERM U1267, 75006 Paris, France
[c] Faculté de Pharmacie, Université Paris Descartes, Université de Paris, 75006 Paris, France
[d] Plateau Technique Imagerie Cellulaire et Moleculaire, CNRS UMS3612, INSERM US25, Université de Paris, 75006 Paris, France

ARTICLE INFO

Keywords:
Hybrid liposome/polymer
Syringe pump
Gelliposomes
Rhodamine
Poloxamer

ABSTRACT

Liposomes are nanocarriers composed of phospholipids, especially designed to potentially carry drugs. However, liposomes suffer in terms of leakage of small hydrophilic drugs. To control the release, a system with lipid shell and polymeric viscous core, namely Hybrid liposome/polymer inside (HLP_{in}), has been designed. For this purpose, we setup a syringe pump apparatus equipped with homemade tubing system. HLPin formulation consisting of poloxamer (5% w/v) was found to be optimal when produced at injection rates of 5 mL.min^{-1}. Then, we tend to characterize the HLP_{in} with DLS, TEM, TRPS, thermal analysis and densitometry in comparison with a polymer added after formation of the liposomes. The optimal formulation was evaluated for its stability and cytotoxicity. The selected conditions and composition resulted in nanocarriers which are highly reproducible with mono-disperse size distribution with an average size of 206 ± 4.8 nm and a polydispersity index of 0.15 ± 0.015. Densitometry and thermal analysis results confirmed the formation of HLP_{in}. Interestingly, HLP_{in} were stable over 2 months, produced no cytotoxicity and exhibited slow release of rhodamine and Doxorubicin in comparison to liposome formulation. Our homemade tubing system coupled with syringe pump apparatus achieved reproducible, precisely controlled production for the HLPin formulation which can be scale up.

1. Introduction

Liposomes are vesicles composed of phospholipid molecules enclosing an aqueous droplet. Initially designed to mimic cell membranes *in vitro*, they were consequently proposed as drug delivery system. Due to high loading capacity as well as similarity with cell membrane, liposomes have been implemented to serve in several applications in the field of pharmaceuticals, such as cancer diagnosis and therapy (Torchilin, 2005). Potential application of liposomes as therapeutic tools is still being challenged by their physical and chemical instability, which may result in increased bilayer permeability and drug leakage (Guan et al., 2015). In order to improve the stability of liposomes, many approaches have been suggested like liposomes coated with PEG polymer. However, the use of an external coating could reduce liposomes cellular uptake (Wollina et al., 2003; Zhang et al., 2013). More recently, a new approach has been investigated in order to alleviate the limitations of liposomes; a system composed of a polymeric-core and a lipid shell have been introduced, in this nanosystem both lipid and polymer are unified to yield theoretically stable particles, enhanced encapsulation, controlled and modified release drug delivery system (Mandal et al., 2013).

Polymers form 3D structures in contact with water. Hydrophilic polymers swells when hydrated and expand by the absorption of water (Peppas, 2000). Poloxamers are non-ionic copolymers arranged in triblock of EOx-POy-EOx consisting of ethylene oxide (EO) and propylene oxide (PO) parts, x and y values can have modulated producing a collection of poloxamer derivatives. Poloxamers exhibit low critical solution temperature (LCST). The poloxamer based nanogels have the

Abbreviations: DOPC, 1,2 dioleoyl-*sn*-glycero-3-phosphocholine; P407, poloxamer 407; CL, conventional liposome; HLP_{in}, hybrid liposome/polymer inside; HLP_{out}, hybrid liposome/polymer outside; TEM, transmission electron microscopy; Rhod, rhodamine B; DLS, dynamic light scattering; DSC, differential scanning calorimetry; TRPS, tunable resistive pulse sensing; CT, cell toxicity; Gelliposomes, Gls

* Corresponding author at: Chemical and Biological Technologies for Health Unit (UTCBS), CNRS UMR8258, 75006 Paris, France.
E-mail address: Nathalie.Mignet@parisdescartes.fr (N. Mignet).

https://doi.org/10.1016/j.ijpharm.2019.118488
Received 30 April 2019; Received in revised form 28 June 2019; Accepted 29 June 2019
Available online 02 July 2019
0378-5173/ © 2019 Published by Elsevier B.V.

particularity to be temperature responsive. Small nanogel particles around 120 nm swelled drastically to over 400 nm when temperature rapidly decreased below LCST (Lee et al., 2008).

In the literature hybrid structures of liposomes with polymer or gel are termed differently such as gelliposome or lipogels. These structures design different compositions which possess various characteristics. To control the release of drug, Kim et al formulated hybrid liposomal lipid bilayers with a Poly(Poly(*N*-Isopropylacrylamide-co-acrylic Acid) core (Kim et al., 1997). In 2015, Guan et al prepared gelliposomes composed of liposomes with a gelatin core to enhance the stability and the structure of liposomes (Guan et al., 2015).

In our case, we were interested in developing interiorly viscous core liposomes with no additional charges or chemical component to avoid the risk of toxicity. The most similar works in the literature were carried by Chandaroy and his team who proposed the hybrid Liposomes and very low concentration of Pluronics, the another similar work in the literature was done by Zhang et al, his team proposed interiorly thickened liposomes with high concentration of poloxamer (Chandaroy et al., 2001; Zhang et al., 2013). This approach lead to an increase of liposomes stability and provided controlled release of encapsulated drugs. The obtained micro particles having an average size of 1.2 µm and exhibiting an important polydispersity (Zhang et al., 2013). In order to enhance the encapsulation of drug and slow their release while keeping a good pharmacokinetics profile, it would be preferable to obtain monodisperse nanoparticles with controlled preparation process. In this work, we aimed to obtain nanosized hybrid liposome/polymer particles with enhanced inner core viscosity using an optimum concentration of poloxamer, that should enhance the encapsulation and delay the release of drug. For this purpose, an appropriate preparation method with controlled experimental conditions had to be set-up.

Several techniques were described for the preparation of liposomes, the conventional ethanol injection technique provides the advantage of being simple to form vesicles without the application of a lot of energy and the possibility of scale up (Akbarzadeh et al., 2013; Batzri and Korn, 1973; Wagner et al., 2002). Automatization of the process by the merger of ethanolic injection technique with a syringe pump apparatus enhanced the reproducibility, while reducing the variability related to the experimenter. Additionally it allows to achieve a large scale production of liposomes (Pham et al., 2012; Pradhan et al., 2008).

In this paper, we developed a hybrid liposome/poloxamer inside (HLP_{in}) formulation using a syringe pump apparatus coupled with a homemade tubing system. We first optimized the composition and the experimental parameters in order to obtain small size and monodispersed particles. The optimal formulation was extensively characterized in term of physico-chemical properties. The cytotoxicity, encapsulation and release kinetics of two hydrophilic drug models were then evaluated.

2. Materials

DOPC (1,2 Dioleooyl-*sn*-glycero-3-phosphocholine) was purchased from Avanti polar Lipids (Alabaster, Alabama, USA), poloxamer 407 (P407), also known by its trade name as Kolliphor P407 was provided by BASF (Ludwigshafen, Germany), Doxorubicin Hydrochloride (Sigma Aldrich, France), Rhodamine B (Sigma Aldrich, France), Iodine and Potassium Iodine were provided by Prolab (Briare, France). Water was purified on Milli-Q system from Millipore (Fontenay-sous-bois, France), Ethanol 96% was purchased from Carlo-Erba reagents (Val-de-Reuil, France). Ultra-filtration units Vivaspin®20 were purchased from Sartorius (Geottingen, Germany), ultra-filtration units NANOSEP 300k was purchased from PALL filtron (Massachusetts, USA), Dialysis device Microfloat-A-lyzer 100 KD was purchased from spectrum laboratories (CA, USA), Polyether ether ketone (PEEK) tubes and T-shaped connectors and ferrules were purchased from IDEX Health & Science (Oak Harbor, WA, USA).

3. Methods

3.1. Preparation of the formulations

In this work, three formulations were designed: Conventional non-ionic liposomes, Hybrid liposome/poloxamer inside (HLP_{in}) and Hybrid liposome/poloxamer outside (HLP_{out}).

Conventional liposomes (CLs) were prepared by the ethanolic injection method using a syringe pump apparatus (Harvard apparatus PHD 2000). One syringe (1 mL) was filled with ethanolic solution of DOPC (20 $mg.mL^{-1}$, 25.4 $\mu mol.mL^{-1}$) and another syringe (10 mL) was filled with Milli-Q® water. Both syringes were fixed on the syringe pump apparatus, injection speed was set to 0.5 $mL.min^{-1}$ for the lipid solution and 5 $mL.min^{-1}$ for the aqueous solution. Apparatus ran for 1 min giving final volume of 5.5 mL, yielding a final concentration of DOPC (2 mg/mL, 2.54 $mmol.mL^{-1}$).

Hybrid liposome/poloxamer inside (HLP_{in}) was prepared using the same procedure as liposomes preparation. The aqueous phase was replaced by poloxamer 407 (P407) solution at different concentration (0.5, 5 and 10% w/v). Different flow rates of P407 solution injection (0.1, 1, 5, 10 and 37 $mL.min^{-1}$) were tested in order to choose the optimal value. Ratio of the injection flow rates between the lipid solution and the P407 solution was kept at 1:10 for all experiments.

Liposomes with gel outside termed as Hybrid liposome/poloxamer outside (HLP_{out}). HLP_{out} was prepared by first preparing conventional liposomes with concentration of DOPC (4 $mg.mL^{-1}$, 5.08 $mmol.mL^{-1}$). A poloxamer solution (10% w/v) was prepared. Liposome suspension and poloxamer solution were then mixed with 1:1 vol ratio to obtain final concentration of lipid and poloxamer similar to HLP_{in}.

In case of rhodamine or Doxorubicin HCL (DOX) encapsulation, the formulations were prepared by following the same procedure discussed above for each formulation. The only difference was the addition of rhodamine or DOX (0.5 $mg.mL^{-1}$ and 5 $mg.mL^{-1}$, respectively) in aqueous phase or in poloxamer solution during preparation.

The theoretical calculation of Reynolds Number to determine the laminar flow in the tubes was computed using the equation,

$$Re = \frac{\rho VD}{\mu}$$

where ρ represents the fluid density, V is the linear velocity of the solution, D the tube diameter and µ the dynamic viscosity of the fluid. The density of a 5% P407 solution was experimentally determined by densitometry (DMA™ 4500 M, Anton Paar) performed at 20 °C.

Where ρ = 1.00612 kg/L, V is the linear velocity which depends on the injection rate, D = 0.25 mm, the viscosity of poloxamer (P407 0.5%) µ = 2.29 cP.

3.2. Evaporation of ethanol

The removal of ethanol was performed using a rotary evaporator. The formulation was collected in an evaporation flask and treated by using a rotavapor (Rotavapor R-144, Büchi, Switzerland) at the following conditions (rotating rate 60 rpm, 35 °C, pressure 10 mbar). These conditions applied for 10–15 min to achieve 25–35% evaporation and 20–30 min to achieve 60–65% evaporation of formulation measured by weight which were later adjusted with by adding Milli-Q® water.

3.3. Densitometry

The density was measured by using a Densitometer (Anton Paar DMA™ 4500 M). Densitometry analysis is based on the principle of oscillating U-tube to determine the density of samples based on an electronic measurement of the frequency of oscillation, from which the density value is calculated. Experiments were performed at temperature 25 and 37 °C. The U-tube was washed with Milli-Q® water then with

ethanol 96% following by drying with air, before and after each utilization. The oscillating U-tube was filled with about 1.5 mL of sample with a syringe. The U-View ™ camera function shows and records live images of the oscillating U-tube to ensure that there should be no bubbles and that the U-tube is entirely filled with the sample.

3.4. Ultrafiltration by centrifugation

Ultrafiltration column (Pall Filtron, USA) with 300 kDa molecular weight cut-off (MWCO) were used to separate free poloxamer and non-encapsulated rhodamine B from liposomal suspension. The filtration was carried out by centrifugation at 13,000 rpm for 30 min in a refrigerated bench-top centrifuge (Hettich Rotanta 460 RF, Germany) at 4 °C.

3.5. Physicochemical characterization

3.5.1. Dynamic light scattering (DLS)

The liposome, HLP_{in} and HLP_{out} diameters were determined at 25 °C by quasi-elastic light scattering using a Zetasizer Nanoseries Nano-ZS (Malvern Instruments, France). The scattering was measured at a 173° fixed angle and the position at 4.65. Each sample was run for 3 measurements. Results were expressed as the average hydrodynamic diameter and the standard deviation of the triplicate.

3.5.2. Transmission electron microscopy (TEM)

The liposome, HLP_{in} and HLP_{out} formulations were observed by Transmission Electron Microscopy (TEM). Briefly, 10 µL of the sample was deposited on a carbon-coated copper grids, excess solution was removed after 2 min by a filter paper. This was followed by the application of 5 µL of uranyl acetate 1% to the same grid for 2 min, excess stain was then removed with filter paper. Sample is subsequently air-dried at room temperature. The grid placed on a slide was inserted in the microscope. The sample analysis was performed with a JEOL JEM 100 S (JEOL Ltd Tokyo, Japan) TEM operating at 80 kV. TEM images were captured using an Orius Sc 200 digital Camera (Gatan-Roper Scientific, Evry, France).

3.5.3. Tunable resistive pulse sensing (TRPS)

Measurements were made using a qNano system from IZON Science equipped with an upper and a lower fluid cell, each one containing an Ag/AgCl electrode. The measurements were done using electrolyte (standard provided with Izon kit) solution and a pressure of 0 mbar to allow the passage of the particles through the pore. The membrane stretch was comprised between 45 and 47 mm and the voltage were adjusted in order to have a baseline current between 120 and 145 nA. Data were acquired using Izon Control Suite V3.1. Each acquisition presented is the result of the passage of at least 500 liposomes. The liposome size and concentration were calculated after the measurement of the calibrated particles solutions with Nano-pore (NP250) allowing a measurement of a total size range between 100 and 400 nm according to manufacturer. The results were determined using the IZON Control Suite software.

3.5.4. Thermal analysis

The Differential Scanning Calorimetry (DSC) experiments were performed on the differential scanning calorimeter 822e (Mettler-Toledo, Switzerland) previously calibrated with high purity indium (T_{fus} = 156.6 °C, $\Delta_{fus}H$ = 28.45 J.g^{-1}) and zinc (T_{fus} = 419.6 °C, $\Delta_{fus}H$ = 107.5 J.g^{-1}). DSC experiments were performed at temperature starting from 5 to 60 °C at 1 K.min^{-1} scan rate under dry air (60 mL.min^{-1}). Empty aluminum pan of 100 µL was hermetically sealed and holed from the top by means of a small pin of controlled size (0.7 mm) and used as a reference.

3.6. Calorimetric assay (Baleux assay)

Poloxamer quantification was carried out by a colorimetric assay as previously described by Baleux and Champetier (1972). Briefly, 12.5 µL Iodine solution (iodine solution at 10 mg/mL and potassium iodide solution at 20 mg/mL) was added to 1 mL of diluted sample. The absorbance of the complex was measured after 5 min at 540 nm using UV–Vis spectrophotometer (Varian CARY® 100). Linearity was checked for standard solutions with concentration ranging from 0.05 to 100 µg.mL^{-1}. Poloxamer concentration of samples were calculated using calibration curve with r^2 of 0.99.

3.7. Stability study

Stability tests were carried out for CLs, HLP_{in} and HLP_{out} formulations for 2 months. The three formulations were prepared, filtered and kept at 4 °C. The liposome and HLP diameters were determined at 25 °C by quasi-elastic light scattering using a Zetasizer Nanoseries Nano-ZS (Malvern Instruments, France).

3.8. Cytotoxicity tests

The murine fibroblast NIH/3T3 (ATCC® CRL1658™) and liver normal epithelial BNL 1ME A.7R.1 (ATCC® TIB75™) cell lines were purchased from the American Type Culture Collection (ATCC, Manassas, USA). The cell line NIH/3T3 was grown at 37 °C and 5% CO_2 in DMEM containing 2 mM L-glutamine, 100 U/mL penicillin and 100 µg/mL streptomycin, 10% bovine serum, whereas cell line BNL was grown in the same medium just replacing the bovine serum by a fetal one. Cells were plated onto 96-well plates at 20,000 cells per well in 100 µL of culture medium. Twenty-four hours after plating, 100 µL of medium containing the compound of interest (final concentrations ranging from 0.06 to 2 mg/mL in terms of lipid or 1.5–50 mg/mL in terms of P407, in 2-fold dilutions) was added to the wells. After 24 h of exposure, the cell viability was evaluated using the MTT test. Then, the absorbance was read at 560 nm in a microplate reader (Infinite F200 Pro – TECAN). Results are expressed in percent of viability compared to the same concentration of solvent.

3.9. Loading content and encapsulation efficiency

The liposome and HLP_{in} formulations encapsulating rhodamine B (0.5 mg.mL^{-1}) or doxorubicin (5 mg.mL^{-1}) were filtered as described in Section 3.4. The sample remained on the filter was re-suspended with Milli-Q® water in order to make up to the initial volume and quantified by spectrofluorometry using a Varian CARY® spectrofluorometer at excitation 490 nm and emission 580 nm for rhodamine and at excitation 490 nm and emission 595 nm for doxorubicin. Linearity was checked for standard solutions with concentration ranging from 0.075 to 1 µg.mL^{-1} for rhodamine and 1 to 25 µg.mL^{-1} for doxorubicin. Rhodamine and doxorubicin concentration of samples were calculated using calibration curve with r^2 of 0.98 and 0.97, respectively. The solutions of rhodamine B and rhodamine B with P407 5% were taken as controls. Loading content and encapsulation efficiency were calculated by using the following equations:

$$Loading\ Content\ (\%) = \left(\frac{weight\ of\ loaded\ drug}{weight\ of\ drug\ loaded\ particles}\right) \times 100$$

$$Encapsulation\ Efficiency\ (\%) = \left(\frac{weight\ of\ loaded\ drug}{weight\ of\ drug\ in\ feed}\right) \times 100$$

3.10. In vitro release

A stock solution of rhodamine B (0.5 mg.mL^{-1}) was used to prepare

two different samples: solution of rhodamine B encapsulated within liposomes and rhodamine B encapsulated within HLP_{in} formulation. Dialysis device (Micro Float-A-Lyzer, France) was filled with the required volume of each sample and kept floating in a beaker with PBS at 37 °C using an agitation rate of 60 rpm, volume of medium to volume of sample ratio was fixed at 1:1000. At defined points, 1 mL of samples were removed from the release medium and replaced with fresh PBS to maintain the volume constant. The amount of rhodamine B released was monitored by spectrofluorometer (Varian CARY®) at excitation 490 nm and emission 580 nm. *In vitro* release test was performed in triplicates. A similar procedure was followed for doxorubicin HCL (5 $mg.mL^{-1}$) release study at excitation 490 nm and emission 595 nm.

3.11. Statistical analysis

For the size measurement and the Stability test, the data was presented as the mean ± SD. The graph Pad Prism software was used to analyses the data and determine statistical significance between groups for cytotoxicity and release test. Cytotoxicity experiment data was treated with Gaussian nonlinear regression fit and two-way ANOVA was applied $p < 0.05^{***}$. The release test graphs presented one phase decay nonlinear regression fit and student *t* test was applied $p = 0.0001^{***}$. All the experiments were performed in triplicates.

4. Results and discussion

4.1. Conception of the formulations

In this study, a hybrid composition of lipid and polymer was selected to achieve a formulation that offers an improved encapsulation and controlled release of the encapsulated drug. The lipid used for this formulation was DOPC and the polymer used was poloxamer 407 (P407). The designed formulation is referred as Hybrid liposome/poloxamer inside (HLP_{in}). Regarding physicochemical properties, the HLP_{in} system is expected to increase the viscosity and the density of the liposome core by incorporating poloxamer into the aqueous core of the liposomes. This approach should enhance the entrapment of drug and avoid its fast release.

4.1.1. Optimization of the experimental conditions

All formulations were prepared according to the principle of ethanolic injection with the help of a syringe pump device and tubing system that we developed (methods Section 3.1). The preparation of formulations with the syringe pump apparatus combines two main principles, the ethanolic injection and microfluidics. The instrumental setting was designed to provide fully controlled and reproducible experimental conditions due to minimum experimenter influence, in addition to offer the possibility to scale up the production (Charcosset et al., 2015). From a formulation standing point, the main advantage is to produce a narrow size distribution of liposomes in a single step, without extrusion or sonication. However, to generate a reproducible formulation having relevant characteristics, several parameters needed to be setup, i) optimization of experimental setup, ii) optimization of formulation regarding the lipid and poloxamer ratio, and iii) optimization of formulation regarding the solvent content.

4.1.1.1. Optimization of experimental setup. In order to optimize the conditions for formulations preparation, the influence of two instrumental parameters on the final preparation properties was studied, a) the tubing internal diameter and b) the injection flow rate. The HLP_{in} formulation with poloxamer concentration (0.5% w/v) was used for the optimization of the experimental conditions. For this experiment, two types of tubbing systems with different compositions and internal diameters were considered in order to select the most suitable to prepare the formulations as emphasized in Fig. 1. Both preparation systems are comprised of 3 distinctive tubes connected to each other by the intermediate of T-shaped connector (Fig. 1A). T-1 tube system was composed of two polyethylene inlet tubes having a 1 mm internal diameter followed after the junction by one outlet tube of 250 µm internal diameter composed of polyether ether ketone (PEEK) which is high performance engineering thermoplastic inert to water and the most common chemical solvents (Haleem and Javaid, 2019). Whereas, T-2 preparation system composed of three PEEK tubes with the same internal diameter (250 µm). HLP_{in} formulation was prepared using both preparation systems according to the procedure described in preparation of the formulations (Section 3.1).

The second parameter requiring optimization was the injection flow rate. For that purpose, HLP_{in} formulation was prepared using different injection flow rates (0.1 $mL.min^{-1}$, 1 $mL.min^{-1}$, 5 $mL.min^{-1}$, 10 $mL.min^{-1}$, 37 $mL.min^{-1}$). The optimal injection flow rate was selected according to the DLS characterization of the final preparation (Fig. 1B: left and right, respectively). First, we verified that both preparation systems would generate to laminar flow which is necessary to obtain liposomes (Yu et al., 2009). For this purpose, we calculated the Reynolds (Re) number for both preparation systems depending on the injection flow rate. As described in the literature, a Reynold number lower than 2000 is representative of laminar flow conditions, favorable for liquid mixing and to the formation of smaller and uniform size liposomes with low PDI (Bessoth et al., 1999; Jahn et al., 2004; Yu et al., 2009). The Reynold number was calculated for each tube (Table 1). Regardless of the flow rates employed, Re number was systematically well within the range of 2000 and lower for the T-2 tube than the T-1 tube demonstrating the formation of a laminar flow and (Table 1). Therefore, the different configurations T-1 and T-2 were suitable for the formation of liposomes.

All preparations produced had acceptable range of average hydrodynamic size and PDI except in the case of the lowest infusion flow rate (0.1 $mL.min^{-1}$) with Tube-1 system. The comparison showed that the polydispersity (PDI) of the liposomes obtained from T-1 tube was significantly higher than the PDI obtained from T-2 preparation system, as the average PDI for all flow rates was 0.232 and 0.098 respectively. As the T-2 preparation system exhibited lower Re number than T-1 system at each flow rate (see Table 1), this could explain the formation of formulations with slightly better PDI obtained with the T-2 tube system (Fig. 1B: left and right).

The two preparation systems designed to be used in conjunction with the syringe pump demonstrated to be suitable for the production of CLs and HLP formulations in a robust manner. This instrumental approach has the advantage to provide an optimal usage of the volume of the different solutions by minimizing the dead volume of the preparation system. In addition, because it relies on the use of PEEK tubbing readily available, it appears as particularly cost-effective approach which can be easily implemented. On the basis of Re numbers and PDI of HLP_{in}, Tube-2 system was considered further for optimizing lipid/poloxamer ratio according to the injection flow rate.

4.1.1.2. Optimization of the formulation regarding lipid and polymer ratio. The lipid and polymer ratio adjustment was the next phase to attain the intended formulation. The lipid to poloxamer ratio was optimized at fixed lipid concentration and varying poloxamer concentration using various flow rates. We observed that the average hydrodynamic size and PDI values increased with the rise of P407 percentage, nearly at all flow rates (Fig. 2A and B). HLP_{in} with poloxamer 0.5% had the smallest size and PDI but at this concentration, it was thought difficult to increase the liposome inner core viscosity. HLP_{in} with poloxamer 5% was found optimal as it exhibits an average size within acceptable range and a slightly better PDI than HLP_{in} with poloxamer 10%.

Finally, the formulation with the optimal average size and PDI was obtained with the T-2 tube system at a flow rate of 5 $mL.min^{-1}$ with 5% of P407 in HLP_{in}. These parameters were also set for the other two formulations taken as controls, Conventional liposomes (CL) and

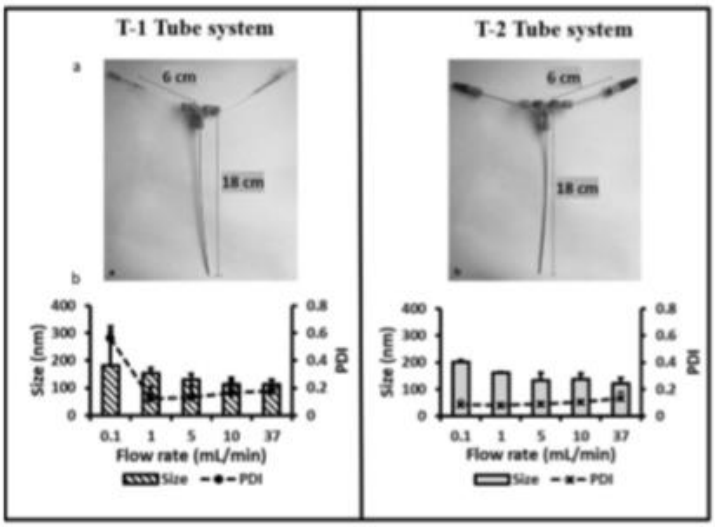

Fig. 1. Comparison between two Tube System T-1 (left) and T-2 (right), (a) Pictorial illustration, (b) Graphical representation of size and PDI of liposomes obtained with different flow rate of each tube system (n = 3).

Table 1
Re numbers obtained by T-1 and T-2 tube system obtained with different flow rate.

Flow Rate (mL.min^{-1})	Reynolds number T-1 tube	Reynolds number T-2 tube
0.1	0.06	0.01
1	0.56	0.07
5	2.80	0.35
10	5.60	0.70
37	20.7	2.59

Hybrid liposome/poloxamer outside (HLP_{out}) in which the poloxamer was added after the formation of liposomes.

4.1.1.3. Optimization of the formulation regarding the solvent content. Density analysis was performed in order i) to optimize the evaporation procedure with respect to HLP integrity, and ii) to evidence the internalization of the polymer within the liposomes. As far as the validation of the evaporation procedure is concerned, it has been demonstrated that the control of ethanol/water quantity in the formulation is necessary to prevent liposomes from dissolving (in case of too high quantity of ethanol, *e.g.* 10% in the present study) or aggregating (in case of water over-evaporation). To optimize the evaporation procedure, the obtained formulations were evaporated up to 25–35% and 60–75% at controlled temperature and pressure. As it can be seen in Table 2, volumetric mass of HLP_{in} and HLP_{out} was differentiated only for formulation evaporated up to 25–35%. In the case of non-evaporated formulations, a slight differentiation was noticed by comparing conventional liposome formulations and water/ethanol 90/10 v/v solutions volumetric masses. Similarly, volumetric mass was quite comparable for the HLP_{in} and HLP_{out} formulations with 60–75% evaporation + q.s. Milli-Q® water. These results could be explained by relative disruption of the liposomes membrane leading to the same P407/lipid system.

Interestingly, densitometry analysis has also demonstrated that with 25–35% of evaporation of the ethanol/water medium, less than 0.3% of ethanol was remaining in the final formulations. Such ratio makes the formulation more stable and suitable for *in vivo* administration.

Furthermore, once the overall formulation procedure has been optimized (*i.e.* 5% P407, 25–35% evaporation + q.s. Milli-Q® water),

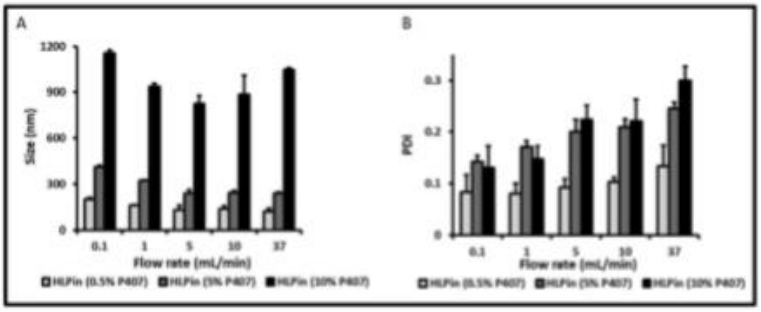

Fig. 2. Flow rate and formulation optimization. Graphical presentation of hydrodynamic average size (A) and polydispersity index (B) of HLP_{in} obtained with different poloxamer (P407) percentages at different flow rates (0.5, 1, 5, 10, and 37 mL.min^{-1}).

Table 2
Volumetric mass of different formulations as function of the ethanol/water ratio at 25 °C.

Formulation	Volumetric mass ($g.cm^{-3}$) 25 °C		
	Without evap.	25–35% evap. + q.s.	60–75% evap. + q.s.
Milli-Q water	0.99705	0.99705	0.99705
Water/ethanol (90/10, v/v)	0.98462	0.99637	0.99702
Conventional liposomes	0.98644	0.99634	0.99685
HLP_{out}	0.99743	1.00214	1.00236
HLP_{in}	0.99171	0.99881	1.00325

densitometry experiments help to have a first insight into HLP_{in} and HLP_{out} properties differentiation. For that purpose, a poloxamer density calibration curve has been firstly established (data not shown) and highlights the fact that volumetric mass of aqueous solution of P407 is directly proportional to the polymer concentration. This could be helpful to estimate the poloxamer amount in the HLP formulations. As far as the present results are concerned, a 5% P407 solution have a volumetric mass of 1.00253 $g.cm^{-3}$ at 25 °C. This density value is similar to that of the optimized HLP_{out} formulation, possibly due to the fact that P407 in the HLP_{out} formulation is present in the continuous medium. For the HLP_{in} formulation, the density is lower compared to the 5% P407 solution but higher compared to the conventional liposome prepared the same way. This suggests that the polymer is encapsulated within the liposomes.

To apprehend the HLP_{in} and HLP_{out} behavior at body temperature, densitometry experiments were also performed at 37 °C (Table 3). A similar behavior is observed, indicating that the liposome as well as the poloxamer entities undergo no change at that temperature. We assume that, at the body temperature, the encapsulation efficiency should be the same as at room temperature. These results will comfort the further *in vitro* and *in vivo* experiments. As far as the current results are concerned, a 5% P407 solution have a volumetric mass of 0.99816 $g.cm^{-3}$ at 37 °C. To resume, the densitometry experiment demonstrated that 25–35% of evaporation of the continuous medium was the best range to optimize the HLP formulations by maintaining its required characteristics.

Concurrently, this procedure allows removing the maximum of ethanol to make the HLP formulations biocompatible. The formulations retained with the help of the densitometry experiments were then filtrated and considered for further characterization studies such as physicochemical experiments, within the objective of accessing the poloxamer encapsulated inside liposome for the HLP_{in} formulations.

4.2. Physicochemical characterization

4.2.1. Dynamic light scattering (DLS)

The results of the particle sizing of our formulations are summarized in Table 4. The table shows the z-average diameters, the polydispersity index obtained for the various liposome, HLP_{in} and HLP_{out} formulations. The z-average diameter values are the mean of measurements

Table 3
Volumetric mass of different formulations after ethanol/water evaporation up to 25–35% + q.s. Milli-Q* water 25 and 37 °C.

Formulation	Volumetric mass ($g.cm^{-3}$) 25 °C	Volumetric mass ($g.cm^{-3}$) 37 °C
Milli-Q water	0.99705	0.99328
Conventional liposomes	0.99634	0.99263
HLP_{out}	1.00214	0.99766
HLP_{in}	0.99881	0.99431

Table 4
DLS results of size and PDI for CL, HLPout and HLP_{in}.

Formulation	Size (nm)	PdI
CL	91 ± 12.8	0.22 ± 0.019
HLP_{out}	183 ± 5.5	0.17 ± 0.016
HLP_{in}	206 ± 4.8	0.15 ± 0.015

repeated on 5 samples of each formulation of CL, HLP_{in} and HLP_{out}. The data shows that the measurements are reproducible for each formulation. In addition, the results show that the size is dependent of the formulation composition. We obtained nanoscale particle size within a range suitable for systemic delivery. This was definitely an advances as regard to the microscale particles gelliposomes reported in the literature (Guan et al., 2015; Zhang et al., 2013).

The physical characterization of liposomes, HLP_{in} and HLP_{out} is of great importance in understanding their stability and suitability for the variety of applications. After size determination, the TEM imaging was carried out to examine the morphological difference between the formulations.

4.2.2. Transmission electron microscopy (TEM) and tunable resistive pulse sensing (TRPS)

TEM images of liposome, HLP_{in} and HLP_{out} revealed the structure and morphology of each system. The morphology of these formulations was different from each other (as shown in Fig. 3 left panel). The liposome exhibits various morphologies lose their defined shape related to the effect of grid drying. HLP_{out} exhibited more defined structures with few clusters. The deformation of the HLP_{out} vesicles can be explained by a significant amount of free poloxamer in the continuous medium. Interestingly, HLP_{in} showed regular structures under TEM observations (Fig. 3A–C, left panel).

To complete the DLS and TEM data, the number of nanoparticles obtained were determined using tunable resistive pulse-sensing. The liposomes and HLP_{out} tend to exhibit a main size distribution between 150 and 200 nm with concentration 1.4×10^9 particles/mL and from 170 to 250 nm with concentration 1.5×10^9 particles/mL respectively (Fig. 3A and B graph at right). HLP_{in} tends to exhibit a broader range from 150 to 200 nm with concentration 7.0×10^8 particles/mL (Fig. 3C graph at right). These interpretations indicate that the HLP_{in} formulation may contain encapsulated poloxamer as it contains a smaller number of particles, which can be due to more homogeneous shape and size as observed in TEM images and a better PDI obtained with DLS. The poloxamer inside the liposome might provide stability, strength and viscosity to the core of liposomes (Zhang et al., 2013). In order to verify this hypothesis, thermal analysis experiments were performed from 5 to 60 °C, as the poloxamer suspension presents a micellization transition in this range of temperature, and since the poloxamer environment may impact such a transition.

4.3. Differential scanning calorimetry (DSC)

Poloxamer behavior as a function of temperature in aqueous medium is well known and discussed in numerous publications (Chen et al., 2013; Dumortier et al., 2006; Pembouong et al., 2011). Indeed, one can have access to the poloxamer micellization transition by deriving the heat flow *vs.* temperature signal obtained from the DSC analysis of the poloxamer solution. An endothermic signal is then obtained with a peak position corresponding to the micellization temperature. This transition corresponds to the removal of water (likely dehydration process) from PPO of the PEO-PPO-PEO chains of the poloxamer during the micelles formation (Alexandridis et al., 1994; Ur-Rehman et al., 2010). Since the micellization temperature decreases with concentration, and since the signal area in proportional to the concentration, the micellization temperature is inversely proportional

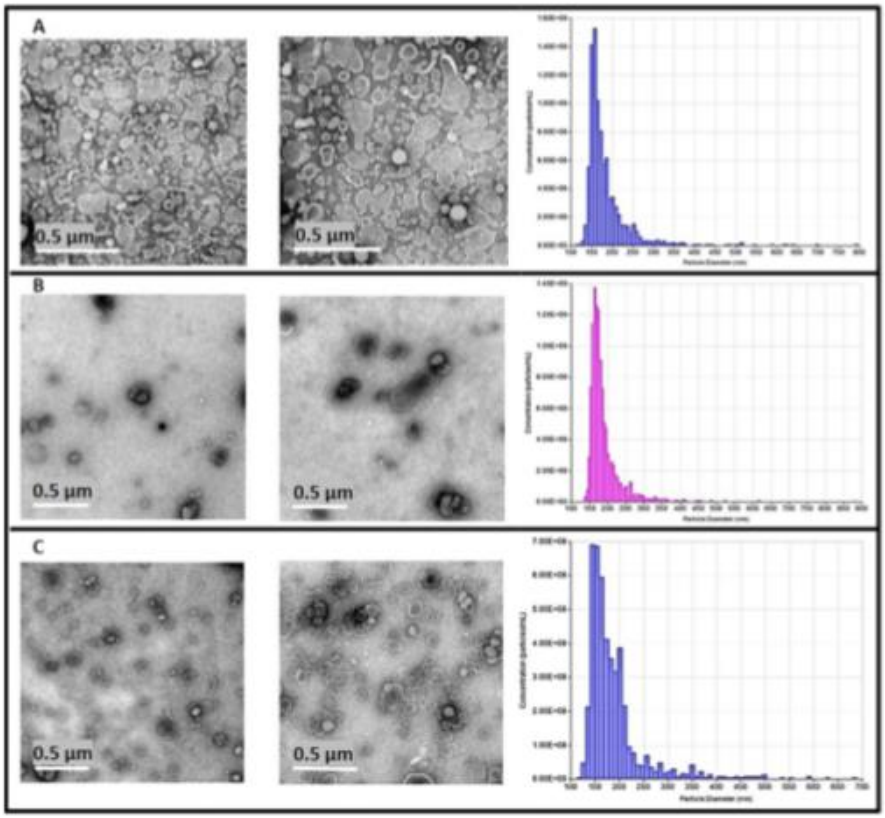

Fig. 3. (A) Conventional liposomes as spherical unilaminar vesicles of variable sizes (24–329 nm), (B) HLP_{out} as heterogenous mixture with non-definite shape particles with size range (30–445), and (C) HLP_{in} as unilaminar vesicles of variable sizes (50–188 nm).

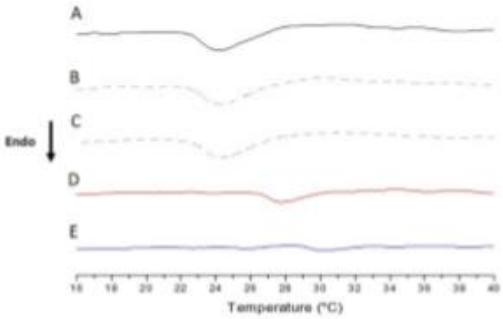

Fig. 4. Derived DSC curves obtained (A) P407 5%, (B) HLP_{out}, before filtration, (C) HLP_{in}, before filtration, (D) HLP_{out}, after filtration, and (E) HLP_{in} after filtration.

to peak height. No difference in micellization was noticed between P407 5% aqueous solution, unfiltered HLP_{in} and HLP_{out} formulations (Fig. 4A–C). This is due to the fact that free poloxamer influences the thermal transition of the overall lipid/polymer systems. But once HLP_{in} and HLP_{out} are filtrated, one can easily distinguish both formulations since their temperatures of micellization are shifted to higher temperatures (Fig. 4D and E). Interestingly, P407 temperature of micellization (T_{mic}) for filtered HLP_{in} is 5.5 °C higher than that of both unfiltered HLP_{in} and free P407 5% formulations. As far as filtered HLP_{out} is concerned, P407, the micellization temperature is 3.6 °C higher than that of both unfiltered HLP_{out} and free P407 5% formulations (see experimental ΔT_{mic} data in Table 5).

This result should support our former hypothesis of encapsulated poloxamer in the HLP_{in} vesicles only if we can certify that decrease in P407 quantity after the filtration process is not the only factor responsible of such a shift in the temperature of micellization. To evaluate the concentration contribution to T_{mic} data for filtrated HLP_{in} and HLP_{out} formulations, a T_{mic} *vs.* concentration curve calibration has been established (results not shown), and then correlated to calorimetric assay of poloxamer in filtrated in and out formulations. The results of the latter experiment are presented hereafter in Section 4.4 and are also considered for some data in Table 5. By measuring temperature of micellization for several P407 aqueous solutions in the 5% to 20% range of concentrations, the relation between T_{mic} and P407 concentration ($C_{\%}$) allowed us to obtain a linear correlation that is fitting by the following equation, $T_{mic} = -0.53 \times C_{\%} + 26.0$ ($r^2 = 0.99999$). P407 concentration will be later determine by calorimetric assay, allowing to recalculate the temperature of micellization (extrapolated T_{mic}) that would correspond to phase transition temperature taking into

Table 5
Experimental and recalculated temperature of micellization.

Formulation	Experimental T_{mic} (°C)	Experimental ΔT_{mic} (°C)	P407 %	Extrapolated T_{mic} (°C)	Effective ΔT_{mic} (°C)
Free P407	23.6	–	5.0%	–	–
HLP_{in}	23.6	–	5.0%	–	–
HLP_{out}	23.6	–	5.0%	–	–
filtrated HLP_{in}	29.1	5.5	3.4%	24.2	4.9
filtrated HLP_{out}	27.2	3.6	2.3%	24.8	2.4

consideration the polymer concentration decrease due to the filtration. Finally, the extrapolated T_{mic} allows determining the effective variation of temperature of micellization (effective ΔT_{mic}) between the filtered and unfiltered formulations, independent to P407 variation of concentration. The latter result clearly indicates that the effective increase of 4.9 °C for filtrated HLP_{in} T_{mic} is due to the poloxamer encapsulation within the liposomes. By similarity, the effective increase of 2.4 °C for filtrated HLP_{out} T_{mic} can be explain by i) a percentage of poloxamer entrapped in the liposomes, and/or ii) a specific interaction between poloxamer and the DOPC. It is noteworthy to mention here that mixtures of unorganized DOPC and poloxamer do not modify the temperature of micellization of poloxamer compared to that of free poloxamer (results not shown).

4.4. Calorimetric assay (Baleux assay)

To determine the quantity of poloxamer entrapped inside the liposomal shell, calorimetric assay was carried out by means of poloxamer/KI_3 interactions. This has been made possible since we demonstrated that DOPC presence does not influence the quantification of poloxamer by such a technic (results not shown). The estimated percentages of entrapped poloxamer for the filtrated HLP_{in} and HLP_{out} formulations were 67% and 45%, respectively. The distinguishable data between these two formulations confirm the TEM images previously described. Indeed, HLP_{in} have higher amount of entrapped poloxamer than HLP_{out}. Additionally, the results obtained allow us to interpret the DSC data.

4.5. Stability

The liposome stability is the limit to which a drug substance or product retains the same properties and characteristics, throughout its period of storage and use (Winterhalter and Lasic, 1993). Stability study of liposome, HLP_{out} and HLP_{in} formulations carried in terms of measurement of average size and PDI. The samples were kept at 4 °C during the whole experiment of 2 months. The results were compared between day 0 and day 58 in terms of average size and PDI. In case of conventional liposomes and HLP_{in} no significant difference was observed in terms of their average size and PDI (Fig. 5). Whereas in HLP_{out}, formulation, the change in average size and PDI was observed that may be due to presence of substantial amount of P407 which leads to liposomal membrane disruption. The stability study was also discussed previously by Guan et al showing that the stability of liposomes was definitely improved in gel core liposomes (Guan et al., 2015).

The stability of our formulation was notable in comparison of HLP_{out} formulation used as control. This experiment confirms that our main formulation HLP_{in} was stable enough and should be considered for next experiments. Therefore, we first assessed its cytotoxicity in two different cell lines.

4.6. Cytotoxicity

To investigate the cytotoxicity of our formulations *in vitro*, the study was carried out on two different cell lines, NIH 3T3 and BNL. Both the cell lines were treated with each formulation (CL, HLP_{out}, HLP_{in} and P407 10%). The viability results for each cell lines are presented in Fig. 6A and B, as a function of lipid (left) and P407 concentration

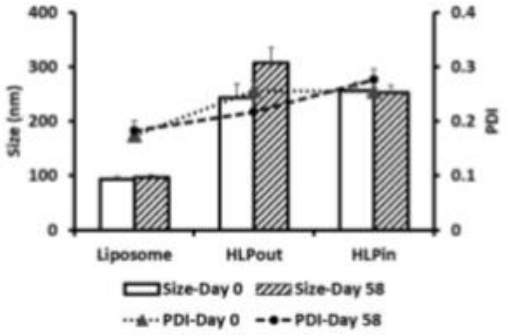

Fig. 5. Stability test graph corresponds to the difference in size and PDI of conventional liposomes, HLPin, and HLP_{out} with in a period of 2 months.

(right). The mean inhibition concentration 50 (IC50) values determined for each curve is shown in Table 6. Cytotoxicity results obtained for HLP_{in} and HLP_{out} formulations in both cell lines were similar to the cytotoxicity of conventional liposomes and poloxamer P407.

In BNL cell line the IC50 value was approximately 1.5 mg/mL in terms of lipid and 35 mg/mL in terms of P407. However, on NIH/3T3 cells, liposome showed low toxicity with 80% of viability at 2 $mg.mL^{-1}$ of lipids ($p < 0.001^{***}$). Hybrid lipid/poloxamer formulations induced a little toxicity in NIH3T3 cell line, probably due to P407 because IC50 was around 35 $mg.mL^{-1}$. The MTT assay revealed the no cytotoxicity over the concentration of poloxamer in our preparations (approximately 30 $mg.mL^{-1}$ for HLP_{in} and 25 $mg.mL^{-1}$ for HLP_{out}, measured after filtration by calorimetric assay). This can be ascribed to the biocompatible nature of lipid and poloxamer in our formulations.

4.7. Encapsulation efficiency and loading content.

The main idea to design this lipid/polymer hybrid a carrier was to improve the encapsulation and/or release kinetic of hydro-soluble drugs. For the evaluation of encapsulation ability, rhodamine B was used as a model drug and doxorubicin as a drug. Three different concentrations of drug solution were used to evaluate the effect of initial drug solution concentration on encapsulation efficiency and loading content. Rhodamine or doxorubicin were added in H_2O or P407 solution and encapsulated during the preparation of CL and HLP_{in}, respectively. The encapsulation efficiency and loading content of HLP_{in} was compared to those of liposomes (Fig. 7A for rhodamine and B for doxorubicin). For both nanosystems, EE% and LC% were increased for both drugs when increasing the initial concentration. Differences in encapsulation values between CLs and HLP_{in} were significant for the low initial concentrations of drugs. It was previously reported that the interior content of liposomes is a key factor for increasing encapsulation (Guan et al., 2015). This implies that the incorporation of rhodamine in thickened liposomes should have been greater than encapsulating rhodamine in empty liposome. However, no difference was observed at the highest concentrations, 0.5 $mg.mL^{-1}$ and 5 $mg.mL^{-1}$ for rhodamine and doxorubicin, respectively.

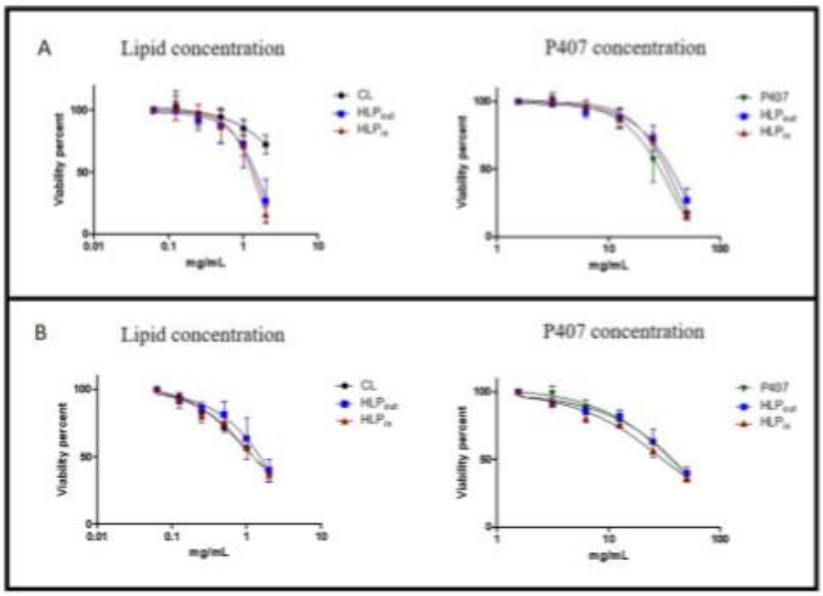

Fig. 6. *In vitro* cell viability curves (A) Graphs for cell line NIH/3T3 cell viability in relation of Lipid and P407 concentration, left and right respectively (B) Graphs for cell line TIB75 cell viability in relation of Lipid and P407 concentration, left and right respectively. Gaussian nonlinear regression fit and two-way ANOVA was applied $p < 0.05$.

Table 6
IC50 values as function of Lipid and P407 on NIH/3T3 and BNL cells.

Cell lines		CL	HLP_{out}	HLP_{in}	P407
NIH 3T3 (IC50)	Lipid	>2	1.4 ± 0.1	1.5 ± 0.2	–
	P407	–	37.9 ± 5.5	35.2 ± 5 0.8	28.1 ± 7.6
BNL (IC50)	Lipid	1.3 ± 0.2	1.5 ± 0.4	1.3 ± 0.2	–
	P407	–	36.6 ± 12.8	32.7 ± 7.0	38.5 ± 4.7

To examine if these two formulations could exhibit a different release kinetics, a release study was carried out on these two formulations. The high concentrations for both drugs was used for the release study, this choice was made considering the volume of release medium and the limit of detection of the spectrofluorometer.

4.8. In vitro release kinetics

In vitro release studies were conducted to determine the difference between drug solutions (rhodamine or doxorubicin), encapsulated drug in liposomes and HLP_{in} from 1 to 24 h (Figs. 8 and 9, respectively). All the experiments were performed in triplicates at 37 °C. The half-life of rhodamine solution, rhodamine release from CL and HLP_{in} were close around 1.83, 1.34 and 2.18 h, respectively. However, the final release from these formulations after 24 h was significantly different. It reached 94% for the rhodamine solution, 91% for CL and only 73% for HLP_{in}. This significant variance is probably due to the viscous core of HLP_{in} which lead to a slower release of rhodamine.

In vitro kinetics were also carried out with doxorubicin. The final release of doxorubicin from these formulations after 30 h was significantly different which was 96% for the doxorubicin solution, 56% for CL and 89% for HLP_{in}. Interestingly, the release of doxorubicin from HLP_{in} displayed delayed release of the drug comparing to the CLs. The amount of doxorubicin released during the first hour was relatively lower as compared to the one of CLs. Noteworthy, HLP_{in} exhibited a release half-life of doxorubicin approximately 3 times higher than the one with CL. This substantial variation between the CLs and HLP_{in} might probably be attributed to the inner core viscosity of HLP_{in} which led to delayed and slower release of doxorubicin.

The release of doxorubicin from CLs reached to a plateau around 4 h whereas a large part of drug payload remained associated to the nanosystem. In contrast, a continuous release throughout the experiment was observed in the case of HLP_{in}, this can be explained by the presence of poloxamer in the nanosystem which released into the release medium that improving the DOX solubility. The characteristic of poloxamer to keep the drugs solubilized and stable in term of their size has been described in previous literature (Bodratti and Alexandridis, 2018; Couilland et al., 2019; Devi et al., 2013).

If we compare HLP_{in} to Gelliposomes (GLs) formulation described in the literature by Zhang et al, the kinetic profile of our formulation was in first order and not biphasic. This could be explained by the fact that the HLP_{in} core was viscous but not gelified like GLs. Moreover, the sustained release of the rhodamine and DOX in HLP_{in} was faster than GLs which have a relatively bigger particle size (1.2 μm) and higher amount of poloxamer.

5. Conclusion

HLP_{in} nanoparticles formulation was effectively produced by using syringe pump system. The poloxamer provides the viscosity to an aqueous core of liposomes which prevents the leakage of small hydrophilic drug and increase the entrapment of drugs. The physicochemical characterization of our HLP systems opens a path for better understanding of formulating vesicles encapsulating polymers. The formation of HLP_{in} was confirmed by DSC and density analysis. *In vitro* release of HLP_{in} showed slow release in comparison of CL in 24 h for rhodamine and 30 h for doxorubicin. HLP_{in} formulation found to be stable for 2 months of storage and shown no cytotoxicity. In conclusion, HLP_{in}

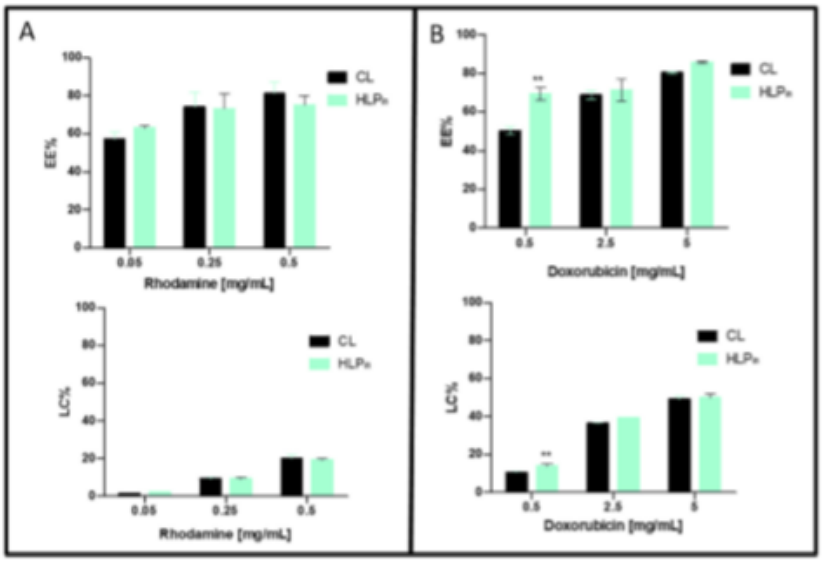

Fig. 7. (A) Encapsulation efficiency and loading content of rhodamine B inside Cls and HLP_{in}. (B) Encapsulation efficiency and loading content of doxorubicin inside Cls and HLP_{in}. Two way ANOVA $p = 0.01^{**}$.

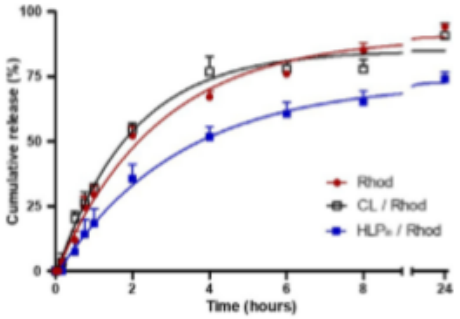

Fig. 8. Release of rhodamine B from nonionic lipids vesicles with and without poloxamer. Formulation composition: (●) rhodamine solution, (□) Liposome encapsulating rhodamine, (■) HLPin encapsulating rhodamine. One phase decay nonlinear regression fit and student *t* test $p = 0.0001^{***}$.

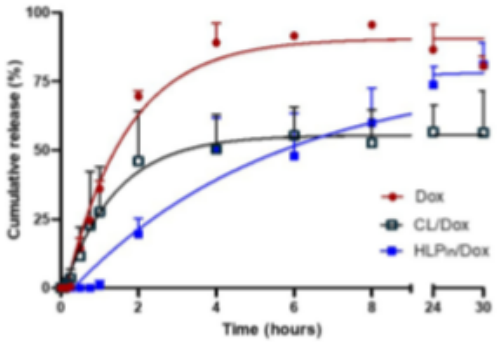

Fig. 9. Release of doxorubicin from nonionic lipids vesicles with and without poloxamer. Formulation composition: (●) doxorubicin solution, (□) Liposome encapsulating doxorubicin, (■) HLP_{in} encapsulating doxorubicin. One phase decay nonlinear regression fit and student *t* test $p = 0.0001^{***}$.

presented different physiognomies to be used as controlled drug delivery systems. Our homemade designed syringe pump tubing achieved reproducible, economical, precisely controlled fabrication for the liposomes and HLP_{in} formulations which can be scale up with a minimal influence of experimenter.

CRediT authorship contribution statement

Shayan Ahmed: Methodology, Validation, Formal analysis, Investigation, Data curation, Writing - original draft, Visualization. **Yohann Corvis:** Conceptualization, Methodology, Writing - review & editing, Visualization, Investigation, Data curation. **Rabah Gahoual:** Methodology, Writing - review & editing. **Arlen Euan:** Data curation, Formal analysis. **Rene Lai-Kuen:** Investigation, Writing - review & editing. **Brice Martin Couillaud:** Data curation, Formal analysis. **Johanne Seguin:** Investigation, Formal analysis, Writing - review & editing. **Khair Alhareth:** Conceptualization, Methodology, Validation, Formal analysis, Investigation, Writing - review & editing, Visualization. **Nathalie Mignet:** Conceptualization, Methodology, Supervision, Methodology, Writing - review & editing, Project administration.

Acknowledgements

The Authors thank Higher Education Commission of Pakistan for providing Shayan Ahmed's scholarship for Ph.D, Master student Pinar Cakilkaya for assisting in the project and BASF (Ludwigshafen, Germany) for providing poloxamer 407.

Declaration of Competing Interest

The authors declare that they have no known competing financial interests.

Authors contributions

NM KA and YC designed the formulation and managed the project. SA and YC performed phsico-chemical analysis. SA and RLK participate for transmission electron microscopy. SA KH and RG designed and optimized the microfluidic system (push syring apparatus). SA, JS and BMC did the cellular *in vitro* studies. AE did release studies. SA NM KH YC wrote the manuscript, JS RG RLK participated in manuscript edition

References

Akbarzadeh, A., Rezaei-Sadabady, R., Davaran, S., Joo, S.W., Zarghami, N., Hanifehpour, Y., Samiei, M., Kouhi, M., Nejati-Koshki, K., 2013. Liposome: classification, preparation, and applications. Nanoscale Res. Lett. 8, 102. https://doi.org/10.1186/1556-276X-8-102.

Alexandridis, P., Holzwarth, J.F., Hatton, T.A., 1994. Micellization of poly(ethylene oxide)-poly(propylene oxide)-poly(ethylene oxide) triblock copolymers in aqueous solutions: thermodynamics of copolymer association. Macromolecules 27, 2414–2425. https://doi.org/10.1021/ma00087a009.

Baleux, B., Champetier, G., 1972. Dosage colorimétrique d'agents de surface non ioniques polyoxyéthylenes al'aide d'une solution iodo–iodurée. CR Acad Sci Paris C 274, 1617–1620.

Batzri, S., Korn, E.D., 1973. Single bilayer liposomes prepared without sonication. Biochim. Biophys. Acta BBA – Biomembr. 298, 1015–1019. https://doi.org/10.1016/0005-2736(73)90408-2.

Bessoth, F.G., deMello, A.J., Manz, A., 1999. Microstructure for efficient continuous flow mixing. Anal. Commun. 36, 213–215. https://doi.org/10.1039/a902237f.

Bodratti, A.M., Alexandridis, P., 2018. Formulation of poloxamers for drug delivery. J. Funct. Biomater. 9. https://doi.org/10.3390/jfb9010011.

Chandaroy, P., Sen, A., Hui, S.W., 2001. Temperature-controlled content release from liposomes encapsulating Pluronic F127. J. Controlled Release 76, 27–37. https://doi.org/10.1016/S0168-3659(01)00429-1.

Charcosset, C., Juban, A., Valour, J.-P., Urbaniak, S., Fessi, H., 2015. Preparation of liposomes at large scale using the ethanol injection method: effect of scale-up and injection devices. Chem. Eng. Res. Des. 94, 508–515. https://doi.org/10.1016/j.cherd.2014.09.008.

Chen, J., Zhou, R., Li, L., Li, B., Zhang, X., Su, J., 2013. Mechanical, rheological and release behaviors of a poloxamer 407/poloxamer 188/carbopol 940 thermosensitive composite hydrogel. Molecules 18, 12415–12425. https://doi.org/10.3390/molecules181012415.

Couilland, B.M., Espeau, P., Mignet, N., Corvis, Y., 2019. State of the art of pharmaceutical solid forms: from crystal property issues to nanocrystals formulation. ChemMedChem 14, 8–23. https://doi.org/10.1002/cmdc.201800612.

Devi, D.R., Sandhya, P., Hari, B.N.V., 2013. Poloxamer: a novel functional molecule for drug delivery and gene therapy. J. Pharm. Sci. 7.

Dumortier, G., Grossiord, J.L., Agnely, F., Chaumeil, J.C., 2006. A review of poloxamer 407 pharmaceutical and pharmacological characteristics. Pharm. Res. 23, 2709–2728. https://doi.org/10.1007/s11095-006-9104-4.

Guan, P., Lu, Y., Qi, J., Niu, M., Lian, R., Wu, W., 2015. Solidification of liposomes by freeze-drying: the importance of incorporating gelatin as interior support on enhanced physical stability. Int. J. Pharm. 478, 655–664. https://doi.org/10.1016/j.ijpharm.2014.12.016.

Haleem, A., Javaid, M., 2019. Polyether ether ketone (PEEK) and its 3D printed implants applications in medical field: an overview. Clin. Epidemiol. Global Health. https://doi.org/10.1016/j.cegh.2019.01.003.

Jahn, A., Vreeland, W.N., Gaitan, M., Locascio, L.E., 2004. Controlled vesicle self-assembly in microfluidic channels with hydrodynamic focusing. J. Am. Chem. Soc. 126, 2674–2675. https://doi.org/10.1021/ja0318090.

Kim, J.-C., Bae, S.K., Kim, J.-D., 1997. Temperature-sensitivity of liposomal lipid bilayers mixed with poly(*N*-isopropylacrylamide-co-acrylic acid). J. Biochem. (Tokyo) 121, 15–19. https://doi.org/10.1093/oxfordjournals.jbchem.a021558.

Lee, S.H., Choi, S.H., Kim, S.H., Park, T.G., 2008. Thermally sensitive cationic polymer nanocapsules for specific cytosolic delivery and efficient gene silencing of siRNA: swelling induced physical disruption of endosome by cold shock. J. Controlled Release 125, 25–32. https://doi.org/10.1016/j.jconrel.2007.09.011.

Mandal, B., Bhattacharjee, H., Mittal, N., Sah, H., Balabathula, P., Thoma, L.A., Wood, G.C., 2013. Core–shell-type lipid–polymer hybrid nanoparticles as a drug delivery platform. Nanomed. Nanotechnol. Biol. Med. 9, 474–491. https://doi.org/10.1016/j.nano.2012.11.010.

Pembouong, G., Morellet, N., Kral, T., Hof, M., Scherman, D., Bureau, M.-F., Mignet, N., 2011. A comprehensive study in triblock copolymer membrane interaction. J. Controlled Release 151, 57–64. https://doi.org/10.1016/j.jconrel.2011.01.007.

Peppas, N., 2000. Hydrogels in pharmaceutical formulations. Eur. J. Pharm. Biopharm. 50, 27–46. https://doi.org/10.1016/S0939-6411(00)00090-4.

Pham, T.T., Jaafar-Maalej, C., Charcosset, C., Fessi, H., 2012. Liposome and niosome preparation using a membrane contactor for scale-up. Colloids Surf. B: Biointerfaces 94, 15–21. https://doi.org/10.1016/j.colsurfb.2011.12.036.

Pradhan, P., Guan, J., Lu, D., Wang, F.G., Lee, L.J., Lee, R.J., 2008. A facile microfluidic method for production of liposomes. Anticancer Res. 28, 943–947.

Torchilin, V.P., 2005. Recent advances with liposomes as pharmaceutical carriers. Nat. Rev. Drug Discov. 4, 145–160. https://doi.org/10.1038/nrd1632.

Ur-Rehman, T., Tavelin, S., Gröbner, G., 2010. Effect of DMSO on micellization, gelation and drug release profile of Poloxamer 407. Int. J. Pharm. 394, 92–98. https://doi.org/10.1016/j.ijpharm.2010.05.012.

Wagner, A., Vorauer-Uhl, K., Kreismayr, G., Katinger, H., 2002. The crossflow injection technique: an improvement of the ethanol injection method. J. Liposome Res. 12, 259–270. https://doi.org/10.1081/LPR-120014761.

Winterhalter, M., Lasic, D.D., 1993. Liposome stability and formation: experimental parameters and theories on the size distribution. Chem. Phys. Lipids 64, 35–43. https://doi.org/10.1016/0009-3084(93)90056-9.

Wollina, U., Dummer, R., Brockmeyer, N.H., Konrad, H., Bunch, J.-O., Kantz, M., Knopf, B., Koch, H.-J., Hauschild, A., 2003. Multicenter study of pegylated liposomal doxorubicin in patients with cutaneous T-cell lymphoma. Cancer 98, 993–1001. https://doi.org/10.1002/cncr.11593.

Yu, B., Lee, R.J., Lee, L.J., 2009. Microfluidic methods for production of liposomes. Methods Enzymol. 465, 129–141. https://doi.org/10.1016/S0076-6879(09)65007-2.

Zhang, B., Chen, J., Lu, Y., Qi, J., Wu, W., 2013. Liposomes interiorly thickened with thermosensitive nanogels as novel drug delivery systems. Int. J. Pharm. 455, 276–284. https://doi.org/10.1016/j.ijpharm.2013.07.020.